Development of site-specific labeling strategies for protein modification and synthesis of Rab probes

Dissertation

zur Erlangung des akademischen Grades

eines Doktors der Naturwissenschaften (Dr. rer. nat.)

des Fachbereichs Chemie der Universität Dortmund

Angefertigt am Max-Planck-Institut für molekulare Physiologie

in Dortmund

vorgelegt von

Long Yi

aus China

Dortmund, October 2012

1. Gutachter : Prof. Dr. Roger Sidney Goody

2. Gutachter : Prof. Dr. Herbert Waldmann

Erklärung/Declaration

Die vorliegende Arbeit wurde in der Zeit von 2009 bis 2012 am Max-Planck-Institut für molekulare Physiologie in Dortmund unter der Anleitung von Prof. Dr. Roger S. Goody, Dr. Yao-Wen Wu und Prof. Dr. Herbert Waldmann, Dr. Gemma Triola durchgeführt.
Hiermit versichere ich an Eides statt, dass ich die vorliegende Arbeit selbständig und nur mit den angegebenen Hilfsmitteln angefertigt habe.

The present work was accomplished from 2009 to 2012 at Max-Planck-Institute for molecular physiology in Dortmund under the guidance of Prof. Dr. Roger S. Goody, Dr. Yao-Wen Wu and Prof. Dr. Herbert Waldmann, Dr. Gemma Triola.
I hereby declare that I performed the work presented independently and did not use any other but the indicated aids.

Dortmund, October 2012 Long Yi

Contents

Abbreviations

Å	Angstrom (1 Å = 0.1 nm = 10^{-10} m)
AA	Amino acid
Boc	tert-Butyloxycarbonyl
BSA	Bovine serum albumin
CBD	Chitin-binding domain
CBR	C-terminus binding region
CHAPS	3-[(3-Cholamidopropyl)-dimethylammonio]-propansulfonat
CHM	Choroideremia
Cmc	Critical micelle concentration
2-Cl-Trt	2-Chlorotrityl chloride
CTAB	Cetyltrimethylammoniumbromide
Da	Dalton
Dansyl	5-Dimethylaminonaphtalin-1-sulfonyl
DTE	1,4-Dithioerythritol
DIPEA	N,N-diisopropylethylamine
DCC	Dicyclohexylcarbodiimide
DIC	N,N'-diisopropylcarbodiimide
EDTA	Ethylenediaminetetraacetic acid
EPL	Expressed protein ligation
EGFP	Enhanced green fluorescent protein
EYFP	Enhanced yellow fluorescent protein
ESI-MS	Electronspray ionization mass spectrometry
Fmoc	Fluorenylmethoxycarbonyl
FTase	Farnesyltransferase
FRET	Fluorescence resonance energy transfer
FITC	Fluorescein 5(6)-isothiocyanate
GAP	GTPase activating protein
GDF	GDI displacement factor
GDI	GDP dissociation inhibitor
GDP	Guaninediphosphate
G.HCl	Guanidinium hydrochloride
GEF	Guaninenucleotide exchange factor
GF	Gel filtration
GG	Geranylgeranyl
GGPP	Geranylgeranylpyrophosphate
GGTase	Geranylgeranyltransferase
GTP	Guaninetriphosphate
GTPase	GTP-binding protein
HEPES	4-(2-Hydroxyethyl)piperazine-1-ethanesulfonic acid
HPLC	High performance liquid chromatography
HRMS	High resolution ESI mas spectra
Hsp	Heat shock protein
IPTG	Isopropyl-β-D-thiogalactoside
KCL	Kinetically controlled ligation
LC-MS	Liquid chromatography-mass spectrometry
MPR	Mannose-6-phosphate receptor
Mant	N-methylanthraniloyl
MALDI-TOF-MS	Matrix assisted laser desorption/ionization-time of flight mass spectrometry
MCS	Multiple cloning site
MESNA	2-Mercaptoethanesulfonic acid
MIC	Maleimidocaproyl
MPAA	(4-Carboxymethyl)thiophenol
MWCO	Molecular weight cut off

NBD	7-Nitrobenz-2-oxa-1,3-diazol-4-yl
NBD-FPP	NBD-farnesyl pyrophosphate
NCL	Native chemical ligation
NHS	N-hydroxysuccinimide
NTA	Nitrilotriacetic acid
NMR	Nuclear magnetic resonance spectroscopy
NSF	*N*-ethyl-maleimide sensitive fusion protein
OD_{600}	Optical density at 600 nm
PEG	Polyethylenglycol
PI(4,5)P2	Phosphatidylinositol 4,5-bisphosphate
PI(3,4,5)P3	Phosphatidylinositol 3,4,5-trisphosphate
PM	Plasma membrane
PMSF	Phenylmethylsulfonyl fluoride
PKA	Protein kinase kines A α-subunit
Rab	Ras-like (protein) from Rat brain
Ras	Rat adeno sarcoma
RBP	Rab binding platform
REP	Rab escort protein
RP-HPLC	Reversed-phase high performance liquid chromatography
RRF	Rab recyling factor
RT	Room temperature
SDS	Sodium dodecyl sulfate
SNAP	Soluble NSF attachment protein
SNARE	Soluble NSF attachment protein receptor
SPPS	Solid phase peptide synthesis
StBu	*S-tert*-butyl
TBTA	Tris[(1-benzyl-1H-1,2,3-triazol-4-yl)methyl]amin
TEV	Tobacco Etch Virus
TFA	Trifluoroacetic acid
TLC	Thin layer chromatography
TTD	(4,7,10)-Trioxa-1,13-tridecanediamine
Yip	Ypt-interacting protein
Ypt	Yeast protein transport

One- and three-letter abbreviations for amino acids were used according to the recommendations of the International Union of Pure and Applied Chemistry (IUPAC) and the International Union of Biochemistry (IUB).

1. General Introduction

"*Most of the important things in the world have been accomplished by people who have kept on trying when there seemed to be no hope at all.*"

Dale Carnegie

1.1. Function of Rab GTPases

1.1.1. Rab proteins

Rab proteins are small Ras-related GTP-binding proteins (GTPases) that are believed to be key regulators of vesicular transport. With more than 60 members identified in mammalian cells and 11 members in yeast (termed Ypt proteins and Sec4p) they form the largest group of the Ras superfamily (Pereira-Leal et al., 2001). Apparently, the increased complexity of vesicular transport routes inside mammalian cell types compared to lower eukaryotes resulted in a significant expansion of the Rab family (Bock et al., 2001). Indeed, certain Rab proteins could be assigned to distinct compartments and transport steps present in all eukaryotes, whereas other Rab isoforms were found to participate in specialized fusion processes in differentiated cells. The number of rab proteins in the eukaryotic cell is dwarfed by the number of rab interacting proteins, reflecting the complexity of Rab controlled networks (for review see Segev, 2001; Ohbayashi et al., 2012). For example, more than 20 proteins were shown to be bound to Rab5 in its GTP bound form (Christoforidis et al., 1999).

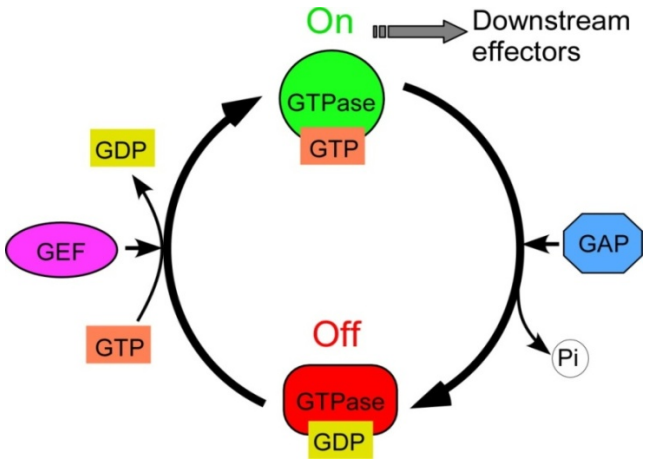

Figure 1.1. The GTPase cycle. GAP: GTPase-activating protein; GEF: guanine nucleotide exchange factor.

As for other GTPases, central to Rab functioning is their ability to cycle between active GTP- and inactive GDP-bound conformations, thereby acting as molecular 'on/off' switches. The GTPase cycle (Figure 1.1) is strictly regulated by guanine nucleotide exchange factors (GEFs) that mediates GDP/GTP exchange and by GTPase-activating proteins (GAPs) that accelerate the otherwise intrinsically slow GTP hydrolysis of GTPases (Bos et al., 2007). In the active conformation Rab proteins recruit Rab effectors, a heterogeneous group of proteins, which exert various functions during vesicular transport. Rabs are converted into the inactive conformation by GTP hydrolysis, which leads to effector dissociation and Rab extraction

from the membrane. The Rab protein is then recycled back to the donor compartment and reactivated by exchange of GDP for GTP. The combined cycles, i.e. GTP/GDP cycling and membrane association/cytosolic localization, are known as the Rab cycle (Figure 1.2).

Several studies suggest a role of rab proteins and their effectors in vesicle formation (Smythe, 2002). For example, the mannose-6-phosphate receptor (MPR), which sequesters cargo proteins into budding clathrin-coated vesicles, was shown to bind indirectly to Rab9-GTP via its effector TIP47 (tail interacting protein of 47 kDa). It seems reasonable that the endosome specific Rab protein triggers the recruitment of TIP47 to MPRs in a organelle specific manner resulting in specific and efficient MPR recycling (Carroll et al., 2001). Besides assisting cargo incorporation into budding vesicles (McLauchlan et al., 1998), Rabs might additionally define the destination of the budding vesicle by recruiting proteins necessary for subsequent docking and fusion steps (Allan et al., 2000).

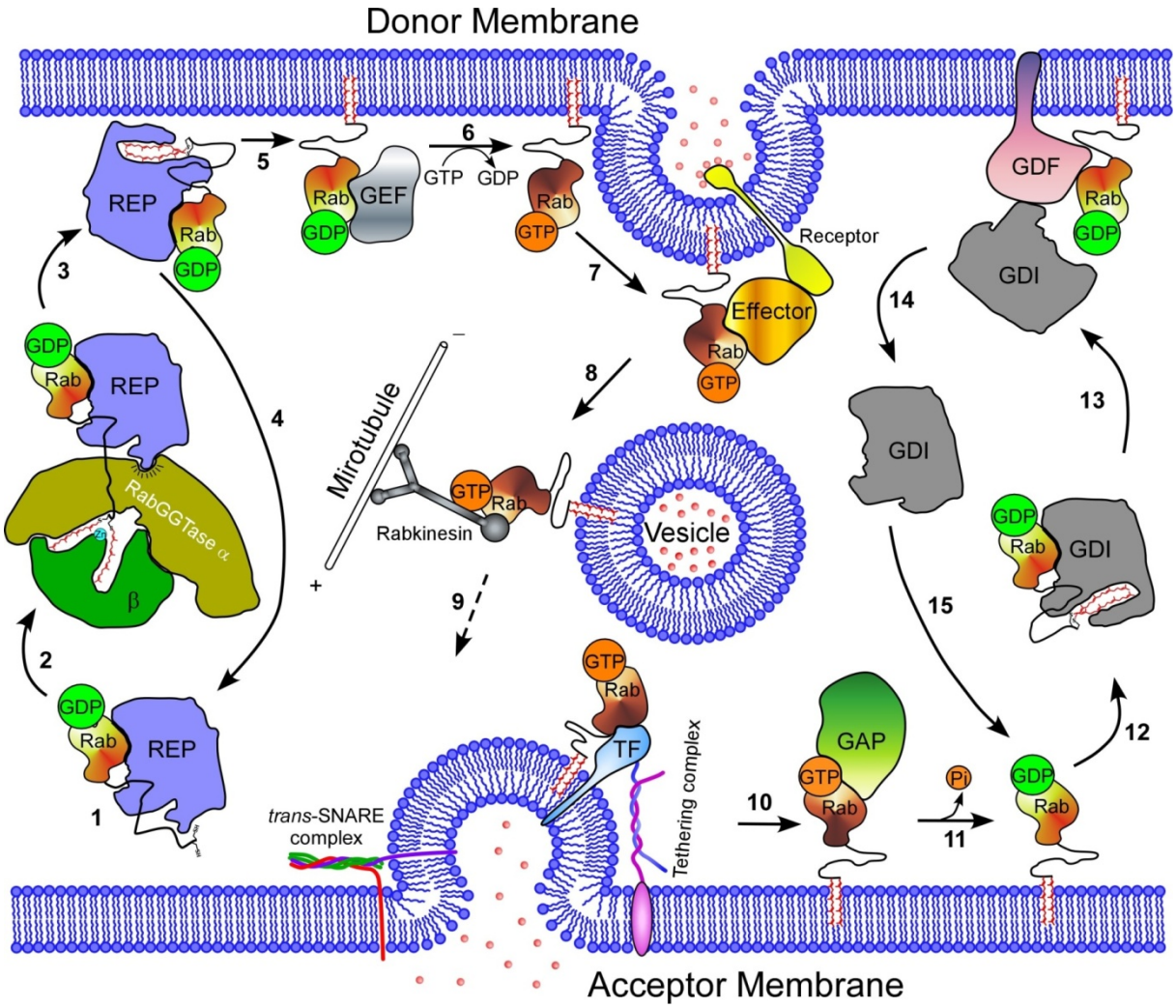

Figure 1.2. Schematic showing the general Rab recycling. (1) Newly synthesized Rab proteins bind to REP. (2) REP presents Rab proteins to heterodimeric RabGGTase for modification of (usually) two geranylgeranyl moieties. (3) REP delivers the prenylated Rab proteins to their target membranes. (4) Once REP is released, it recycles into cytosol to

support additional rounds of Rab prenylation. (5) Prenylated Rab proteins associate with the membrane. (6) Subsequently GEFs facilitate exchange of GTP for GDP. (7) GTP bound Rab proteins can bind to effectors that are involved in vesicle budding and cargo selection. (8) GTP-Rab proteins directly or via effectors recruit motor proteins to drive the movement of vesicles along microtubules and actin filaments. (9) The vesicles are transported to the target compartment. GTP-Rab proteins mediate recruitment of effectors, tethering factors, SNAREs, facilitating tethering, docking and fusion of vesicles at the target membrane. (10, 11) Hydrolysis of GTP is accelerated by GAPs, resulting dissociation of related effectors. (12) Extraction of GDP-bound Rab proteins from membranes is medicated by GDI. This extraction process may involve Rab recycling factors (13) GDI makes prenylated Rab proteins soluble in cytosol and delivers them to the donor membrane. GDF (GDI-displacement factor) facilitates dislodgement of prenylated Rab proteins from GDI, enabling them to re-associate with the donor membrane. (14, 15) GDI is released and is reused in additional rounds of Rab extraction. (The picture is from Dr. Yao-Wen Wu's PhD thesis)

Following vesicle formation, at least some Rabs link transport vesicles to the cytoskeleton via kinesin/dynein-like motor-proteins, which confer actively directed vesicle movement along these structures (Hammer et al., 2002; Murray et al., 2003). Rab6 has been shown to interact directly with a kinesin-like effector protein, termed Rabkinesin-6, which probably acts as a microtubule plus-end directed motor (Figure 1.2, step 8) and has been implicated in cytokinesis during mitosis (Echard et al., 1998; Hill et al., 2000). Another well studied example involves the interaction of Rab27a with Myosin Va via melanophilin, the potential Rab27a effector (Fukuda et al., 2002). Myosin Va is believed to tether melanosomes to the actin cytoskeleton, which actively retains these organelles near the cell peripherie of melanocytes, where they are eventually transferred to keratinocytes for proper skin and hair pigmentation (Hume et al., 2001; Bahadoran et al., 2001). This model is supported by several mutations in Rab27a (Menasche et al., 2000) and Myosin Va (Pastural et al., 1997) that lead to Griscelli Syndrome, a rare inherited disorder of pigmentation arising from the arrest and the accumulation of melanosomes in the perinuclear region of melanocytes, that is accompanied by severe immunological or neurological defects (Stein et al., 2003).

When the transport vesicle approaches its target membrane (Figure 1.2, step 9), Rab proteins initiate the assembly of tethering complexes by interacting with soluble effector proteins (Cao et al., 1998; Ungermann et al., 1998). Tethering effectors fall into two main classes: a group of proteins forming extended homodimeric coil-coil structures (e.g. EEA1, Uso1p, p115) and oligomeric complexes (e.g. HOPS, Exocyst, TRAPP and COGcomplexes) (Deneka et al., 2003; Whyte et al., 2002). Although the details of their functioning remains elusive, most of them could be assigned to a distinct transport step and were shown to bind to Rabs and membranes (Guo et al., 1999; Sacher et al., 1998). Apparently, tethering complexes and Rabs

precede *trans*-SNARE pairing representing the first specificity determinant during vesicle fusion. Moreover, Rabs and the tethering complexes might either directly or indirectly trigger SNARE pairing and subsequent fusion, as can be inferred from their numerous interactions with components of the SNARE fusion machinery (e.g. with NSF (McBride et al., 1999), Sec1-like proteins (Seals et al., 2000), or SNAREs directly (Sato et al., 2000; Zerial et al., 2001)).

Rab GTP hydrolysis is not obligatory for fusion (Stenmark et al., 1994; Rybin et al., 1996), rather the rate of nucleotide hydrolysis seems to define the time frame for rab effector recruitment and therefore influences the progression of tethering, docking and fusion steps (Richardson et al., 1998). Hence, the steady-state level of activated Rab-GTP regulates the extent of fusion reactions and is, not surprisingly, highly regulated by additional factors. For example some of the above mentioned tethering complexes were shown to preserve the GTP bound state, thereby locking Rabs in the activated state by either promoting GDP to GTP exchange (Horiuchi et al., 1997) or inhibiting GTPase activating protein (GAP) induced GTPase activity (Kishida et al., 1993). Following fusion, Rab proteins are inactivated by GTP hydrolysis stimulated by GAPs (Figure 1.2, step 10), which converts them back to their GDP bound form (Figure 1.2, step 11) (Bernards, 2003).

GDP-bound Rab is targeted by Rab GDPdissociation inhibitor (RabGDI), which upon binding inhibits Rab reactivation (Sasaki et al., 1990) and extracts them from the membrane into the cytosol (Araki et al., 1990) (Figure 1.2, step 12). It is likely that this step is mediated by additional factors, termed Rab recycling factors (RRFs) (Luan et al., 1999). One potential RRF candidate essential for Rab3A membrane extraction at the synapse was identified as a heat shock protein (Hsp) complex, consisting of Hsp90, Hsc70 and cysteine string protein (CSP) (Sakisaka et al., 2002). RabGDI delivers Rab proteins back to the donor membrane (Figure 1.2, step 13), consequently ensuring efficient Rab recycling (Soldati et al., 1994; Ullrich et al., 1994). The delivery process probably involves proteins termed GDI displacement factors (GDFs), that serve as the membrane receptor for Rabs and are believed to be key for the Rab compartment specific localization (DiracSvejstrup et al., 1997). Although the above mentioned Hsp complex might potentially also serve as a GDF (Sakisaka et al., 2002), the precise identity of GDFs has remained elusive, hindering a deeper understanding of the process. Recently, human Yip3p (PRA-1) was shown to catalytically displace RabGDI and to specifically recruit endosomal Rabs to reconstituted liposomes (Sivars et al., 2003). Yeast Yip (Ypt-interacting protein) family members (analogs exist in mammals, termed prenylated Rab acceptor (PRA)) were initially identified as proteins that

can interact with Rabs in either their GDP or GTP bound state (Martincic et al., 1997) and with each other (Calero et al., 2002; Matern et al., 2000), and some members were found to be essential for yeast viability and vesicular transport (Yang et al., 1998). Although the assigned GDF activity offers an interesting model for Yip mediated Rab recruitment, additional interactions with other components of the fusion machinery (e.g. with SNAREs (Martincic et al., 1997) and vesicle coat proteins (Tang et al., 2001)) suggest a broader role for Yips in vesicular transport, which needs to be addressed (Barrowman et al., 2003). Upon membrane binding, Rabs are converted to the active form by GDP to GTP exchange mediated by GEF (Figure 1.2, step 6) and the cycle starts again (Ullrich et al., 1994). Interestingly, Rab activation seems often to be spatially and temporally restricted to the site of function, which is supported by the finding that numerous GEFs are in fact members of large protein complexes, which also act as rab effectors (Jones et al., 2000; Wurmser et al., 2000).

1.1.2. The structural basis of Rab function

Rab GTPases contain conserved sequence elements that mediate GDP/GTP binding, effector recognition and subcellular localization. Although distantly related to Ras and other small GTPases (< 30 % amino acid overall identity), they share short highly conserved motifs, termed PM and G motifs, which participate in phosphate/magnesium and guanine base binding, respectively (see Figure 1.3 B,C) (Valencia et al., 1991). The Rab structural fold is similar to all small GTPases of the Ras superfamily (also referred to as the GTPase-fold) consisting of a six stranded beta sheet surrounded by five alpha helices (Dumas et al., 1999; Sprang, 1997).

Conformational changes accompanying GTP to GDP hydrolysis and γ-phosphate release, as originally observed in Ras (Schlichting et al., 1990; Milburn et al., 1990), were also confirmed for Rab proteins (Stroupe et al., 2000; Constantinescu et al., 2002; Brennwald et al., 2004), although significant variations exist, which might explain differences in the rates of GTP hydrolysis and GDP exchange. These regions of major conformational changes, were termed switch I and switch II and form the β,γ-phosphate-magnesium ion binding pocket together with the so called P-loop (Figure 1.3). As mentioned above, key to Rab functioning is their participation in numerous interactions with upstream regulators and downstream effector molecules. The interacting proteins were proposed to recognize the correct nucleotide bound state by binding to switch I (also known as effector domain) and switch II regions based on genetic and functional studies employing mutant chimeric Rab proteins (Brennwald et al., 1993; Dunn et al., 1993). Further extensive sequence analysis studies revealed the

presence of five Rab family motifs (RabF1-5) and four Rab subfamily motifs (RabSF1-4), which localize mainly around switch I and II and are conserved among different species (Figure 1-3) (Pereira-Leal et al., 2000). RabF motifs can be used for unambiguous identification of Rab proteins, whereas RabSF motifs determine the relatedness to one of the four Rab subfamilies.

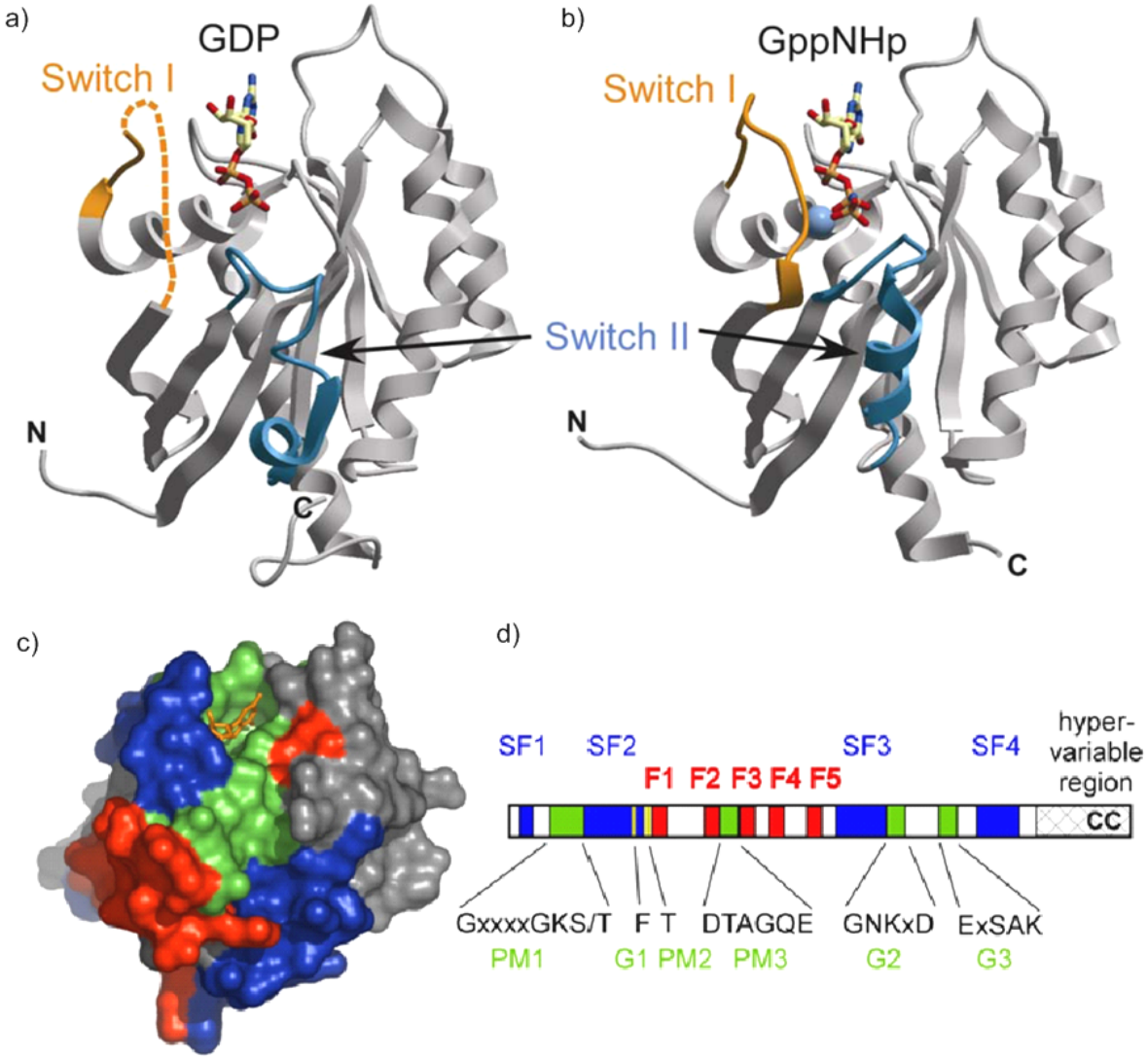

Figure 1.3. a) and b) Structures of Rab4a in GDP (PDB code: 2BMD) and GppNHp (non-hydrolysable analogue of GTP) (PDB code: 2BME) bound form, respectively. Rab4a is displayed in ribbon representation, nucleotides in stick representation and Mg^{2+} in cyan sphere. Switch I is orange and switch II is light blue. The dashed ribbon in Rab4a-GDP represents the invisible part in the crystal structure. c) Surface representation of location of PM and G motifs (green), Rab family motifs (F, red) and Rab subfamily motifs (SF, blue). d) Organization of the identified motifs along the primary sequence. CC represents the prenylation motif.

Concerning the binding of interacting proteins, RabF motifs were proposed to be mainly recognized by general Rab regulators (such as GDI and REP), whereas specific interactions

with a certain subset of Rabs additionally require RabSF regions (e.g. most Rab-effector interactions and to some extent GEFs and GAPs). Confirmation of this model comes from several mutagenesis studies (Pereira-Leal et al., 2003) and the structure of Rab complexed to its effector. The structure of Rab7-RILP complex showed that RabSF1 and RabSF4 regions of Rab7 are important for interaction with RILP (Wu et al., 2005). However, in some cases different subsets of residues within the switch regions determine specificity. Rabex-5 VPS9 domain, a RabGEF, selects for the Rab5 subfamily primarily through a strict requirement for a small nonacidic residue preceding the invariant phenylanaline in the switch I **T**(I/V)GA(A/S)**F** motif, while the selectivity for Rab21 also involves Gln53 in the TLQASF motif (Delprato et al., 2004; 2007). Sec2p, the specific GEF for Sec4p GTPase, discriminates its substrates via the switch regions (Dong et al., 2007). In contrast, MSS4, which is a less specific RabGEF and activates a range of Rabs, interacts with switch I, interswitch regions, and the N-terminus, but not with switch II (Itzen et al., 2006). Different elements contribute to the interacting specificity between Rab and its effectors. Furthermore, other nonconserved residues in Rab that alter the conformation of those conserved residues in direct effector contacts may also contribute to the binding specificity (Merithew et al., 2001).

Another important structural feature of Rab proteins was identified by Chavrier et al (Chavrier et al., 1991; Stenmark et al., 1994) and termed hypervariable region that comprises about 35 amino acid residues in the C-terminal region (Figure 1.3D). This region is presumed to serve as a targeting signal for the subcellular localization of Rab proteins and is at least in some cases subject to additional regulation. For example, phosphorylation within the hypervariable region of Rab4 during mitosis was shown to prevent membrane recruitment leading to accumulation of Rab4 in the cytosol (Vandersluijs et al., 1992; Ayad et al., 1997). At or near the C-terminus, the conserved cysteine(s) in the Rab prenylation motif (CC, CXC, CCX, CCXX, CCXXX and CAAX) are post-translationally modified by geranylgeranyl group(s) (Kinsella et al., 1991). This hydrophobic modification mediates the reversible attachement of Rab proteins to membranes and is essential for proper Rab functioning (Newman et al., 1992).

1.1.3. Rab geranylgeranylation

Geranylgeranylation of Rab proteins is a posttranslational process catalyzed by geranylgeranyltransferase type II (GGTase-II or RabGGTase), which transfers geranylgeranyl moieties from geranylgeranylpyrophosphate (GGPP) to C-terminal cysteine residues linking them via stable thioether bonds (Figure 1.4) (Moores et al., 1991). GGTase-II belongs to the

family of protein prenyltransferases together with Farnesyltransferase (FTase) and GGTase-I, which act on Ras and Rac/Rho GTPases, respectively (Casey et al., 1996). FTase and GGTase-I are also known as CaaX prenyltransferases. The term refers to the short C-terminal substrate sequences recognized by both enzymes, where 'C' stands for the cysteine that is to be modified, 'a' designates an aliphatic residue and the identity of 'X' determines whether 'C' will be farnesylated by FTase (X = Ala, Gln, Met, Ser) or geranylgeranylated by GGTase-I (X = Leu) (Moores et al., 1991; Caplin et al., 1994; Roskoski, et al., 1998). In contrast, Rab prenylation motifs are more heterogenic including terminal CXC, CC, CCX, CCXX and CCXXX sequences (Khosravifar et al., 1991; Kinsella et al., 1992), where both cysteines are modified by GGTaseII (Farnsworth et al., 1994). Rabs terminating with CXC sequences are additionally methyl esterified by a S-adenosylmethionine (SAM) dependant enzyme activity following the prenylation reaction (Smeland et al., 1994).

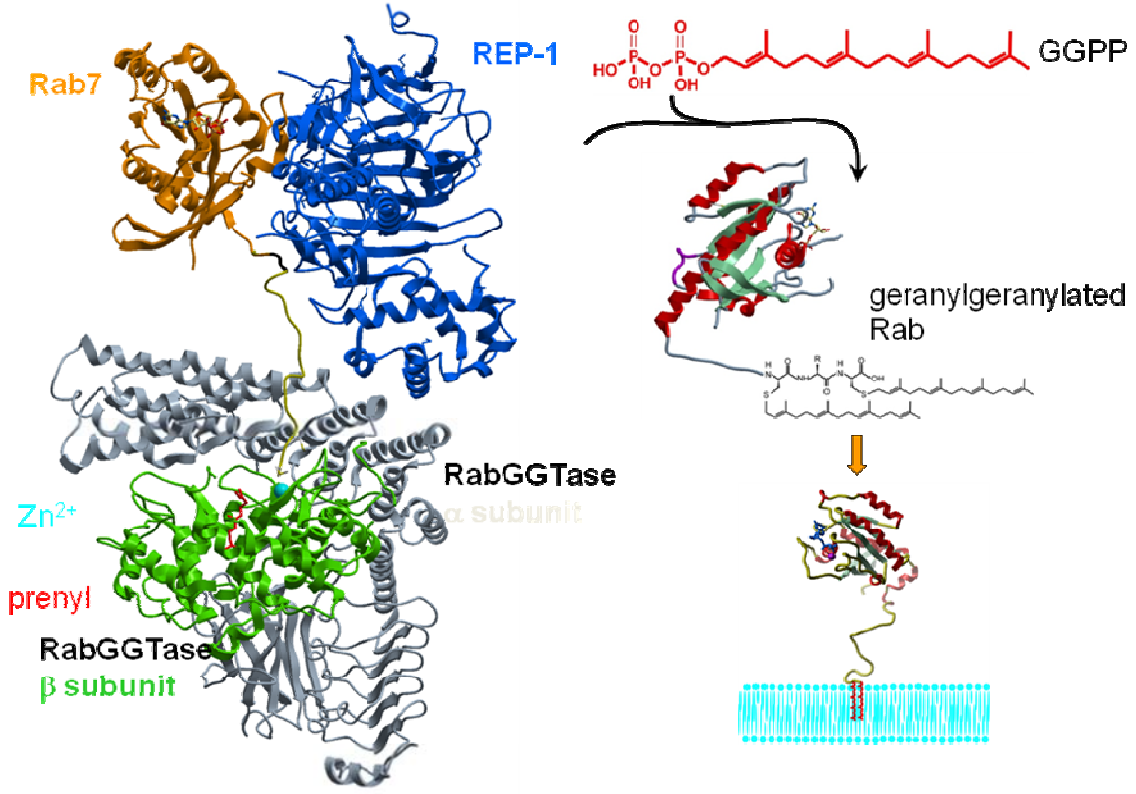

Figure 1.4. GGTase-II catalyzed geranylgeranylation of Rab proteins. Rab-GDP, REP-1 and GGTase-II form a ternary complex (Wu et al., 2009). Prenyl groups are transferred in two consecutive reactions from GGPP to Rab. Structure of the complex GGTase-II (α and β subunits are colored gray and green, respectively), REP-1 (blue) and Rab7 (organe) based on structures of prenylated Rab7:REP complex (PDB code, 1VG0) and REP-1:RabGGTase (PDB code, 1LTX). The farnesyl group is show in stick representation in red, and Zn^{2+} as a turquoise ball in cyan.

GGTase-II consists of two subunits (α and β) forming a heterodimer of ca. 100 kDa that requires Zn^{2+} and Mg^{2+} for activity (Figure 1.4) (Seabra et al., 1992). In contrast to the other

prenyltransferases, GGTase-II additionally requires a protein cofactor, originally termed component A, which was later identified as the product of the choroideremia (CHM) gene and eventually renamed as rab escort protein (REP) (Andres et al., 1993). REP associates with the unprenylated Rab protein preferentially in its GDP bound form (Seabra, 1996) and facilitates its recognition by the catalytic GGTase α/β-heterodimer (Alexandrov et al., 1999). Upon ternary complex formation, GGTase-II transfers both isoprenoids in two independent, consecutive reactions, with the monoprenylated intermediate being strongly bound to the enzyme (Thoma et al., 2001).

Elucidation of the RabGGTase reaction mechanism was carried out by the combination of classical biochemical and spectroscopic methods that utilized isoprenoid and protein-based fluorescent probes (Anant et al., 1998; Dursina et al., 2006; Alexandrov et al., 2002; Durek et al., 2004; Wu et al., 2006). Detailed biophysical information generated by these studies promoted structure solution of the complexes between RabGGTase and REP-1, as well as between Rab7 and REP-1 (Pylypenko et al., 2003; Rak et al., 2004). Although the structure of the catalytic ternary complex has not been solved, it was computationally modeled and biochemically validated by using structural information from the binary complexes (Figure 1.4) (Wu et al., 2009). It transpires from the model that the main specificity and affinity determinant is conferred by the interaction of the Switch I and II regions of the Rab GTPase domain with the Rab binding platform (RBP). An additional determinant of Rab:REP complex formation and prenylation is the interaction of a hydrophobic patch on the surface of REP, which is referred to as the C-terminal binding region (CBR), with the CBR binding motif (CIM) within the Rab C terminus (Rak et al., 2004; Wu et al., 2009). In most Rab sequences, the CIM consists of two large hydrophobic residues flanking a more polar residue.

Computational modeling of the catalytic ternary complex suggests that its assembly proceeds sequentially, starting from the recognition of the Rab GTPase domain by the RBP of REP, thus leading to a low- to intermediate-affinity complex (Nguyen et al., 2010) (Figure 1.5). The affinity of the complex is further increased by an order of magnitude through association of CBR with CIM; this targets the Rab C terminus towards the REP-associated RabGGTase. The cysteines that contain part of the C terminus bind to the active site of RabGGTase through a series of weak interactions. One consequence of this arrangement is that the protein substrate specificity does not need to be encoded in the prenylatable C terminus, that is, both the enzyme and the Rab GTPases “outsource” their specificity for each other to the accessory protein REP. This sequential complex assembly, engaging progressively weaker and smaller binding interfaces, enables any cysteine residue near the C

terminus to be prenylated by RabGGTase. This arrangement also enables multiple prenylation events on a single substrate of arbitrary sequence, a feature that is uncommon in protein-modifying enzymes.

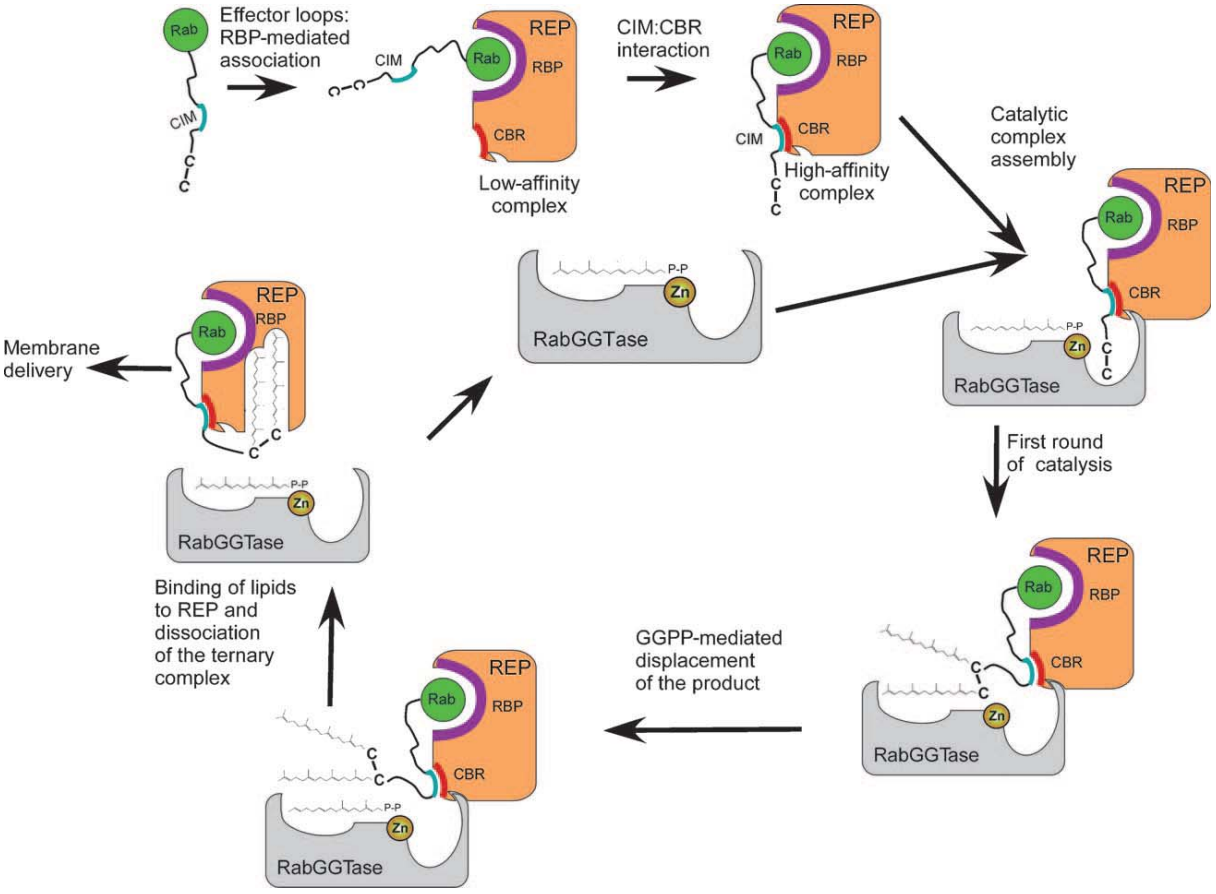

Figure 1.5. Mechanistic model of RabGGTase-mediated protein prenylation. REP: Rab escort protein, CIM: C terminus interacting motif, RBP: Rab binding platform, CBR: C terminus binding region. (The picture is from ChemBioChem, 2010, *11*, 1194)

Following double prenylation, binding of another GGPP molecule triggers release of the prenylated Rab:REP complex (Thoma et al., 2001), and Rab is delivered to the membrane with assistance of REP (Figure 1-5) (Alexandrov et al., 1994). Two ubiquitiously expressed isoforms of REP have been identified in mammalian cells (REP-1 and REP-2) (Cremers et al., 1994), whereas only a single protein named Mrs6p mediates Rab prenylation in yeast (Fujimura et al., 1994). Loss of REP-1 function has been linked to CHM, an X-linked inherited disease characterized by progressive retinal degeneration leading to complete blindness in adults (Seabra et al., 1993). The molecular mechanism underlying CHM was proposed to involve inefficient prenylation of certain Rabs (such as Rab27) due to malfunctioning of REP-1, which cannot be compensated by the REP-2 isoform. The

consequence of this accumulation of unfinished Rab27 proteins is a massive apoptosis of retinal cells, which leads to a progressive degeneration of the retina.

Interestingly, REP and RabGDI (see above) share approximately 30 % sequence identity and are structurally and functionally related (Seabra et al., 1992). Both proteins form the RabGDI/CHM family (Wu et al., 1996) can bind prenylated Rabs preferentially in their GDP bound state, inhibit GDP release from the GTPase domain and can deliver the Rab proteins to their proper membrane site. However, RabGDI cannot replace REP in the prenylation reaction due to its low affinity for unprenylated Rabs (Araki et al., 1991, Wu et al., 2007), whereas REP cannot functionally replace RabGDI´s ability to extract Rab proteins from membranes. Consequently, both proteins are not functionally interchangeable as was demonstrated by complementation experiments performed in yeast (Garrett et al., 1994) and by semisynthesis of Rab protein probes (Wu et al., 2007).

In summary, geranylgeranylation is believed to be crucial for the proper functioning of all Rab proteins. On a molecular level the role of the lipids seems to be at least two-fold: Firstly, the geranylgeranyl groups are integral components of Rab interactions with other regulatory proteins. Currently several factors are known, that require prenylation for productive binding to Rab proteins: RabGDI (Araki et al., 1991), several members of the Yip family (Calero et al., 2002; Figueroa et al., 2001), Rab3GAP (Fukui et al., 1997) and Rab3-GEF (Wada et al., 1997). Secondly, the hydrophobic isoprenoids mediate the essential membrane attachment of Rab proteins, probably by inserting into the lipid bilayer. Unprenylated Rabs cannot associate with membranes and are intracellularly restricted to the cytosol where they cannot fulfill their biological role. Recent studies suggest that double prenylation is required for correct localization of Rab proteins to their characteristic subcellular target membrane, whereas single prenylated Rabs are mistargeted and appeared to be non-functional (Gomes et al., 2003; Calero et al., 2003).

1.1.4. Rab targeting

More than 60 Rab proteins have been described in humans, some of which are ubiquitous while others are subject to tissue specific and developmentally regulated expression (Pereira-Leal et al., 2001; Seabra et al., 2002). Each Rab shows a characteristic subcellular distribution. In fact, Rabs may serve as important determinants of organelle identity and membrane organization (Munro, 2002; Seabra et al., 2004). Through the recruitment of specific effector molecules, Rabs can give rise to membrane subdomains within a compartment. Rab5a and Rab4, although both localized to early endosomes, are largely

present on distinct domains (De Renzis et al., 2002; Sonnichsen et al., 2000). Similarly, Rab7 and Rab9 occupy separate domains within late endosomal membranes (Barbero et al., 2002). Surprisingly, the molecular mechanisms regulating the specific association of Rabs with cellular membranes remain obscure. Though geranylgeranylation of Rab proteins is essential for their correct intracellular localization (Calero et al., 2003; Gomes et al., 2003), it is a common feature of all Rabs and thus cannot in itself account for their organelle-specific targeting. The C-terminal hypervariable region of about 35 amino acids shows the highest level of sequence divergence between Rab family members, and was postulated to act as a signal for subcellular targeting (Chavrier et al., 1991). Over a decade ago, Zerial and co-workers showed that replacing the C-terminal 35 residues of Rab5 with the equivalent C-terminal region of Rab7 resulted in re-localization of the hybrid Rab to Rab7-positive late endosomal structures. Targeting of Rab proteins via the hypervariable region is a widely accepted model, but the underlying molecular mechanisms have not been elucidated further. Despite the attractiveness of this proposal, recent studies indicated that this is not the case for several Rabs. Replacing the hypervariable domain of Rab5a with that of Rab1a, Rab2a, Rab7 and Rab27a had no effect on its localization to early endosomes or its function in endosomal fusion activity (Ali et al., 2004). However, replacing the hypervariable domain of Rab27a with that of Rab1 or Rab5a failed to re-target the hybrid proteins away from melanosomes in melanocytes and the hybrid proteins reversed the Rab27a null phenotype (melanosomes clustering) in *ashen* cells indicating preservation of function despite exchanging the hypervariable domain (Ali et al., 2004).

The first step of the molecular mechanisms for Rab targeting should be the dissociation of the tight binding GDI-Rab complex. Based on this point, several mechanisms for Rab membrane targeting are proposed.

Delivery of Rab proteins to membranes by Rab GDF: The binding affinity of prenylated Rab proteins to RabGDI is relatively high with the dissociation constant (K_d) of 4.5 nM for GDP-bound Rab7 (Wu et al., 2010). This high affinity led to the proposal that the dissociation of Rab proteins from GDI and their subsequent association to membranes requires a displacement factor, named GDF (Figure 1.6) (Dirac-Svejstrup et al., 1997). Attempts to purify this GDF activity from membranes proved extremely difficult, but Pfeffer et al. used a candidate-screening approach to show that human Yip3 exhibits GDF activity towards the prenylated endosomal Rab protein Rab9 and to a lesser extent towards Rab5 (Sivars et al., 2003). Prenyl Rab9–GDI complexes were used to test whether purified human Yip3 could dissociate Rab–GDI complexes as monitored by an increase in the rate of ^{35}S-GTPγS binding.

Once released from GDI, a Rab will exchange bound GDP for GTPγS and then be incapable of rebinding GDI. Yip3 catalytically stimulated GTP[S] nucleotide binding to Rab9, thus implying the dissociation of the Rab protein from GDI, as this is a prerequisite for GTP[S] binding. This activity was reconstituted by using liposomes and is distinct from GEF activity because Yip3 failed to stimulate the intrinsic nucleotide exchange of the endosomal Rab proteins. Yip3 was specific to endosomal Rabs, Rab9 and Rab5, and failed to act on Rab1 or Rab2. Yip3 remains the only GDF identified thus far and other members of the Yip family (Ypt interacting proteins) have been assigned other functions. For example, despite the ability of Yip1 and Yif1 to interact with Rab proteins, the disruption of either of the two proteins did not result in Ypt1 mislocalization or dysfunction (Barrowman et al., 2003; Heidtman et al., 2003). More examples of the involvement of Yip protein family members as GDFs are needed before a generalization of their function as GDFs can be confirmed.

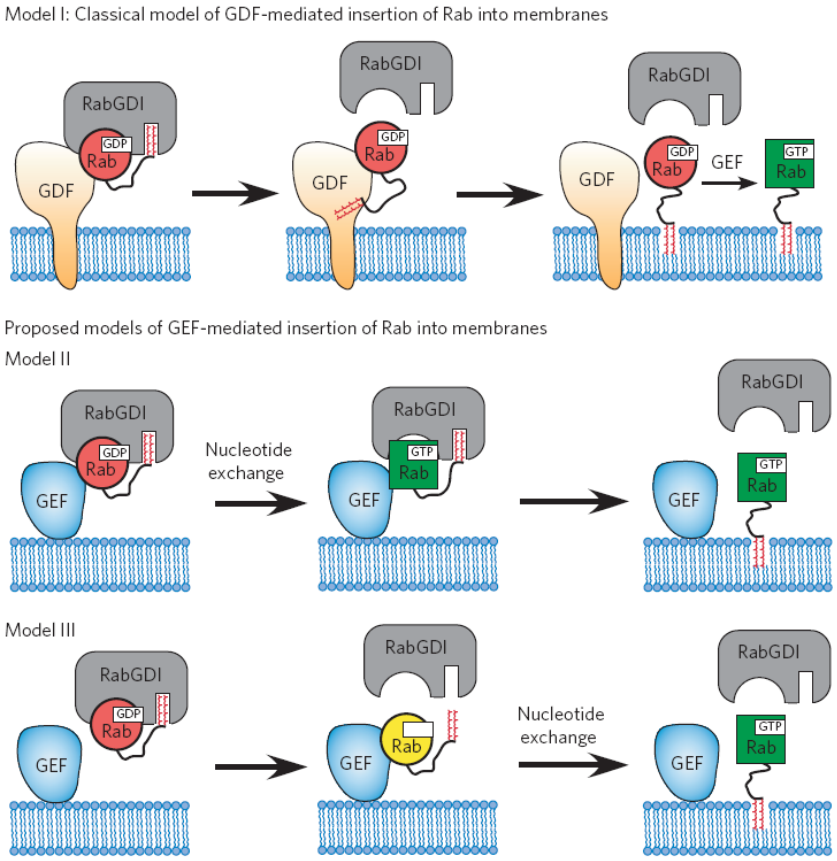

Figure 1.6. Models of modulation of Rab targeting of Rabs to membranes by the state of bound nucleotide. In model I, GDF-facilitated GDI dissociation is followed by membrane attachment and GEF-mediated nucleotide exchange. In a variant of this model that has not yet been discussed specifically here or elsewhere, the complex between Rab and GDF would be directly available for GEF action and exchange would occur before membrane attachment. In the other models for GEF-mediated insertion, either there is direct interaction of GEF with the Rab–GDI complex, leading to nucleotide exchange and Rab dissociation (model II), or

spontaneous dissociation is rendered effectively irreversible by GEF activity and membrane attachment. (The picture is from Nat. Chem. Biol. 2010, 6, 534)

Delivery of Rab proteins to membranes by nucleotide exchange factors (GEF): It is an accepted notion that once a Rab protein has been deposited on to the target cellular membrane, it is activated by its nucleotide exchange factor (GEF). However, only a few Rab GEFs have been identified thus far. Some GEFs have been shown to consist of multisubunit protein complexes. For example, the Rabex5–rabaptin complex is GEF for Rab5 and the TRAPP complex for Ypt1 (Rab1 in *Saccharomyces cerevisiae*). An interesting observation is the finding that the activation of one Rab protein is a prerequisite for the targeting and recruitment of another. For example, activation of Ypt31/Ypt32 results in the recruitment of Sec2, a GEF for Sec4, which is the Rab downstream of Ypt31/Ypt32 in yeast secretory pathway (Ortiz et al., 2002). This provided the basis for the cascade model, where the activation of one Rab would trigger the recruitment and activation of the following Rab, a process mediated by a common protein complex being an effector for one Rab and a GEF for the other. Like Rab proteins, GEFs generally have exquisite localization within the cell and therefore it has been postulated that GEFs might be the receptors or the targeting determinants of their client Rab proteins (Figure 1.6).

Delivery of Rab proteins to membranes by GEFs is further proved by recent research of the DrrA protein in Goody's group. The *Legionella pneumophila* protein DrrA displaces GDI from Rab1:GDI complexes, incorporating Rab1 into Legionella-containing vacuoles and activating Rab1 by exchanging GDP for GTP (Ingmundson et al., 2007; Machner et al., 2007). DrrA efficiently catalyzes nucleotide exchange and mimics the general nucleotide exchange mechanism of mammalian GEFs for Ras-like GTPases. The GEF activity of DrrA is sufficient to displace prenylated Rab1 from the Rab1:GDI complex (Stefan et al., 2009; Wu et al., 2010). Thus, GEFs are necessary and sufficient for membrane targeting of GTPases and that the previously proposed GDFs are not thermodynamically required for this process (Wu et al., 2010).

Retrieval of Rab proteins from membranes mediated by Rab recycling factor: Once the Rab protein completes its designated function on the membrane, it becomes inactivated by hydrolyzing the bound GTP to GDP. This is usually accelerated and regulated by GAP. As has already been mentioned, inactive (GDP-bound) Rab proteins are removed from the membranes by GDI. Similar to the delivery process, it is thought that protein factors on the membrane are needed for the efficient and regulated extraction process. A fraction of the synaptic membrane-associated GDI is in complex with a chaperone complex containing

Hsp90, Hsc70 and cysteine string protein (Sakisaka et al., 2002). The ability of GDI to recycle Rab3A from membranes was enhanced by Hsp90 and inhibited by geldanamycin, an Hsp90 inhibitor. Similarly, neurotransmitter release was affected in a similar manner. These results led to the conclusion that Hsp90 chaperone complex is a Rab recycling factor. It will be interesting to see if Hsp90 plays a similar role for other Rabs and cell systems other than neuronal cells. Curiously, Hsp90 was co-immunoprecipitated with REP from brain cytosol and enhanced the REP-mediated Rab prenylation *in vitro*. However, the physiological significance of this interaction is still unclear (Ali et al., 2005).

Targeting plasma membrane with a polybasic-prenyl motif: Rab35 protein has to be localized to the plasma membrane (PM) in order to carry out its function. The C-terminal sequence (KLTKNSKRKKRCC) of Rab 35 contains a cluster of positively charged amino acids. To test whether this polybasic cluster binds negatively charged phosphatidylinositol 4,5-bisphosphate [PI(4,5)P2] lipids, Meyer et al. developed a chemical phosphatase activation method to deplete PM PI(4,5)P2 (Heo et al., 2006). Unexpectedly, proteins with polybasic clusters dissociated from the PM only when both PI(4,5)P2 and phosphatidylinositol 3,4,5-trisphosphate [PI(3,4,5)P3] were depleted, arguing that both lipid second messengers jointly regulate PM targeting. The polybasic-prenyl PM-targeting motif includes proteins such as K-Ras for which a 20–amino acid tail sequence (Prior et al., 2011) is sufficient for farnesylation and PM targeting, as well as Rab35 for which an intact GTPase domain is required for geranylgeranylation and a polybasic sequence for PM targeting. They further compared the roles of farnesylation and geranylgeranylation by creating a Rab35 mutant with a consensus CAAX farnesylation sequence in place of the geranylgeranylation sequence (Heo et al., 2006). This mutant showed PM localization indistinguishable from that of the geranylgeranylated Rab35. They reported that the polybasic-geranylgeranyl motifs of Rab35 can be equally effective in PM targeting as the polybasic-farnesyl motif of K-Ras, which supports the notion that both types of prenylation motifs can be grouped into a single polybasic-prenyl PM-targeting motif.

Post-translational modifications of Rab proteins contributing to membrane targeting: In order to allow the necessary recruitment of the Rab to its specific target membrane, it is necessary to efficiently replace GDI from the Rab:GDP:GDI complex by GDF or GEF (such as DrrA). It is reported that posttranslational modifications of Rabs can also modulate the affinity for GDI and thus cause effective displacement of GDI from Rab:GDI complexes (Oesterlin et al., 2012). These activities have been found associated with the phosphocholination and adenylylation activities of the enzymes AnkX and DrrA/SidM,

respectively, from the pathogenic bacterium Legionella pneumophila (Mukherjee et al., 2011; Müller et al., 2010). Both modifications occur after spontaneous dissociation of Rab:GDI complexes within their natural equilibrium. Therefore, the effective GDI displacement that is observed is caused by inhibition of reformation of Rab:GDI complexes. Interestingly, in contrast to adenylylation by DrrA, AnkX can covalently modify inactive Rabs with high catalytic efficiency even when GDP is bound to the GTPase and hence can inhibit binding of GDI to Rab:GDP complexes. They further speculate that human cells could employ similar mechanisms in the absence of infection to effectively displace Rabs from GDI.

In summary, membrane targeting mechanism of Rab GTPases remains not totally clear. Several factors including GDF, GEF and posttranslational protein modification are reported to release GDI from the tight complex Rab:GDP:GDI, which should be responsible for Rab targeting. Considering the fact that more than 60 Rab proteins show their specially characteristic subcellular distribution (Pereira-Leal et al., 2001), we still need to do much work to understand Rab targeting at molecular level.

1.2. Orthogonal reactions for protein chemistry

The investigation of biological processes by chemical methods, commonly referred as chemical biology, often requires chemical access to biologically relevant macromolecules such as peptides and proteins. Chemoselective reactions are employed for this purpose. Chemoselective reactions in biological systems, also known as bioorthogonal reactions, are defined as functional groups that react rapidly and selectively with each other under physiological conditions in the presence of biological-relative groups. For example, a variety of bioorthogonal chemical reactions, such as the Cu(I)-catalyzed [3+2] azide-alkyne cycloaddition (Lin et al., 2006; Gauchet et al., 2006; Seo et al., 2011), the native chemical ligation (Dawson et al., 1994; Girish et al., 2005; Camarero et al., 2004), the Staudinger ligation (Soellner et al., 2003; Watzke et al., 2006), the Diels-Alder cycloaddition (de Araujo et al., 2005; Pauloehrl et al., 2012), the oxime ligation (Christman et al., 2007; Lempens et al., 2009; Dettin et al., 2011), the click sulfonamide reaction (Govindaraju et al., 2008) and the photochemical thiol-ene reaction (Jonkheijm et al., 2008; Weinrich et al., 2010) have been successfully applied for site-specific protein modification and immobilization. The oxime ligation, the native chemical ligation and the click ligation are employed in this project and highlighted as follow.

1.2.1. Oxime ligation

The reaction between oxyamines and aldehydes or ketones yields an oxime adduct (Figure 1.7). Because this reaction is mild, the oxime ligation finds wide use in a variety of bioconjugation applications, including site-specific protein labeling *in vitro* (Cornish et al., 1996), labeling of proteins on the bacterial cell surface (Zhang et al., 2003), and metabolic labeling of glycans on the mammalian cell surface (Mahal et al., 1997).

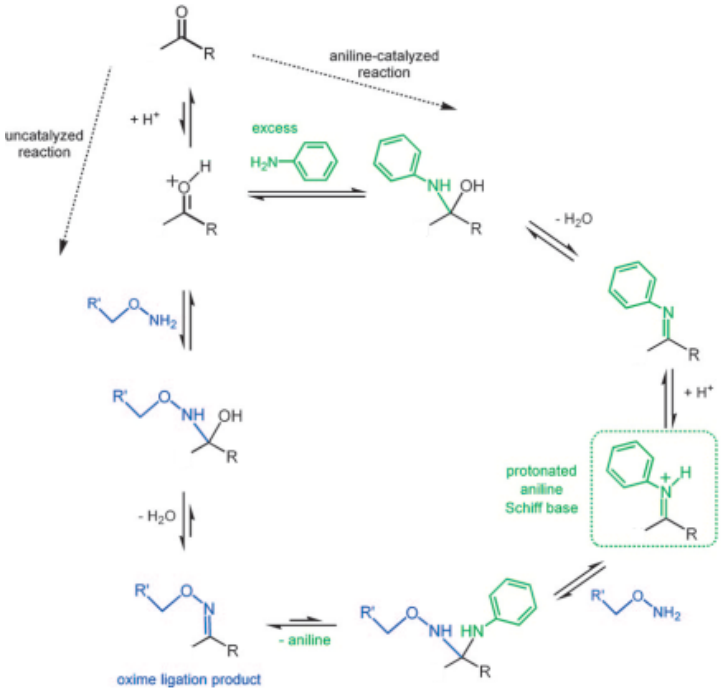

Figure 1.7. Aniline catalysis of oxime ligations. The uncatalyzed oxime ligation begins with addition of an aminooxy reagent to a ketone, forming a carbinolamine. This initial step is slow because it requires protonation of the ketone, but not the aminooxy group. Next, the carbinolamine undergoes dehydration to form the oxime ligation product. The oxime ligation can be catalyzed by excess aniline, which reacts with the ketone to form an imine. The aniline imine is readily protonated, enabling it to react with aminooxy reagent. Subsequent loss of aniline leads to formation of the stable oxime product.

The ability of ketones and aldehydes to participate in chemoselective reactions offers a conceptually simple way to selectively tag these functional groups. But, in practice, the chemistry of the reaction imposes limitations. The reaction between a ketone and the nitrogen present in an aminooxy group is optimal under slightly acidic conditions (pH 5–6) and even then, proceeds at only a modest rate. The slow reaction kinetics can be partially overcome by using high concentrations of the aminooxy, but quantitative labeling remains elusive. The sluggish kinetics and pH dependence of these reactions result from the requirement for protonation of the carbonyl oxygen (Rosenberg et al., 1974; Sayer et al., 1974). Lowering the pH of the reaction mixture increases the concentration of protonated carbonyl, but simultaneously decreases the reactivity of the aminooxy nucleophile by protonating that

molecule as well, so it is difficult to achieve rapid kinetics at any pH. The ingredient that has been lacking in these reactions is an appropriate nucleophilic catalyst.

Aniline has the unique ability to fill this role. Aniline catalyzes oxime ligations through a transimination mechanism (Figure 1.7). Like α-effect nitrogens, aniline reacts with protonated carbonyls to form imines, but the pK_a of these aniline imines is such that they are significantly protonated at the pH of the reaction mixture. Thus, the protonated aniline Schiff base is poised to react rapidly with an aminooxy reagent, forming an oxime product that does not readily re-react with aniline. The ability of aniline to function as a catalyst in these types of reactions was first reported in 1961 (Cordes et al., 1962), but has only recently been applied to bioconjugation reactions (Dirksen et al., 2006; Yi et al., 2010). The addition of aniline results in a ten-fold increase in ligation efficiency, and transforms a mediocre labeling reaction into highly effective one.

1.2.2. Click ligation

The reaction of alkynes with organoazides has been known as a valuable method for triazole synthesis for more than a century (Michael, 1893). It is a typical example of a Huisgen-type 1,3-dipolar cycloaddition (Huisgen, 1963). However, the high reaction temperatures limited the biological application of this reaction. However, the groups of Meldal and of Sharpless reported an ideal regio-specifity and an extreme rate enhancement in the reaction of terminal alkynes with azides in the presence of copper(I) catalysis at room temperature (Sharpless, et al., 2001; Berry et al., 2010). Such a discovery dramatically changed the scope of its application in chemical biology.

This Cu(I)-catalyzed Huisgen 1,3-dipolar cycloaddition reaction is commonly known as "click" reaction (Sharpless, et al., 2001). A stepwise pathway with copper(I) acetylide catalysts and a copper(I) triazolide intermediate is generally assumed (Figure 1.8) (Nolte et al., 2007). The rate-limiting step apparently changes from the protonation of the triazolide complex (H_2O or alkyne as proton source) to the alkyne deprotonation–cycloaddition sequence (excess of acetic acid). Direct evidence of this mechanism was proven by the isolation of the copper(I)-triazolide complex (Nolte et al., 2007). Though the click reaction is accelerated by approximately 7 orders of magnitude compared to the uncatalyzed version, the catalytic copper(I) is not much stable in aqueous solution. As a ligand-assisted process, the reaction is further accelerated by Cu(I)-stabilizing ligand tris[(1-benzyl-1*H*-1,2,3-triazol-4-yl)methyl]amine (Chan et al., 2004). Due to these fast reaction kinetics and exquisite

selectivity, this click reaction has gained widespread utilization in chemical biology and materials science.

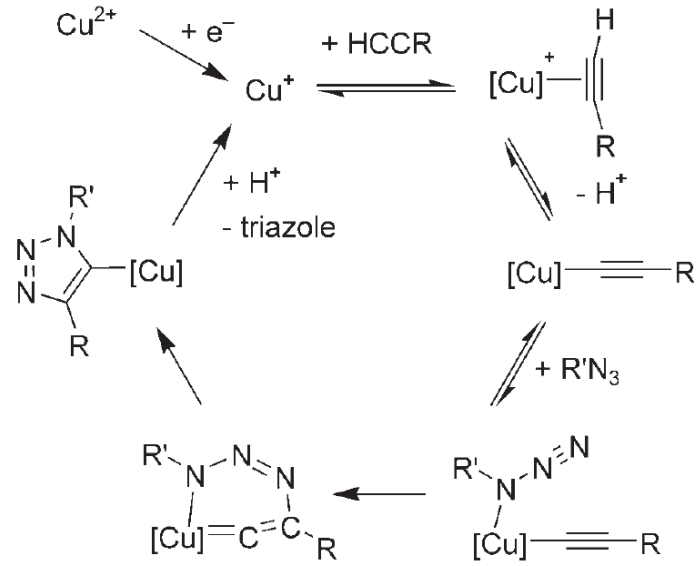

Figure 1.8. Proposed mechanism in the alkyne–azide click reaction; [Cu] represents either mononuclear or dinuclear copper(I) complex fragments. (Angew. Chem. Int. Ed. 2007, *46*, 2101)

1.2.3. Native chemical ligation

Chemical synthesis is an attractive alternative to biological methods for protein production. Synthetic chemistry provides almost unlimited modulation of the structure of a polypeptide chain in order to understand the protein function. However, since proteins are large molecules, applying chemical synthesis to them is a considerable challenge. In 1994, Kent and coworkers introduced the approach of native chemical ligation (NCL), which is now a general method in chemical protein synthesis (Dawson et al., 1994) and protein modification. In this method, two unprotected synthetic peptide fragments are joined together in neutral aqueous conditions with the formation of a native peptide bond at the ligation site. The principle of NCL is depicted in Figure 1.9.

The approach is based on the chemoselective reaction between a peptide containing a C-terminal thioester and another peptide containing an N-terminal cysteine. The initial chemoselective transthioesterification in NCL is essentially reversible, whereas the subsequent S→N acyl shift is spontaneous and irreversible. Thus, the reaction is driven to form an amide bond specifically at the ligation site, even in the presence of unprotected internal cysteine residues. NCL has been widely used in the total chemical synthesis of small proteins and protein domains, with a number of refinements in ligation methodology and

strategy, such as auxiliary group-facilitated ligation (Offer et al., 2002; Meutermans et al., 1999), catalytic thiol cofactors (Johnson and Kent, 2006; Dawson et al., 1997b), kinetically controlled ligation (KCL) (Bang et al., 2006), and convergent chemical protein synthesis (Durek et al., 2007). The utility of NCL was significantly broadened by the demonstration that both essential components (C-terminal thioester and N-terminal cysteine residue containing fragments) can be produced recombinantly.

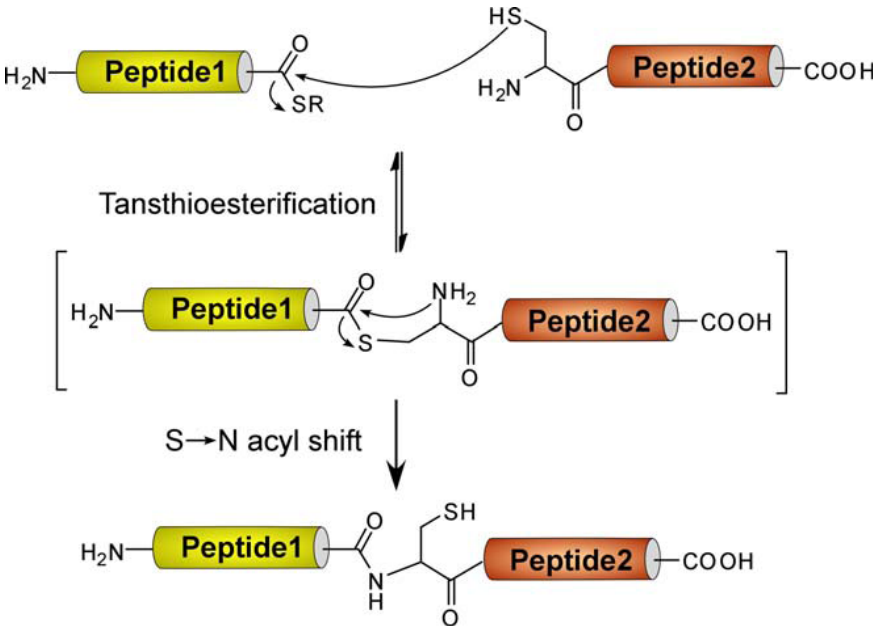

Figure 1.9. Principle of native chemical ligation. Both peptide fragments are fully unprotected and the reaction proceeds in aqueous and neutral conditions, given that one contains a C-terminal α-thioester and the other contains N-terminal cysteine (Dr. Thomas Durek's PhD thesis, 2004).

1.2.4. Expression protein ligation

Expressed protein ligation (EPL) is a variation of NCL in which one or more of the peptide segments used to assemble a protein is produced recombinantly, permitting synthetic peptides to be chemo- and regioselectively coupled to recombinant proteins (Muir et al., 1998) by the NCL reaction. EPL combines the structural flexibility of chemical (peptide) synthesis with the ability of recombinant DNA methodologies to generate large polypeptides (proteins), thereby enabling the semi-synthesis of much larger proteins.

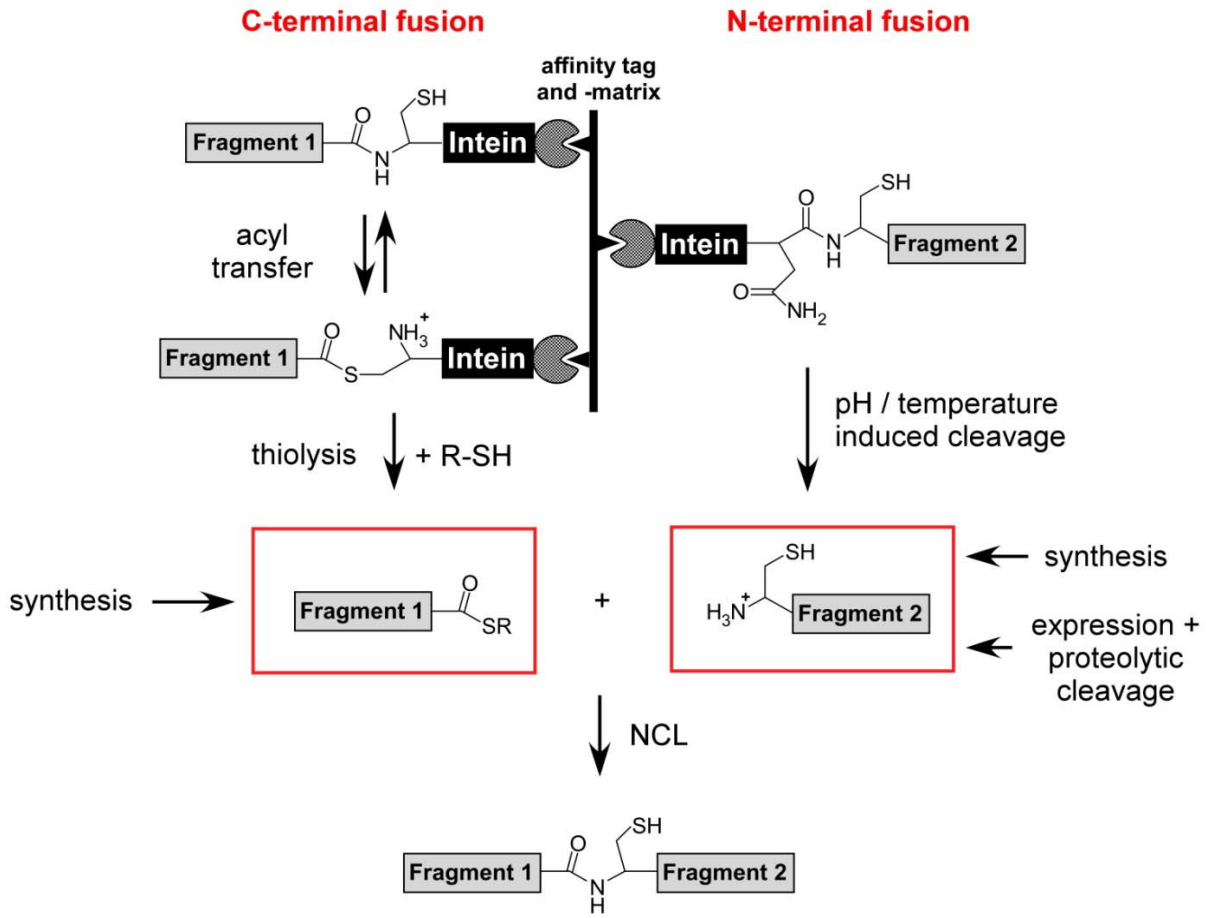

Figure 1.10. Basic concept of EPL. Recombinantly expressed proteins bearing a C-terminal thioester or an N-terminal cysteine can be prepared by fusion to and subsequent cleavage of engineered inteins. The isolated fragments are ligated in a manner similar to NCL.

As shown in Figure 1.10, α-thioester derivatives of recombinant proteins can be prepared by thiolysis of mutated intein fusions. In this case the target protein is fused to the N-terminus of a modified intein, which cannot undergo C-terminal cleavage. The intein catalyzes an N→S acyl shift leading to a linear thioester linked intermediate, which can be cleaved by transthioesterification with thiols, liberating the α-thioester tagged protein. Commercially available systems additionally use affinity tags (mainly chitin-binding domain (CBD)), which allow facile affinity purification and inducible self-cleavage of expressed proteins. In contrast, preparation of recombinant proteins bearing an N-terminal cysteine is often more complicated and always involves specific removal of an N-terminal leader sequence from a precursor protein. Proteolytic cleavage of an expressed protein precursor with the cysteine residue adjacent to a protease cleavage site was demonstrated by *in vitro* processing with tobacco etch virus (TEV) protease (Tolbert et al., 2002) and Factor Xa protease (Erlanson et al., 1996; Chytil et al., 1998), as well as *in vivo,* utilizing endogenous methionylaminopeptidase

(MetAp) (Iwai et al., 1999). In summary, protein splicing and its modulation provide the means for site-specific and genetically codeable labeling of recombinant proteins, which can be further exploited by EPL or other techniques.

Since its introduction, EPL has been applied to many different proteins (Muir, 2003). One of the most important advantages of EPL is that it allows the creating essential tools for the exploration of important functional questions. Most applications aim at modifications located within ~ 50 residues of the N- or C-terminus, which allows target molecule assembly from two fragments, one synthetic and one recombinant. Furthermore, sequential EPL strategies (i.e. the ligation of three or more fragments) offer the possibility to modify any residue within the entire primary protein sequence (Cotton et al., 1999, 2000).

1.3. Lipoprotein synthesis

Lipidation of proteins is an important mechanism to regulate protein trafficking, localization and activity in cell and tissues. The targeting of proteins to membranes by lipidation plays key roles in many physiological processes and when not regulated properly can lead to cancer and neurological disorders. Dissecting the precise roles of protein lipidation in physiology and disease is a major challenge. The biochemical generation of fully functionalized and modified lipidated proteins is difficult, time consuming, and in the case of S-palmitoylation, leads to heterogeneous mixtures and is therefore in most cases not practical or applicable.

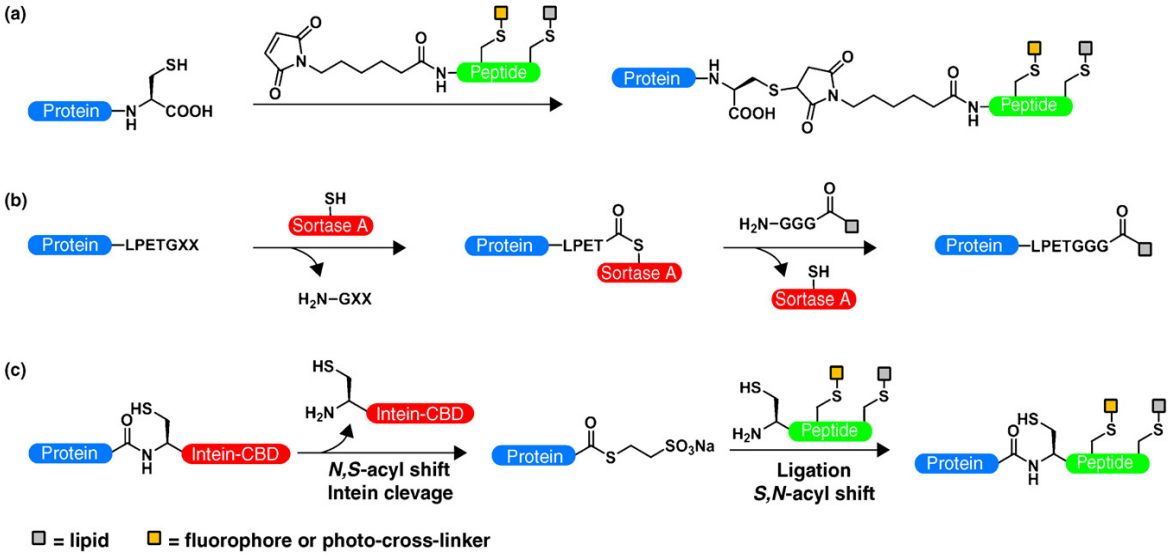

Figure 1.11. Semi-synthetic synthesis of lipidated proteins. (a) Conjugation of proteins with lipidated and/or fluorescently tagged peptides by MIC ligation on cysteine residues. (b) Lipidation by sortase-mediated trans-peptidation. (c) Lipidation and/or fluorescent tagging of proteins by EPL.

In contrast, chemical-biological approaches have been developed in the last years, giving access to the fully functional lipidated proteins bearing natural and non-natural modifications, thereby enabling the study of the complete functional proteins. This was achieved through two techniques that were developed more or less in parallel: 1) protein ligation and chemical synthesis of proteins (Muir, 2003; Kent, 2009) and 2) lipidated peptide synthesis, both in solution and on solid support. Notably, the development of solid-phase synthesis methods for generation of fatty-acylated and prenylated peptides has provided key tools to characterize these proteins (Brunsveld et al., 2006).

For example, the conjugation of fluorescent lipopeptides to proteins bearing C-terminal cysteines by maleimidocaproyl (MIC) ligation afforded fluorescent Ras lipoprotein variants to interrogate their partitioning into membranes *in vitro* (Weise et al., 2009; Nicolini et al., 2006; Bader et al., 2000) and trafficking in living cells (Rocks et al., 2005) (Figure 1.11a). The analysis of S-palmitoylated and non-hydrolyzable thioether analogs of lipidated Ras demonstrated that dynamic S-palmitoylation of proteins is an important feature for the distribution and trafficking of lipidated proteins in cells (Rocks et al., 2005). Photo-crosslinkers such as the benzophenone group can also be installed via MIC ligations to investigate lipidated protein–protein interactions (Alexander et al., 2009; Volkert et al., 2003). In addition to isoprenoid and fatty acid analogs, other lipids such as cholesterol can be conjugated to proteins by MIC ligation (Peters et al., 2004).

Sortase-catalyzed transpeptidation provides an alternative method for the semisynthesis of C-terminal lipid-modified proteins (Antos et al., 2008) (Figure 1.11b). While these methods have provided access to fully unmodified lipoproteins, both approaches introduce non-native peptide linkages that may have an effect on protein structure or activity.

Expressed protein ligation (EPL) has emerged as a powerful method for the semisynthesis of proteins bearing various posttranslational modifications linked to the protein through native peptide bonds (Muir, 2003) (Figure 1.11c). Indeed, EPL has enabled the production of various lipidated protein constructs for biochemical and biophysical studies (Gottlieb et al., 2006; Alexandrov et al., 2002; Becker et al., 2008; Paulick et al., 2007). Of note, the semisynthesis of fluorescently modified and prenylated isoforms of Rab7, a member of the RabGTPase family of proteins involved in vesicular transport and membrane fusion, has revealed geranylgeranylation dependent protein–protein interactions (Wu et al., 2007). For example, synthetic unmodified or monogeranylgeranylated Rab7 binds to REP for further RabGGTase-mediated geranylgeranylation and subsequent membrane targeting, whereas GDP dissociation inhibitor (GDI) preferentially binds mono-geranylgeranylated and dually geranylgeranylated

Rab7 to modulate RabGTPase membrane activity (Wu et al., 2007). These biochemical studies provide important mechanistic insight into the cyclic regulation of RabGTPases, which are further supported by structural analysis of a monoprenylated Rab protein, Ypt1 also generated by EPL, in complex with GDI (Rak et al., 2003).

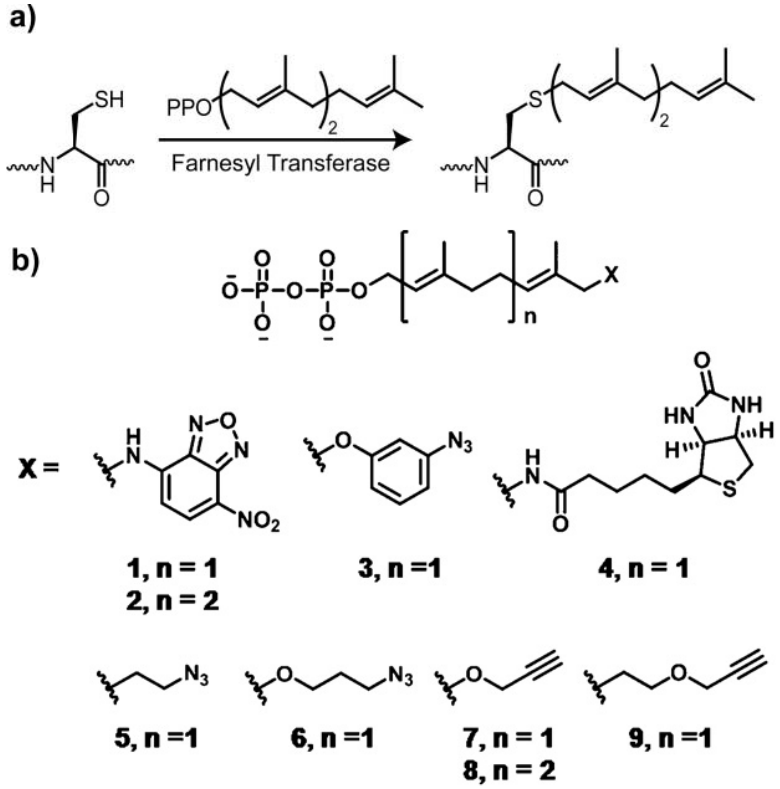

Figure 1.12. a) Farnesyltransferase (FTase) catalyzed protein modification. The native activity of FTase is to attach farnesyl isoprenoid group to a Cys residue of the modified protein. b) Isoprenoid analogs functionalized with fluorophore, photo-crosslinker, biotin, azide or alkyne group for *in vitro* protein S-prenylation studies.

Chemoenzymatic methods can complement semisynthetic approaches for generating functionalized lipoproteins. For example, fluorescent nitrobenzoxadiazole (NBD) analogs of farnesyl and geranylgeranyl pyrophosphates were shown to be efficient *in vitro* substrates for FTase, and GGTase I/II, respectively (Dursina et al., 2006; Wu et al., 2006) (Figure 1.12). These fluorescent substrates provide a rapid non-radioactive assay for protein prenylation *in vitro* that facilitated the high-throughput screening of selective FTase and RabGGTase inhibitors (Guo et al., 2008). Prenyl pyrophosphate analogs bearing photoaffinity crosslinkers such as arylazides can also be enzymatically installed by FTase to map interactions of prenylated proteins with other proteins and membranes (Katadae et al., 2008) (Figure 1.12). In addition, a biotinylated geranyl pyrophosphate (BGPP) derivative can be utilized by RabGGTase for the site-specific modification of recombinant proteins with an affinity tag

(Nguyen et al., 2007, 2009). While BGPP is not a substrate for wild-type FTase or GTTase I, mutants of both enzymes have been identified that can utilize this biotinylated isoprenoid analog. Alternatively, lipid analogs bearing smaller chemical tags (azide or alkyne) can serve as substrates of protein lipidation enzymes and subsequently functionalized with fluorophores or affinity tags by click chemistry (Rostovtsev et al., 2002).

Chemical approaches have provided very important insight into the biosynthesis and functions of protein lipidation in biology (Rak et al., 2003; Rocks et al., 2010). The advances in the semisynthesis of lipidated peptides and proteins have yielded homogeneous materials for fundamental biochemical and cellular studies. These new chemical tools (semi-synthetic protein probes) should help to dissect the functions of protein lipidation in physiology and disease as well as to facilitate the development of effective therapeutics for cancer and neurological disorders.

2. Aims of the project

“Truth in science can be defined as the working hypothesis best suited to open the way to the next better one.”

Konrad Zacharias Lorenz

2. Aims of the project

The recent advances in the field of protein chemistry paved the way for the application of methods of synthetic organic chemistry to the modification of large proteins. Such a symbiosis of chemistry and biology can be considered to be extremely useful in various fields, including the development of new methods for protein labeling and immobilization, the semi-synthesis of lipoproteins and the generation of synthetic protein probes for biological studies.

In order to generate homogeneous protein layers (also as protein microarray) as well as to maintain the native structure and bioactivity of the immobilized proteins, site-specific protein immobilization methods are advantageous, as opposed to random attachment. Moreover, to attain high linkage stability, covalent protein immobilization is preferable to non-covalent methods. The development of operationally simple and practical, mild and general techniques for immobilization of functional proteins on solid supports remains a central challenge. In particular, the development of methods that enable the direct immobilization of expressed proteins from cellular lysates is of great value since it streamlines the entire process of protein microarray fabrication and greatly enhances practicability and efficiency. We aim to develop a facile, efficient and mild strategy for the site-specific immobilization of proteins on surfaces by means of oxyamine ligation to generate protein microarrays. Furthermore, this strategy should enable the direct immobilization of expressed proteins from crude cellular lysates without prior purification. The produced protein biochips can be used for the study of protein-protein interactions. The work should expand the repertoire of protein immobilization methods and provides an alternative means to meet the various requirements for protein immobilization.

Multi-color labeling is a valuable technique for the characterization of proteins with respect to their structure, folding, and interactions both as single molecules and in cellular investigations. The key technique for such studies is based on fluorescence resonance energy transfer (FRET). FRET applications require the attachment of donor and acceptor molecules to specific sites of a given protein or proteins. Such labeling is typically achieved through conjugation at cysteine residues or amino groups or by genetic fusion to different fluorescent proteins. However, site-specific incorporation of multiple fluorophores into a single protein remains a considerable challenge. Herein, we aim to develop a general, facile and efficient method for one-pot dual-labeling of a protein based on two chemoselective reactions. The

produced dual-labeling protein probes should be used for studying protein-protein interactions and protein refolding.

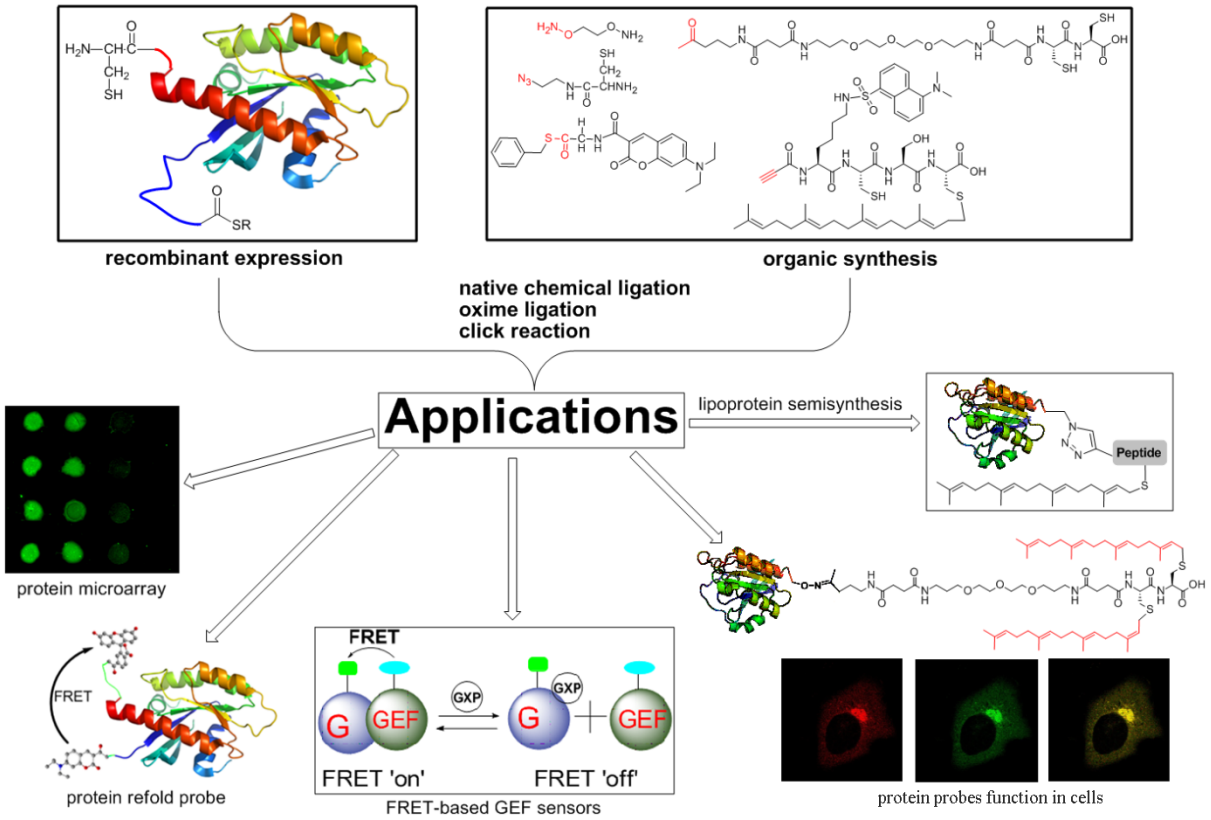

Figure 2.1. Overview of the project. The combination of organic synthesis and molecular biology produced modified proteins. The lower part of the figure shows some applications of such modified proteins, which were explored in this study.

The GTPase cycle is strictly regulated by GEFs that mediates GDP/GTP exchange. GEFs are often multidomain proteins or members of large protein complexes, which activate GTPases at specific subcellular sites. GEFs have been considered as promising therapeutic targets, due to their function in regulating disease-relevant GTPase signaling. Investigation of GEF mechanisms and identification of GEF inhibitors require appropriate assays for the GEF activity. The frequently used method for monitoring GEF activity is based on the intrinsic fluorescence of the protein or that of GDP/GTP analogues labeled with an environmentally sensitive fluorophore, such as N-methylanthraniloyl (mant). Though mant is a small fluorescent group, mant-GDP or -GTP might not behave identically to the native nucleotides. Thus, kinetic parameters obtained using mant-GDP/GTP are not identical to those of native nucleotides. An assay using radio-labeled GDP/GTP is not appropriate for monitoring fast kinetics of GEF-mediated nucleotide exchange. We aim to develop a sensitive and versatile assay based on intermolecular FRET between GEF and GTPase for monitoring GEF-

mediated nucleotide exchange. Transient kinetic studies based on the FRET signal changes can be used to monitor the GEF activity and inhibition. This strategy may open up a new avenue for the identification of GEF inhibitors and for studying GEF mechanisms.

Tools for generating protein-lipid conjugates are valuable for studying the role of post-translational lipid modification in controlling protein function and localization. However, recombinant production of post-translationally modified proteins is usually challenging in terms of homogeneity and output. The site-specific attachment of lipids to proteins remains a significant challenge in bioconjugation. Only a relatively limited set of chemical and chemoenzymatic strategies are available for this purpose. We aim to develop a general and fast ligation strategy for preparing lipid-protein conjugates based on tandem EPL and click chemistry. The lipid-protein bioconjugate should be quantitative, which can make the purification of ligated protein much facile. The ligation strategy may open up a new avenue for production of lipoproteins that are used in various biological studies.

In order to further understand the mechanism of Rab prenylation, we want to know whether there is nothing required for Rab C-terminal sequence and to what extent the Rab prenylation machinery could tolerate the change in the Rab C-terminal sequence. We also hope to use chemical-biological tools to probe whether the C-terminal hypervariable region of Rabs contains a general targeting signal for Rab localization. We aim to replace Rab C-terminal sequence and cysteines with unnatural linkers (such as a polyethylenglycol (PEG) linker) and thiols, respectively. The produced protein probes can be used to elucidate the mechanism of Rab prenylation. A further aim of this work was to provide sufficient amounts of PEGylated Rab protein probes for intracellular localization.

3. Results and Discussion

“Things should be made as simple as possible, but not any simpler.”

Albert Einstein

3.1. Development of a universal strategy for C-terminal protein modification and immobilization

3.1.1. Introduction

Site-specific protein modification can facilitate the characterization of proteins with respect to their structure, folding, and interaction with other proteins both in biochemical and in cellular investigations. Although many chemical reactions are applicable in principle, methods for site-specific modification of proteins remain in high demand and there is a requirement for readily available ligation reagents (Hackenberger et al., 2008; Kurpiers et al., 2009). Moreover, the structural sensitivity of proteins calls for chemical transformations that proceed under mild conditions (room temperature, neutral pH) and are compatible with all functional groups present in proteins. Oxime-based reactions have found wide application in the conjugation of biomolecules due to the absence of oxyamine groups in proteins and their orthogonal reactivity with ketones to give stable oximes (Sohma et al., 2009; Muralidharan et al., 2006; Kalia et al., 2010; Sletten et al., 2009; Lim et al., 2010; Zeng et al., 2009; Dirksen et al. 2006; Huang et al., 2010). The oxime reaction has been exploited in protein modification mainly via incorporating ketone groups into proteins by various chemical (Geoghegan et al., 1992), enzymatic (Lee et al., 2010) and molecular biological methods (Cornish et al., 1996; Brustad et al., 2008). To expand the application of this efficient methodology to protein ligation, we planned the development of a simple and general method to incorporate oxyamine groups into proteins and its further reaction with ketone-containing molecules as an alternative method for protein modification.

It is well known that hydroxyamine of thioesters can lead to expose the free thiol groups (Figure 3.1a). On the other hand, it was shown that during NCL the nitrogen atom of oxyamines can react with a thioester group intramolecularly (Figure 3.1b) (Canne et al., 1996). Therefore, we reasoned that in theory, highly nucleophilic oxyamines could also selectively react intermolecularly with a C-terminal thioester of a protein. If this reaction would be performed with a linker carrying two oxyamine groups, one oxyamine could form a hydroxamic acid with the protein and the second oxyamine still would be available for a subsequent ligation reaction (Figure 3.1c). This project describes how a bis(oxyamine) molecule **1** was first incorporated at a protein C-termini to produce oxyamine-modified proteins, and how the subsequent efficient and specific reaction of the second oxyamine group with ketones was achieved to modify/immobilize proteins site-specifically under mild

conditions. The labeling strategy has been commercialized for a wide application by Jena Bioscience (http://www.jenabioscience.com).

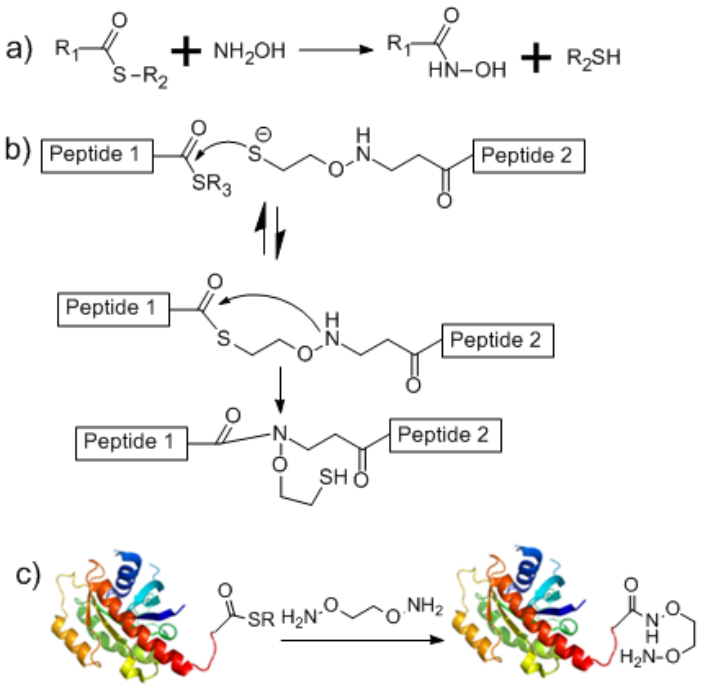

Figure 3.1. a) Intermolecular aminolysis of thioester by oxyamine. b) Intramolecular aminolysis of thioester by oxyamine. c) A strategy for production of an oxyamine-modified protein.

3.1.2. Preparation of oxyamine-modified proteins

The bacterial expression strategy for the generation of protein C-terminal thioesters is shown in Figure 3.2. This requires the truncated target protein gene to be inserted upstream of an intein-chitin-binding-domain (CBD) or intein-His-tag construct. Following expression and affinity purification of the three-part fusion protein, the protein of interest is precisely cleaved from the intein as a C-terminal α-thioester. Several *E. coli* expression vectors are now commercially available that allow the target DNA to be easily subcloned in frame of various engineered inteins (Xu et al., 2000). These vectors utilize the T7/lac promoter to provide stringent control of fusion protein expression and a CBD from *Bacillus circulans*. The pTWIN1 vector that was frequently used in this study is depicted in Figure 3.2a. Another pTWIN1-His vector whose CBD is replaced by His-tag was also used (Figure 3.2b).

All protein thioesters in this thesis were expressed as C-terminal intein fusions using pTWIN1 or pTWIN1-His expression vectors. Vectors were prepared by using standard PCR subcloning procedures employing in most cases ligation sites recommended by New England Biolabs. The various expression vectors were then transformed into BL21(DE3) cells and a

series of preliminary studies were undertaken to identify optimal expression conditions (IPTG concentration, induction time and temperature were varied). For soluble fusion protein expression the induction temperature had to be lowered to 18-22 °C in all cases examined so far. Purification of the fusion proteins from crude cell extracts employing chitin agarose beads or Ni-NTA (nitrilotriacetic acid) column was straightforward. However, starting with crude cell lysate the whole procedure should reach the thiol induced cleavage stage within 4-6 hours. Cleavage was in all cases performed in the presence of 500 mM 2-mercaptoethanesulfonic acid (MESNA) at room temperature for 12-16 h. Incubation of the intein-fusion protein with such high concentrations of MESNA (0.5 M) resulted in almost quantitative cleavage. Firstly, Rab1-thioester as a model protein was generated through intein-mediated partial protein splicing. The successful expression and purification of Rab1 were indicated by SDS-PAGE (Figure 3.2), with typical yield of 5-10 mg per liter of bacterial culture in excellent purity (> 90 %).

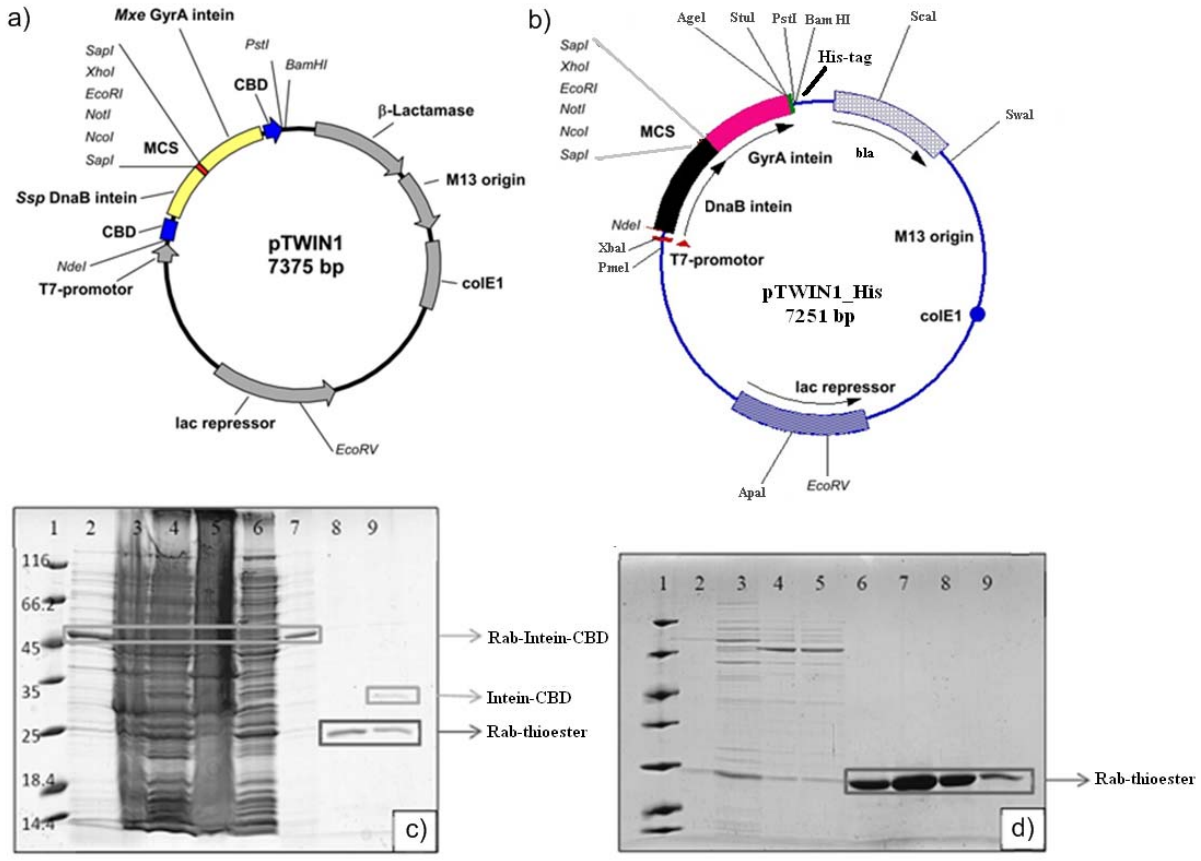

Figure 3.2. a) The pTWIN1 vector utilizes two mini-inteins. Depending on the cloning strategy, target proteins can be fused C- and/or N-terminally to the inteins. b) The pTWIN1-His vector employs the His-tag instead of CBD in a). MCS = multiple cloning site. c) Expression and purification of Rab1-thioester. Lane 1: Marker, Lane 3: cell lysate before induction, lane 4: cell lysate after induction with IPTG overnight (o/n), lane 5: pellet of the cell lysate, lane 6: flow-through from the chitin column, lanes 2 and 7: chitin beads after washing, lane 8: fraction of the eluted protein after an overnight incubation with 0.5 M

MESNA at 20 °C, lane 9: chitin beads after the cleavage; d) Further purification by gel filtration assay, Lane 1: Marker, Lanes 2-5: fractions before gel filtration, Lanes 6-9: fractions after gel filtration.

The synthesis of bis(oxyamine)·2HCl (**1**·2HCl) started from the commercially available and inexpensive reagent N-hydroxyphthalimide and 1,2-dibromoethane (Figure 3.3) (Bauer et al., 1963). The economic yielded **1**·2HCl in a convenient manner without chromatography (yield > 20% over two steps; for details see experimental part) is important for the wide use of the method developed herein. The resulting white solid **1**·2HCl was dissolved in a 2 M NaOH solution to prepare a 1-2 M stock solution with a pH around 7.5. This stock solution **1** is stable at 4 °C for at least two years. It should be noted that compound **1** (rather than its HCl salt) is liquid and readily explosive. However, the stock solution is safe enough for common protein ligation operations.

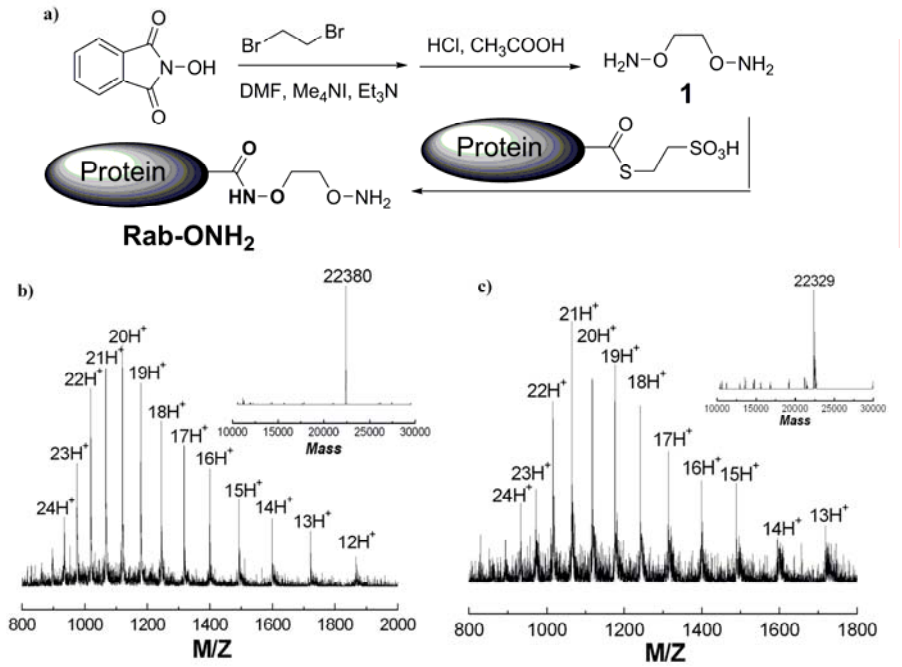

Figure 3.3. a) Synthesis of bis(oxyamine) **1** and the generation of Rab-ONH_2. b) and c) ESI-MS spectra of Rab1-thioester ($M_{calc.}$ = 22380) and Rab1-ONH_2 ($M_{calc.}$ = 22330), respectively. (Rab1-thioester is a gift from Nathalie Bleimling)

Once bis(oxyamine) **1** was prepared, its use for protein modification was investigated. In order to introduce an oxyamine group into a protein, the reaction of Rab1-thioester and **1** was performed on ice for 4 h. As shown in Figure 3.3, ESI-MS analysis revealed that the main protein peak had a mass of 22329 Da (expected mass 22330 Da), implying that most of the Rab1 protein was modified with the oxyamine moiety. The bis(oxyamine) could react directly

with the thioester group to form a stable O-alkyl hydroxamic acid bond. It should be noted that there is no sign of bis(oxyamine) bridged proteins as indicated by SDS-PAGE. There was also no detectable thioester hydrolysis during this reaction. Excess of **1** in the Rab1-ONH_2 preparation was removed by simple dialysis against sodium phosphate buffer (pH 7.5). Under neutral conditions oxyamine-modified protein could be stored at -80 °C for more than two years, generally without any detectable decomposition or loss of oxime ligation efficiency. This strategy should be general for preparation of oxyamine-modified proteins.

3.1.3. Optimization of the oxyamine ligation conditions

The reactivity of the oxyamino group on proteins was first tested using acetone. After simple incubation of Rab1-ONH_2 (1 mg/mL, ESI-MS 22330) and acetone (10 mM) at pH 5.5 on ice, the reaction was finished within 20 minutes (ESI-MS 22371), indicating that the reaction was rapid and generated a protein carrying a single acetone modification. In order to achieve fluorescent labeling of proteins, the same reaction was investigated with a ketone-containing fluorophore. Keto-coumarin was chosen firstly, since this fluorophore has good water-solubility and an excellent quantum yield, and is easy to synthesize (Sethna et al., 1945). On incubation of keto-coumarin **2** and Rab1Δ3-ONH_2 on ice for four hours, full conversion of the oxyamine to an oxime was achieved (Figure 3.4b). Unreacted small molecules were then removed by passing the reaction mixture over a PD-10 desalting column pre-equilibrated with 30 mM sodium phosphate buffer (pH 7.5, 50 mM NaCl, 1 mM $MgCl_2$, 10 μM GDP, and 5 mM DTE). Excitation/emission scans of a solution of Rab1-coumarin revealed that, as expected from the reporter group used, the fluorescence spectrum has an excitation maximum at 332 nm and an emission maximum at 412 nm (Figure 3.4c).

In order to further examine the fluorescent labeling efficiency of the protein by SDS-PAGE, keto-fluorescein **3** was synthesized and incubated with Rab1Δ3-ONH_2 on ice for various reaction times. The fluorescence gel image (Figure 3.4d) showed that the reaction was rapid and complete within 2 h on ice at pH 5.5. Rab1-thioester did not show any detectable labeling with **3,** further confirming that the reaction was chemoselective. The labeling reaction appeared to be highly efficient, since the starting Rab1-ONH_2 was not detected by ESI-MS (Figure 3.4e).

To further validate this ligation method as a general method for protein C terminal modification, it was also applied to an enhanced yellow fluorescent protein (EYFP). As for Rab1, the EYFP thioester was generated from an intein fusion protein, which was further

modified with the oxyamine group by direct incubation of protein and **1** in buffer. The obtained oxyamine-modified protein EYFP-ONH_2 was then incubated with **3** for different times on ice. The fluorescence intensity of the band corresponding to the product increased with time, and was essentially complete within 2 h at pH 5.5 (Yi et al., 2010). Formation of the product with the expected mass was detected by ESI-MS. These results indicate that the C-terminal modification strategy is general and efficient.

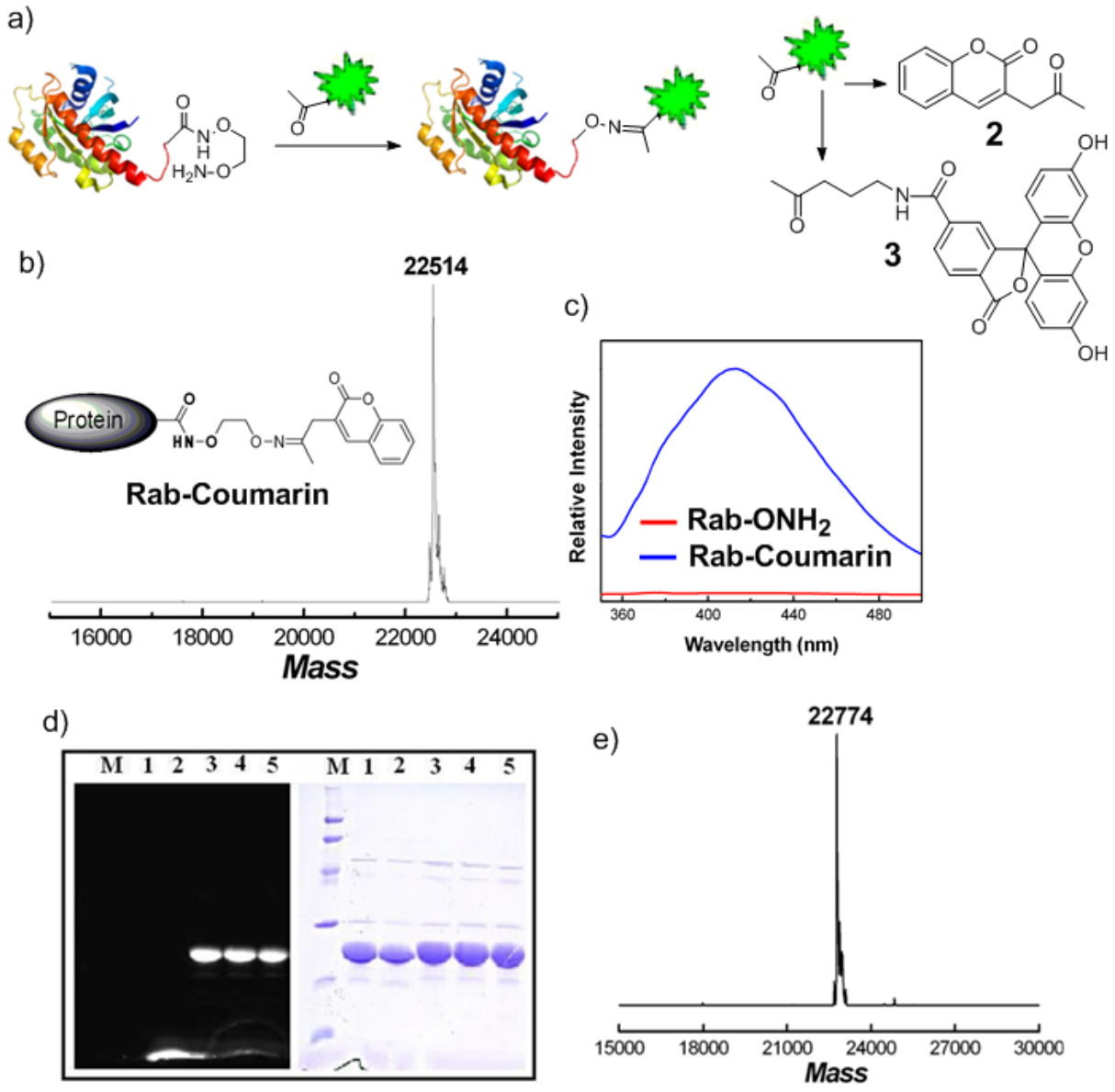

Figure 3.4. a) C-terminal fluorescence labeling by oxyamine-ketone ligation with different keto-fluorophores. b) ESI-MS spectrum of the reaction product between Rab1-ONH_2 and **2** ($M_{calc.}$ = 22516). c) Emission spectra of Rab1-ONH_2 (1 μM) and Rab1-coumarin (1 μM) excited by 332 nm. d) Fluorescence (left) and Coomassie staining (right) images of a gel loaded with Rab1-ONH_2 labeled with keto-fluorescein **3** (M, marker of 97, 66, 45, 30, 20.1, 14.4 KD; Lane 1, Rab1-ONH_2; Lane 2, Rab1-thioester and **3** for 30 min incubation on ice; Lanes 3-5, reaction between Rab1-ONH_2 and **3** for 30 min, 1 h and 2 h at pH 5.5 on ice,

respectively.) e) ESI-MS spectrum of the ligation product of Rab1-ONH_2 and **3** ($M_{calc.}$ = 22771).

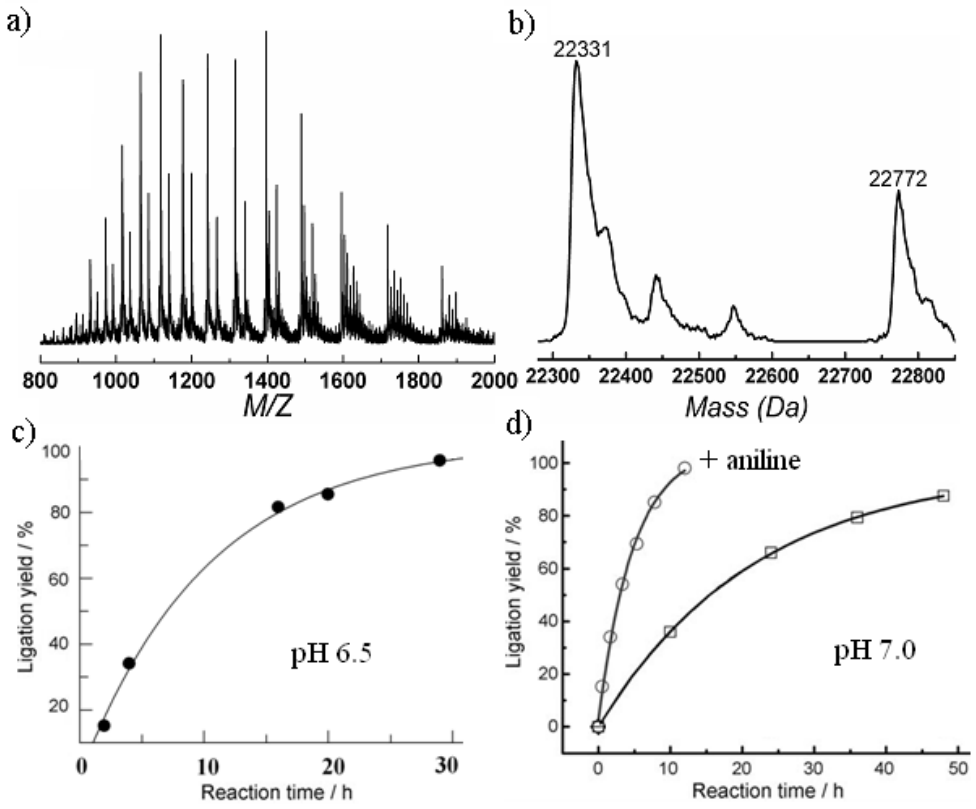

Figure 3.5. Reaction kinetics of 1 mg/mL Rab1-ONH_2 and 1 mM **3** through incubation on ice in sodium phosphate buffer (30 mM). a) Typical ESI peaks of the reaction mixture through incubation on ice at pH 6.5 for 4 hours, which shows both ligated and unligated proteins. b) Deconvolution mass spectra for that in a). c) and d) Ligation yield versus reaction time at pH 6.5 and 7.0, respectively. The ligation yield was calculated based on the ratio of the spectral integration values of the peaks of ligated and unligated proteins. The solid lines show a first-order reaction fit giving half-live value of 7.1 h, 15.1 h and 2.8 h for that at pH 6.5, pH 7.0 without and with 100 mM aniline, respectively.

ESI-MS analysis is an excellent tool to detect the protein ligation efficiency, and can be used to monitor the reaction kinetics in this work. Further experiments showed that the oxime reaction of 1 mg/mL Rab1Δ3-ONH_2 and 1 mM keto-fluorescein **3** could be achieved quantitatively at pH 6.5 (Figure 3.5c). The reaction is about ten-time slower than that at pH 5.5. Surprisingly, the protein ligation could be accomplished efficiently at pH 7.0 within 2 days (Figure 3.5d). Aniline can catalyze the oxime ligation in neutral buffer (Dirksen et al., 2006), and in our case the ligation rate can be further improved (by about fivefold) in the presence of 100 mM aniline at pH 7.0 (Figure 3.5d). Therefore, we can achieve quantitative labeling of oxyamine-modified proteins at pH 7.0 by incubation the reaction on ice overnight.

The oxime ligation normally cannot proceed efficient at neutral pH value. It is plausible that the particular functional moiety introduced at the protein C terminus might contribute to the fast oxime ligation kinetics in this work. Kinetic studies based on the model molecule **4** where the same bis(oxyamine) function was added to Fmoc-lysine compared to O-benzylhydroxylamine **5**, were performed at pH 7.0 buffer in pseudo-first-order reaction conditions (Figure 3.6). The oxime reaction of **3** with **4** was about tenfold faster than that for **5**, implying that our bisoxyamine is a particularly effective nucleophile for rapid reactions with ketones in protein modification, and may be the responsibility of the increase in efficiency.

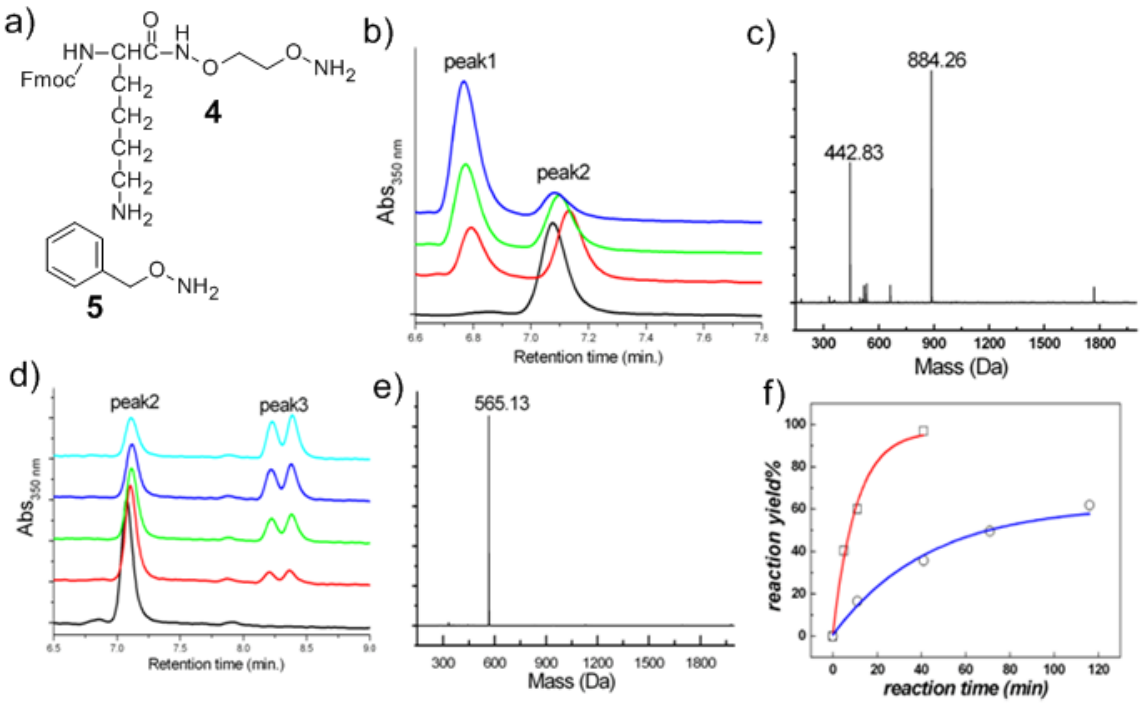

Figure 3.6. a) Chemical structures of **4** and **5**. b) HPLC traces for the reaction of 1 mM **3** and 10 mM **4** at pH 7.0 buffer at different time (0, 5, 11, 41 minutes). c) Mass spectrum of the peak 1 in b) at retention time of around 6.7 min. The calculated $[M+H]^+$ mass for **6**+H of the oxime product of **3** and **4** is 884.35. d) HPLC traces for the reaction of 1 mM **3** and 10 mM **5** at pH 7.0 buffer at different time (0, 11, 41, 71, 116 minutes). e) Mass spectrum of the peak3 in d) at retention time of around 8.3 min. The calculated $[M+H]^+$ mass for **7**+H of the oxime product of **3** and **5** is 565.20. f) Reaction kinetics of **5** (○) and a model molecule **6** (□) with **3**. The reaction yield was calculated based on the ratio of the integrated peaks values of reacted and unreacted fluorescein in HPLC traces. The solid lines show a first-order reaction fit giving half-life values of 7.3 and 70.7 min. for **4** and **5**, respectively.

To test the oxime-bond stability, the oxime-bond-containing Rab1-fluorescein protein (about 45 μM) was dialyzed against 1 L sodium phosphate buffer (50 mM, pH 7.4) at 4 ºC and analyzed by LC-MS after 4 h, 1 day and 2 days. No hydrolyzed protein was detected according to the mass spectra. We also mixed 1 mM **5** and 1 mg/mL Rab1-fluorescein (about

45 μM) in sodium phosphate buffer (50 mM, pH 7.4) and incubation on ice for three days. We found no evidence by mass spectrometry for replacement of the bisoxyamino moiety by **5** or for hydrolysis under these conditions. The oxime protein can be kept at -80 ºC for at least 3 months without hydrolysis. These results indicate that the oxime bond was stable enough at neutral pH to allow typical applications in biochemical experiments. Thus, the fast oxime ligation under mild conditions to form a stable oxime bond should provide a potentially general method for C-terminal modification of proteins.

The unique position and chemistry of protein C termini has stimulated efforts to target this site for selective protein modification. In one approach, a protein tag is appended to a target protein, and an enzymatic reaction is used to covalently introduce a C-terminal modification onto a protein (Antos et al., 2009; Tsukiji et al., 2009; Keppler et al., 2002; Chen et al., 2005). However, the protein tag is still retained in the labeled protein, which may interfere with protein function. An intein-based protein cleavage reaction has generated very useful approaches to protein C-terminal modification (Blaschke et al., 2000), mainly based on thioester-mediated ligation chemistry (Dawson et al., 1994; Lue et al., 2004; Watzke et al., 2006). A limitation of this method is that it generally leads to introduction of a cysteine residue into the target protein, regardless of whether this corresponds to the native structure or not. In addition, the thioester could undergo potential hydrolysis during the ligation reaction. Recently, it was reported that the C-terminal carboxylate can also be transformed into a thioacid, followed by protein C-terminal modification via thioacid/azide amidation in the presence of 6 M G.-HCl and 3 mM 2,6-lutidine (Zhang et al., 2009). However, these conditions are too harsh to maintain the proper folding of a protein. Moreover, the thioacid group is prone to hydrolysis under such conditions. In contrast to these methods, we could introduce an oxyamine group into the C-terminus of protein in mild conditions, and this can subsequently undergo fast and chemoselective oxime ligation on ice for site-specific protein labeling. No hydrolysis of thioester bonds is found in the reaction.

3.1.4. Functional characterization of the labeled proteins

In order to determine whether proteins still retain their activity after fluorescent labeling, we chose another Rab GTPase, Rab7, which binds to Rab escort protein (REP-1) with nanomolar affinity (Alexandrov et al., 1999). Fluorescence labeling of Rab7Δ2 was performed as for Rab1 with keto-coumarin. ESI-MS of the protein peaks gave masses of Rab7Δ2-ONH_2 and Rab7-coumarin of 23273 and 23458 Da, respectively, consistent with the expected values of 23275 and 23459 Da. Rab7Δ2-coumarin and REP-1 were incubated on ice for 1 hour,

separated by gel filtration and analyzed by SDS-PAGE (Yi et al., 2010). It is clear that Rab7-coumarin and REP-1 form a complex, implying that the modification of coumarin at the C-terminus did not significantly perturb the Rab7:REP-1 interaction (Wu et al., 2007; Sidorovitch et al., 2002).

To assess whether this method can be used for studying protein-protein interactions, we attached an environmentally sensitive fluorophore dansyl group to the protein C-terminus by the oxime ligation (keto-dansyl **8**). When the synthetic Rab7Δ7-dansyl protein probe was titrated with REP-1, a dose-dependent and saturatable increase of the fluorescence emission signal was observed when excited at 340 nm (Figure 3.7a).

Titration data could be fitted using a quadratic equation describing the binding curve and were consistent with 1:1 stoichiometry. The K_d value obtained (2.6 nM) is close to the one determined previously using mant-GDP-bound Rab7 (1 nM) (Alexandrov et al., 1998). Our results demonstrate that the oxyamine-ketone ligation offers an advantageous and novel approach for the site-selective functionalization and labeling of proteins for protein-protein interaction studies.

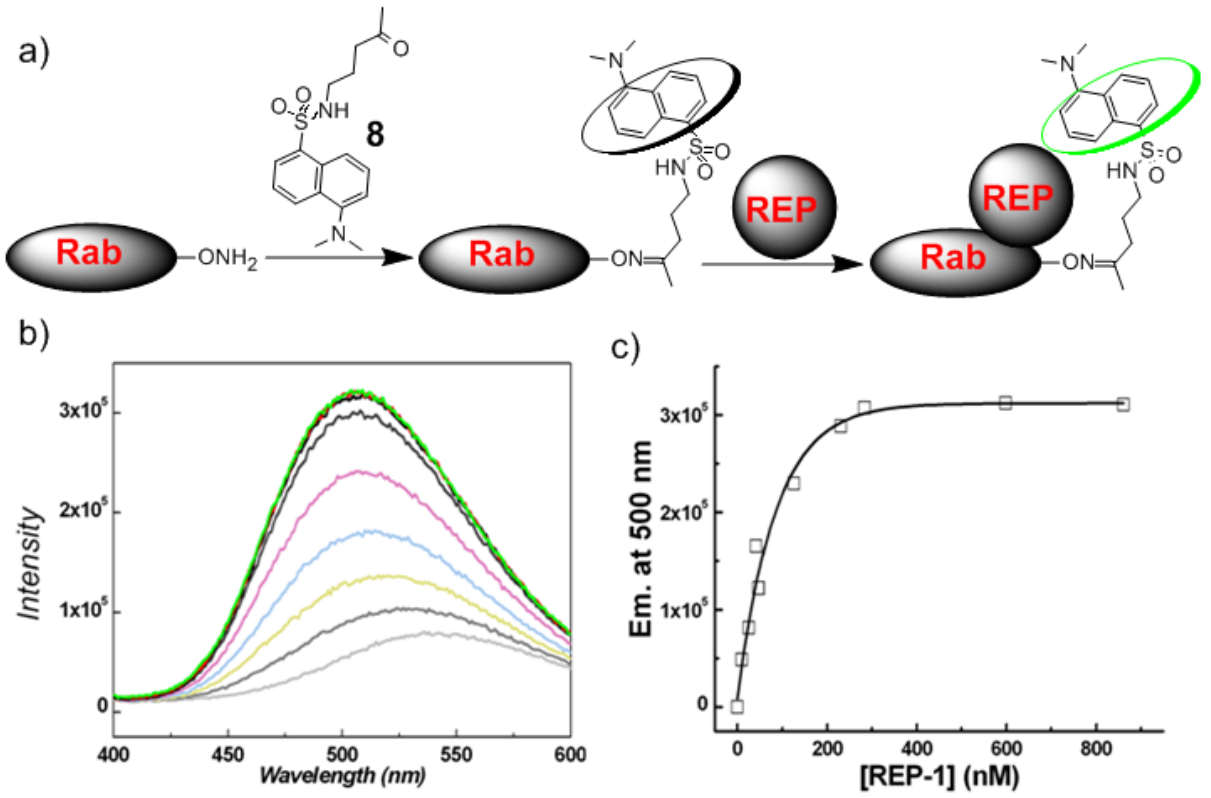

Figure 3.7. a) Schematic drawing of dansyl-modified Rab probe for Rab:REP interaction. b) Titration of REP-1 (10.5, 26.2, 47.2, 89.2, 126, 231, 283.5, 598.5, 861 nM) to a nominal concentration of 140 nM Rab7Δ7-dansyl using direct fuorescence as a signal for binding (excitation wavelength 340 nm). c) The emission intensity at 500 nm was fitted by using a quadratic equation to give 2.6 nM for the K_d.

In a further application of the method, we applied it to the generation of a dual-color labeled Rab. Dual-color protein labeling is a valuable tool for fluorescence resonance energy transfer (FRET) studies of dynamic biomolecular dynamics and associations (Joo et al., 2008). We expressed the protein mCherry-Rab7Δ3-intein, since mCherry is a FRET acceptor for fluorescein. After performing the labeling reaction of mCherry-Rab7Δ3-ONH_2 with **3** as described above, fluorescent imaging of the protein bands on the gel displays green and red fluorescence (Yi et al., 2010). Figure 3.8 shows that FRET occurred within the mCherry-Rab7Δ3-fluorescein molecule, since a strong fluorescent signal at 610 nm could be observed when mCherry-Rab7Δ3-fluorescein was excited at 490 nm (excitation wavelength for fluorescein). Compared with mCherry-Rab7Δ3-ONH_2 at the same concentration and excited at the same wavelength, this represents ca. 6 fold signal increase due to FRET. In contrast, denatured mCherry-Ypt7Δ3-fluorescein only displayed a strong signal of fluorescein fluorescence at emission wavelength 510 nm, suggesting that the FRET disappeared due to unfolding of the protein. FRET signal could be used to test the folding state of the construct under the ligation conditions (i.e. at pH 5.5). Thus, storing mCherry-Rab7Δ3-fluorescein in the ligation buffer for one week on ice did not lead to significant change in the fluorescent spectra, further suggesting that the ligation conditions are mild for Rab protein modification, although this remains to be tested in further individual cases.

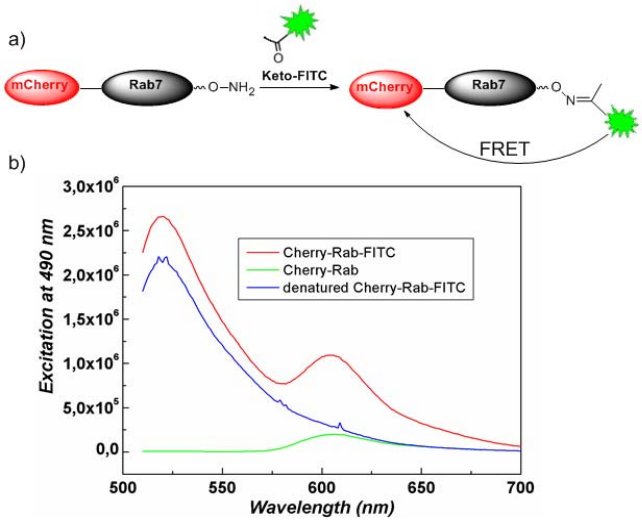

Figure 3.8. a) Schematic representation of generation of a dual-color protein showing FRET between fluorescein and mCherry. b) Emission spectra of mCherry-Rab7Δ3-fluorescein showing a FRET effect, while the denatured protein just shows the emission band of fluorescein.

3.1.5. Immobilization of oxyamine-modified proteins

The immobilization of proteins on surfaces plays an important role in various field of the life sciences, such as quick and comprehensive biomarker detection in clinical samples (Knickerbocker et al., 2011; Lee et al., 2008), proteome-wide interaction screens (MacBeath et al., 2000), and applications in drug discovery (Terstappen et al., 2007; Yu et al., 2011; Lynch et al., 2004), which could facilitate systematic understanding of biological phenomena at the molecular level (Phizicky et al., 2003; Weinrich et al., 2009). In order to generate homogeneous protein layers as well as to maintain the native structure and bioactivity of the immobilized proteins, site-specific protein immobilization methods are superior to random attachment (Jonkheijm et al., 2008; Lin et al., 2010; Wong et al., 2009). Moreover, in terms of linkage stability, covalent protein immobilization methods are particularly preferable. A variety of bioorthogonal chemical transformations have been successfully applied for site-specific protein immobilization (Jonkheijm et al., 2008). Each of them have their own advantages and limitations. However, the development of operationally simple and practical, mild and general techniques for immobilization of functional proteins on solid supports remains a central challenge. Furthermore, the development of methods that enable the direct immobilization of expressed proteins from cellular lysates would be of great value (Weinrich et al., 2010; Sielaff et al., 2006). To address this issue, this work aims to develop a new strategy for the immobilization of proteins equipped with oxyamine groups at the *C*-terminus on ketone-coated surfaces to generate protein microarrays, which can be further used to study protein-protein interactions (Figure 3.9).

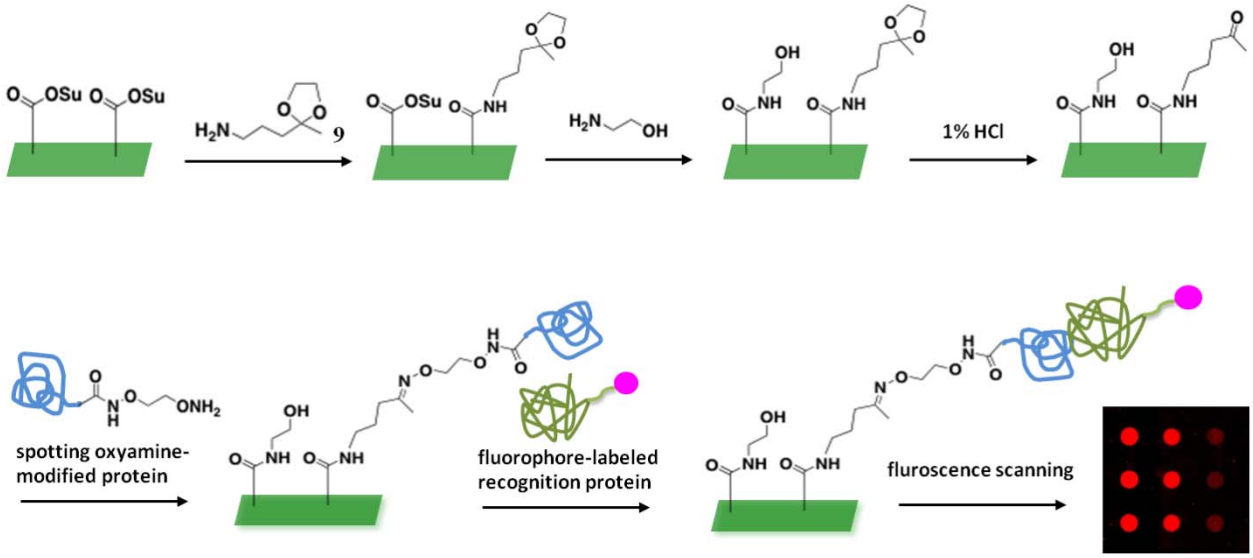

Figure 3.9. Schematic illustration of the immobilization of proteins equipped with oxyamine groups at the *C*-terminus on ketone-coated surfaces and its use for the detection of protein-

protein interactions. Su = succinimide. (This work is in close cooperation with Dr. Yong-Xiang Chen in Prof. Waldmann's group)

To establish the method, glass slides activated with *N*-hydroxysuccinimide (NHS) esters (SCHOTT NEXTERION® Slide P) were firstly coated with a linker incorporating a 5-amino-2-pentanone ethylene ketal **9**, and then blocked with ethanolamine (Figure 3. 9). After the deprotection of the ketone by treatment with a 1% HCl solution, the ketone-coated slides were ready for protein immobilization via the oxyamine ligation.

To this end, an enhanced green fluorescent protein tagged Rab7 protein equipped with an oxyamine group at the *C*-terminus (EGFP-Rab7Δ15-ONH_2) was prepared by EPL approach as previously described. EGFP-Rab7Δ15-ONH_2 and EGFP-Rab7Δ15-thioester (negative control) in neutral buffer (pH 7.0) were spotted on a ketone-functionalized slide and incubated in a humidity chamber at room temperature. After washing out non-reacting proteins, the protein immobilization efficiency can be demonstrated by quantifying the fluorescence intensity of protein spots on the slides. The preliminary experiments showed that immobilization of EGFP-Rab7Δ15-ONH_2 gave intense fluorescence signals, whereas almost no signal was observable for EGFP-Rab7 thioester (Figure 3.10a). The ratio of average fluorescence intensity between these two proteins was 478:1, indicating that the oxyamine proteins could be selectively and efficiently immobilized on the ketone-coated slides by the oxyamine ligation.

Aniline can catalyze the oxime ligation in neutral buffer (Dirksen et al., 2006; Yi et al., 2010). However, when a 100 mM solution of aniline was included in the protein solution, the immobilization efficiency improved only moderately (Figure 3.10b, ratio of average fluorescence intensity 1:1.8). Considering the need of an organic cosolvent to solubilize aniline (see experimental part for detail) and the potentially negative effect of organic solvents on protein samples, we decided to investigate an aniline-free oxyamine ligation for preparation of protein biochips.

In order to optimize the conditions for protein immobilization, EGFP-Rab7-ONH_2 was incubated with ketone-coated slides for different time frames at room temperature after spotting. The time-dependent immobilization efficiencies were reflected by average fluorescence intensities (Figure 3.10c), and incubation for 6 hours appeared to be an optimal condition. Therefore, six hours was selected as general incubation time for immobilizing oxyamine-modified proteins on ketone-coated slides.

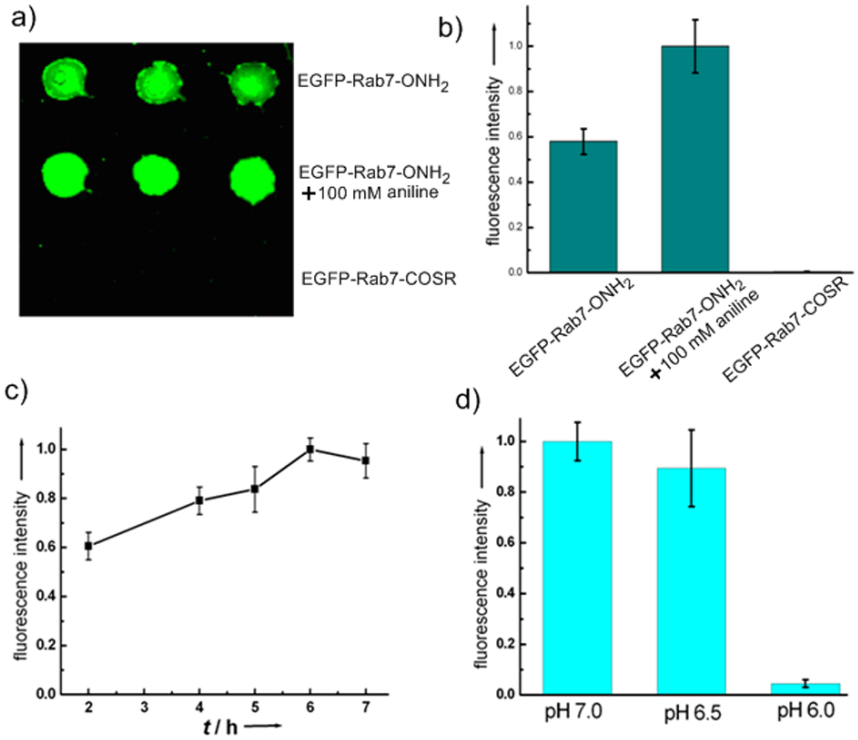

Figure 3.10. Optimization of the immobilization conditions for EGFP-Rab7-ONH_2 on the ketone-coated slides. a) Fluorescence image of the slide with EGFP-Rab7-ONH_2 without and with 100 mM aniline and the control EGFP-Rab7-COSR at pH 7.0 for 6 hours b) Quantified relative fluorescence intensities after immobilization of proteins at pH 7.0 for 6 hours. c) Time-dependent immobilization efficiency of EGFP-Rab7-ONH_2 under neutral condition reflected by relative fluorescence intensity. d) Relative fluorescence intensity of the immobilization of EGFP-Rab7-ONH_2 at different pH values.

The oxime ligation normally proceeds much faster at lower pH (4.5) than at pH 7.0 (Dirksen et al. 2006). The oxime ligation has been used previously for site-specific protein immobilization on oxyamine-coated surfaces under weakly acidic conditions, which employ proteins equipped with ketone groups (Christman et al., 2007). Hence, we probed the immobilization of EGFP-Rab7-ONH_2 at different pH values. The quantification of fluorescence intensities (Figure 3.10d) indicated that the immobilization of EGFP-Rab7-ONH_2 at pH 7.0 and 6.5 proceeded with similar efficiency whereas almost no signal was observable for the protein at pH 6.0, probably due to the instability of EGFP-Rab7-ONH_2 on the slides at lower pH value. Similar results were obtained for oxyamine-modified mCherry-Rab7 (Figure 3.11). Immobilization of mCherry-Rab7-ONH_2 at pH 7.0 gave intense fluorescence signals, whereas almost no signal was observable for mCherry-Rab7 thioester or for the oxyamine-modified protein at pH lower than 6.5 (Figure 3.11), again implying that our oxyamine ligation strategy is general and efficient for protein immobilization. Moreover, since most proteins are more stable under neutral conditions than under weakly acidic

conditions, the use of neutral pH for protein immobilization renders the oxyamine ligation a more general method for protein immobilization.

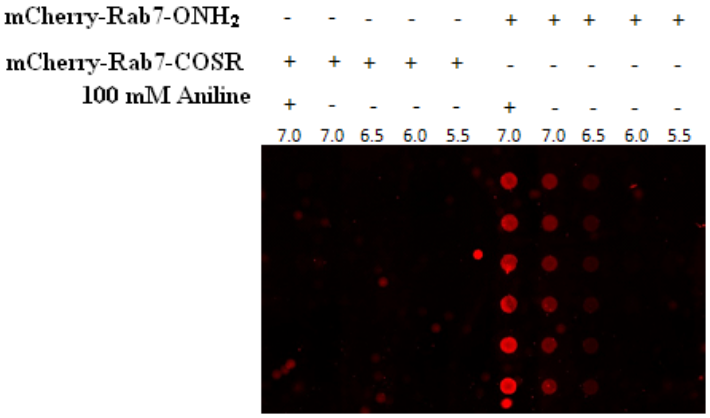

Figure 3.11. Immobilization of mCherry-Rab7-COSR and mCherry-Rab7-ONH_2 on ketone-coated slides at different pH values with and without aniline catalysis. The slides were incubated with the protein solution at room temperature for 4 hours.

3.1.6. Chip-based protein-protein interactions

The generated protein biochips should be valuable tools for the study of protein-protein interactions. To investigate this possibility, we used the EGFP-Rab7 protein microarray for the analysis of a protein-protein interaction (Figure 3.12). Hence, the slides with immobilized EGFP-Rab7 were treated with a 200 nM solution of a Cy3-labeled Rab escort protein 1 (Cy3-REP-1) and with a 1 µM solution of Cy3-labeled Rab GDP dissociation inhibitor (Cy3-RabGDI), respectively. REP-1 has high binding affinities (nM) for unprenylated Rab proteins. In contrast, RabGDI binds unprenylated Rab proteins with micromolar or even lower affinity (Wu et al., 2007). After treatment of the slide with Cy3-REP-1, clear fluorescence signals were detected, which indicated the recognition of EGFP-Rab7 by Cy3-REP-1. For Cy3-RabGDI (1 µM), almost no fluorescence signal was detected, indicating no interaction between immobilized EGFP-Rab7 and Cy3-RabGDI at this concentration (Figure 3.12b). We further employed protein kinase A α-subunit (PKA) for protein immobilization and used a fluorescein-labeled PKA antibody for detection. As shown in Figure 3.12c, the slide with immobilized PKA-ONH_2 shows strong fluorescence after treatment with a FITC-labeled PKA antibody, while in the case of PKA-COSR the fluorescence is weak. The efficiency of the immobilization was investigated employing different protein concentrations. PKA-ONH_2 was immobilized at concentrations ranging from 100 µM to 5 µM. A concentration-dependent signal was detected in all cases (Figure 3.12d). These results demonstrate that the

immobilization of oxyamine-functionalized proteins on ketone-coated slides maintains the correct tertiary structure of the proteins, and that the generated protein chips can be used for the study of protein-protein and antigen-antibody interactions even at low protein concentrations.

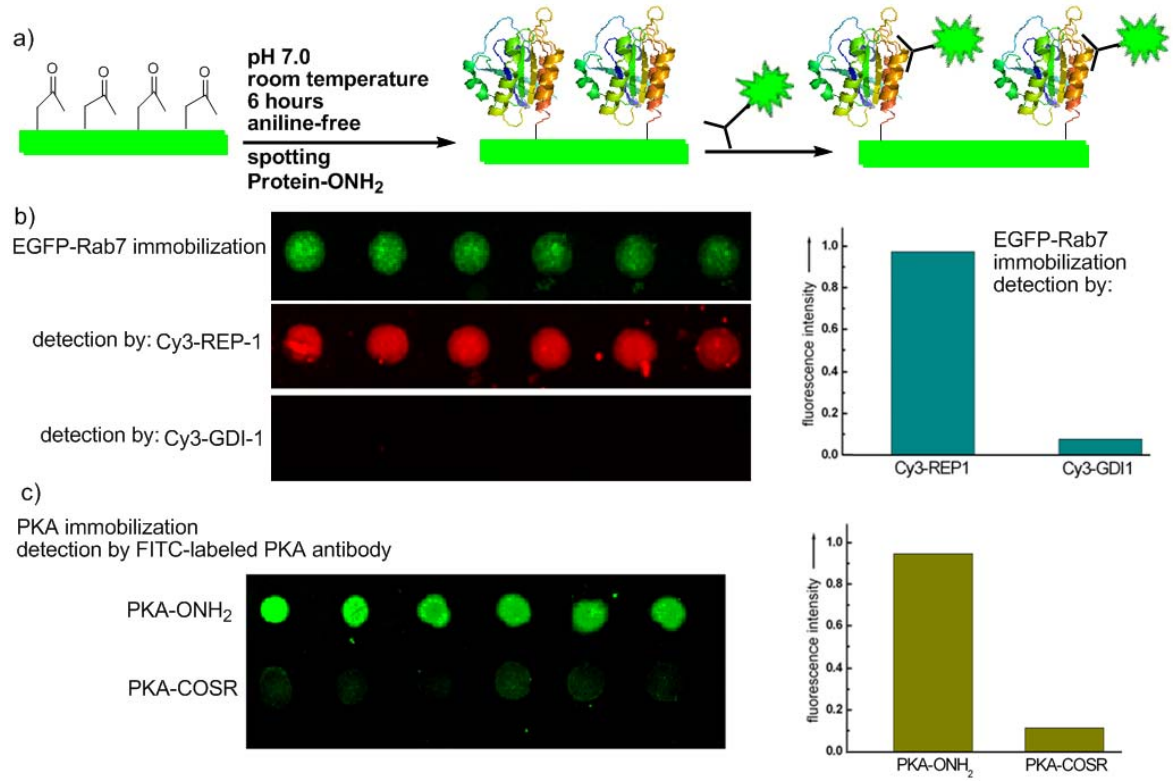

Figure 3.12. Interaction analysis of immobilized proteins with fluorescently-labeled recognizing proteins. a) Schematic showing the spotting conditions and subsequent protein-protein interaction analysis. b) Immobilization of 50 µM EGFP-Rab7 followed by detection with 200 nM Cy3-REP-1 and 1 µM Cy3-RabGDI. The ratio of average fluorescence intensity between that of REP-1 and GDI-1 is about 20:1. c) Immobilization of 50 µM PKA followed by detection with 500 nM FITC-labeled PKA antibody. The ratio of average fluorescence intensity between that of PKA-ONH_2 and PKA-COSR is about 8:1. d) Different concentrations of PKA-ONH_2 were immobilized on ketone-coated microarray and then detected by incubation with a 500 nM solution of FITC-labeled antibody.

3.1.7. Labeling and immobilization of target proteins from cell lysates

The selective reactivity of bis(oxyamine) towards thioester bonds at high concentrations and the tandem bioorthogonal oxyamine ligation should enable the direct modification and immobilization of expressed proteins from crude cellular lysates without further purification.

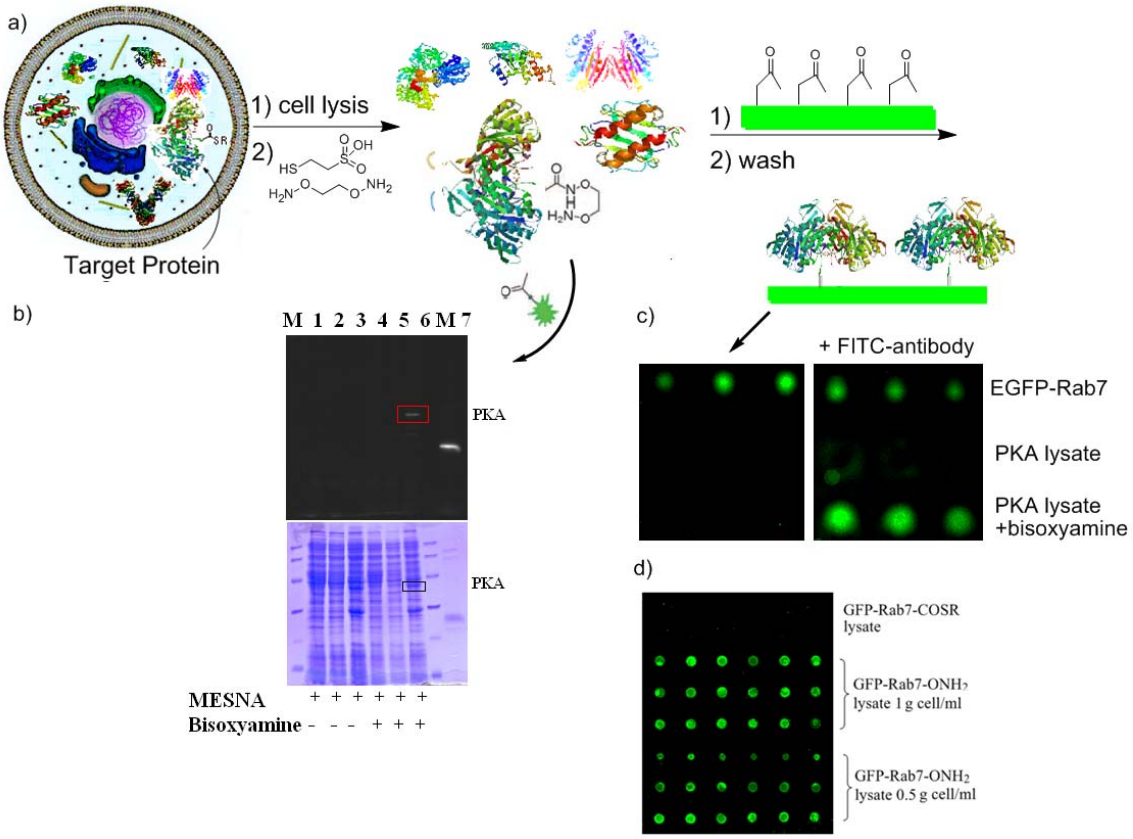

Figure 3.13. Proteins can be site-specific tagged with bis(oxyamine) and subsequently labeled with fluorophores or direct immobilized on ketone-coated surfaces. a) Schematic showing the principle of the method. b) SDS-PAGE analysis of *E. coli* lysates after treatment with MESNA and bis(oxyamine) followed by incubation with keto-fluorescein. Lanes 1 and 4, no transfection of PKA gene; lanes 2 and 5, transfection of PKA gene but without induction by IPTG; lanes 3 and 6, transfection with PKA gene and induction by IPTG. Lane M, maker for 97, 66, 45, 30, 20, 14.4 KDa; lane 7, Rab7-fluorescein (Yi et al., 2011) as a fluorescent marker. c) Direct immobilization of cellular lysates containing expressed PKA on ketone-coated slides followed by detection with 500 nM FITC-labeled PKA antibody. Pure oxyamine-modified EGFP-Rab7 protein was used as positive control. d) Direct immobilization of cellular lysates containing expressed GFP-Rab7 on ketone-coated slides.

To investigate this possibility we explored the selective labeling and site-specific immobilization of PKA from cell lysates (Figure 3.13). To this end, the PKA-intein fusion protein was overexpressed in *E. coli* and the corresponding soluble cellular fractions without further purification were treated overnight with a 500 mM solution of MESNA at room temperature followed by reaction with a 300 mM solution of bis(oxyamine) on ice for 4 hours. After dialysis against phosphate buffer (pH 7.5) in the presence of protein inhibitor, the resulting solution was incubated with keto-fluorescein for 6 h. The oxyamine-modified PKA was selectively labeled with keto-fluorescein as indicated by the presence of a fluorescent band with the correct molecular weight on SDS-PAGE (Figure 3.13b), thus demonstrating the successful labeling of proteins directly from *E. coli* expression lysates.

The direct immobilization of oxyamine-modified proteins was investigated by employing PKA expression lysates directly for spotting (Figure 3.13c). The strong fluorescence signal of the microarray obtained after treatment with a FITC-labeled PKA antibody proves the successful immobilization of oxyamine-modified PKA from *E. coli* lysates. Similarly, direct immobilization of EGFP-Rab7 in cellular lysates resulted in a strong fluorescence signal indicating the covalent attachment of the proteins (Figure 3.13d) and thus the selective immobilization of oxyamine-modified GFP-Rab7 from cellular lysates, while no signal could be detected when the cellular lysates were not treated with bis(oxyamine) (GFP-Rab7-COSR).

3.1.8. Conclusion

A facile, chemoselective, efficient and potentially general strategy for C-terminal protein modification and immobilization has been developed. Some key points are highlighted as follow:

1. For the first time, a high concentration of oxyamine is used for the selective aminolysis of thioester bonds in proteins.
2. Oxyamine-modified proteins can be produced by this new chemical reaction of bis(oxyamine) with protein thioester at pH 7.5.
3. The oxyamine group on protein C-terminus is efficient for oxyamine ligation both in solution and on solid surface at pH 7.0.
4. The selective reactivity of bis(oxyamine) towards thioester bonds at high concentrations and the tandem bioorthogonal oxyamine ligation enable the direct modification and immobilization of expressed proteins from crude cellular lysates.

As a useful alternative to existing approaches for protein labeling, the rapid reaction of the oxyamine-modified proteins with ketones under mild condition is intriguing and potentially advantageous for many biological applications including synthesis of Rab protein probes and construction of protein microarray. The produced protein probes and biochips can be used for the study of protein-protein interactions, as indicated by Rab-REP and PKA-antibody interaction studies. This strategy expands the repertoire of protein labeling and immobilization methods and provides an alternative means to meet the various requirements for protein modification and immobilization.

3.2. Development of universal strategies for quantitative labeling of N-Cys-proteins and one-pot dual-color labeling of a protein

3.2.1. Introduction

Multi-color labeling is a valuable technique for the characterization of proteins with respect to their structure, folding, and interactions both as single molecules and in cellular investigations. The key technique for such studies is based on FRET (Giepmans et al., 2006; Piston et al., 2007; Roy et al., 2008; Weiss, 1999). FRET applications require the attachment of donor and acceptor molecules to specific sites of a given protein or proteins. Such labeling is typically achieved through conjugation at cysteine residues or amino groups or by genetic fusion to different fluorescent proteins (Hong et al., 2003; Schleifenbaum et al., 2004; Lee et al., 2010; Szilvay et al., 2009). However, site-specific incorporation of multiple fluorophores into a single protein remains a considerable challenge. Dual-labeling of a single protein has been achieved using multi-step reactions. For example, sortases with different substrate specificity were used for site-specific C- and N-terminal labeling of a single protein (Antos et al., 2009). The Muir lab reported a method for producing a dual-labeled protein through a multi-step expressed protein ligation approach (Cotton et al., 2000). Recently, Yang et al. used a three-step strategy based on split inteins for site-specific two-color protein labeling (Yang et al., 2009). This work aims to develop a facile and efficient method for dual-labeling of proteins based on two chemoselective reactions.

Frequently used chemoselective reactions include NCL, Staudinger ligation, click chemistry, oxime ligation, strain-promoted cycloaddition, and Diels-Alder ligation (Sletten et al., 2009). We reasoned that by employing two chemoselective reactions for protein labeling, it should be possible to obtain dual-color labeled proteins in a one-pot reaction in a straightforward fashion (Figure 3.14a).

A facile and efficient method for C-terminal modification of proteins is developed in part 3.1. For N-terminal labeling, a protein containing an N-terminal cysteine can undergo NCL with thioester probes (Dawson et al., 1994; 2000). Hence, we speculated that both NCL and oxime ligation could be employed for one-pot dual-color labeling of a given protein (Figure 3.14b) (Rose, 1994; Canne et al., 1995). Coumarin as FRET donor and fluorescein as FRET acceptor were chosen, considering both of which can be easily prepared from commercially available reagents (see experimental part for details). Herein we develop a strategy for constructing a

dual-labeled Rab7 GTPase in a one-pot reaction with quantitative conversion and illustrate the use of the produced Rab probe for studying protein refolding and protein-protein interactions.

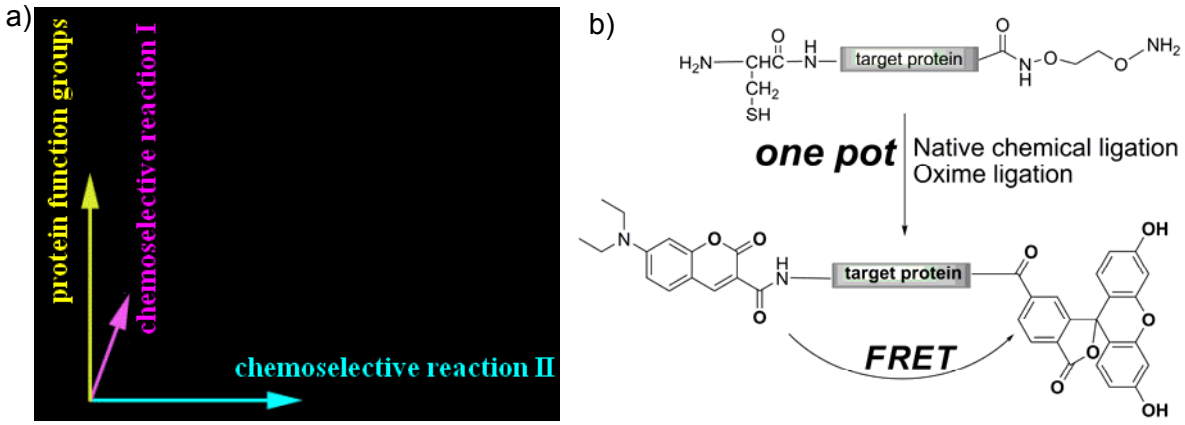

Figure 3.14. a) Schematic showing the orthogonality for two chemoselective reactions and protein function groups. b) Strategy for preparation of a dual-color coumarin-fluorescein protein by one-pot oxime ligation and native chemical ligation.

3.2.2. N-terminal modification of N-Cys-proteins

The exposure of an N-terminal cysteine can be achieved via a TEV (tobacco etch virus) protease cleavage. Hence, a hexahistidine-tag (His6-tag) followed by the TEV protease cleavage sequence was fused to the N-terminus of the target protein. A cysteine mutation was introduced at the P1′ position of TEV cleavage site (Figure 3.15a). The resulting plasmid was transformed into *E. coli* BL21(DE3) cells for expression of TEV-Cys-proteins. After protein expression and purification, the TEV protease cleavage of the His_6-tagged proteins was carried out at room temperature (see experimental part for detail). The produced N-terminal cysteine proteins were purified on a Ni-NTA column to remove His_6-TEV protease and uncleaved His-tagged proteins and characterized by SDS-PAGE (Figure 3.15c) and ESI-MS (Figure 3.15d). Such a general strategy for preparing N-Cys-proteins has been successfully applied to DrrA (GEF of Rab1) and Rcc1 (GEF of Ran).

Our next goal aimed to achieve quantitative conversion during the NCL-based N-terminal protein modification. We chose coumarin thioester **10** (quantum yield of 0.27) as FRET donor and keto fluorescein **3** (quantum yield of 0.97) as FRET acceptor, both of which can be easily prepared from commercially available reagents. A dansyl-thioester **11** was also prepared (from Dr. Wei Liu in Wu's group), since that the dansyl fluorophore under UV exposure is much brighter than that of coumarin. The NCL reaction for N-terminal modification was not complete after incubation on ice for three days using MESNA as a thiol cofactor (checked by

LCMS). We then used **11** for optimization of reaction conditions on SDS-PAGE. Kent et al. reported that the addition of 200 mM MPAA ((4-carboxymethyl)thiophenol) can significantly accelerate the native chemical ligation during protein total synthesis (Johnson et al., 2006). Herein we tested the reaction of N-Cys-Rcc1 with **11** (Figure 3.16b,c) and found that 200 mM MPAA can greatly increase the protein labeling efficiency. The further reaction kinetics of N-Cys-Rcc1 and **11** in the presence of 200 mM MPAA indicated that the half-life reaction time is about 24 minutes (Figure 3.16d). The reaction can be complete within 2-3 h under such reaction conditions. Quantitative modification of N-Cys-DrrA with **10** can also be achieved by similar reaction condition, as indicated by both SDS-PAGE and ESI-MS (Figure 3.16e-g).

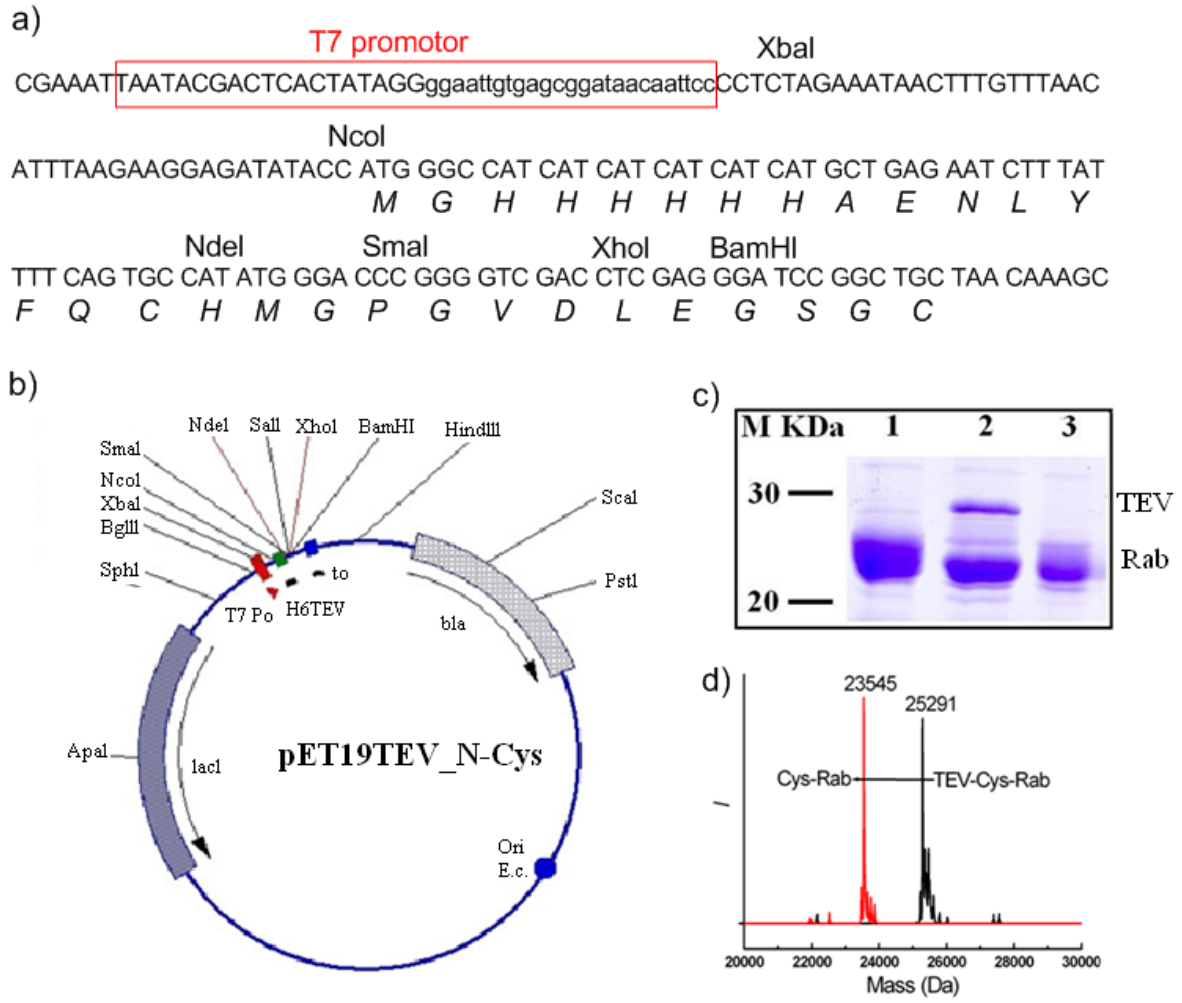

Figure 3.15. a) and b) The gene sequence around T7 promotor in the pET19TEV_N-Cys vector. c) SDS-PAGE analysis of Rab7 proteins. Lane 1, TEV-tag-Rab7Δ3-ONH_2; Lane 2, N-Cys-Rab7Δ3-ONH_2 before removing TEV protease; Lane 3, N-Cys-Rab7Δ3-ONH_2. d) ESI-MS spectra of TEV-tag-Rab7Δ3-ONH_2 ($M_{calc.}$ 25291) and N-Cys-Rab7Δ3-ONH_2 ($M_{calc.}$ 23544).

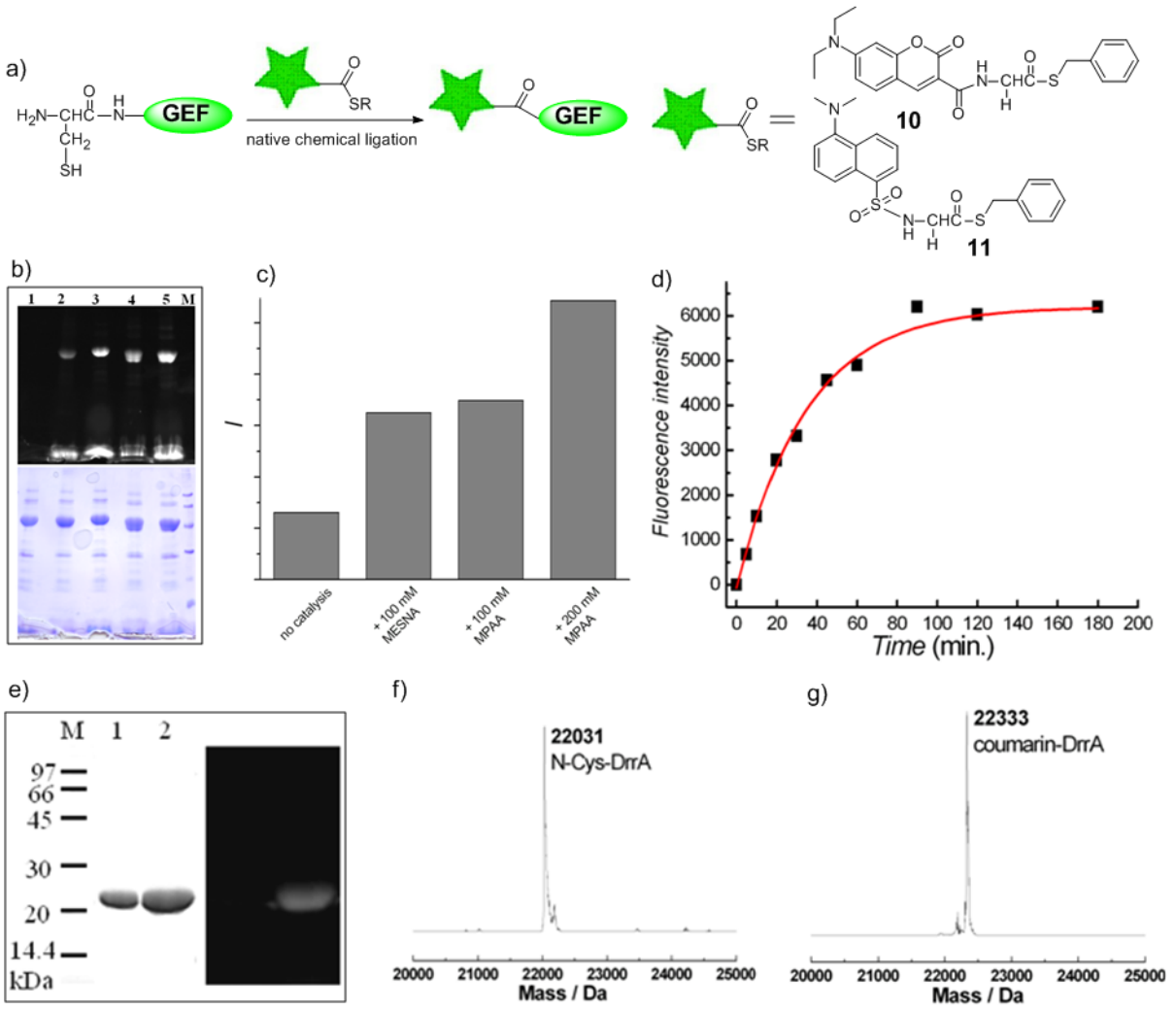

Figure 3.16. a) Strategy for N-terminal protein modification with thioester-containing fluorophores **10** and **11**. b) SDS-PAGE of N-Cys-Rcc1 (50 μM) with **11** (500 μM) at room temperature for 2 h with fluorescence scan (up) and Coomassie staining (down). Lane 1, Rcc1 only; lanes 2-5, the reaction with no thiol catalysis, 100 mM MESNA, 100 mM MPAA, 200 mM MPAA, respectively. c) Relatively fluorescent intensities of labeling Rcc1 proteins in SDS-PAGE. d) Reaction kinetics of N-Cys-Rcc1 (50 μM) with **11** (500 μM) at room temperature in the presence of 200 mM MPAA revealed by relatively fluorescent intensities of labeling Rcc1 proteins in SDS-PAGE. e) SDS-PAGE of N-Cys-DrrA (lane 1) and N-coumarin-DrrA (lane 2) with Coomassie staining (left) and fluorescence scan (right). f) and g) ESI-MS spectra of N-Cys-DrrA (M_{calcd} = 22028) and coumarin-DrrA (M_{calcd} = 22328), respectively.

There are many strategies for site-specific protein modification at the N terminus because the N-terminal amine of a protein has unique pH-dependent reactivity. Its decreased pK_a value relative to amine groups on lysine side chains renders selective modification possible in the presence of many competing lysine side chains. For example, transamination reactions optimized by Francis et al. have been particularly successful for selective modification of the N-terminal amine (Gilmore et al., 2006). Extensive characterization revealed that the

transamination reaction proceeded best when Ala, Gly, Asp, Glu, or Asn occupied the N-terminal position. This reaction also occurred with many other N-terminal residues, but the yields were variable (Scheck et al., 2008). Very recently, a method of highly selective N-terminal modification of proteins (modified α-amino group/modified ε-amino group > 99:1) by an isolated ketene at pH 6.3 was developed by Che et al. (Chan et al., 2012). Other chemical methods for N-terminal modification rely on a specific residue at the N terminus. For example, N terminal serine and threonine residues undergo periodate oxidation to form glyoxylamides (Geoghegan et al., 1992). The aldehyde moiety of the glyoxylamide can then be modified with hydrazide or aminooxy reagents. A Pictet–Spengler reaction can selectively modify N-terminal tryptophan and histidine residues with aldehyde probes (Li et al., 2000). N-Terminal cysteine residues have also been exploited in the highly successful method of protein modification known as native chemical ligation (Tolbert et al., 2002). In this project, I have developed the MPAA-catalysis NCL as a universal strategy for labeling of protein N terminus with advantages containing: 1) quantitative modification; 2) potentially orthogonal reaction with the oxyamine ligation; 3) operationally facile and practical. The reaction conditions were mild enough for labeling of different proteins such as Rabs, DrrA and Rcc1.

3.2.3. N/C-terminal dual-labeling of N-Cys-Rab7Δ3-ONH_2

To generate a doubly functionalized Rab7 protein with an N-terminal cysteine and a C-terminal oxyamine, N-Cys-Rab7Δ3-ONH_2, a TEV cleavage peptide sequence was firstly fused to the N terminus of the Rab7Δ3 protein as described above (part 3.2.2). Rab7Δ3 fused N-terminally to an engineered Mxe GyrA intein domain can undergo initial N→S acyl transfer and be subsequently cleaved by thiol reagents, releasing a thioester-tagged protein. Subsequently, the Rab7Δ3-thioester (10 mg/mL, 400 μM) was treated with 500 mM bis(oxyamine) at pH 7.5 to produce the oxyamine-modified protein. After dialysis to remove bis(oxyamine), TEV protease was then added to cleave the N-terminal protection sequence to expose the N-cysteine (Figure 3.17). The produced N-Cys-Rab7Δ3-ONH_2 was purified on a Ni-NTA column to remove His_6-TEV protease and uncleaved His-tagged proteins.

Before performing the one-pot dual-labeling of N-Cys-Rab7Δ3-ONH_2, it was necessary to prove that both native chemical ligation and oxime ligation are orthogonal in the labeling conditions.

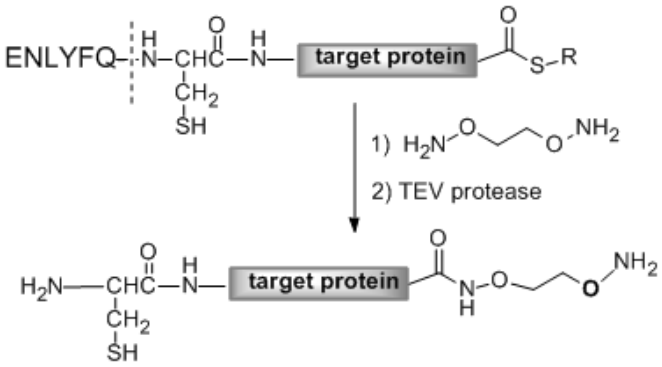

Figure 3.17. A strategy for producing of N-Cys-Rab7Δ3-ONH_2.

In order to show the specificity of the N-terminal labeling reaction, oxyamine-tagged proteins without the N-terminal cysteine, TEV-Rab7Δ3-ONH_2 and Rab7Δ7-ONH_2, were chosen as controls. Under the same reaction conditions, coumarin-thioester (**10**) did not show cross reaction with oxyamine tagged proteins (Figure 3.18a), suggesting the chemoselectivity of the NCL reaction. This was further confirmed by evaluating the reaction using ESI-MS. A mixture of about 0.23 mM Rab7-ONH_2 and 0.5 mM coumarin-thioester in the presence of 200 mM MPAA was incubated on ice in the phosphate buffer (pH 7.5) for 24 h. LC-ESI-MS of the protein before and after reaction suggested no reaction between coumarin-thioester and Rab7-ONH_2 under these conditions (Figure 3.18b).

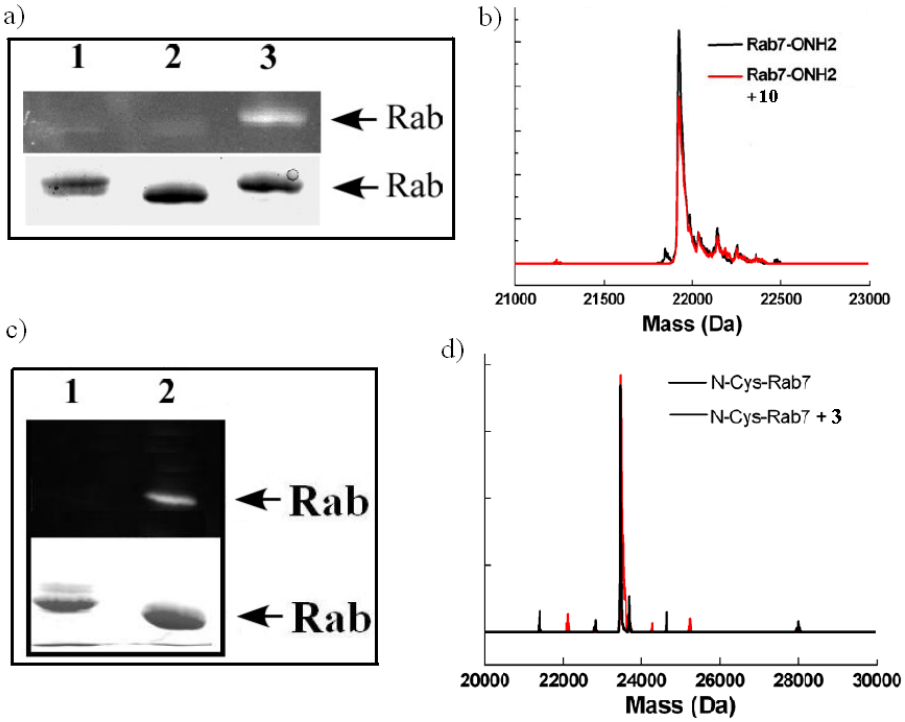

Figure 3.18. a) SDS-PAGE of the reaction of **10** with TEV-Rab7-ONH_2 (lane 1), Rab7Δ7-ONH_2 (lane 2) and N-Cys-Rab7Δ3-ONH_2 (lane 3). Fluorescence scan and Coomassie staining were shown in the upper and lower panel, respectively. Reaction conditions: 1 mg/mL (43 μM)

protein, 0.7 mM **10**, 200 mM MPAA, room temperature, 3 h. b) ESI-MS spectra of Rab7-ONH_2 before (black line) and after (red line) reaction with **10**. c) SDS-PAGE of the reaction of **3** with N-Cys-Rab7Δ3-CONHOH (lane 1) and Rab7Δ7-ONH_2 (lane 2). Fluorescence scan and Coomassie staining were shown in the upper and the lower panel, respectively. Reaction conditions: 1 mg/mL (43 μM) protein, 1 mM **3**, 100 mM aniline, pH 7.0, on ice for 6 h. d) ESI-MS spectra of N-Cys-Rab7Δ3-CONHOH before (black line) and after (red line) reaction with **3**.

In order to show the specificity of the C-terminal labeling reaction, a Rab protein containing N-terminal cysteine, N-Cys-Rab24, was used as a control. Under the same reaction conditions, keto-fluorescein did not show cross reaction with N-Cys-Rab24 (Figure 3.18c), suggesting the chemoselectivity of the oxime ligation reaction under these conditions. This was further confirmed by evaluating the reaction using ESI-MS. A mixture of about 43 μM N-Cys-Rab7Δ3- CONHOH or Rab7Δ7-ONH_2 and 1 mM keto-fluorescein in the presence of 100 mM aniline was incubated on ice in the phosphate buffer (pH 7.0) for 6 h. LC-ESI-MS of the protein before and after reaction suggested no reaction between keto-fluorescein and N-Cys-Rab7Δ3-CONHOH under these conditions (Figure 3.18d).

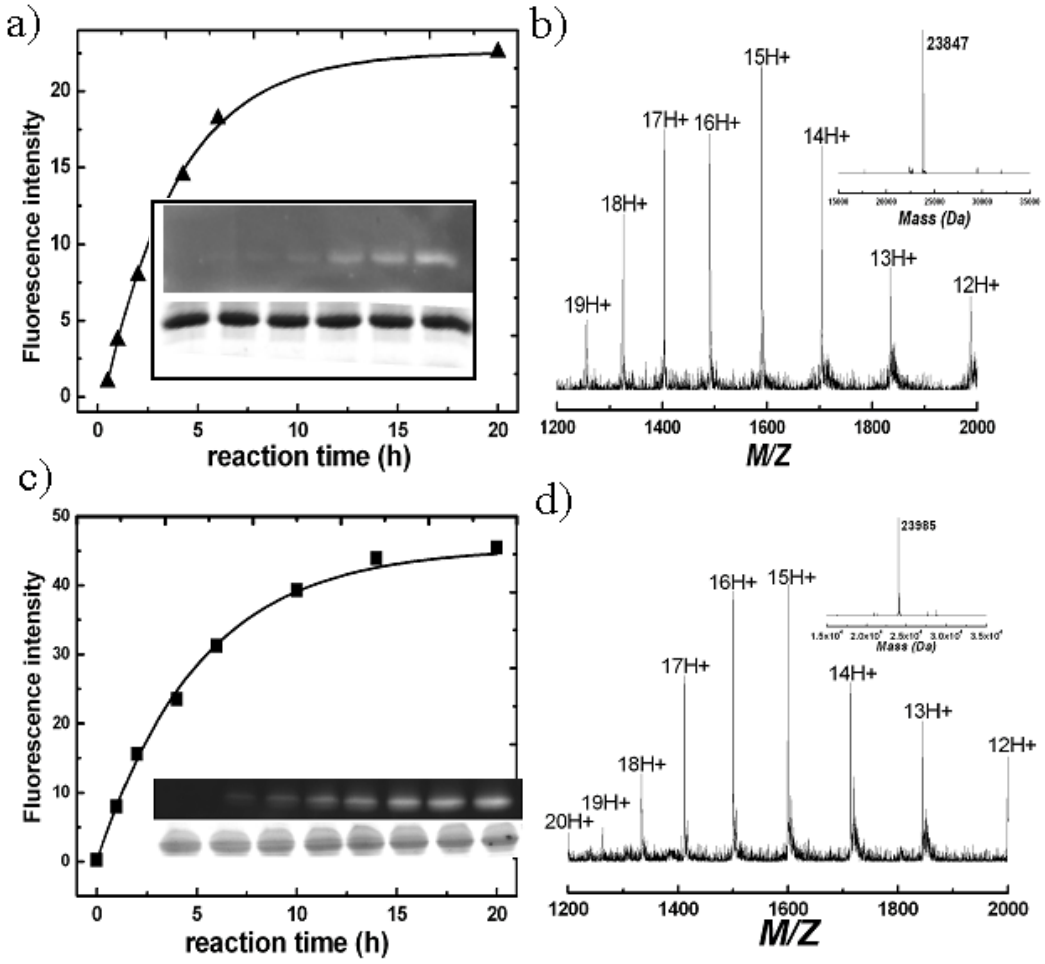

Figure 3.19. Reaction kinetics of 40 µM N-Cys-Rab7Δ3-ONH_2 protein and 160 µM **10** in the presence of 200 mM MPAA (a) or 0.4 mM **3** in the presence of 100 mM aniline (b) through incubation on ice in sodium phosphate buffer (pH 7.0) and the approximations of the first-order reactions (solid lines) with reaction half-lives of about 2.5 and 3.5 hours, respectively. c) and d) The ESI-MS spectra indicated that both reactions were finished after one day incubation.

Now that the cross reaction of coumarin thioester with oxyamine tagged proteins and keto-fluorescein with N-Cys-proteins were not observed, the next step was to optimize the quantitative conversion of both N- and C-terminal modification for the double-functionalized N-Cys-Rab7Δ3-ONH_2 protein. The first-order reaction of the Rab protein and **3** or **10** was performed on ice in the presence of catalysis, and the extent of protein labeling was monitored over 20 hours by SDS-PAGE. Following protein separation on a SDS-PAGE gel, the labeled protein was visualized and quantified by a fluorescence gel scanner (Figure 3.19). In both cases, the labeling was shown to reach near completion (> 95% labeling) within 20 hours of the reaction. The site-specific nature of both labeling reactions was confirmed by ESI-MS results (Figure 3.19).

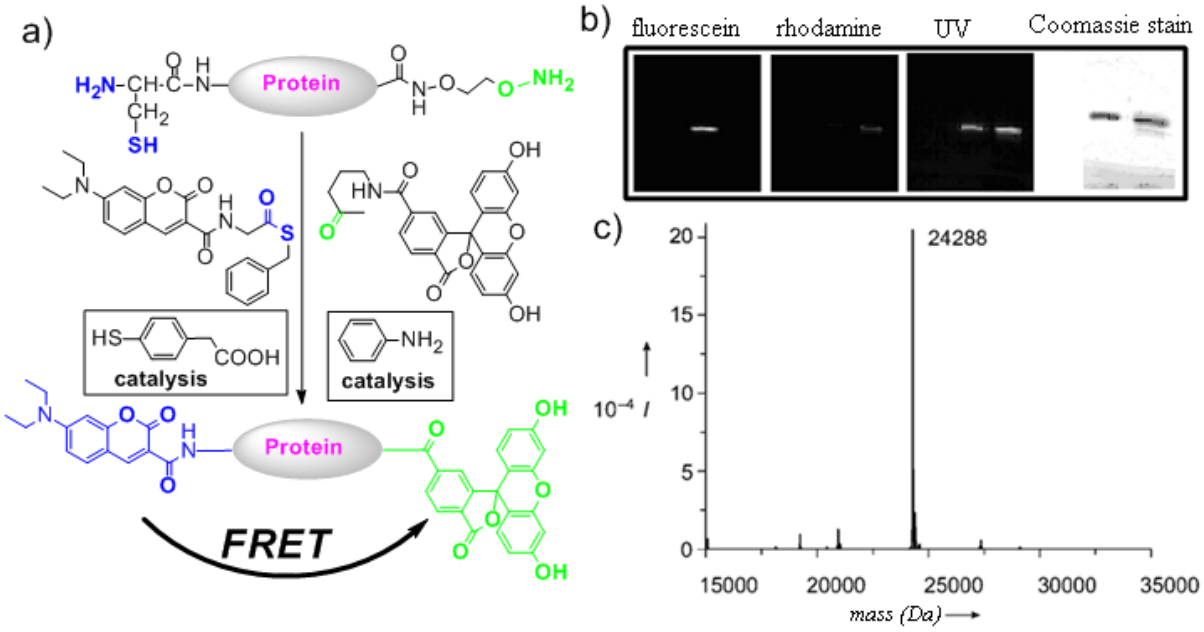

Figure 3.20. a) Strategy for the preparation of a two-color Rab7 protein by two chemoselective reactions. b) SDS-PAGE of the dual-label proteins N-coumarin-Rab7Δ3-fluorescein (left lane) and N-coumarin-Rab7Δ3-rhodamine (right lane). Photos from left to right: emission in the blue fluorescence mode with cut-off filter at 530 nm showing mainly fluorescein fluorescence; emission in the green fluorescence mode with cut-off filter at 605 nm showing mainly rhodamine fluorescence; excitation with UV light and emission without cut-off filter; Coomassie blue staining result. c) ESI-MS spectrum of coumarin-Rab7-fluorescein (M_{calcd} = 24287).

Because both labeling reactions are near quantitative and show not cross reaction under the reaction conditions, the tandem NCL and oxime ligation reactions could be used for producing two-color labeled proteins (Figure 3.20). A mixture of 3 mg/mL (130 μM) protein and 0.7 mM coumarin **10** in the presence of 200 mM MPAA was incubated at room temperature for 3 h. The resulting solution was diluted into 4 volumes of sodium acetate buffer (50 mM, pH 5.5) and incubated with **3** (0.5 mM) in the presence of 100 mM aniline on ice. The quantitative dual-labeling of Rab7 protein was confirmed by LCMS and SDS-PAGE after overnight reaction (Figure 3.20).

Encouraged by these results, I next tested whether the orthogonality of the transformations suffices from one-pot dual-labeling of a protein. I found that the oxime ligation was not affected by MPAA and coumarin thioester. Further experiments showed that one-pot dual-labeling could be achieved simply by incubation of both 0.5 mM **10** or keto-rhodamine **12** and 0.5 mM **3** with 43 mM protein N-Cys-Rab7Δ3-ONH_2 on ice for one day in the presence of catalysts 200 mM MPAA and 100 mM aniline. Quantitative conversion of N-Cys-Rab7Δ3-ONH_2 to the dual-labeled N-coumarin-Rab7Δ3-fluorescein and N-coumarin-Rab7Δ3-rhodamine protein was observed by ESI-MS and fluorescent SDS-PAGE (Figure 3.20). High yields of fluorescent labeled proteins are very important, because poor labeling efficiency reduces the quality of FRET measurements or requires additional purification steps. After removing excess small molecules on a desalting column, the obtained dual-labeled protein could be used for biophysical studies.

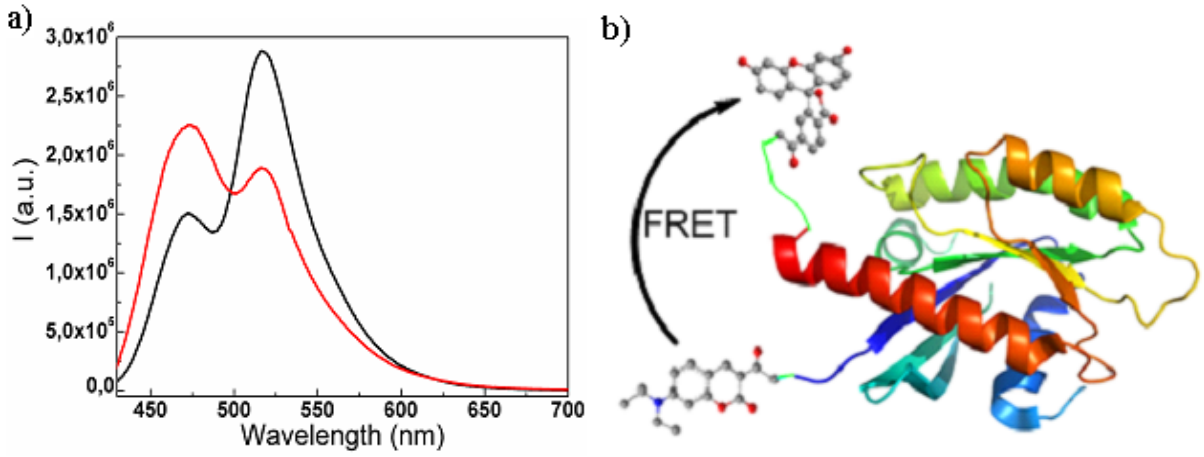

Figure 3.21. a) Emission spectra of N-coumarin-Rab7-fluorescein before (black line) and after (red line) subtilisin treatment. Excitation was at 400 nm. b) Schematic drawing of the dual-color labeling Rab7. Structures of fluorophores were generated by CHEM3D. The three-dimensional probe structure was generated by manually attached fluorophores at N-/C-terminus of Rab7 (PDB code, 1VG1).

As expected, the optical properties of the dual-labeled protein N-coumarin-Rab7Δ3-fluorescein are dominated by the acceptor chromophore (Figure 3.21a), indicating that the two fluorescent dyes located at the N- and C-terminus of Rab7 are close enough to produce an efficient FRET effect, which is consistent with the crystal structure (Figure 3.21b) (Rak et al., 2004). Digestion of Rab7 by subtilisin protease led to loss of the FRET signal. The ratio of fluorescein to coumarin emission intensities (517 nm/471 nm) upon excitation at 400 nm changes from 1.92 to 0.84 on loss of energy transfer after proteolytic digestion (Figure 3.21a). These results imply that the dual-labeling protein probe has potential to monitor protease activity.

The development of methods for specific protein decoration in multiple sites shows great relevance and impact in many fields of life science. In previous reported methods, the covalent and selective modification of multiple cysteines in an expressed protein has been achieved, taking advantage of the different solvent accessibility and reactivity of Cys residues. An alternative multiple-labeling strategy involves the modification of cellular ribosomal machinery for the introduction of unnatural amino acids with functional properties or ability to react selectively with specific probes (Sletten et al., 2009). Compared with these methods, the present labeling strategy allows for simultaneously N- and C-terminal labeling by two bioorthangonal chemical reactions with nearly quantitative conversion and without obvious cross reaction.

3.2.4. Application of the dual-labeling Rab probe

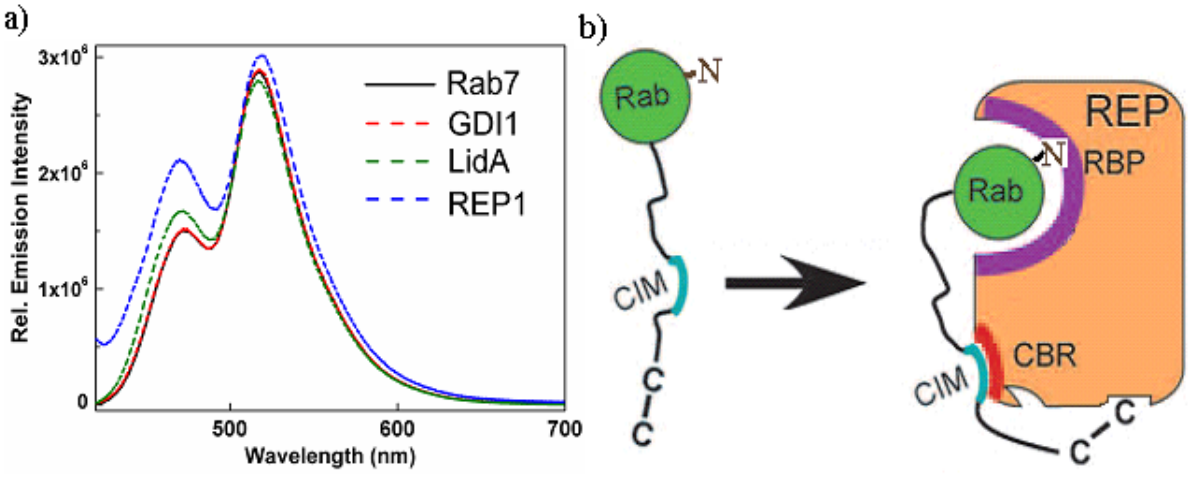

Figure 3.22. a) Binding of dual-labeled Rab7 (100 nM) with its effectors. Change of emission (excitation, 400 nm) of coumarin-Rab7-fluorescein in the presence of 10 times GDI-1, REP-1 and LidA. b) Schematic drawing of the Rab:REP interaction with the Rab C-terminal conformation change and Rab N-terminal interaction with REP.

To demonstrate the potential use of dual-labeled protein probes for protein-protein interaction studies, we examined the interaction of the dual-labeled Rab7 protein with the Rab binding proteins GDI and REP-1. As expected, addition of GDI-1 does not perturb the FRET signal (Figure 3.22), since GDI binds unprenylated Rab proteins only with micromolar or even lower affinity (Wu et al., 2007). Addition of the tightly binding REP-1 to the labeled Rab led to an increase in the fluorescence intensities of both the donor and acceptor, while the ratio of acceptor to donor intensities decreased. From a previous structural analysis (Rak et al., 2004), it was envisaged that the C-terminus of Rab7 interacts with REP-1 and becomes stretched away from the globular GTPase domain upon binding to REP-1. This would be expected to lead to an increase in the distance between the N- and C-termini of Rab7, in accordance with the decrease in FRET efficiency in the dual-labeled Rab7. The increase in fluorescence intensity may result from the fluorescence enhancement of the relatively environmentally sensitive coumarin when it binds REP-1. This was confirmed by using a single-labeled N-coumarin-Rab7 (Yi et al., 2011). When LidA, a Rab effector from *Legionella pneumophila* (Machner et al., 2006), was added to N-coumarin-Rab7Δ3-fluorescein, the interaction led to a change of the emission ratio (517 nm/471 nm) from 1.92 to 1.67, suggesting a slight conformational change when Rab7 binds to LidA. Further biophysical and structural biology studies are needed to investigate the interaction between LidA and Rab GTPases.

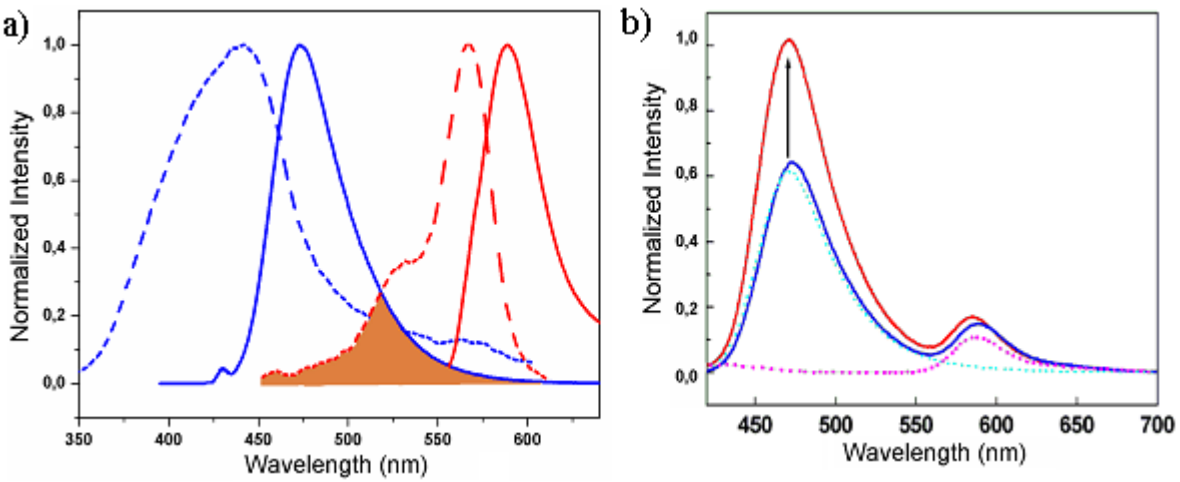

Figure 3.23. a) Absorption (dotted line) and emission (solid line) spectra of **10** (blue) and **12** (red) in phosphate buffer (pH 7.0). The spectra overlaps of the emission spectra of the donor and the absorption spectra of the acceptor are colored in orange. b) Emission spectra of N-coumarin-Rab7Δ3-rhodamine (blue line), N-coumarin-Rab7Δ3-rhodamine after the addition of REP-1 (red line), N-coumarin-Rab7Δ3-ONH_2 (dashed cyan line), and N-Cys-Rab7Δ3-rhodamine (dashed pink line). Excitation was at 400 nm.

Another dual-labeled protein, N-coumarin-Rab7Δ3-rhodamine, was prepared using the one-pot method with keto-rhodamine **12** instead of keto-fluorescein **3**. Since there is not much overlap between the absorption spectrum of rhodamine and the fluorescence emission spectrum of coumarin (Figure 3.23a), almost no intramolecular FRET was observed for this protein, which is therefore suitable to study Rab-REP interactions based solely on the change in fluorescence intensity of coumarin (Figure 3.23b). Titration of REP-1 to 80 nM N-coumarin-Rab7-rhodamine gives a value of 3.8 nM for the K_d (excitation was at 400 nm, emission was collected at 464 nm) from three independent measurements. This is close to the result determined previously using Rab7-dansyl (see Part 3.1). These results demonstrate that the dual-labeled Rab protein retains its activity for interaction with its regulator/effector, suggesting that the labeling strategy is mild enough for protein modification.

In further experiments, the use of N-coumarin-Rab7Δ3-fluorescein for protein folding studies was tested. The protein (20 µL, 0.1 mg/mL) in buffer A (50 mM HEPES, pH 7.2, 50 mM NaCl, 2 mM $MgCl_2$, 5 mM DTE) was added into 980 µl buffer A containing 0-8 M guanidine hydrochloride (G.HCl). Then the emission spectra (420-700 nm) with excitation at 400 nm were recorded. The intramolecular FRET signal decreased with increasing denaturant concentrations from 0 to 8 M (Figure 3.24a). We observed a time-dependent decrease in the FRET signal in the presence of 2 M G.HCl (Figure 3.24b). This suggests the average distance between the two dyes increased when G.HCl was used to unfold the protein.

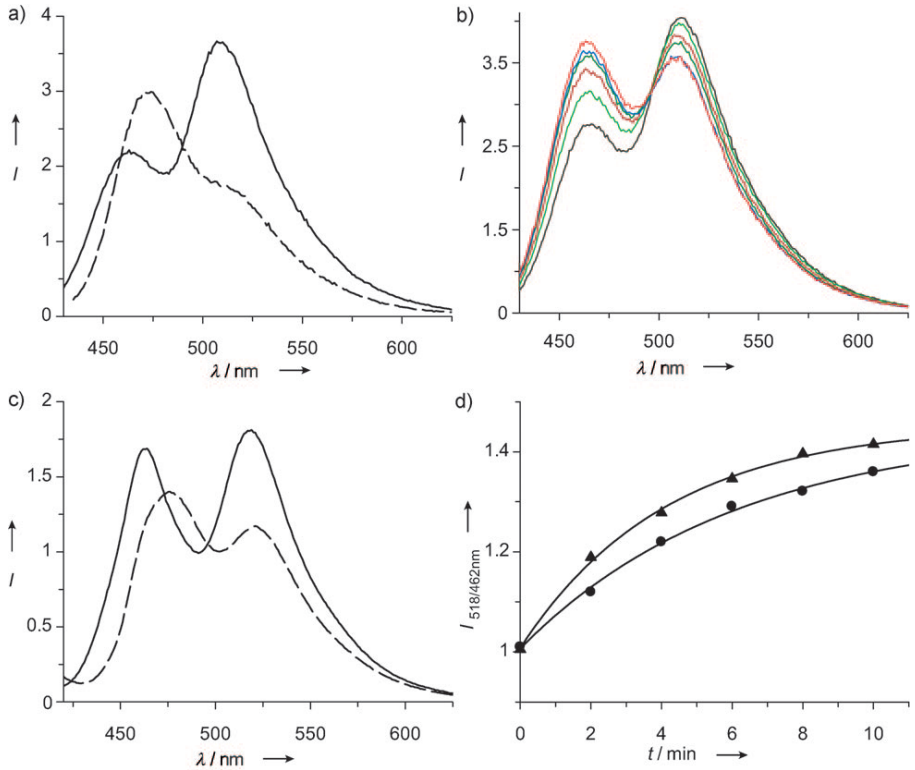

Figure 3.24. Unfolding and refolding of the dual-labeled Rab protein probe. a) Fluorescence spectra of N-coumarin-Rab7-fluorescein before (—) and after denaturation in 8 M G.HCl for 30 min (- -). Excitation was at 400 nm. b) Emission spectra of N-coumarin-Rab7-fluorescein in 2 M G.HCl. Each spectrum was recorded at 2 min intervals. T = 0 min (black), t = 10 min (pink line). c) Emission spectra of the denatured Ncoumarin-Rab7-fluorescein in 6 M G.HCl (—) and after diluting into the refolding buffer (- -). Excitation was at 400 nm. d) The emission ratio of 518 nm/462 nm (excitation at 400 nm) as function of time for refolding in the presence of GDP (●) and GppNHp (▲).

Refolding was carried out by diluting the denatured protein into refolding buffer A. In this study a 1:100 dilution of the denatured protein into refolding solution was performed. Firstly, 20 µl protein (0.1 mg/mL) was precipitated by addition of 200 µl cold methanol. Before starting renaturation the precipitated protein material had to be solubilized by strong denaturants such as 6 M G.HCl. Herein 10 µl denaturing buffer (50 mM HEPES, pH 7.2, 6 M G.HCl) was added to dissolve the protein pellet, and the resulted solution was added into 990 µl buffer A containing 50 µM GDP or GppNHp (a nonhydrolysis analog of GTP). It is reported that the presence of cofactors or substrates (e.g. GDP or GTP) during refolding has been shown to dramatically increase the yields of renaturation for Rab proteins (Durek et al., 2004). The emission ratio of 518 nm/462 nm (excitation at 400 nm) as function of time was recorded to monitor the refolding in real time. The protein was refolded with observed with refolding rate constants of 0.16 and 0.24 min^{-1} in the presence of 50 µM GDP and GppNHp, respectively (Figure 3.24c,d), suggesting similar stabilizing effects of the two nucleotides. This is in aggrement with the similar affinities of the nucleotides to Rab7 (Simon et al., 1996). Although the protein is maintained in the soluble fraction, this does not necessarily prove that it is correctly folded. The refolded Rab was intended for complexation with interacting proteins such as REP, which are expected to discriminate between the correctly folded and misfolded protein due to the dependence of this interaction on the integrity of the GTPase fold (Khosravifar et al., 1992). In this study, the refolded GDP-bound Rab7 protein is able to bind REP-1 and displays a similar response in the emission spectra as that of the native Rab7 protein (Yi et al., 2011), suggesting that the protein is correctly refolded and functional.

It is generally assumed that the folding of a polypeptide chain is a spontaneous process intrinsically determined by its primary structure (i.e. amino acid sequence) and depending on the appropriate environment. Small single-domain proteins derived from total- or semi-synthesis or from bacterial inclusion bodies have been refolded with excellent yields in the past, including small GTPases of the Ras superfamily proteins (Durek et al., 2004; Wu et al., 2011). Based on a FRET-based protein probe in this study, we found that supplementing the

refolding buffer with different nucleotides (GDP or GppNHp) could easily give access to differently nucleotide-loaded Rab proteins, which would meet the needs of various other applications. For example, we can prepare GppNHp-bound GTPases through this refolding strategy, which is indicated in the semisynthesis of GppNHp-bound RhoA GTPase.

3.2.5. Synthesis of RhoA-GG by refolding methods

Now that the protein refolding results of the FRET-based Rab probe point out a way to produce GppNHp-bound GTPase, we aim to semisynthesize the lipidated RhoA in both GDP- and GppNHp-bound forms through a refolding strategy. In mammals, Rho family consists of 20 proteins, belonging to the superfamily of small GTPases. RhoA as one of the best characterized Rho GTPases was described as master regulators of the actin cytoskeleton (Pedersen et al., 2012). Unlike Rab GTPases, RhoA contains a polybasic sequence together with one GerGer group at the C-terminus. The synthesis of lipidated RhoA (RhoA-GG) was achieved by EPL of RhoA-thioester and a geranylgeranylated peptide **13** (Figure 3.25).

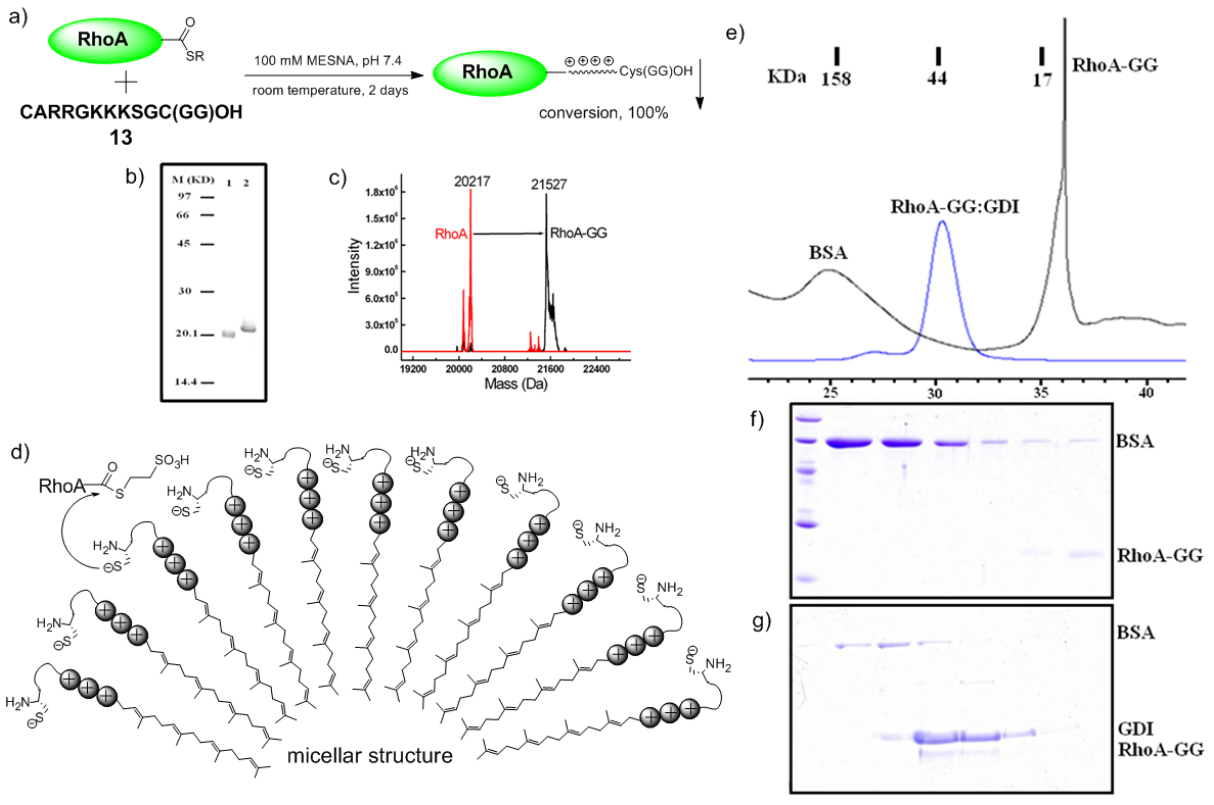

Figure 3.25. a) The ligation conditions of RhoA-thioester and **13**. b) SDS-PAGE of RhoA before (lane 1) and after (lane 2) the ligation reaction. c) ESI-MS spectra of RhoA before (M_{calcd} = 20203) and after (M_{calcd} = 21526) the ligation reaction. d) A micellar structure of **13** is proposed in buffer during the ligation. e) Gel filtration traces of refolded GppNHp-bound RhoA-GG (black line) and its complex with RhoGDI (blue line) and analysis of their resulting fractions by SDS-PAGE of refolded GppNHp-bound RhoA-GG (f) and its complex with

RhoGDI (g). Compound **13** was synthesized by Dr. Debapratim Das from the Department of Chemical Biology, MPI Dortmund.

Since the GerGer-containing peptide **13** is water-soluble, the ligation between RhoA-thioester and **13** can be performed in buffer without addition of detergents. This is different from what it was observed with Rab proteins, since their geranylgeranylated peptides were found to be essentially insoluble in pure aqueous solutions and high concentrations of the detergents were necessary for solubilizing the lipidated peptides for EPL (Durek et al., 2004). As shown in Figure 3.25, EPL for RhoA is carried out in aqueous buffers (pH 7.4) at room temperature with **13** in large molar excess (10 times) in the reaction mixture in order to improve the ligation yields. MESNA (100 mM) as catalytic thiol cofactors was added that can retain the cysteine side chains in the reduced state, reverse the formation of unproductive thioesters and activate less reactive thioesters by transthioesterification. The quantitative conversion was indicated by SDS-PAGE and ESI-MS after incubation of the reaction for 2 days. After the reaction, the geranylgeranylated RhoA (RhoA-GG) precipitated from the ligation buffer.

The lipidated peptide **13** might form micellar structures in solution, e.g., the hydrophobic region (GerGer moiety) forms the micelle interior while the polybasic region interacts with thioester groups in the Stern-layer (Figure 3.25d). The relatively high charge density on the micelle surface could additionally contribute to the polarization of the carbonyl thioester, thereby enhancing its reactivity with protein-thioesters. The micellar structure may render **13** soluble in solution. After the ligation, lipidated proteins on the micellar structure contact each other, resulting in protein aggregration and precipitation.

The RhoA-GG pellets were resolubilized in 6 M G.HCl buffer containing the reductant DTE and the detergent CHAPS. Renaturation of the denatured protein was achieved by pulse-refolding approach in which the denatured protein was titrated into refolding buffer of typical 30-fold dilution in pulses (Durek et al., 2004). It is reported that prenylated Rab proteins could be stabilized in solution using delipidated BSA (Dirac-Svejstrup et al., 1994), but required higher molar excess of the later. Herein, 10 time delipidated BSA was added into the refolding buffer in order to stabilize the GerGer group in RhoA. The resulting RhoA-GG protein remained in solution after refolding in the presence of GDP or GppNHp, which is an atypical behavior because the geranylgeranylated protein tends to form aggregates in buffer (Wu et al., 2007). The ligated protein eluted from a size exclusion column at a position corresponding to a molecular mass < 10 kDa, suggesting that the protein does not form

multimers and that its migration is retarded on the column probably by hydrophobic interaction with the matrix. The solubility of RhoA-GG is surprising. From the SDS-PAGE (Figure 3.25f), RhoA-GG co-elute with small amount of BSA, which should help to stabilize RhoA-GG in solution. Furthermore, the ploybasic sequence at the C-terminus should also contribute to the water-solubility of RhoA-GG, since Rab-GG in the presence of small amount of BSA tends to form aggregates in buffer (Dr. Yaowen Wu, PhD thesis, 2008). Semisynthetic GppNHp-bound RhoA-GG was correctly folded as judged by its ability to form a stoichiometric complex with GDI (Figure 3.25e,g). These results imply that the refolding strategy for preparation of GppNHp-bound lipidated Rho GTPases is feasible, considering that the biochemical generation of such GppNHp-bound lipidated proteins in multi-milligram scale is difficult or in most cases not practical or applicable.

3.2.6. Conclusion

In summary, a universal and quantitative method for N-terminal labeling of N-Cys-proteins was achieved. A general, facile and efficient strategy for N- and C-terminal dual-color labeling of a protein was achieved by using both native chemical ligation and oxime ligation in an one-pot manner. The produced protein probes based on these labeling methods were used to study protein refolding and protein-protein interactions by FRET. It is found that both GDP and GppNHp can help GTPase to refold, and therefore point out a way to produce GppNHp-bound GTPase as indicated in the case of semisynthesis of RhoA-GG.

3.3. Development of a FRET-based strategy for monitoring GEF-mediated activation of GTPases

3.3.1. Introduction

GEFs are essential partners of GTPases involved in intracellular signal transduction and regulatory mechanisms (Bos et al., 2007). GEFs are often multidomain proteins or members of large protein complexes, which activate GTPases at specific subcellular sites (Garcia-Mata et al., 2007; Yoshimura et al., 2010; Quilliam et al., 2002). Thermodynamic and kinetic analyses of interaction of GEFs have suggested a common mechanism involving allosteric competition between nucleotide and GEF interacting with a GTPase (Klebe et al., 1995; Lenzen et al., 1998; Hutchinson et al., 2000; Gromadski et al., 2002). GEFs catalyze dissociation of the tightly bound nucleotide from the GTPase by reducing the affinity of the nucleotide, and vice versa, binding of the nucleotide decreases the affinity of GEF. As a result, the nucleotide is displaced and subsequently replaced by GTP due to much higher cellular concentration of GTP than GDP. The binding of the nucleotide consequently releases the GEF (Goody, 2002; Guo et al., 2005). The interactions of GEFs with GTPases have been resolved at the atomic level. Binding of a GEF to a GTPase induces conformational changes in switch I and II and the P loop, resulting in disruption of the nucleotide binding site (Vetter et al., 2001).

GEFs have been considered as promising therapeutic targets, due to their function in regulating disease-relevant GTPase signaling (Morishige et al., 2008; Gonzalez-Garcia et al., 2005; Malliri et al., 2002; Vega et al., 2008). For example, GEP100, a GEF for Arf6, connects EGFR signaling to Arf6 activation and is responsible for invasive activity of breast cancer cells, suggesting that Arf6 and its regulator could be therapeutic targets for the prevention of breast cancer metastasis (Morishige et al., 2008). Tiam1 (a RacGEF) knock-out mice develop, grow and reproduce normally, but are resistant to the development of Ras-induced skin tumors (Malliri et al., 2002). This suggests that inhibition of Tiam1 may be a safe and efficient approach for anti-tumor therapy. GEF inhibitors have been used in chemical genetic studies to reveal the function of specific GEFs, such as ArfGEFs and RhoGEFs (Hafner et al., 2006; Gao et al., 2004; Bouquier et al., 2009; Blangy et al., 2006).

Investigation of GEF mechanisms and identification of GEF inhibitors require appropriate assays for the GEF activity. The frequently used methods for monitoring GEF activity are based on the intrinsic fluorescence of the protein or that of GDP/GTP analogues labeled with an environmentally sensitive fluorophore, such as N-methylanthraniloyl (mant) (Klebe et al.,

1995). Though mant is a small fluorescent group, mant-GDP and -GTP might not behave identically to the native nucleotides. Thus, kinetic parameters obtained using mant-GDP/GTP are not identical to those of native nucleotides (Schoebel et al., 2009; Itzen et al., 2007). An assay using radio-labeled GDP/GTP is not appropriate for monitoring fast kinetics of GEF-mediated nucleotide exchange. The specific binding of an effector domain with a GTP-bound protein has been used as a sensor for the activation of GTPases *in vitro* and *in vivo* (Kraynov et al., 2000; Mochizuki et al., 2001; Galperin et al., 2003). Such interactions can be detected by FRET and pull-down assays (Bill et al., 2011; Knaus et al., 2007; Niebel et al., 2011). Although the activation-dependent interaction assay reports the extent of GTPase activation, it could not be used to visualize the interaction of GEFs in real time. Furthermore, these probes require a tedious search for an appropriate effector domain (Nakamura, 2005). These prompted us to develop a sensitive and versatile assay based on intermolecular FRET between GEF and GTPase (Figure 3.26). FRET-based detection produces large Stokes shift together with a dual-wavelength readout that provides an internal normalization (Förster, 1946). The development of FRET probes has significantly facilitated the analysis of enzyme activity, the elucidation of structures and conformational changes of biomolecules, and the detection of biomolecular interactions involved in various biological events (Sapsford et al., 2006). In this work, FRET is employed to analyze protein-protein and protein-ligand interactions.

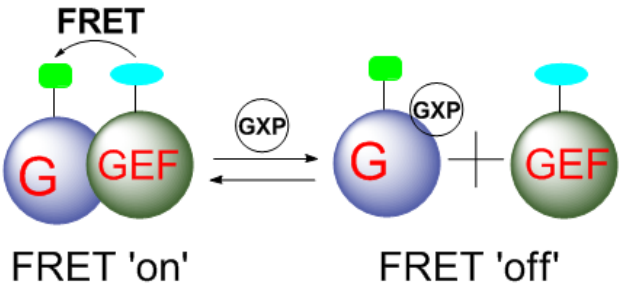

Figure 3.26. A FRET strategy for monitoring GEF mechanism. G = GTPase, GXP = GDP/GTP.

3.3.2. Construction of FRET-based GEF sensors

The construction of a FRET system based on the interaction between GEF and GTPase requires the specific attachment of donor and acceptor fluorophores to the proteins (Figure 3.26). Methods for facile, specific and efficient modification at the C- and N-termini of proteins were established by using chemoselective reactions under mild conditions (see part 3.1 and 3.2). In this work we further employ these methods to label both GTPases and their

GEFs with FRET dyes coumarin and fluorescein. As a proof of principle, we chose Rab1 GTPase and its GEF from *Legionella pneumophilathe*, DrrA, of which the GEF domain (340-533) was used (we refer to it as DrrA hereinafter) (Schoebel et al., 2009), and Ran GTPase and its GEF, RCC1 (Klebe et al., 1995). To generate GEF with an N-terminal cysteine, we fused a peptide sequence containing a TEV cleavage site (ENLYFQ¦C; dotted line indicates the cleavage site) to the N-terminus of the GEF protein. TEV protease was then added to expose the N-terminal cysteine, resulting in N-Cys-DrrA and N-Cys-Rcc1 that can subsequently undergo NCL with coumarin-thioester (Figure 3.27). GTPases were fused C-terminally to an intein domain and were subsequently cleaved by MESNA to release the α-thioester-tagged proteins. The resulting proteins were treated with a high concentration of bis(oxyamine) at pH 7.5 to produce the oxyamine-modified proteins that were subject to oxime ligation with keto-fluorescein (Figure 3.27). All labeled proteins were characterized by mass spectra and SDS-PAGE.

It is noted that the C-terminal hypervariable region of Rab1 together with prenylatable cysteines are deleted, since they are not involved in interactions with RabGEF (Schoebel et al., 2009). However, GDP-bound Ran_{1-178} without the C-terminal region is very unstable during protein purification. This point is consistent with a previous crystal structural analyisis that the C-terminal sequence of Ran is involved in nucleotide binding (Scheffzek et al., 1995). The full-length Ran_{1-205} is enough stable and choosen in this study.

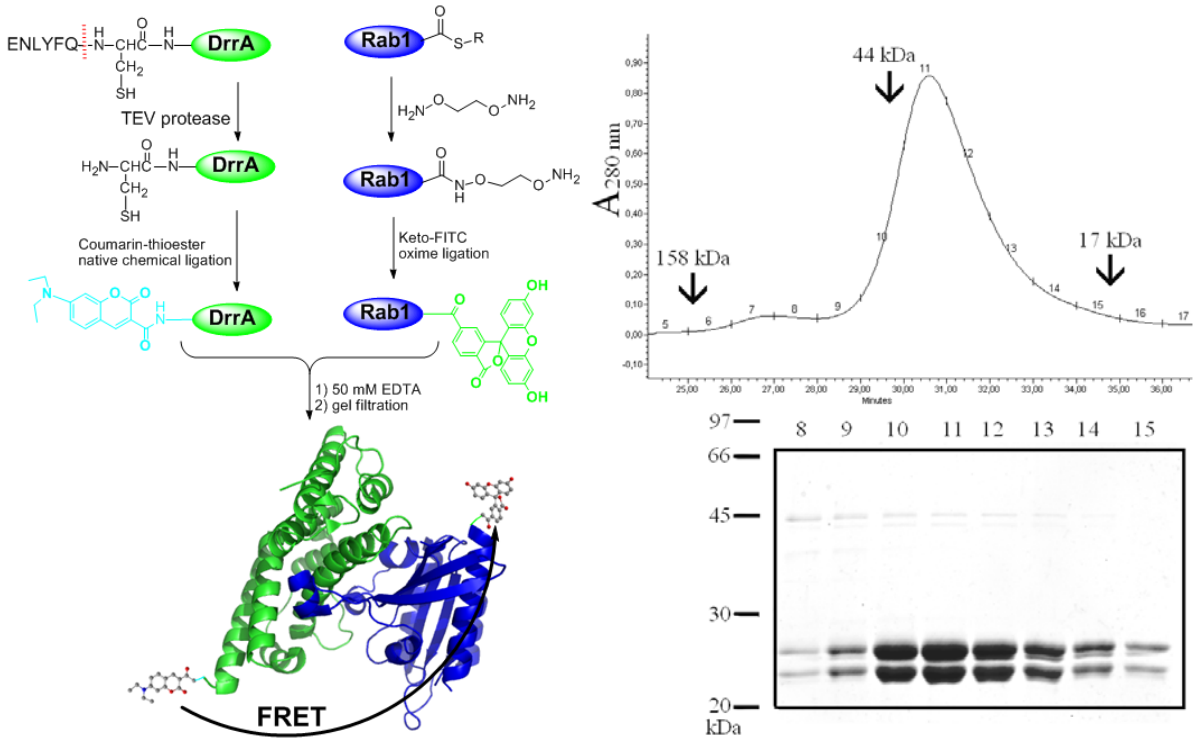

Figure 3.27. Site-specific labeling of DrrA and Rab1b (left) to form a coumarin-DrrA:Rab1b-fluorescein complex and its gel filtration trace at 280 nm (right). The fractions 8-15 were analyzed by SDS-PAGE as shown in the lower panel.

With fluorophore-modified proteins in hand, we prepared the DrrA:Rab1b and Rcc1:Ran complexes by mixing stoichiometric amounts of the proteins with 10-fold excess of EDTA (ethylene diamine tetra acetic acid) over Mg^{2+} (Figure 3.27). The coordination of Mg^{2+} by EDTA can greatly reduce the GDP-binding ability of GTPases, and therefore is beneficial for the replacement of GDP by GEF. After run a gel filtration in nucleotide-free buffer, the 1:1 GEF:GTPase protein complex eluted out in the position with correct molecular weight. SDS-PAGE was further employed to indicate the formation of the 1:1 GEF:GTPase complex. Such labeling strategy could also be successfully applied to a Rho GTPase, Cdc42, and its GEF, Dock9.

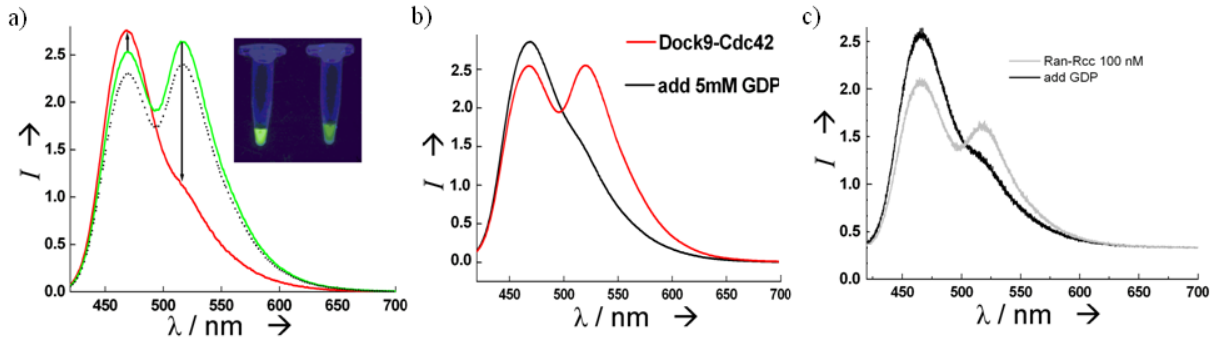

Figure 3.28. a) Emission spectra of coumarin-DrrA:Rab1b-fluorescein complex before (green line) and after GDP treatment (red line) or after buffer treatment (black dotted line). Inset: photographs of coumarin-DrrA:Rab1b-fluorescein complex before (left) and after GTP treatment (right) under a UV lamp. b) Emission spectra of coumarin-Dock9:Cdc42-fluorescein complex before (red line) and after GTP treatment (blank line). c) Emission spectra of coumarin-Rcc1:Ran-fluorescein complex before (gray line) and after GTP treatment (blank line). All spectra were excited at 400 nm.

The coumarin-DrrA:Rab1b-fluorescein complex displayed green fluorescence under a UV lamp, while addition of 100-fold excess of GTP led to cyan fluorescence. This color change can be observed by the naked eye (Figure 3.28). Upon excitation of coumarin (FRET donor) at 400 nm, two emission peaks at 471 nm (coumarin) and 517 nm (fluorescein) were observed, indicating an efficient FRET effect. Addition of GDP or GTP into the complex led to loss of the FRET signal, with a change in the ratio of fluorescein to coumarin emission intensities (517 nm/471 nm) from 1.04 to 0.41 (Figure 3.28a). In contrast, the FRET signal ($I_{517\ nm/471\ nm}$) of the protein complex remained constant upon buffer dilution or AMP treatment. These

results show that the association of GDP/GTP with DrrA:Rab1b complex displaced DrrA. This process can be monitored by the significant decrease of the FRET signal (FRET-off signal). We also observe such FRET-off signal in other GTPase:GEF pairs including Cdc42:Dock9 and Ran:Rcc1 (Figure 3.28). As expected, the ratio of fluorescein to coumarin emission intensities (517 nm/471 nm) decrease from 1.00 to 0.54 and from 0.78 to 0.44 for Dock9:Cdc42 and Ran:Rcc1, respectively. These results imply that the association of GDP/GTP with GEF:GTPase complexes displaced GEF (Figure 3.29). This process can be monitored by the significant decrease of the FRET-off signal.

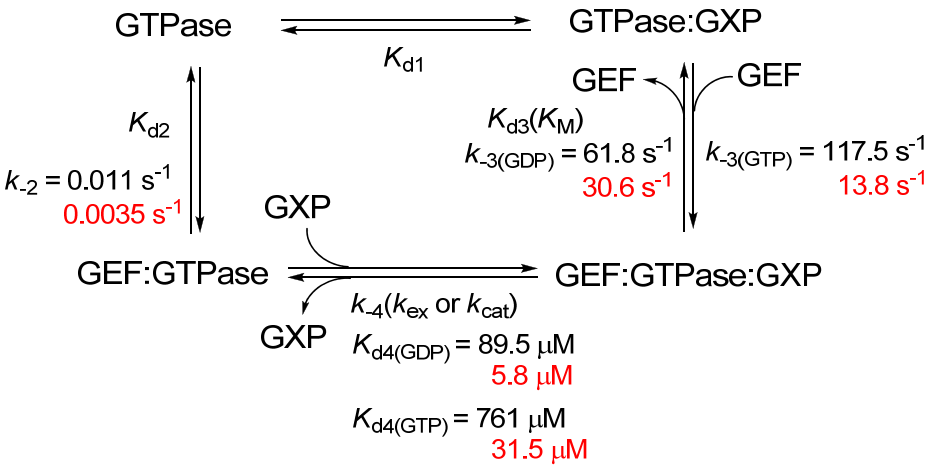

Figure 3.29. Kinetics and equilibria of the reversible GEF:GTPase:GXP interaction cycle. The parameters shown in black are for DrrA and Rab1b and red for RCC1 and Ran.

3.3.3. Kinetics for monitoring the dissociation of the GEF:GTPase complex

In order to answer the question whether the kinetics of association of GDP or GTP to the GTPase:GEF complex are different, we performed the transient kinetic experiment in the reverse direction under pseudo first order conditions. Firstly, the transient kinetics of the reaction were examined in stopped flow experiments in which a 1:1 complex of DrrA:Rab1b was mixed rapidly with varying concentrations of GDP or GTP. The FRET-off signal on displacement of DrrA from Rab1b by GDP or GTP was a pseudo-first-order process (Figure 3.30a). The observed rate constants for the displacement showed a hyperbolic dependence on nucleotide concentration, indicating a two-step reaction (Figure 3.30b,d). These hyperbolic dependence curves allow the determination of K_{d4} and k_{-3} (Figure 3.29) through the following relationship:

$$k_{\text{obs, GXP association}} = \frac{k_3}{1 + \frac{K_{d4}}{c(\text{GXP})}}$$

The affinity of GDP for the DrrA:Rab1b complex was 8-fold higher than that of GTP, with a K_{d4} value of 89.5 µM for GDP or 761 µM for GTP (Figure 3.29). The K_{d4} value for GDP was comparable with the previously determined value using tryptophan fluorescence as the binding signal (Schoebel et al., 2009). Although the affinity of GTP with the GEF:GTPase complex is relatively low, the higher concentration of GTP (up to 1 mM) in cells (Kleinecke et al., 1979) allows efficient GTP binding with the complex to achieve nucleotide exchange. The result also implies that the DrrA:Rab1b complex does not have much selectivity towards GDP or GTP, namely, GDP or GTP is an allosteric competitive factor in the GEF-catalyzed reaction (Goody, 2002).

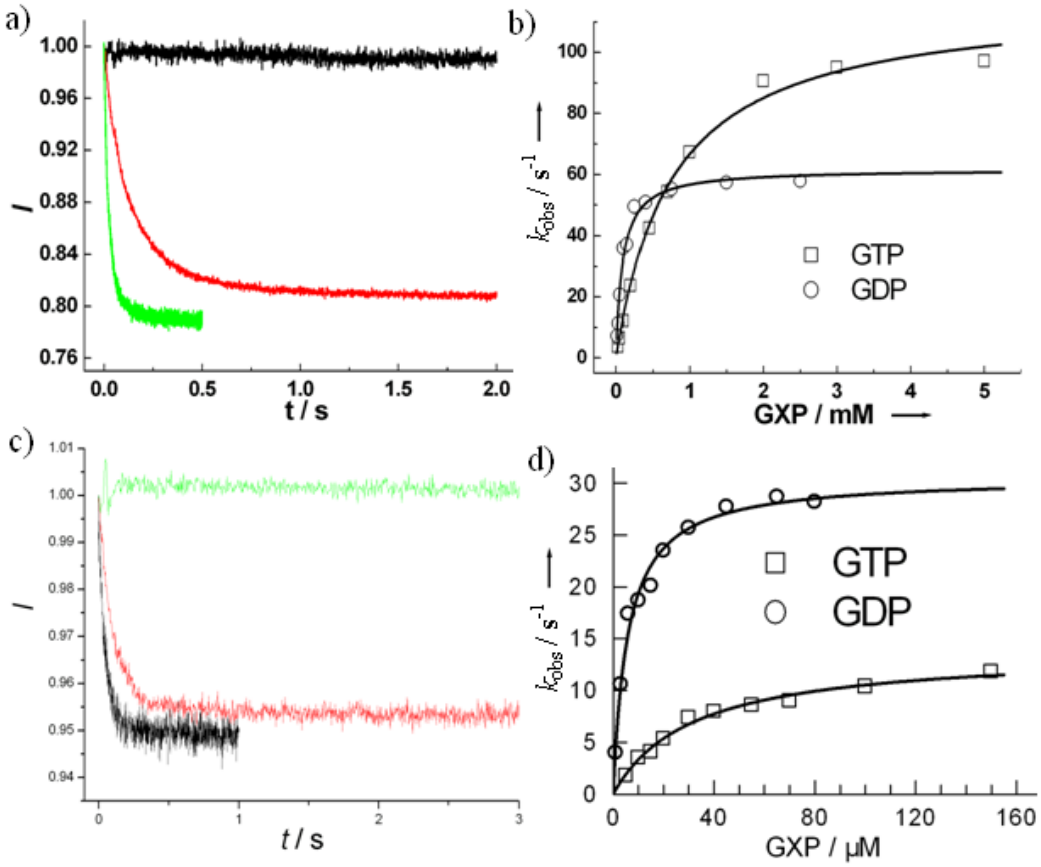

Figure 3.30. a) Stopped-flow traces of the dissociation of the coumarin-DrrA:Rab1b-fluorescein complex by addition of GDP of 15 µM (red line) and 150 µM (green line). The black line represents the control on mixing the protein complex and buffer. The final concentration of coumarin-DrrA:Rab1b-fluorescein is 50 nM. b) Hyperbolic dependence of the observed rate constant for FRET-off signal change from the coumarin-DrrA:Rab1b-fluorescein complex on various concentrations of GDP or GTP. The time-courses of the FRET-off signal were fitted to a single exponential function, and the resulting rate constants (k_{obs}) were plotted against GDP or GTP concentration. The hyperbolic fittings (solid lines) gave K_{d4} values of GDP/ GTP with the DrrA:Rab1b complex and the dissociation rate

constant (k_{-3}) of DrrA from Rab1b:GDP or GTP complex as shown in Figure 3.29. c) Stopped-flow traces of the dissociation of the coumarin-Rcc1:Ran-fluorescein complex (500 nM) by addition of GDP of 3 μM (red line) and 15 μM (black line). The green line represents the control on mixing the protein complex and buffer. d) The hyperbolic fittings (solid lines) gave K_{d4} values of GDP/GTP with the Rcc1:Ran complex and k_{-3} of Rcc1 from Ran:GDP or GTP complex similar with that in the Rab1b:DrrA complex.

We also employed the Ran:Rcc1 pair to study the association of GDP or GTP to the GTPase:GEF complex. Using identical nucleotide concentrations, we find that the association of GTP to Ran-RCC1 is slower than that of GDP. Quantitative evaluation of the two reaction steps was performed as that of the DrrA:Rab1 pair by hyperbolically fitting the secondary plot of k_{obs} against GXP concentration (Figure 3.30d). The affinity of GDP for the Rcc1:Ran complex was about 5-fold higher than that of GTP, with a K_{d4} value of 5.8 μM for GDP or 31.5 μM for GTP. These K_{d4} values were comparable with the previously determined value using tryptophan fluorescence as the binding signal (Klebe et al., 1995).

Using mdGTP, we cannot obtain the reaction rate at saturating nucleotide concentrations due to the high background signal at these concentrations. The present strategy will not have this problem. While using the change of intrinsic tryptophan fluorescence as a signal (Klebe et al., 1995), one could observe single exponential time traces with rate constants similar with that in Figure 3.30d. However, the present strategy allows direct measurement of the displacement of GEF with unlabeled nucleotide, and, is thus superior to the approach using Mant-GDP/GTP or tryptophan fluorescence, which only provides the information on nucleotide association.

It was interesting to observe whether ATP could disrupt the DrrA:Rab1b binary complex, especially since an equivalent experiment cannot be performed using fluorescent nucleotides. To this end, the FRET-off signal of the coumarin-DrrA:Rab1b-fluorescein complex was monitored by addition of 1 mM ATP or GTP. The results showed that association of ATP with DrrA:Rab1b complex is three orders of magnitude slower than that of GTP (Figure 3.31). The kinetics imply that GEF:GTPase complex binds with GTP rather than ATP *in vivo*. From the thermodynamic view point, GTPases bind to ATP with a 10^6 lower affinity than GTP (John et al., 1990; Simon et al., 1996).

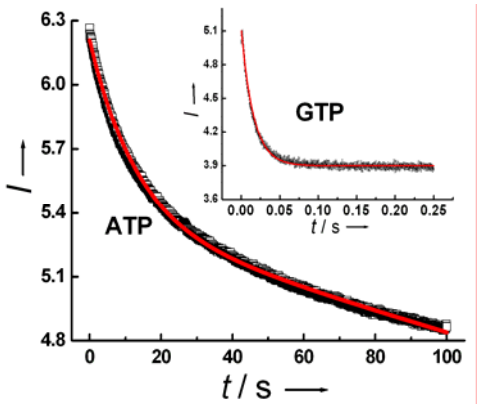

Figure 3.31. Time-dependent decrease of the FRET-off signal of the 50 nM coumarin-DrrA:Rab1b-fluorescein complex by treatment with 1 mM ATP or GTP (inset). The traces were fitted to a single exponential function to give k_{obs} value of 0.076 s^{-1} for ATP and 67.14 s^{-1} for GTP.

The dissociation of the GEF:GTPase complex could be monitored by displacing labeled GEF with excess of non-labeled GEF (Figure 3.32a). This dissociation caused a significant decrease of the FRET signal (Figure 3.32b,c). Single exponential fitting of the trace gave the dissociation constants for DrrA:Rab1b (k_{off} = 0.011 s^{-1}) and RCC1:Ran (k_{off} = 0.0035 s^{-1}), indicating a tightly bound GEF:GTPase complex. It is noted that this kind of the rate constants could not be determined directly in earlier studies, indicating the advantage of our FRET-based strategy. For the first time, we could directly monitor the dissociation of the GEF:GTPase complex in this work.

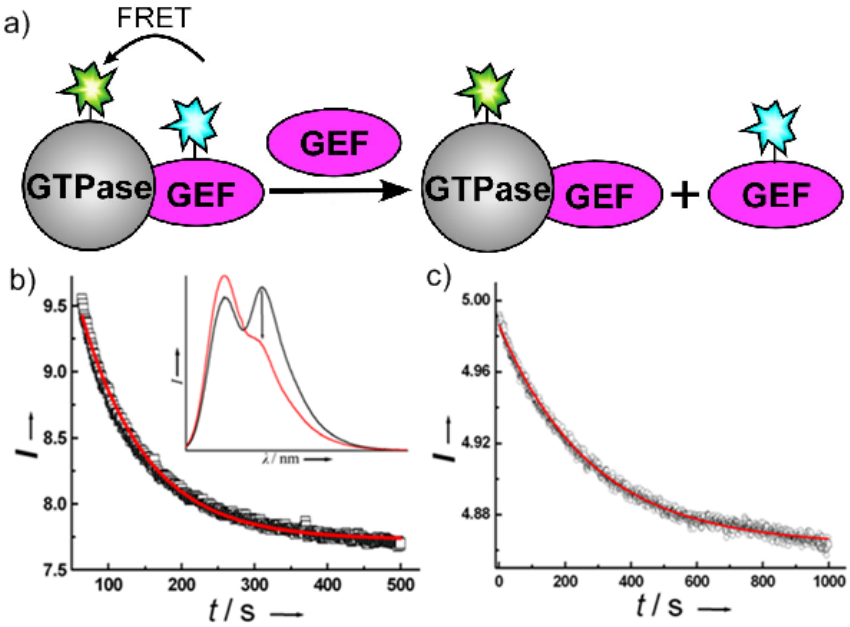

Figure 3.32. a) A FRET-based strategy to monitor the dissociation of GEF from the GEF:GTPase complex. b) Dissociation kinetics of 50 nM coumarin-DrrA:Rab1b-fluorescein

complex on addition of 1 µM non-labeled DrrA. The red line represents a fit to a single exponential function to give a k_{obs} value of 0.011 s^{-1}. Inset: the emission spectra of the sample before addition non-labeled DrrA (black line) and after reaction for 500 s (red line). c) Dissociation kinetics of 500 nM coumarin-Rcc1:Ran-fluorescein complex on addition of 10 µM non-labeled Rcc1. A fit (red line) to a single exponential function gives a k_{obs} value of 0.0035 s^{-1}.

3.3.4. Kinetics for monitoring protein-protein interactions

We next examined the association of coumarin-GEF with GDP:GTPase-fluorescein. GEF can displace GDP from GTPase to form the GEF:GTPase complex, which can be monitored by the increase of the FRET signal (FRET-on signal) (Figure 3.33). The observed first-order rate constant showed a linear dependence on GEF concentration in the concentration range we have used. This suggests that the affinity of GEF with GTPase:GDP is low, i.e. K_{d3} is high, which is in line with the previously determined K_{d3} of 10-40 µM (Schoebel et al., 2009). The plots indicated that the exchange rate constant k_{-4} for GDP was higher than the one determined using mant-GDP (k_{-4} of 7.6 s^{-1} for DrrA and 21 s^{-1} for RCC1) (Schoebel et al., 2009; Klebe et al., 1995). The slope in Figure 3.33a of the linear fit provides an estimation of the GEF catalytic efficiency of DrrA (k_{cat}/K_M = 1.5 × 10^6 $M^{-1}s^{-1}$), which is comparable with the reported value of 0.91 × 10^6 $M^{-1}s^{-1}$ (Suh et al., 2010). These results demonstrate that the FRET strategy can be used to monitor GEF activity.

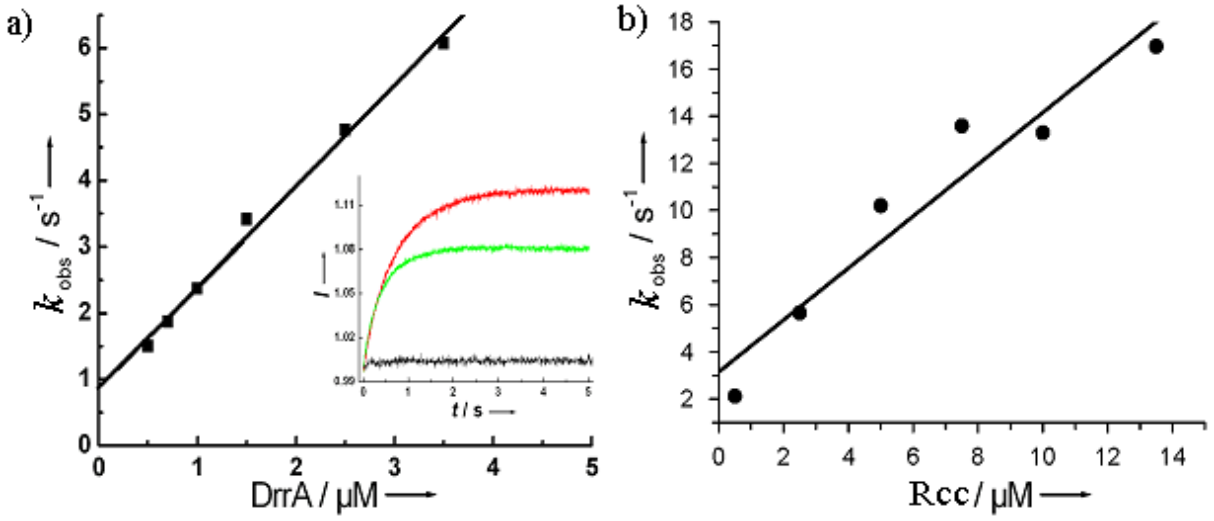

Figure 3.33. Characterization of the GEF activity using FRET-on signal. a) 50 nM GDP:Rab1b-fluorescein was rapidly mixed with varying concentrations of DrrA. The time-courses of FRET-on signal were fitted to a single exponential function, and the resulting rate constants (k_{obs}) were plotted against DrrA concentration. Inset: time-dependent increase of FRET signal at different concentrations of DrrA. b) 500 nM GDP:Ran-fluorescein was rapidly mixed with varying concentrations of Rcc1. The time-courses of FRET-on signal were fitted

to a double exponential function, and the resulting rate constants (k_{obs}) were plotted against Rcc1 concentration.

3.3.5. Conclusion

In summary, we have presented the general principle of a FRET-based strategy for monitoring GEF-mediated nucleotide exchange using site-specifically labeled GEF and GTPase proteins. Using NCL and oxime ligation, we prepared N-terminal coumarin-labeled GEFs and C-terminal fluorescein-labeled GTPases. We constructed two pairs of coumarin-GEF:GTPase-fluorescein complexes, which showed a significant intermolecular FRET effect. The FRET signal was disrupted by binding of GDP or GTP and allowed direct detection of the GEF:GTPase interaction. Transient kinetic studies based on the FRET signal changes were used to monitor the GEF activity and nucleotide binding. The studies led to a consistent conclusion on the GEF mechanism involving allosteric competition between GDP/GTP and GEF's interaction with a GTPase. The strategy presented here could be a general method that is applicable to other GEFs and GTPases, and may open up a new avenue for the identification of GEF inhibitors and for studying GEF mechanisms.

3.4. Development of a general strategy for preparation of lipid-protein conjugates

3.4.1. Introduction

Post-translational modification of proteins with lipids (e.g. fatty acids, isoprenoids) is an essential biological process in eukaryotic cells. Tools for generating protein-lipid conjugates are valuable for studying the role of post-translational lipid modification in controlling protein function and localization. However, recombinant production of post-translationally modified proteins is usually challenging in terms of homogeneity and output. The site-specific attachment of lipids to proteins remains a challenge in bioconjugation. Only a relatively limited set of chemical (Brunsveld et al., 2006; Kadereit et al., 2000; Grogan et al., 2005; Alexandrov et al., 2002) and chemoenzymatic (Owen et al., 1999; Mcgeady et al., 1995; Antos et al., 2008) strategies are available for this purpose. EPL has proven to be a chemoselective and efficient method for construction of lipidated Rab GTPases (Durek et al., 2004). Herein we aim to develop a general and quantitative bioconjugate method as an alternative strategy for preparing lipid-protein conjugates.

In this work Rab proteins were chosen as model proteins, since they have single or double modification of geranylgeranyl isoprenoids at the C terminus. Studies of Rab protein function as well as the mechanism of Rab prenylation require methods that allow for generating enough amounts of prenylated Rab proteins with new functionalities such as fluorophores, photoreactivity, and isoprenoid groups at non-native positions. Herein we employed the click reaction to construct lipid-protein conjugates because: 1) the formed 1,2,3-triazole has only a low steric demand and is also regarded as a peptide-bond mimetic (Tron et al., 2008); 2) the reaction confers superior efficiency (high reaction rate) and selectivity (Rostovtsev et al., 2002; Berry et al., 2010); 3) the quantitative click ligation would enable to make pure lipidated proteins. This is particularly important, since the separation of modified protein from unmodified one may be highly problematic. Recently, the strategy where a protein or peptide equipped with an alkyne or azide moiety undergo rapid click reaction has been widely employed in protein/peptide modifications (Yi et al., 2009; Weikart et al., 2010; Xiao et al., 2009; Flavell et al., 2008; Binda et al., 2011; Wang et al., 2011; Cai et al., 2011). In this work, we firstly incorporated an azide group into the C-terminus of Rab proteins based on EPL and subsequently ligated alkyne-modified prenylated peptides or lipidated molecules to the proteins using click reaction (Figure 3.34). Using this approach we can generate prenylated

Rab proteins that form complexes with their natural chaperones REP-1 and GDI-1, which were used to study Rab prenylation *in vitro*.

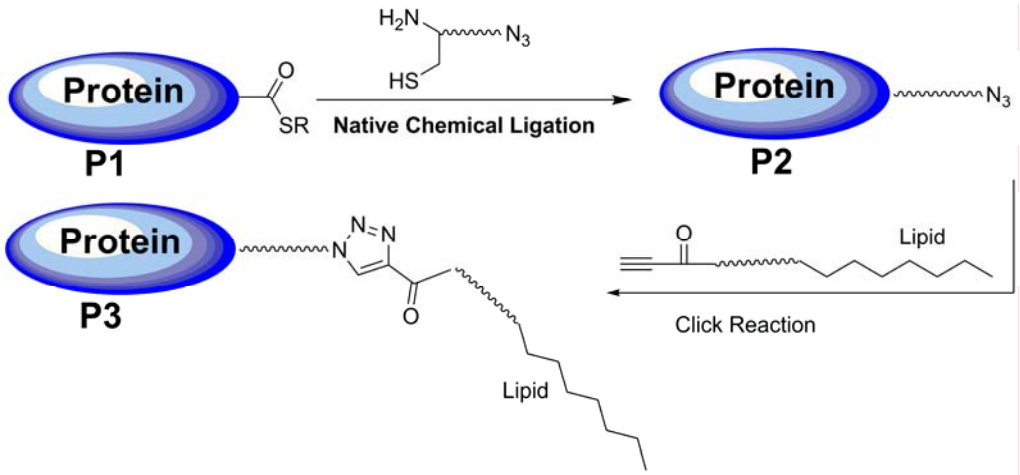

Figure 3.34. Strategy for the semi-synthesis of geranylgeranylated Rab proteins. Firstly, an azide group is introduced into protein C-terminus by NCL, and then the Click reaction between an alkyne-containing lipid and the resulted azide-modified protein produces a lipid-modified protein bioconjugate.

3.4.2. Preparation of azide-modified proteins

In order to incooperate an azide moiety into a protein in a site-specific fashion and using the EPL reaction, compound **14** was designed and synthesized (Figure 3.35). The synthesis of **14** starts from Fmoc-Cys(StBu)OH and 2-azidoethanamine (see experimental part for details). The cysteine moiety in **14** is protected by t-butylthio (StBu), which can be easily removed by treatment with high concentration of thiol additives during EPL. The co-existence of thiol and azide groups in one molecule is stable (Riedrich et al., 2007), however, the azide group in **14** can be reduced to an amino group by high concentration of thiols. We finally found that 100-150 mM MESNA can efficiently remove the StBu group in buffer without reducing the azide group.

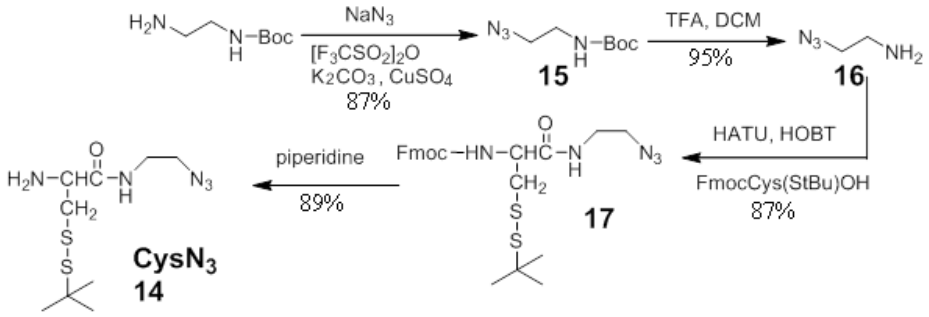

Figure 3.35. Synthesis of **CysN$_3$ 14**.

The reaction of **14** and Rab-thioesters in the presence of 150 mM MESNA resulted in azide-modified proteins, and then the mixture was dialyzed to remove excess of **14**. In the optimized conditions (Figure 3.36), the thioester proteins were quantitatively converted to azide-modified proteins as indicated by LCMS. Partial dimerization of the azide-modified proteins was observed during the storage at -80 °C probably due to the disulfide cross-linking of C-terminal cysteines. However, protein cross-linking did not influence the subsequent click ligation (see following results). Though the azide groups in protein can be significantly reduced to amino groups in the presence of 500 mM MESNA, the azide-modified proteins are stable in the buffer for click ligation.

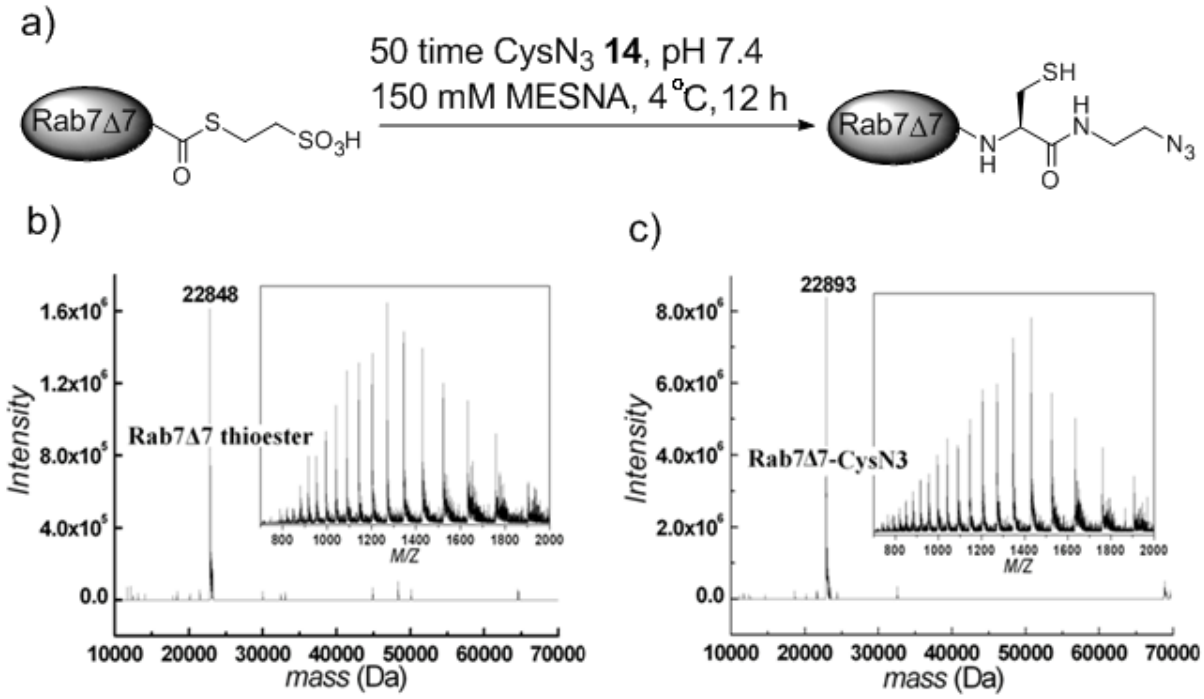

Figure 3.36. a) An optimized ligation conditions for preparation of azide-modified proteins. b) and c) ESI-MS spectra of Rab7Δ7 thioester proteins (M_{calcd} = 22842) and azide-modified proteins (M_{calcd} = 22892), respectively.

3.4.3. Synthesis of alkyne-containing lipid molecules

The GerGer-containing peptides were synthesized based on solid-phase lipidated peptide synthesis (SPPS) developed by Waldmann et al. (Gottlieb et al., 2006). The GerGer group was firstly incorporated into cysteine to produce the building block Fmoc-Cys(GerGer)OH (Brown et al., 1991). It is noted that the reaction intermediate, Cys(GerGer)OH, has relatively low solubility in CH_2Cl_2. If small amount CH_3OH (0.5%) is added during the reaction, the

yield (from GerGerOH) can be greatly improved to reach more than 80% (Figure 3.37), which is important because the commercial available GerGerOH is expensive.

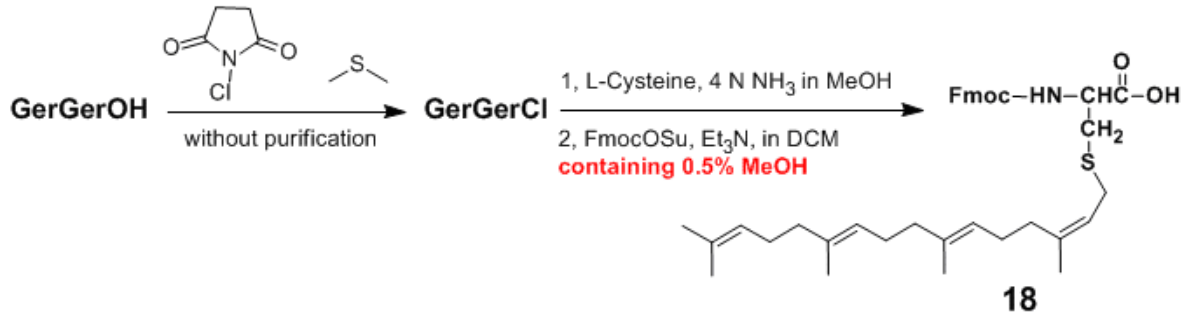

Figure 3.37. synthesis of the lipid building block **18**.

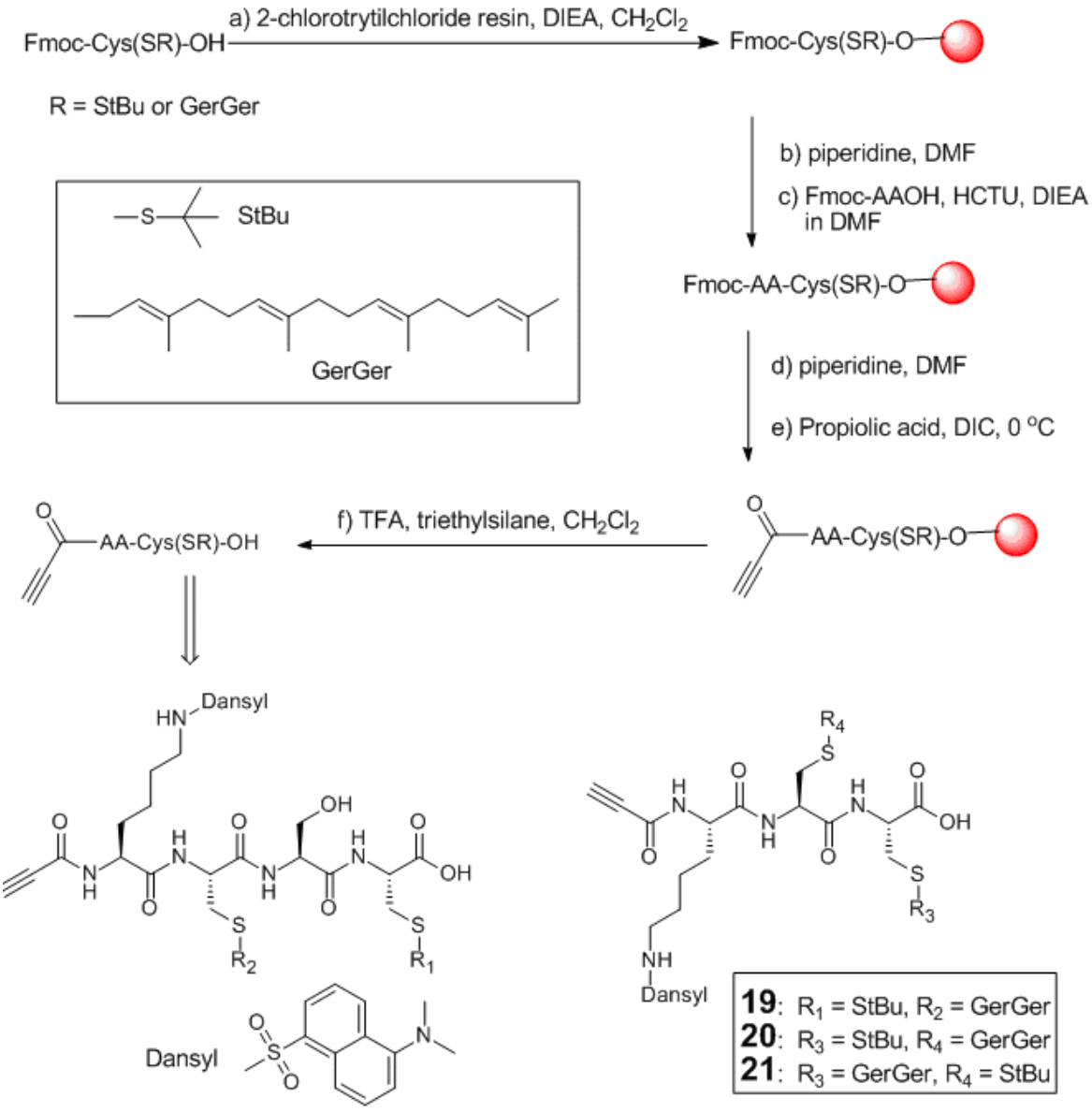

Figure 3.38. Solid-phase peptide synthesis of the geranylgeranylated peptides with N-terminal alkyne moieties.

The lipid building block was loaded onto 2-chlorotrityl chloride (2-Cl-Trt) resin or linked to peptide by standard Fmoc technique (Figure 3.38). The coupling of propiolic acid encountered the problem of precipitation upon addition of N,N-diisopropylethylamine (DIPEA) (Neukamm et al., 2008). Eventually I found that the mixture of 3 eq. (equivalent) propiolic acid and 3 eq. N,N'-diisopropylcarbodiimide (DIC) in cold CH_2Cl_2 can react with the resin at 0 °C. Though this reaction was performed in weak acid condition, no significant lipidated peptides were cleaved from resin during the couple reaction. The mono-geranylgeranylated fluorescently labeled peptides **19-21** were obtained after cleavage from the 2-Cl-Trt resin using a standard procedure. The peptides were purified by flash chromatography with about 50% yield and characterized by MALDI-TOF and high resolution ESI mass spectra (HRMS).

3.4.4. Click ligation for lipid-protein conjugate

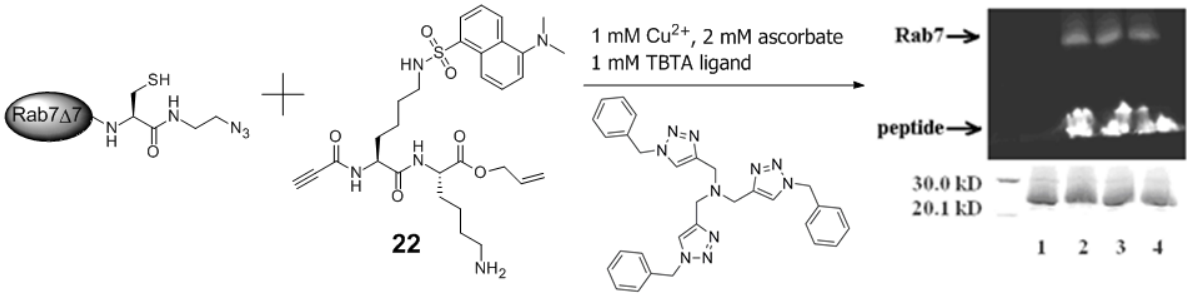

Figure 3.39. SDS-PAGE shows the fluorescent labeling of protein by click reaction. Lane 1, azide-modified Rab7; Lanes 2-4, click reaction of azide-modified Rab7 and the fluorescent peptide with reaction time of 15, 30, 60 minutes, respectively.

With both azide-modified proteins and alkyne-modified peptides in hand, we next aimed to perform the click ligation in buffer without protein precipitate and decomposition. In the first tests, I found that Rab proteins were totally decomposed in the presence of copper. It was reported that the reactive oxygen species produced by Cu(I) can damage biomacromolecules (Devaraj et al., 2005). The ligand tris[(1-benzyl-1*H*-1,2,3-triazol-4-yl)methyl]amin) (TBTA) is reported to greatly increase the click reaction rate and to reduce protein decomposition during the Click reaction. A dansyl-containing fluorescent peptide **22** (Figure 3.39) was employed to optimize the protein ligation. This fluorescently labeled peptide permits easy detection of protein ligation products by means of SDS-PAGE when the unstained gel is exposed to UV light. In such a case, appearance of a fluorescent band in the 20-30 kDa molecular weight region indicates the formation of the ligation product. Firstly, a 10 × click catalysis was prepared as: 10 mM $CuSO_4$ (from 100 mM stock solution), 10 mM TBTA

ligand (from 20 mM methanol stock solution), 20 mM sodium ascorbate (from 200 mM freshly stock solution) were mixed and incubated at room temperature for 5 minutes. Then the catalysis solution was added into a mixture of azide-modified Rab7 (1 mg/mL) and **22** (1 mM) at pH 7.4 buffer. After the reaction, the solution was centrifuged and 1 mM EDTA was added to quench the reaction. Based on SDS-PAGE, I found that the Rab protein was highly efficient modified within 15 minutes without obvious protein decomposition, implying that this copper-catalyzed click ligation is very fast as expected.

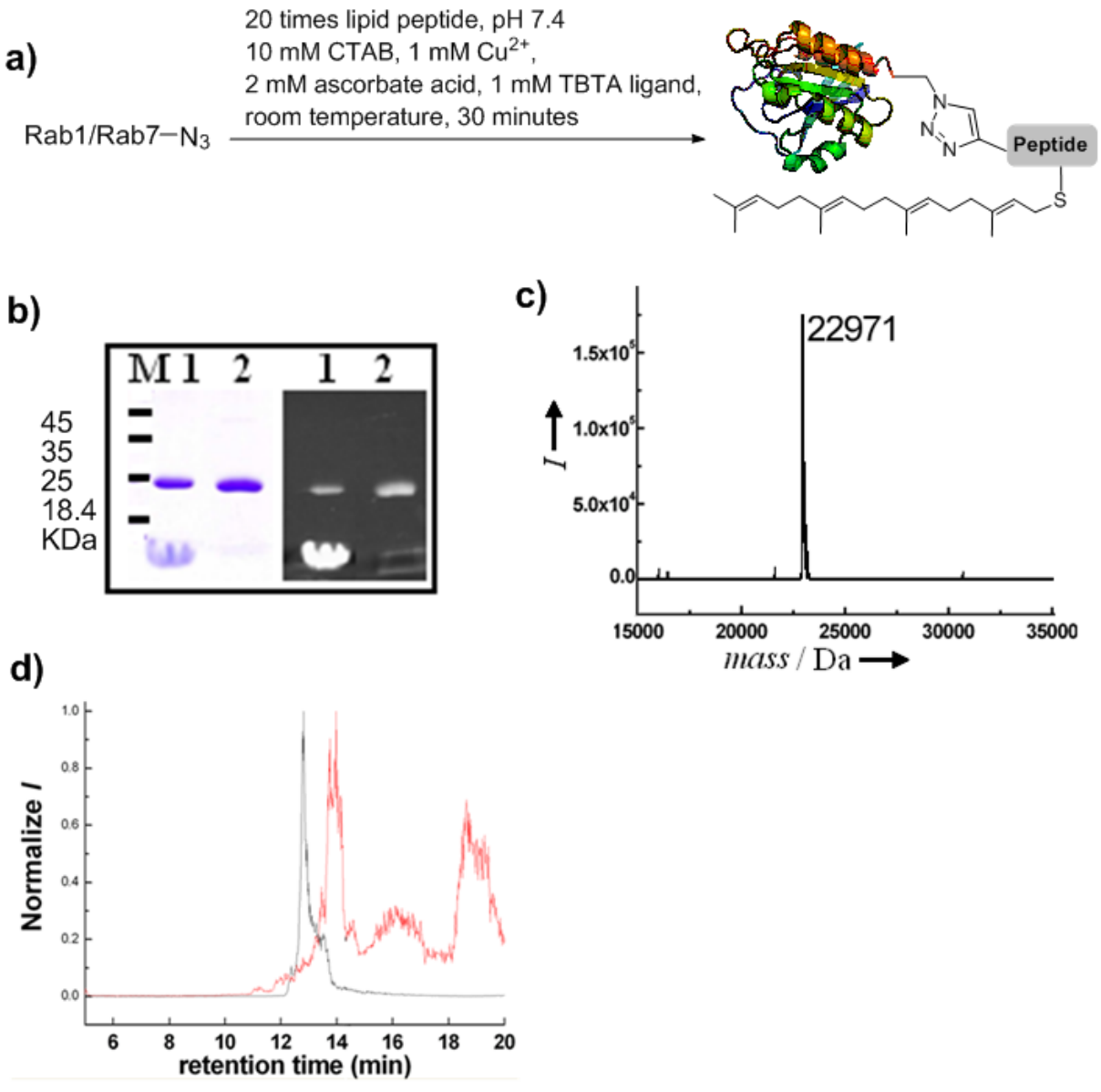

Figure 3.40. a) The click protocol for semisynthesis of geranylgeranylated Rab GTPases. b) SDS-PAGE of the ligated product of Rab1 with peptide **20** before (lane 1) and after (lane 2) purification. Lane M, molecular marker. The gel was photographed both in the UV light to show fluorescence (right) and in the visible light after Coomassie blue staining (left). c) ESI-MS spectrum of the ligation product of Rab1 and peptide **20** (M_{calcd} = 22965 Da). d) HPLC-MS profiles of Rab1-N_3 (black line) and the ligation product with prenylated peptide (red line). The elution condition: buffer A, 0.1% HCOOH in H_2O; buffer B, 0.1% HCOOH in

CH3CN; flow rate of 1 mL/min for RP-C4 column; 0-5 min, 80% buffer A; 5-15 min, 80-30% buffer A with gradient mode; 15-17 min, 30-10% buffer A; 17-19 min, 10-80% buffer A; then keep in 80% buffer A. The ESI-MS spectra between 12-15 min further indicated the quantitative conversion from Rab1-N_3 to Rab1-G.

Encouraged by these results, we tested the click reaction of azide-modified Rab with alkyne-containing lipidated peptides. Not surprisingly, the geranylgeranylated peptides **19-21** are very hydrophobic, which are insoluble in 30% methanol or 50 mM CHAPS-containing buffer. In previous studies, it was found that cetyltrimethylammonium bromide (CTAB) can efficiently solubilize the GerGer-containing peptides in buffer (Durek et al., 2004). In this study, the click reaction of prenylated peptides and azide-modified Rab proteins proceeded rapidly in the presence of CTAB. The appearance of fluorescent bands of 24 kDa in SDS-PAGE indicated the formation of the ligated product Rab1-G (Figure 3.40b). LC-MS analysis further indicated the quantitative ligation of Rab1 with prenylated peptides (Figure 3.40c). The HPLC traces of Rab1 before and after ligation with lipopeptide (Figure 3.40d) indicated the click reaction can be finished within 30 minutes.

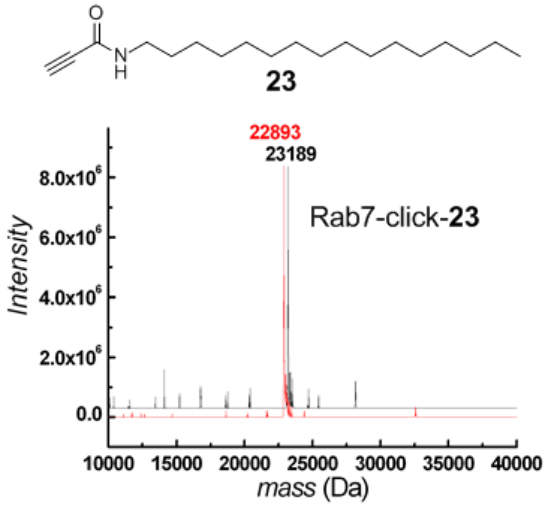

Figure 3.41. The chemical structure of **23** and ESI-MS spectra of Rab7-N_3 and the ligation product with **23**.

We further used an alkyne-containing hexadecyl chain **23** (a palmitoyl analogue, Figure 3.41) for lipid–protein bioconjugation. The click reaction between azide-modified Rab7 and **23** was complete within 30 min in the optimized click ligation protocol, as indicated by LC-MS. These results suggested that the click ligation strategy is general applicable for the generation of lipidated proteins.

EPL has successfully enabled the production of various lipidated Rab protein constructs for biochemical and biophysical studies (Thomas Durek PhD thesis, 2004; Yao-Wen Wu PhD thesis, 2008). It is proposed that the high charge density on the micelle surface (Figure 3.42) could additionally contribute to the polarization of the carbonyl thioester, thereby enhancing its reactivity. However, such effect leads to unavoidable hydrolysis of thioesters in CTAB buffer. Using two-step ligation strategy here, we can achieve the quantitative lipid-protein bioconjugate. The first-step of EPL is quantitative, since the ligation of **14** and thioester proteins can proceed smoothly without addition of CTAB. Now that the thioester groups have been transferred into azide groups, no hydrolysis will happen in this case (Figure 3.42). The tandem Click ligation is highly efficient to achieve quantitative conversion of azide-modified proteins into lipidated proteins.

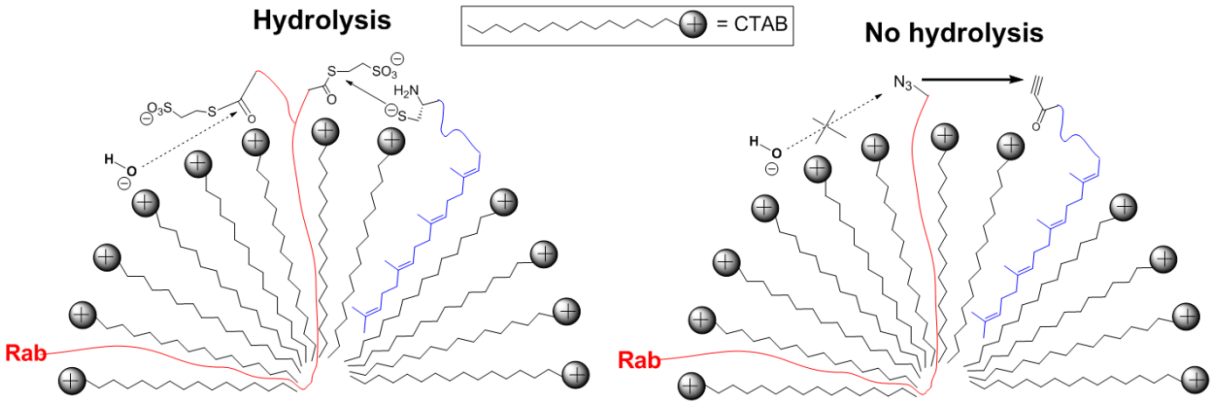

Figure 3.42. Hypothetical model of the micelle catalysis effect of CTAB for EPL (left) and Click ligation (right). Rab thioester is colored red and the geranylgeranylated peptide is shown in blue.

3.4.5. Development of a purification strategy

Upon completion of the click reaction, ligated proteins must be purified from contaminating lipidated peptides, and detergent (CTAB) or additive (MESNA), which unexpectedly turned out to be highly problematic. To this end, the reaction mixture was treated with ice-cold acetone or methanol (at least 10-fold volume), which resulted in fully protein precipitation and partly extraction of unligated peptide into the organic phase (Figure 3.43). It appeared that the geranylgeranylated Rab tightly associates with the prenylated peptide and CTAB, which is presumably due to the result of strong hydrophobic interactions. Therefore, the protein pellet was washed with organic solvents such as methanol and dichloromethane and then with water to remove unreacted prenylated peptides and detergents. Using this approach peptide free ligation proteins could be obtained.

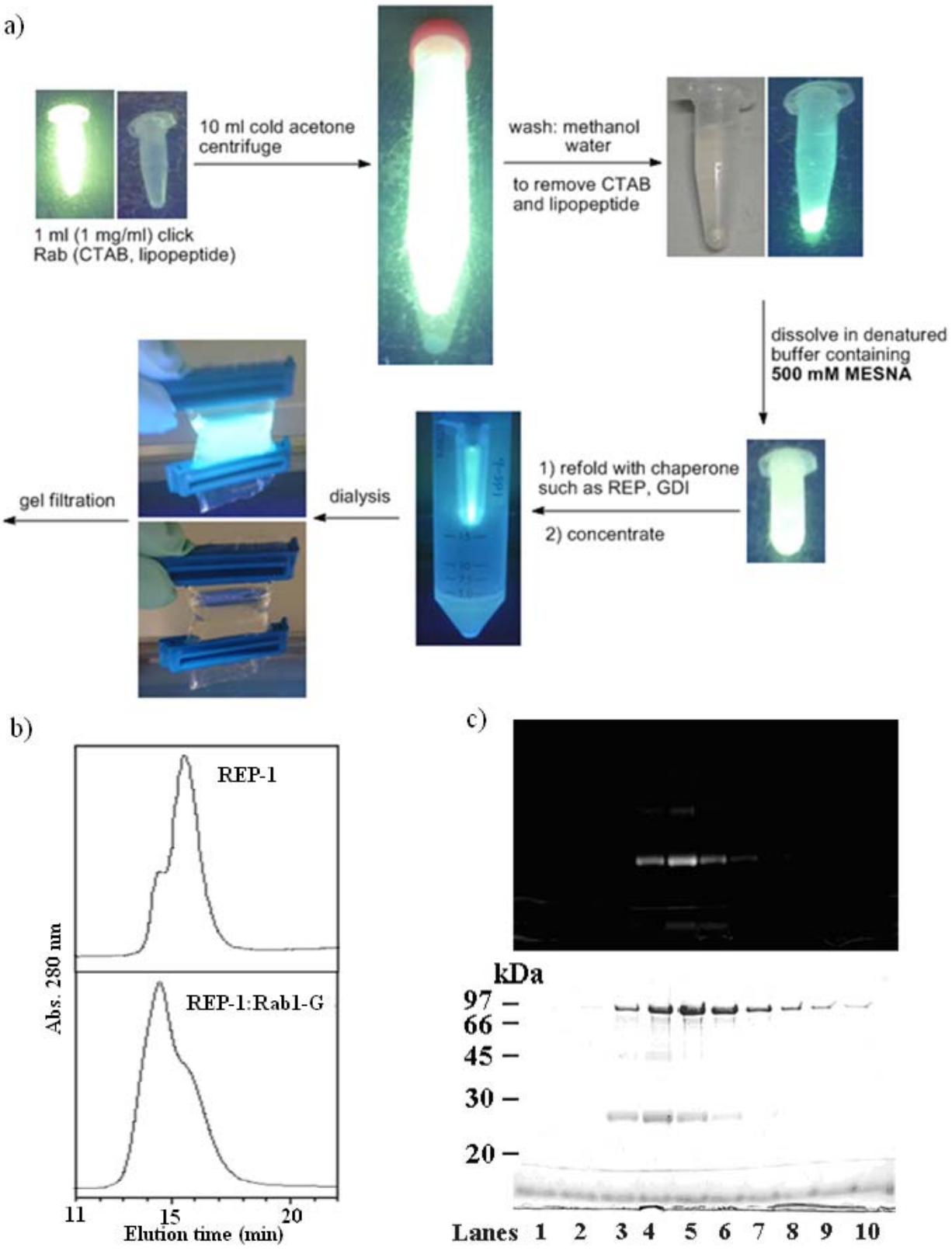

Figure 3.43. a) Photograph showing the general purification protocol for semisynthetic prenylated proteins. b) Gel filtration chromatography of Rab1C(G)C:REP-1 complex and REP-1. c) SDS-PAGE analysis of the resulting fractions of the Rab1C(G)C:REP-1 complex from 12 to 21 min (elution time) as resolved in lane 1-10, respectively. The gel was photographed both in the UV light (up) and the visible light after Coomassie blue staining (down).

The renaturation step is necessary to achieve functional lipidated proteins. The protein pellet was firstly dissolved in 8 M guanidinium-HCl containing 500 mM MESNA that successfully disrupted the disulfide crosslinking and the protecting group StBu of the C-terminal cysteine. The resulting protein was refolded by pulse dilution into refolding buffer. To stabilize the lipidated protein after removal of the detergent, Rab chaperones such as REP-1 or GDI-1 were added. After renaturation of the lipid-modified Rab protein further purifications turned out to be straightforward using standard biochemical procedures including dialysis and gel filtration (Figure 3.43). The large volumes of very dilute protein solutions had to be concentrated before gel filtration. The yield of proteins from this refolding procedure is about 40% (based on azide-modified proteins).

Based on the present method, we constructed prenylated Rab1 proteins and REP-1 complexes arising from the ligation of Rab1 with peptide **20** and **21**, termed Rab1-CC(G) and Rab1-C(G)C, respectively. The prenylated Rab1 (Rab1-G):REP-1 complexes were subject to size-exclusion chromatography. A single protein peak eluted earlier than the REP-1 peak contained both prenylated Rab1 and REP-1 proteins as indicated by SDS-PAGE of the eluted fractions (Figure 3.43), suggesting that prenylated Rab1 form a tight complex with REP-1 (Alexandrov et al., 1999).

3.4.6. *In vitro* protein prenylation of lipoproteins

The binding activity of the semi-synthetic Rab1-G protein with REP-1 implies its functionality. This prompted us to ask whether the obtained mono-geranylgeranylated Rab protein could function as a prenyl acceptor in the prenylation reaction meditated by RabGGTase. Using NBD-farnesyl pyrophosphate (NBD-FPP) (Wu et al., 2006), a fluorescent analogue of geranylgeranyl pyrophosphate (GGPP), we performed an *in vitro* prenylation assay in which the Rab1-G:REP complex was incubated with RabGGTase and NBD-FPP. As shown in Figure 3.44a, incorporation of NBD-isoprenoids to Rab1-G proteins was observed (Figure 3.44a, Lane 6 and 7), while no incorporation was observed when RabGGTase was omitted (Figure 3.44a, Lane 4 and 5). This suggests that the semi-synthetic Rab1-G can accept another prenyl group through the prenylation reaction. This result indicated that the semisynthetic lipidated proteins were correctly refolded and functional.

We further used the fluorescence change of the C-terminal dansyl group upon prenylation to monitor the prenylation of both mono-geranylgeranylated Rab intermediates. The time course of fluorescence decrease could be fitted with a double-exponential function (Figure 3.44b). The observation of non-single exponential reaction kinetics is probably due to a

conformational change following the chemical step. This is not surprising, since diprenylated C-terminus has to move out of the active site of RabGGTase and associates with the lipid binding site on the REP molecule (Thomä et al., 2001; Pylypenko et al., 2006; Wu et al., 2009). Prenylation of Rab1-C(G)C (k_1 = 0.002 s^{-1}) is slightly faster than that of Rab1-CC(G) (k_1 = 0.0015 s^{-1}), suggesting that the protein with the first prenyl group at the N-terminal cysteine may adapt more favourable conformation for the second prenyl transfer. Thus, we conclude that the N-terminal cysteine of Rab1 is preferred for the first round of prenylation. This is consistent with the previous finding that the prenylation of Rab1-CS is slightly faster than that of Rab1-SC (Shen et al., 1996). In contrast, in the case of Rab7 with CXC C-terminal motif the upstream cysteine is preferred for the first prenyl transfer (Durek et al., 2004; Thomä et al., 2001). It is conceivable that C-terminal motif (CC or CXC) of Rab proteins might determine which cysteine is preferred for the first prenyl transfer. These scenarios could be explained by the fact that Rab C-terminus is flexible and adapts a variety of conformations during prenylation (Wu et al., 2009). Nevertheless, the order of cysteine residues does not appear to significantly affect the extent of Rab protein prenylation *in vitro* (Farnsworth et al., 1994), and both C-terminal cysteines of Rabs were geranylgeranylated. However, the biological role of ordered digeranylgeranylation remains elusive.

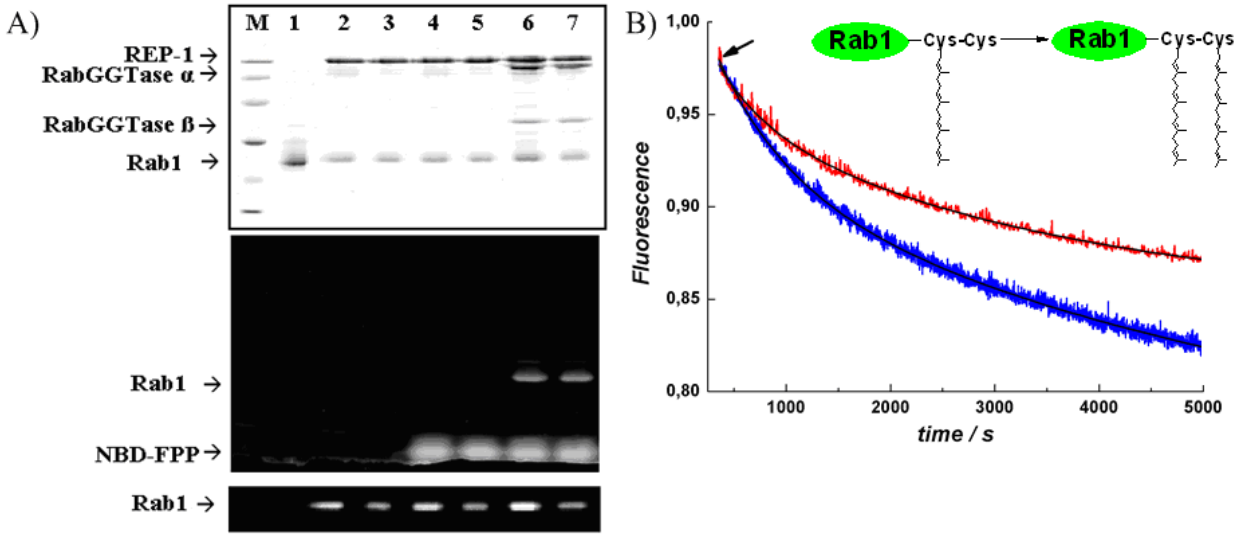

Figure 3.44. The activity of Rab1-G in complex with REP-1 was confirmed by *in vitro* prenylation assay. A) Incorporation of NBD-FPP to Rab1-G upon *in vitro* prenylation resolved by SDS-PAGE (top: Coomassie blue staining; middle: scan of NBD fluorescence (ex: 488 nm); bottom: scan of dansyl fluorescence in UV light. Lane 1: Rab1Δ5-thioester, Lanes 2: Rab1-C(G)C:REP-1 complex, Lane 3: Rab1-CC(G):REP-1 complex. Lanes 6 and 7, prenylation of the Rab1-C(G)C (lane 6) and Rab1-CC(G) (lane 7) in complex with REP-1 in the presence of RabGGTase and NBD-FPP for 1 h at room temperature. Lanes 4 and 5: the same reactions as shown in lane 6 and 7 in the absence of RabGGTase. It is noted that there was no crosstalk between dansyl and NBD fluorescence under these conditions. B)

Prenylation reactions of semisynthetic Rab1-G. 75 nM Rab1-G:REP complex was incubated with 75 nM RabGGTase, and 30 μM GGPP was added at the point indicated by arrows. The solid lines represent fits to a double-exponential equation for Rab1-CC(G) in red (k_1 = 0.0015 s^{-1} and k_2 = 0.00016 s^{-1}) and Rab1-C(G)C in blue (k_1 = 0.002 s^{-1} and k_2 = 0.0003 s^{-1}).

4.4.7. Conclusion

In summary, we have presented a new strategy using tandem EPL and click chemistry to site-specifically install hydrophobic lipids into proteins. The two-step ligation reaction is quantitative, which makes the purification of ligated protein much facile. The approach yielded correctly folded and functional geranylgeranylated Rab GTPases, as could be inferred by their ability to interact with REP/GDI as well as to accept the second prenyl group in prenylation. The ligation strategy may open up a new avenue for the production of lipidated proteins that are used in various biological studies. What is more, the replacement of Rab C-terminal sequence with unnatural triazole moiety did not influence Rab prenylation, which encourages further modifications at the Rab C-terminus for the investigation of Rab GTPases functions. Based on this study, we aim to use chemical linkers to replace the C-terminal hypervariable region of about 35 amino acids of Rabs to probe Rab prenylation and subcellular localization mechanism in following studies.

3.5. Semisynthesis of PEGylated proteins for probing Rab prenylation and localization mechanism

3.5.1. Introduction

Rab proteins require a posttranslational modification that is conferred by RabGGTase together with an additional factor REP, which attaches geranylgeranyl moieties onto (usually) two cysteines at their C-terminus. Rab prenylation requires the formation of a catalytic Rab-REP-RabGTPase ternary complex (Alexandrov et al., 1999). Although the structure of the ternary complex is not available, a model of the complex has been established based on the crystal structures of Rab-REP and REP-RabGGTase binary complexes (Pylypenko et al., 2003; Rak et al., 2004; Wu et al., 2009). Structure and interaction analysis suggest that three binding interfaces contributed from 1) the GTPase domain; 2) C-terminal interacting motif (CIM) of Rab with REP; 3) RabGGTase with REP confer the establishment of the ternary complex (Guo et al., 2008; Wu et al., 2009). Computational simulation of the disordered Rab C-terminal peptide in the ternary complex and biochemical validation suggest that the flexible C terminus of Rab substrate forms a series of weaker and less specific interactions that channel it into the active site of RabGGTase. In order to further understand the mechanism of Rab prenylation, we want to know whether there is anything required for Rab C-terminal sequence and to what extent the Rab prenylation machinery could tolerate the change in the Rab C-terminal sequence. We speculated that the assembly of Rab prenylation machinery could allow any C-terminal cysteine residue that is presented into the active site of RabGGTase to undergo prenylation, and therefore, if we replace the Rab C-terminal sequence with a non-native peptide chain such as a polyethylenglycol (PEG) linker, Rab could still be prenylated.

On the other hand, the C-terminal hypervariable region of 35 to 40 amino acids shows the highest level of sequence divergence between Rab family members, and was postulated to act as a signal for subcellular targeting. Zerial and co-workers showed that replacing the C-terminal 35 residues of Rab5 with the equivalent C-terminal region of Rab7 resulted in re-localization of the hybrid Rab to Rab7-positive late endosomal structures (Chavrier et al., 1991). Targeting of Rab proteins via the hypervariable region is a widely accepted model, but the underlying molecular mechanisms have not been elucidated further. Despite the attractiveness of this proposal, recent studies indicated that this is not the case for several Rabs. We reason that if we replace the C-terminal hypervariable region of Rabs with a non-

native peptide chemical linker, the result protein probes could be used for studying Rab localization mechanism.

In this work, we semisynthesized a series of Rab probes that the C-terminal hypervariable region and prenylatable cysteines are replaced by PEG linkers and thiols, respectively. Biochemical analysis suggested that the resulting PEGylated Rab probes were prenylated as efficiently as the wild type Rab proteins. Using the EGFP-tagged Rab probes, we found that the flexible C-terminal sequences of some Rabs (such as Rab1 and Rab5) have no contribution for their cellar localization.

3.5.2. Replace the peptide after CIM by a chemical linker

Firstly, we chose a well-characterized Rab7 protein as the model protein. We aimed to replace the peptide after the essential CIM motif by a PEG linker. Since the length of the linker is critical for Rab prenylation (Wu et al., 2009), we sought to produce a PEGylated Rab7 protein conjugate that has a similar C-terminal length as that of the wild type protein (Figure 3.45a). To this end, we truncated the amino acid residues after the CIM motif of Rab7 protein and cloned the truncated Rab7 gene in an intein vector (pTWIN1). Rab7Δ15-thioester protein was produced through intein-medicated protein splicing using MESNA as the thiol reagent. Subsequently, Rab7Δ15-thioester was treated with bis(oxyamine) at pH 7.5 on ice for 4 h to achieve oxyamine-modified protein, Rab7Δ15-ONH_2, which is competent for oxime ligation with a chemical linker containing a ketone moiety (see part 3.1 for details).

As shown in Figure 3.45, we designed a chemical linker **24** containing a ketone group for oxime ligation, a PEG linker, and two prenylatable cysteines. This linker was synthesized by stepwise solid-phase synthesis using Fmoc-Cys(StBu), (4,7,10)-trioxa-1,13-tridecanediamine (TTD), succinic anhydride, and 3-(2-methyl-1,3-dioxolan-2-yl)propan-1-amine as building blocks (Figure 3.45b). Firstly, Fmoc-Cys(StBu) was loading on 2-Cl-Trt resin with loading efficiency of 0.4-0.5 mmol/g. After deprotection of the Fmoc group, the linker was extended by standard coupling protocols (see synthesis details in the experimental part). It is noted that after the coupling of TTD, the coupling reaction on resin became inefficiency, probably due to the long and flexible structure of this TTD linker. Finally, the linker was cleaved from the resin by treatment with 5% TFA in CH_2Cl_2, and in this case the protection group of ketone was also cleaved. The result crude product was purified by prep-HPLC with the final yield of about 8%.

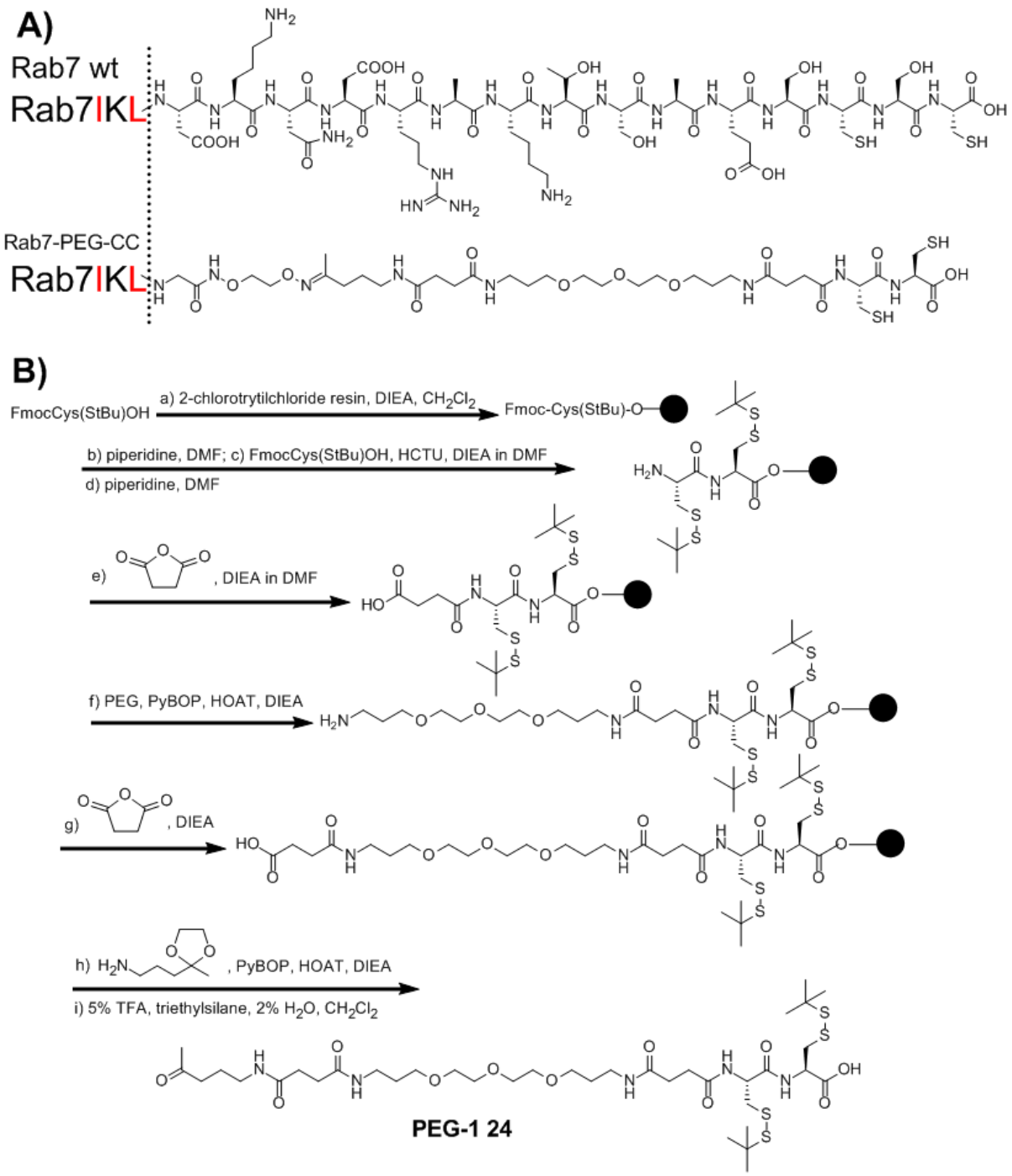

Figure 3.45. A) Chemical structures of the C-terminus of Rab7 wild type and the design bioconjugate Rab7-PEG-CC. B) Synthesis route for the chemical linker **24**.

The PEG-1 linker **24** contains two cysteines protected with StBu groups, which can be removed by the treatment with reducing reagents after protein ligation. Incubation of **24** and Rab7Δ15-ONH_2 on ice overnight resulted in full conversion of the oxyamine to an oxime adduct, Rab7-PEG-1, as shown by SDS-PAGE (Figure 3.46). It is noted that because **24** has little water-soluble, 10% methanol had to been added into the ligation buffer to keep **24** soluble. Though organic solvents have the potentially negative effect on protein samples, I

found that reaction at the low-temperature (protein ligation on ice) is enough mild to keep protein stable under these conditions. The overall yield of the semisynthesis protein is larger than 90%, implying that the ligation conditions are mild and efficient. After the oxime ligation, the unreacted linker **24** can be easily removed by a desalting column. The StBu groups in the semisynthesis Rab7-PEG-1 cannot be removed efficiently by treatment with 200 mM DTE overnight (data not shown). I speculate that the steric effect of two StBu groups from two neighbor cysteines may be responsible for this slow reaction kinetics. A smaller thiol reagent instead of DTE may be more efficient for this cleavage. Finally, we found that 500 mM MESNA can be used to cleave both StBu groups fast and completely, as indicated by LCMS (Figure 3.46c), to achieve thiol-free protein Rab7-PEG-1-CC.

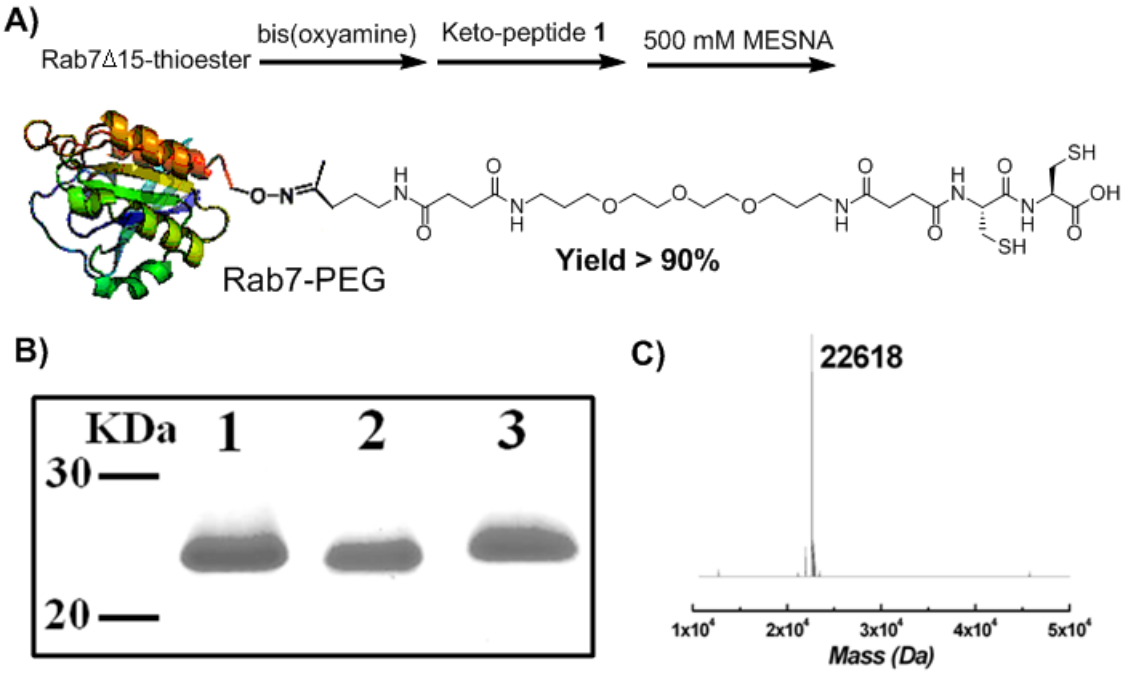

Figure 3.46. A) Semisynthesis of Rab7-PEG-CC. B) SDS-PAGE analysis of Rab7Δ15-thioester (lane 1), Rab7Δ15-ONH_2 (lane 2) and Rab7-PEG-CC (lane 3). C) ESI-MS spectrum of Rab7-PEG-CC (M_{calcd} = 22613).

The obtained Rab7-PEG-1-CC was subjected to *in vitro* prenylation assay using substrates NBD-FPP and GGPP. The prenylation reaction was allowed to proceed for 1 h at 37 °C and was quenched by addition of SDS-PAGE sample buffer, after which the samples were resolved on a 15% SDSPAGE gel and scanned for fluorescence using a laser fluorescent image reader followed by Coomassie blue staining. As shown in Figure 3.47, Rab7-PEG-1-CC displays nearly identical prenylation efficiency to that of the wild type Rab7 protein. The prenylation kinetics at room temperature further supported that Rab7-PEG-1-CC can be

prenylated as efficient as that of wide-type Rab7. Prenylation of Rab7-PEG-CC using GGPP also led to the doubly geranylgeranylated protein as shown by ESI-MS. These results suggest that, as expected, replacing the peptide between the CIM motif and the prenylatable cysteines with a non-peptidic PEG linker does not affect Rab prenylation, and the Rab protein substrate specificity is not encoded in this C-terminal region.

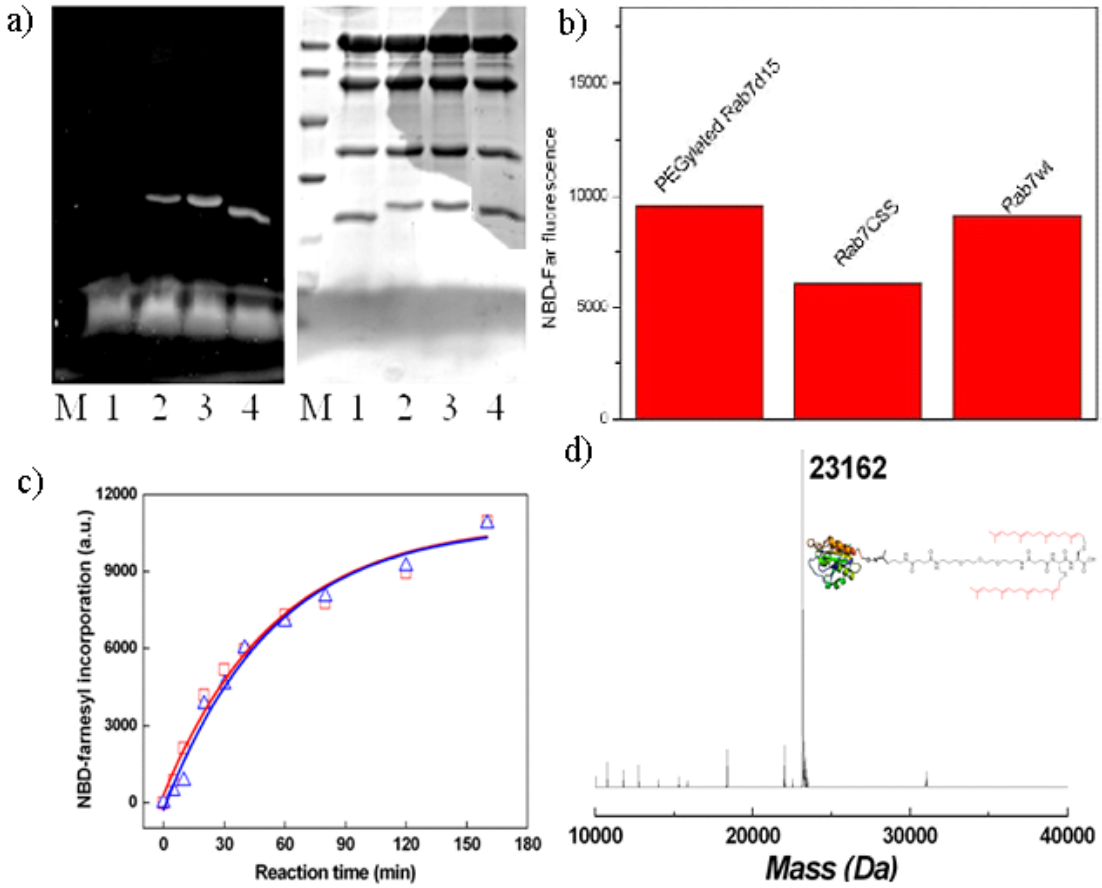

Figure 3.47. a) The activity of semisynthesis protein probe Rab7-PEG-1-CC was confirmed by *in vitro* prenylation reaction through incorporation of NBD-FPP to Rab resolved by SDS-PAGE (left: scan from a laser fluorescent image reader excitation at 473 nm; right: photograph in visible light after Coomassie blue staining). Lane 1: Rab7Δ15-ONH_2; Lane 2: Rab7CSS; Lane 3: Rab7 wide type; Lane 4: Rab7-PEG-1-CC. b) The relative fluorescence intensity of the Rab bands in a). c) Reaction kinetics of the *in vitro* prenylation by an end-point assay based on NBD-FPP for Rab7-PEG-1-CC. d) LCMS spectra of the prenylation reaction in the presence of the RabGGTase substrate GGPP (M_{calcd} = 23157 Da). Reaction condition: 6 µM PEGylated Rab7, 10 µM REP, and 6 µM RabGGTase were mixed with 100 µM GGPP in prenylation buffer and incubated for 1 h at 37 °C. Before reaction, the Rab protein eluted at about 12.7 min, while after geranylgeranylated reaction, the protein eluted at about 17 min, and the prenylation reaction was clearly shown by the change of mass spectra.

4.5.3. Replace prenylatable cysteines with a thiol group

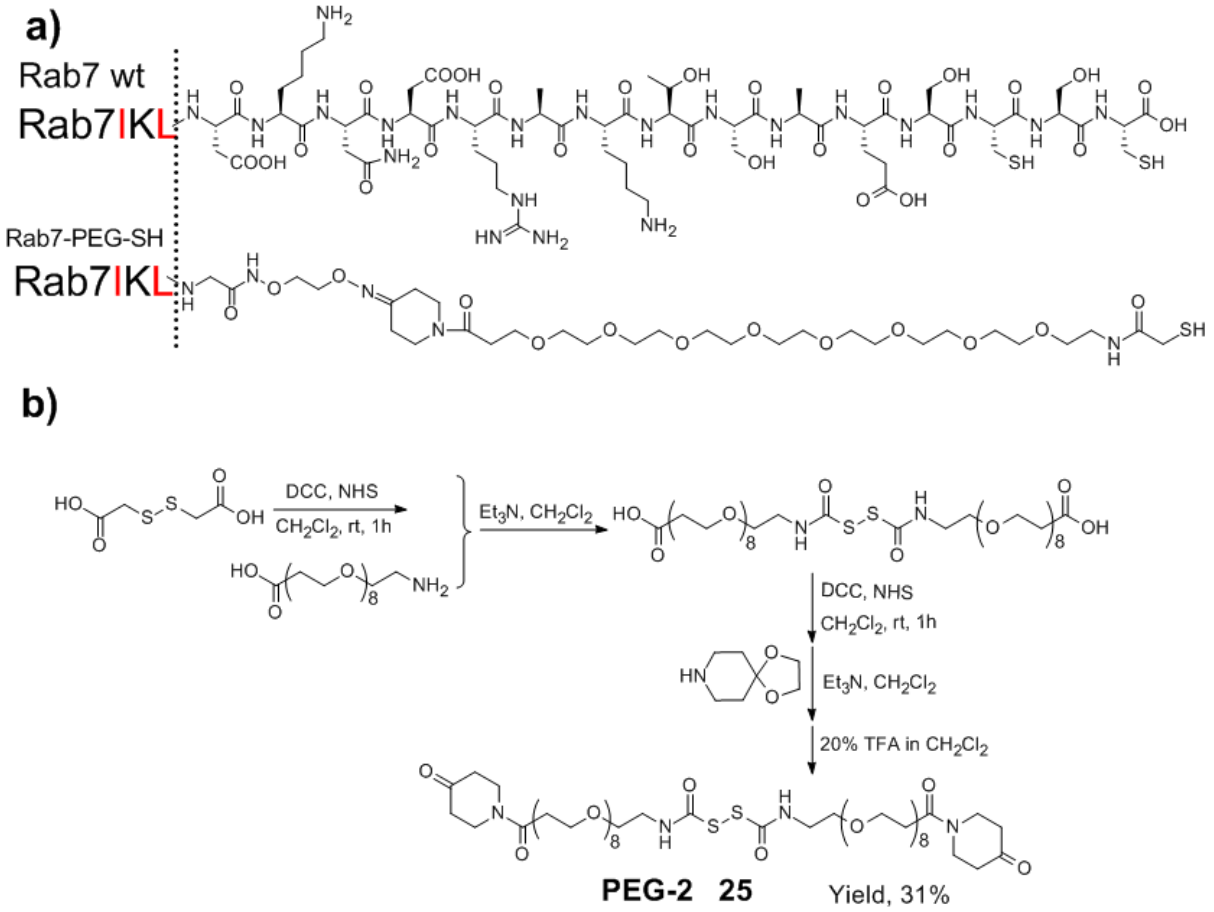

Figure 3.48. a) Chemical structures of the C-terminus of Rab7 wild type and the design bioconjugate Rab7-PEG-2-SH. b) Synthesis route for the chemical linker **25**.

From above studies, we know that the Rab7 C-terminus downstream the conserved CIM motif does not encode specificity for Rab prenylation. We hope to further probe whether the prenylatable cysteines can be replaced by thiols. A chemical linker PEG-2 **25** was designed (Figure 3.48), which contains a ketone group for protein ligation, a $(PEG)_8$ linker and a prenylatable thiol linked by disulfide bond, which can be easily cleaved by using 5 mM DTE during protein ligation.

Unlike PEG-1 **24**, the PEG-2 **25** is water-soluble. So we can perform the oxime ligation of **25** and Rab7Δ15-ONH_2 in buffer without addition of methanol co-solvent. The LCMS spectrum indicated the successful protein ligation to give a protein peak at 22508 (Figure 3.49). The result bioconjugate Rab7-PEG-2-SH can be prenylated by RabGGTase (Figure 3.49b-d). Using NBD-FPP, Rab7-PEG-2-SH displays faster prenylation efficiency than that of the wild type Rab7 protein. This is reasonable considering that there is only one thiol in the semisynthesis protein rather than two cysteines in wide-type protein. Prenylation of Rab7-

PEG-2-SH using GGPP led to the geranylgeranylated protein (Figure 3.49d). These results imply that the thiol group in Rab7-PEG-SH can be prenylated as efficient as cysteines at the Rab C-terminus, suggesting a flexibility within RabGGTase prenylation machine!

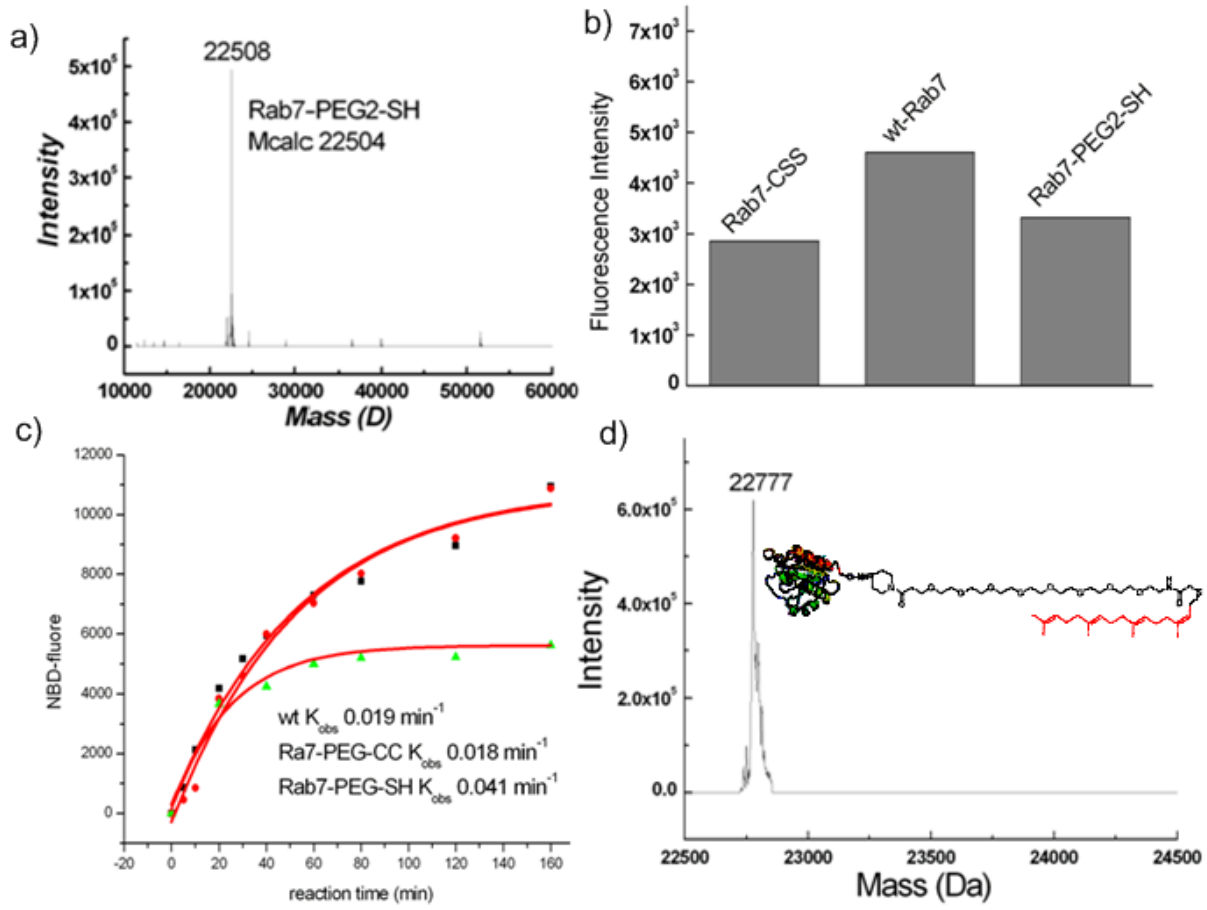

Figure 3.49. a) LCMS spectrum of the Rab7-PEG-2-SH protein. b) The relative fluorescence intensity of the Rab bands in *in vitro* prenylation reaction through incorporation of NBD-FPP to Rab resolved by SDS-PAGE. c) Reaction kinetics of the *in vitro* prenylation by an end-point assay based on NBD-FPP. d) LCMS spectra of the prenylation reaction in the presence of the RabGGTase substrate GGPP (M_{calcd} = 22780 Da). Reaction condition: 6 μM PEGylated Rab7, 10 μM REP, and 6 μM RabGGTase were mixed with 100 μM GGPP in prenylation buffer and incubated for 1 h at 37 °C.

4.5.4. Replace the C-terminal hypervariable region with chemical linkers

Considering the fact that the C-terminal hypervariable region of about 30-40 amino acids shows the highest level of sequence divergence between Rab family members, we further argue that whether the C-terminal hypervariable region before the CIM motif contributes to Rab prenylation. In order to answer this question, we firstly designed and synthesized a very long PEGylated chemical linker PEG-3 (Figure 3.50) to try to replace the Rab7 C-terminal hypervariable region of 34 amino acids. It is noted that the CIM motif, which is necessary for the Rab:REP interaction, must be kept in the linker.

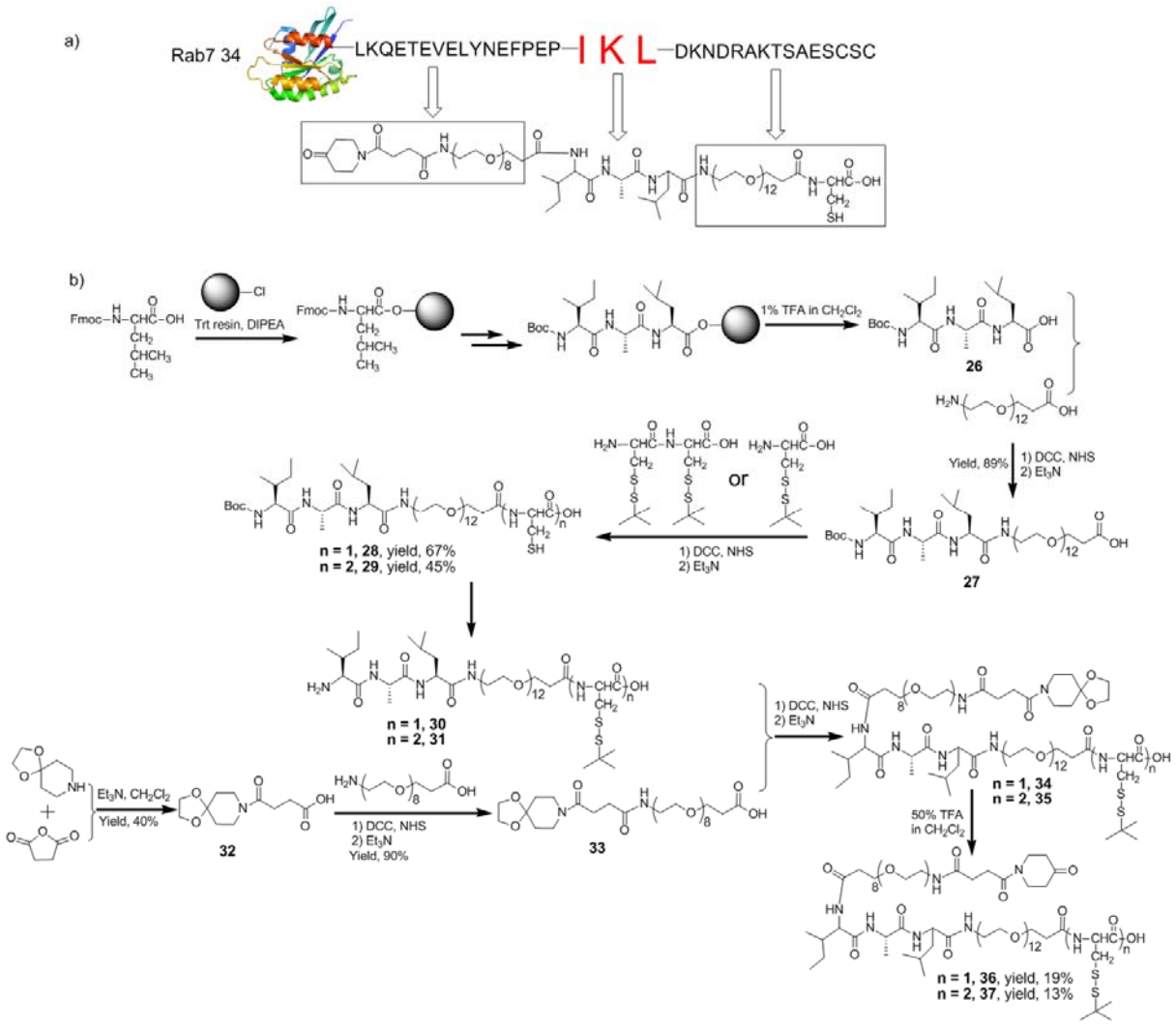

Figure 3.50. a) The design of PEG-3 linker based on wide-type Rab7. b) The synthesis route for the linkers **36** and **37**. DCC: dicyclohexylcarbodiimide. NHS: N-hydroxysuccinimide.

As shown in Figure 3.50a, the C-terminal sequence before the IKL motif is replaced by a ketone-containing $(PEG)_8$ fraction. Considering the facile synthesis for PEG-3 liker, we replace lysine in the IKL motif as alanine. The amino acids after the IKL motif were replaced by a PEG_{12} fraction. One or two cysteines were appended at the C-terminus of the linker for prenylation.

The synthesis of PEG-3 **36** and **37** were achieved by the combination of SPPS and solution synthesis (Figure 3.50b). Firstly, the tripeptide IAL was prepared in SPPS. Cleavage of peptide **26** at weak acid condition (1% TFA) is mild enough for keeping the Boc group. The selective coupling between **26** and an amino group in PEG_{12} was achieved by firstly preactivating **26** with DCC and NHS, and then reacting with the amine group in the presence of carboxylate group (Brunsveld et al., 2005). Such a two-step strategy is efficient (normally yield > 80%) for following coupling reactions. Finally, the Boc group was deprotected to give

30 and **31** for subsequent coupling reaction. An N-terminal fragment **33** was prepared separately. The coupling of **33** and **30** or **31** gave the final linkers with protected ketones. Surprisingly, the deprotection of ketones in **34** or **35** becomes more difficult than that in **24** or **25**. I could not remove the protection group in normal condition (5% TFA in CH_2Cl_2). Finally, the deprotection condition was optimized as 50% TFA in CH_2Cl_2 for overnight reaction. The ketone group in these long and flexible PEG-3 linkers (**36**, **37**) could be schielded from the deprotection reaction, and this point is further supported by their very slow oxime ligation.

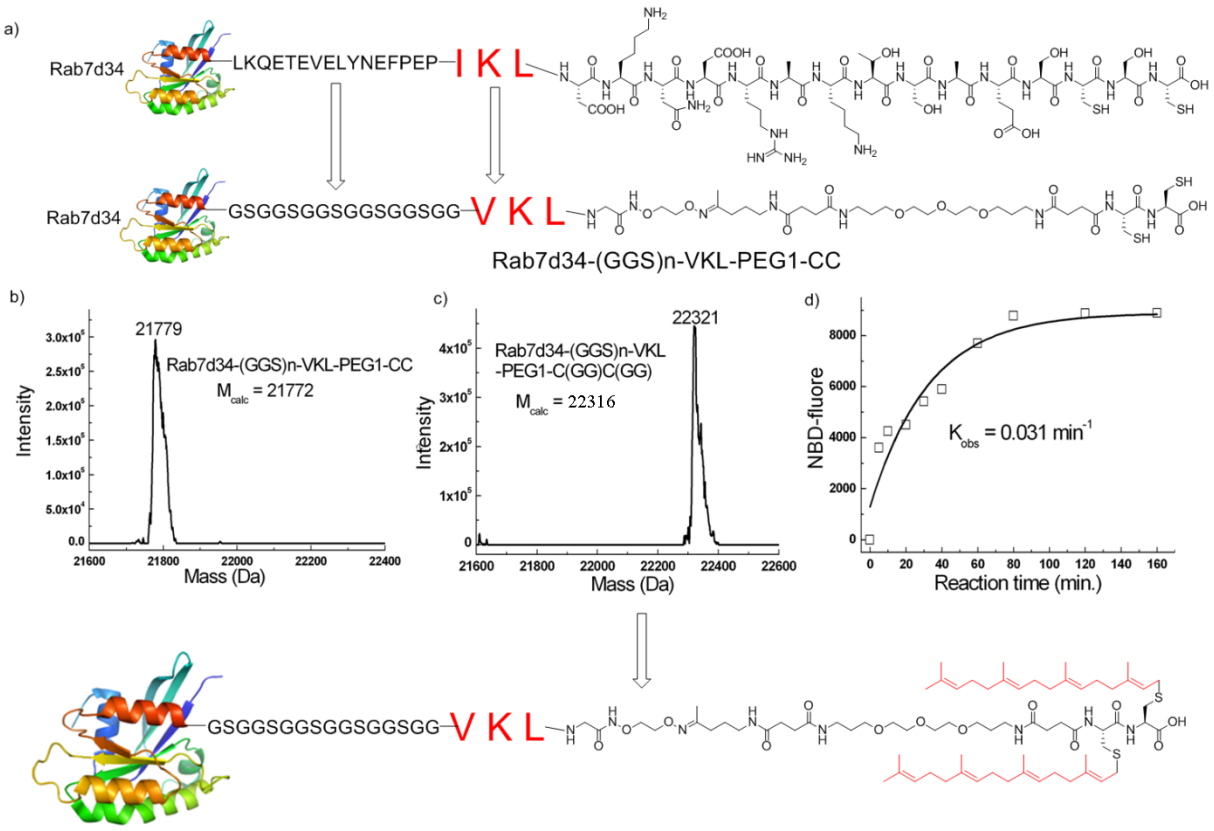

Figure 3.51. a) Design of Rab7-GGS-PEG1-CC. b) and c) LCMS spectra of the semisynthesis protein probe and its prenylation product based on GGPP. The prenylation condition was similar with that for Rab7-PEG1-CC. d) Reaction kinetics of the *in vitro* prenylation by an end-point assay based on NBD-FPP.

The oxime ligation between oxyamine-modified proteins and **36** or **37** cannot be achieved based on the establishment ligation conditions (data not shown). On the other hand, the protein expression and purification of Rab7Δ34-thioester were highly problematic. Though the Rab7Δ34-intein protein was soluble, the Rab7Δ34-thioester was unstable and precipitated during purification procedures. I have met a similar case in the protein purification of $Ran_{1\text{-}178}$, a C-terminal deleted construct of Ran. The C-terminal amino acids of Rab GTPases could contribute to the protein stability. We then re-consider the experimental design, since it looks very difficult to achieve the ligation of Rab7Δ34 and PEG-3 linkers.

Consequently, we try to use a non-specific sequence linker (Pedersen, et al., 1998), (GGS)n, to replace the C-terminal hypervariable region before the CIM motif. As shown in Figure 3.52a, we aim to use (GGS)n-VKL-PEG1-CC to replace the C-terminal 35 amine acids of Rab7 and other Rabs. The successful semisynthesis of the protein probe Rab7Δ34-(GGS)n-VKL-PEG1-CC is indicated by LCMS (Figure 3.51b) and SDS-PAGE. Prenylation of Rab7Δ34-(GGS)n-VKL-PEG1-CC using GGPP led to the double-geranylgeranylated protein as indicated by LCMS result (Figure 3.51c). Using NBD-FPP, this protein probe displayed a little faster prenylation efficiency than that of the wild type Rab7. These results imply that the Rab C-terminal hypervariable region besides CIM motif does not encode Rab prenylation signal specificity.

The study presented here further elaborated the model for Rab prenylation. The specificity of Rab prenylation machinery is conferred by three binding interfaces, including GTPase domain and CIM of Rab with REP and RabGGTase with REP. Once the ternary protein complex is established, Rab C-terminus is concentrated within the micro-environment of the ternary complex, thus, enhances the chances of C-terminal cysteines or even thiols reaching the active site of RabGGTase. Rab C-terminal hypervariable sequence upstream and downstream the CIM does not contribute specificity and binding energy to the assembly of ternary protein complex. As a consequence, Rab protein substrate specificity does not need to be encoded in the prenylatable C-terminus. The model is consistent with the fact that RabGGTase has essentially no sequence preference for the context of the prenylatable cysteines, and the C-terminal sequences occurring in Rab GTPases include CC, CXC, CCX, CCXX, CCXXX, and CXXX (Pereira-Leal et al., 2001). Hence any cysteine-containing fragment, even any thiol-containing fragment, which can properly present the thiols into the active site of RabGGTase, is able to undergo prenylation. This point is proved by our results that Rab C terminus replaced by a thiol-containing chemical linker did not affect its *in vitro* prenylation efficiency. The very flexible prenylation ability of RabGGTase prenylation machine allows it to process a family of over 60 Rab proteins with hypervariable C-terminal sequences, a feature that is uncommon in protein-modifying enzymes. In this study, we further find that using (GGS)n-VKL-PEG1-CC to replace the C-terminal 35 amino acids of Rab7 did not influence prenylation by RabGGTase. Therefore, the unique feature of Rab prenylation machinery enables it to process unnatural Rab C-terminal moieties that contain cysteines or thiols. Based on this study, it is also possible to produce di-gernaylgeranyled peptides by using a cleavable linker at the Rab C-terminus.

3.5.5. Synthesis of GFP-tagged Rab probes for studying membrane targeting

The next question we are interested in is whether the C-terminal hypervariable region of Rab proteins contributes to Rab subcellular localization. We intended to use the semisynthesis protein probes to address this point. EGFP is tagged to Rab N-terminus as a fluorescent indicator, since it is reported that such tagging do not interfere Rab localization and function in living cells (Ali et al., 2004). In this work, we produced a series of EGFP-tagged Rab proteins (Rab1, Rab5, Rab7, Rab8, Rab35) without the flexible C-terminal sequence. The expressed Rab proteins were ligated with chemical linkers **24** and **25** as described above (Figure 3.52a-c). All semisynthesis proteins were characterized by LCMS spectra (Table 3.1) and SDS-PAGE, indicating the successful preparation of these protein probes.

Table 3.1. LCMS results of Rab protein probes used in this study. (calculation mass)

Protein (P)	P-COSR	P-ONH2	P-PEG1	P-PEG1-CC	P-PEG1-C(GG)C(GG)	P-PEG2-SH	P-PEG2-S(GG)
Rab7Δ15	21974 (21972)	21926 (21922)	22792 (22789)	22617 (22613)	23162 (23157)	22508 (22500)	22777 (22772)
EGFP-Rab1 Δ13	49732 (49752)	49683 (49702)	50553 (50569)	50378 (50393)		50271 (50280)	
EGFP-Rab5 Δ14	50001 (50019)	49954 (49969)				50545 (50547)	
EGFP-Rab5-Q79L-Δ14	49988 (50004)	49943 (49954)	50798 (50821)			50520 (50532)	
EGFP-Rab7 Δ15	50889 (50905)	50836 (50855)	51707 (51722)	51532 (51546)		51459 (51433)	
EGFP-Rab8 Δ13	49659 (49652)	49602 (49602)				50168 (50180)	
EGFP-Rab35 Δ11	50527 (50542)	50481 (50492)	51346 (51359)	51170 (51183)			
Rab7Δ34-(GGS)n-VKL-GG	21135 (21131)	21086 (21081)	21954 (21948)	21779 (21772)	22321 (22316)		
EGFP-Rab1 Δ31-(GGS)n-VKL-GG	49122 (49134)	49078 (49084)	49938 (49951)	49775 (49975)			
EGFP-Rab5-Q79L-Δ35-(GGS)n-VKL-GG	49186 (49191)	49150 (49140)	50007 (50007)	49834 (49834)			
EGFP-Rab7 Δ34-(GGS)n-VKL-GG	49025 (49037)	48977 (48987)	49841 (49855)	49678 (49679)			

All EGFP-tagged Rab probes were tested for *in vitro* prenylation reaction through incorporation of NBD-FPP to Rabs resolved by SDS-PAGE. As shown in Figure 3.52d, strong fluorescence of the semisynthesis Rab probes can be observed in SDS-PAGE, while in the case of pure EGFP-tagged Rabs, only weak fluorescence is indicated by the fluorophore of EGFP. All Rab probes can be prenylated based this fluorescence assay. These results imply that Rab probes were efficiently prenylated *in vitro*, and again indicate that the RabGGTase machine is indeed very flexible for protein prenylation.

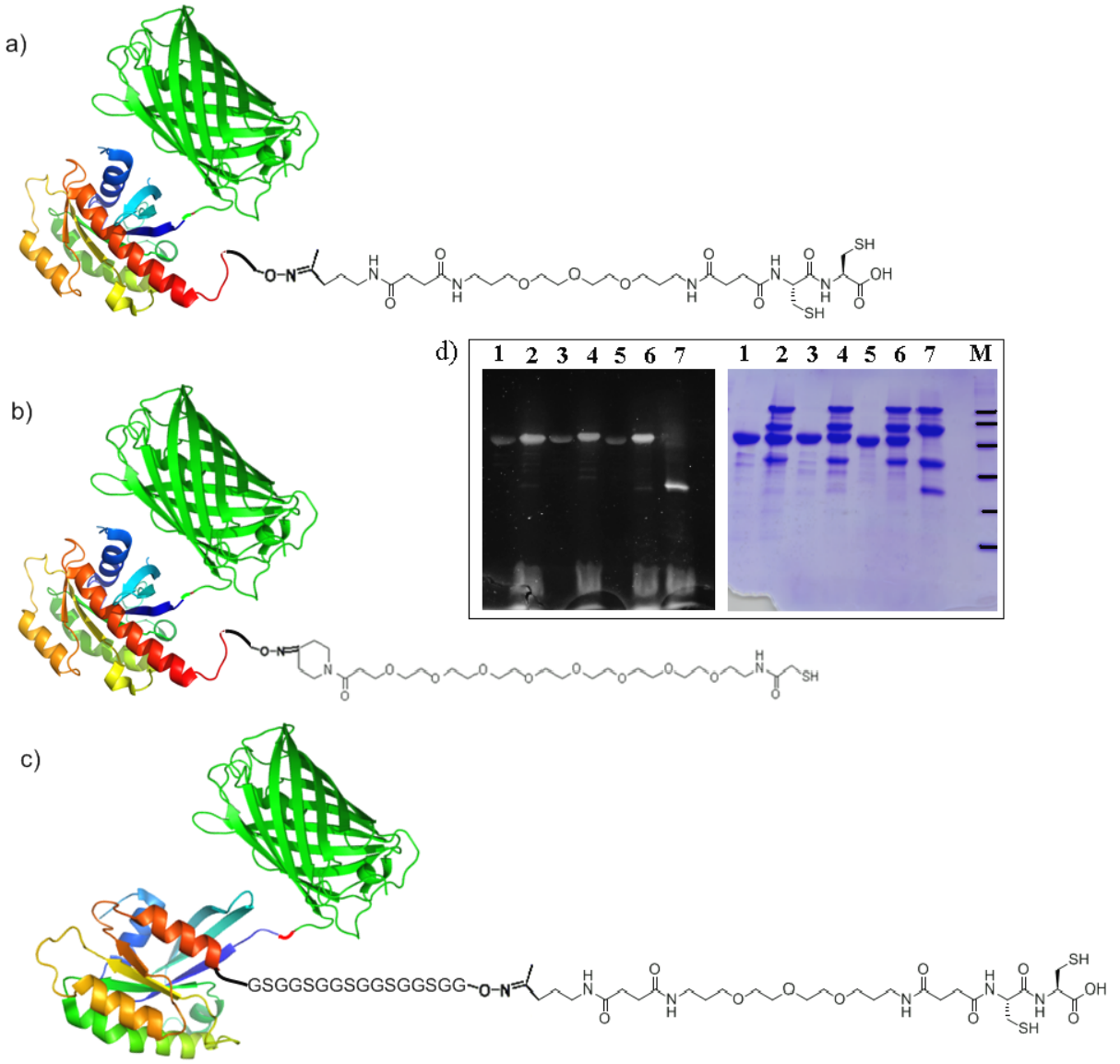

Figure 3.52. a)-c) Design of EGFP-tagged Rab probes. d) The activity of semisynthesis protein probes EGFP-Rab-(GGS)n-PEG-1-CC were confirmed by *in vitro* prenylation reaction through incorporation of NBD-FPP to Rab resolved by SDS-PAGE (left: scan from a laser fluorescent image reader excitation at 473 nm; right: photograph in visible light after Coomassie blue staining). Lanes 1, 3, 5: pure Rab1, Rab5, Rab7 proteins as negative control; Lanes 2, 4, 6: prenylation reaction samples of Rab1, Rab5, Rab7 proteins, respectively; Lane 7, prenylation reaction sample of Rab7 wide type; Lane M: marker 97, 66, 45, 30, 20.1, 14.4 KD.

These semisynthetic Rab probes were further microinjected into living HeLa cells for *in vivo* prenylation and localization studies (Figure 3.53, this work was performed by Fu Li in Wu's group). The plasmids of cherry-tagged wide-type Rab proteins were transfected as positive control. The steady-state localization of the microinjected proteins was determined by means of confocal fluorescence microscopy and compared to the localization of transfected cherry-tagged Rabs. The co-localization results are Rab-dependent.

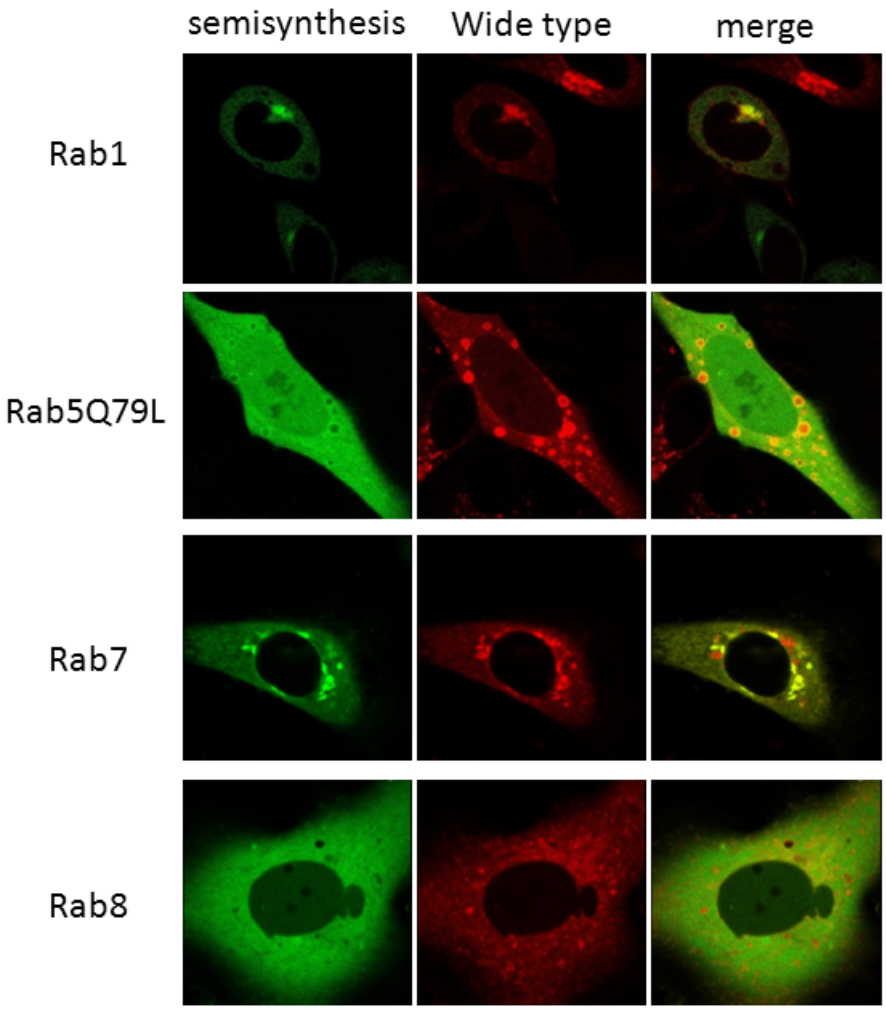

Figure 3.53. Subcellular distribution of various Rab family small GTPases in HeLa cells (provided by Fu Li in Wu's group). Semisynthesis protein represents EGFP-Rab-PEG1-CC or EGFP-Rab-PEG2-SH (Rab8); wide-type protein represents transfected mCherry-Rab.

A steady-state distribution comparable to native Rab1 protein could be observed for the EGFP-Rab1-PEG1-CC probe, which localize with wild type at the Golgi apparatus. This result implies that the C-terminal hypervariable region of Rab1 do not encode membrane-targeting signal. The recent research in Goody's group indicates that a RabGEF DrrA can dissociate Rab1:GDP:GDI complex efficiently (Schoebel et al., 2009), suggesting that RabGEF may play a key role in Rab1 membrane targeting. This point is consistent with our finding that the semisynthetic Rab1 probes can co-localize with wide-type Rab1, namely, the Rab1 localization is determined by RabGEF rather then Rab C-terminal sequence. The successful co-localization of semisynthetic protein probes and wide-type proteins also implies that these protein probes can be prenylated *in vivo*, considering the fact that Rab proteins without C-terminal prenylation cannot target to membranes (Gomes et al., 2003; Calero et al., 2003).

For further functional studies, a Rab5Q79L mutant was selected because this Q79L mutant was found mainly in the GTP-bound form *in vivo* (Stenmark et al., 1994). Expression of Rab5Q79L is known to cause formation of enlarged early endosomes. Therefore, this phenotype can be used to indicate the biological activity of semisynthetic Rab probes. We found that EGFP-Rab5Q79L-PEG-CC probe could co-localize with mCherry-Rab5Q79L and induce appearance of unusually large early endocytic structures (Figure 3.53). The replacement of flexible C-terminus of Rab5 with chemical linkers did not perturb Rab functionality in living cells.

However, while in the case of Rab7, Rab8 and Rab35, the semisynthesis Rab probes and wide-type proteins have different distribution in cells (Figure 3.53). For Rab35, replacement of the polybasic sequence with the PEG linker may disrupt the electrostatic interaction with the PIPs lipids on the PM, leading to mistargeting of Rab35 from the PM to the Golgi (Heo et al., 2006). For Rab7, we found that the C-terminal hypervariable sequence before CIM is essential for targeting to late endosome or lysoyomes (from Fu Li's data in Wu's group). Further study is needed to fully understand the contribution of C-terminal sequence of Rab7 and Rab8 for membrane targeting.

3.5.6. Conclusion

In conclusion, we have used a facile method of oxime ligation to produce a series of PEGylated Rab protein probes for prenylation and localization studies. The replacement of Rab C-terminal peptide with an unnatural PEG moiety did not perturb Rab prenylation *in vitro* and *in vivo*. These results further elucidated the mechanism of Rab prenylation, i.e. there is no specificity required in Rab C-terminus hypervariable regions before and after the CIM motif for Rab prenylation. Using these Rab probes, we further investigated the issue that whether the C-terminal hypervariable region contributes to Rab targeting. We found that the membrane targeting mechanisms for Rab-family proteins are more complex than previous proposal. For several Rab proteins, the C-terminal hypervariable regions do not contribute to the membrane targeting. However, the replacement of C-terminal sequence with chemical linkers in several Rab proteins disrupted Rab membrane targeting, implying that in these Rab proteins the C-terminal sequence is important for biological function. Further work is needed to fully understand membrane targeting mechanisms of various Rab proteins.

4. Summary

"An expert is a man who has made all the mistakes which can be made,

in a narrow field."

Niels Bohr

4. Summary

The development of methods for the chemical ligation of synthetic small molecules or peptides to proteins is a current frontier in chemical biology. Expressed protein ligation (EPL) has been extremely useful for the synthesis of various proteins in the past. In particular the concept of EPL elegantly demonstrates the usefulness of combining the fields of synthetic organic chemistry and molecular biology in order to address complex physiological and biochemical questions. The present study aimed at two facets: 1) establish several universal strategies to extend the EPL technology for site-specific protein modification and immobilization; 2) adapt the EPL methodology to the semi-synthesis of Rab proteins probes, which exert many important functions during vesicular transport in eukaryotic cells.

Firstly, we developed a facile, efficient and mild strategy for the site-specific immobilization of proteins on surfaces by means of oxyamine ligation to generate protein microarrays. In our strategy the proteins are first readily modified with oxyamine groups at the C-terminus and then immobilized on ketone-coated slides. This immobilization strategy proceeds efficiently at neutral conditions (pH 7.0), and is exceptionally mild for protein immobilization in comparison to other methods. Furthermore, this strategy enables the direct immobilization of expressed proteins from crude cellular lysates without prior purification. The produced protein biochips can be used for the study of protein-protein interactions, as indicated by Rab-REP and PKA-antibody interaction studies. Our strategy expands the repertoire of protein immobilization methods and provides an alternative means to meet the various requirements for protein immobilization.

Secondly, we presented the principle of using two chemoselective reactions to site-specifically label a single protein in a one-pot reaction. We developed a general, facile and efficient strategy for N- and C-terminal dual-color labeling exemplified for the Rab7 protein using native chemical ligation and oxime ligation. The method is low in cost and easy to carry out. The reaction conditions are biocompatible and mild enough for protein modifications. The strategy presented here could be a general method for generating dual-labeled proteins, which could also have a wide range of applications for studying protein functions at the single molecule and cellular level. We have shown the the produced protein probe can be used to study protein refolding and protein-protein interactions by FRET studies. This study leads to the finding that both GDP and GppNHp can help GTPase to refold, and therefore point out a way to produce GppNHp-bound GTPase as indicated by successful semisynthesis of a RhoA-GG protein.

Thirdly, we presented the principle of a FRET strategy for monitoring GEF-mediated nucleotide exchange using site-specifically labeled GEF and GTPase proteins. Using NCL and oxime ligation, we prepared N-terminal coumarin-labeled GEFs and C-terminal fluorescein-labeled GTPases. We constructed the coumarin-GEF:GTPase-fluorescein complex, which showed a significant intermolecular FRET effect. The FRET signal was disrupted by binding of GDP or GTP and allowed direct detection of the GEF:GTPase interaction. Transient kinetic studies based on the FRET signal change were used to monitor the GEF activity and nucleotide binding. The studies led to a consistent conclusion on the GEF mechanism involving allosteric competition between GDP/GTP and GEF's interaction with a GTPase. The strategy presented here could be a general method that is applicable to other GEFs and GTPases, and may open up a new avenue for the identification of GEF inhibitors and for studying GEF mechanisms.

Fourthly, we presented a general strategy using tandem EPL and click chemistry to site-specifically install hydrophobic GerGer modifications into proteins. The two-step ligation is quantitative, which makes the purification of ligated protein much facile. The approach yielded correctly folded and functional geranylgeranylated Rab GTPases, as could be inferred by their ability to interact with REP as well as to accept the second GerGer group in prenylation. The ligation strategy may open up a new avenue for production of lipoproteins that are used in various biological studies.

Finally, we have used a facile method of oxime ligation to produce a series of PEGylated Rab protein probes for prenylation and localization studies. The replacement of Rab C-terminal region with an unnatural PEG moiety did not perturb Rab prenylation *in vitro* and *in vivo*. These results further elucidated the mechanism of Rab prenylation, i.e. there is no specificity required in Rab C-terminus hypervariable regions before and after the CIM motif for Rab prenylation. Using this series of Rab probes, we further investigated the issue that whether the C-terminal hypervariable region contributes to Rab targeting. We found that the membrane targeting mechanisms for Rab-family proteins are more complex then previous propose. For Rab1 and Rab5, the C-terminal hypervariable regions do not contribute to the membrane targeting. However, the replacement of C-terminal sequence with chemical linkers in several Rab proteins indeed disrupt their membrane targeting, implying that in these Rab proteins the C-terminal hypervariable region is important for biological function. This work provides an example of chemical tools can be used to challenge native biomolecular functions, leading to better understanding the Rab prenylation and targeting mechanisms.

4. Summary (german)

Die Entwicklung von Methoden für die chemische Ligation von synthetischen kleinen Molekülen oder Peptiden, Proteinen ist eine aktuelle Grenze in der chemischen Biologie. Exprimierte Protein-Ligation (EPL) war äußerst nützlich für die Synthese von verschiedenen Proteinen in der Vergangenheit. Insbesondere das Konzept der EPL elegant zeigt den Nutzen der Kombination der Felder der synthetischen organischen Chemie und Molekularbiologie, um komplexe physiologische und biochemische Fragen anzugehen. Die vorliegende Studie an zwei Facetten einzuführen: 1) herzustellen mehrere universale Strategien, um die EPL-Technologie für eine ortsspezifische Proteinmodifikation und Immobilisierung erstrecken; 2) Anpassung der EPL Methodik auf die Halbsynthese Rab Proteine Sonden, die mehrere wichtige Funktionen ausüben während vesikulären Transport in eukaryotischen Zellen.

Erstens haben wir eine einfache, effiziente und leichte Strategie für die ortsspezifische Immobilisierung von Proteinen an Oberflächen durch Ligation an Oxyamingruppe Proteinmikroarrays erzeugen. In unserer Strategie die Proteine werden zunächst leicht mit Oxyamingruppe Gruppen am C-Terminus modifiziert und anschließend immobilisiert auf Keton-beschichtete Objektträger. Diese Immobilisierung Strategie effizient verläuft bei neutralen Bedingungen (pH 7,0), und ist besonders mild zur Immobilisierung von Proteinen im Vergleich zu anderen Methoden. Darüber hinaus ermöglicht diese Strategie die direkte Immobilisierung von exprimierten Proteinen aus rohem Zelllysaten ohne vorherige Reinigung. Die produzierten Protein Biochips können für die Untersuchung von Protein-Protein-Wechselwirkungen, wie durch Rab-REP und PKA-Antikörper-Wechselwirkung Studien gezeigt verwendet werden. Unsere Strategie erweitert das Repertoire der Immobilisierung von Proteinen Methoden und bietet eine alternative Möglichkeit, um die verschiedenen Anforderungen für die Immobilisierung von Proteinen erfüllen.

Zweitens haben wir das Prinzip der Verwendung von zwei chemoselektive Reaktionen auf ortsspezifisch kennzeichnen ein einzelnes Protein in einer Eintopfreaktion. Wir entwickelten einen allgemeinen, einfache und effiziente Strategie für die N-und C-terminalen zweifarbige Kennzeichnung für das Protein unter Verwendung Rab7 native chemische Ligation und Oxim veranschaulicht. Das Verfahren ist kostengünstig und einfach durchzuführen. Die Reaktionsbedingungen sind biokompatibel und mild genug für die Protein-Modifikationen. Die Strategie hier vorgestellte könnte ein allgemeines Verfahren zur Erzeugung doppelt markierte Proteine, die ebenfalls könnte eine Vielzahl von Anwendungen zum Studium Proteinfunktionen am einzigen Molekül und zellulärer Ebene. Wir haben gezeigt, das das gebildete Protein-Sonde verwendet werden, um Protein-Umfaltung und Protein-Protein-

Wechselwirkungen durch FRET-Untersuchungen zu untersuchen. Diese Studie führt zu der Erkenntnis, dass sowohl BIP als auch GppNHp kann GTPase helfen, falten, und deshalb darauf, einen Weg zu GppNHp-gebundenen GTPase, wie sie durch erfolgreiche Semisynthese eines RhoA-GG Protein angegeben.

Drittens haben wir das Prinzip einer FRET-Strategie für die Überwachung GEF-vermittelten Nukleotid-Austausch mit Website-spezifisch markierten GEF und GTPase-Proteine. Verwendung NCL und Oxim bereiteten wir N-terminalen Cumarin-markierten GEFs und C-terminalen fluoresceinmarkierten GTPasen. Wir konstruierten die Cumarin-GEF:GTPase-Fluorescein-Komplex, der eine signifikante intermolekulare FRET-Effekt zeigte. GTPase Interaktion: das FRET-Signal wurde durch Bindung von GDP oder GTP und erlaubt den direkten Nachweis des GEF gestört. Transient kinetische Studien zur FRET Signaländerung bezogen wurden verwendet, um die Aktivität und GEF Nukleotidbindung überwachen. Die Untersuchungen führten zu einer konsistenten Rückschluss auf die GEF Mechanismus mit allosterischen Wettbewerb zwischen GDP / GTP und GEF die Interaktion mit einer GTPase. Die vorgestellte Strategie könnte hier eine allgemeine Methode, die für andere GEFs und GTPasen ist, und kann eröffnen einen neuen Weg für die Identifizierung von GEF-Inhibitoren und für das Studium GEF-Mechanismen.

Viertens stellten wir eine allgemeine Strategie mit Tandem EPL und klicken Chemie ortsspezifisch installiert hydrophoben Gerger Modifikationen in Proteine. Das zweistufige Ligation ist quantitativ, wodurch die Reinigung des Proteins wesentlich ligierten facile. Der Ansatz ergab korrekt gefaltete und funktionelle geranylgeranyliert Rab GTPasen, wie durch ihre Fähigkeit, mit REP sowie interagieren, um die zweite Gruppe in Gerger Prenylierung akzeptieren abgeleitet werden könnten. Die Ligation kann eröffnen einen neuen Weg zur Herstellung von Lipoproteinen, die in verschiedenen biologischen Studien verwendet werden.

Schließlich haben wir ein einfaches Verfahren von Oxim Ligierung, um eine Reihe von PEGyliertem Rab-Protein-Sonden für Prenylierung und Lokalisationsstudien produzieren. Der Ersatz von Rab C-terminalen Region mit einer unnatürlichen PEG-Gruppierung nicht stören Rab Prenylierung in vitro und in vivo. Diese Ergebnisse den Mechanismus aufgeklärt Rab Prenylierung, dh es besteht keine Spezifität in Rab C-Terminus hypervariablen Regionen vor und nach dem Motiv für CIM Rab Prenylierung erforderlich. Mit diesen Reihe von Sonden Rab wir weiter untersucht, ob das Problem, dass die C-terminalen hypervariablen Bereich nach Rab Targeting beiträgt. Wir fanden, dass die Membran Targeting-Mechanismen für die Rab-Proteine Familie komplizierter als in früheren schlagen sind. Für Rab1 und Rab5, werden die C-terminalen hypervariablen Regionen nicht an die Membran-Targeting beitragen.

Allerdings ist die Ersetzung der C-terminalen Sequenz mit chemischen Linker in mehreren Rab Proteine tatsächlich stören ihrer Membran-Targeting, was bedeutet, dass in diesen Rab-Proteine der C-terminalen hypervariablen Region ist wichtig für biologische Funktion. Diese Arbeit stellt ein Beispiel für chemische Werkzeuge verwendet werden, um einheimische biomolekularen Funktionen anzufechten, was zu einem besseren Verständnis der Rab Prenylierung und Targeting-Mechanismen.

5. Materials and Methods

“Scientific knowledge aims at being wholly impersonal.”

Bertrand Russell

5. Materials and Methods

5.1. General methods

Silica gel flash liquid chromatography:

Purifications were performed using silica gel from J. T. Baker or Merck (particle size 40-60 μm) under approximately 0.5 bar pressure.

Nuclear magnetic resonance spectroscopy (NMR):

^{1}H- and ^{13}C-NMR spectra were recorded using a Varian Mercury 400 spectrometer (400 MHz, ^{1}H and 100 MHz, ^{13}C). Chemical shifts are expressed in parts per million (ppm) from internal deuterated solvent standard ($CDCl_3$: δ_H = 7.26 ppm, δ_C = 77.0 ppm; CD_3OD: δ_H = 4.84 ppm, δ_C = 49.05 ppm; ^{d6}DMSO: δ_H = 2.50 ppm, δ_C = 39.43 ppm; D_2O: δ_H = 4.79 ppm). Coupling constants (*J*) are given in Hertz (Hz) and the following notations indicate the multiplicity of the signals: s (singlet), d (doublet), t (triplet), dd (doublet of doublet), m (multiplet), br (broad signal).

Electronspray ionization mass spectrometry (ESI-MS):

Electrospray mass spectrometric analyses (ESI-MS) were performed on a Finnigan LCQ spectrometer. Calculated masses were obtained using the software ChemDraw Ultra (CambridgeSoft Corporation) or Xcalibur.

Reversed-phase liquid chromatography-ESI (LCMS) for small molecules:

LCMS measurements were carried out on a Hewlett Packard HPLC 1100/Finnigan LCQ mass spectrometer system using Nucleodur C_{18} Gravity, Nucleosyl 100-5 C_{18} Nautilus (Macherey-Nagel) or Jupiter C_4 (Phenomenex) columns and detection at 215 and 254 nm.
Method A: Positive linear gradients of solvent B (0.1% formic acid in acetonitrile) and solvent A (0.1% formic acid in water) were used at 1 mL/min flow rate.
Method B: Negative linear gradients of solvent B (10 mM NH_4OH in acetonitrile) and solvent A (10 mM NH_4OH in water) were used at 1 mL/min flow rate.
Method C: Positive linear gradients of solvent B (0.1% formic acid and 5% THF in methanol) and solvent A (0.1% formic acid in water) were used at 1 mL/min flow rate.
Method D: Negative linear gradients of solvent B (10 mM NH_4OH and 5% THF in methanol) and solvent A (10 mM NH_4OH in water) were used at 1 mL/min flow rate.

Analytical reversed-phase high performance liquid chromatography (HPLC) for small molecules:

Analyses were performed on a Varian prostar system using CC 125/4 Nucleodur C_4 Gravity columns (Macherey-Nagel), autosampler prostar 410 and UV/Vis detector with Varian prostar 335. Linear gradients were used at 1 mL/min flow rate (A: water, B: acetonitrile, C: 2% TFA in water).

Method:

95% A $\xrightarrow{1\text{ min}}$ 95% A $\xrightarrow{10\text{ min}}$ 15% A $\xrightarrow{2\text{ min}}$ 10% A $\xrightarrow{7\text{ min}}$ 10% A $\xrightarrow{2\text{ min}}$ 95% A $\xrightarrow{3\text{ min}}$ 95% A

Preparative reverse-phase high performance liquid chromatography (prep HPLC):

Purification of compounds was performed on an Varian Prostar system using VP 250/21 Nucleodur C_4 Gravity 5 mm column (Macherey-Nagel), fraction collector prostar 701 and detection at 220 ~ 240 nm with UV/Vis prostar 340. Linear gradients of solvent A (water) and solvent B (acetonitrile) were used at 6 mL/min flow rate.

Method:

90% A $\xrightarrow{5\text{ min}}$ 90% A $\xrightarrow{15\text{ min}}$ 20% A $\xrightarrow{2\text{ min}}$ 10% A $\xrightarrow{3\text{ min}}$ 10% A $\xrightarrow{2\text{ min}}$ 95% A $\xrightarrow{3\text{ min}}$ 95% A

Thin layer chromatography (TLC):

TLC was carried out on Merck precoated silica gel plates (60F-254) using ultraviolet light irradiation at 254 nm and 360 nm or the following solutions as developing agents:

Staining solution A: molybdatophosphoric acid (25 g) and cerium (IV) sulfate (10 g) in concentrated sulfuric acid (60 mL) and water (to 1 L);

Staining solution B: (for detection of free amino groups): ninhydrin (300 mg) in ethanol (100 mL) and acetic acid (3 mL).

Staining solution C: $KMnO_4$ (1 g), K_2CO_3 (6.6 g), 5% NaOH solution (1.7 mL) in H_2O (to 100 mL).

MALDI-TOF-mass spectrometry:

MALDI spectra were recorded on a Voyager-DE Pro Biospectrometry workstation from Applied Biosystems (Weiterstadt, Germany). Protein samples were desalted using small GF spin columns (Quiagen, Hilden, Germany) and mixed with an equal volume of sample matrix (10 mg/mL sinapinic acid or 2,5-dihydroxybenzoic acid in water/acetonitril (1:1) containing 0.1 % (v/v) TFA). The mixture was quickly spotted on a MALDI sample plate, air-dried and spectra were measured with the following device settings: acceleration voltage = 25 kV, grid

voltage = 93%, extraction delay time = 750 ns and guide wire = 0.3%. The laser intensity was manually adjusted during the measurements in order to obtain optimal signal to noise ratios. Calibrations were carried out using a protein mixture of defined molecular mass (Sigma). Spectra recording and data evaluation was performed using the supplied Voyager software package. The accuracy of the method for proteins within the molecular weight range of 20-30 kDa is ca. ± 20.

LCMS measurements for proteins:

LCMS analysis was performed on an Agilent 1100 series chromatography system (Hewlett Packard) equipped with an LCQ electrospray mass spectrometer (Finnigan, San Jose, USA) using Jupiter C_4 columns (5 µm, 15 x 0.46 cm, 300 Å pore-size) from Phenomenex (Aschaffenburg, Germany). For LC-separations a gradient of buffer B (0.1 % formic acid in acetonitrile) in buffer A (0.1% formic acid in water) with a constant flow-rate of 1 mL/min was employed. Upon sample injection, a ratio of 20% buffer B was kept constant for 4 min. Elution was achieved using a linear gradient of 30-80% buffer B in buffer A for 5-15 min followed by a steep gradient (70-90% buffer B) for 15-17 min. The column was extensively flushed for 17-19 min with 90-10% buffer B. Data evaluation and deconvolution was carried out using the Xcalibur software package. The accuracy of the method for proteins within the molecular weight range of 20 kDa is ca. ± 5 Da; 50 KDa is ca. ± 20 Da.

Analytical reversed-phase (RP) and gel filtration (GF) HPLC for proteins:

Analytical RP and GF chromatography were performed on a Waters 600 chromatography instrument equipped with a Waters 2475 fluorescence detector and a Waters 2487 absorbance detector (Waters, Milford, MA, USA). Jupiter C_4 columns (5 µm, 15 x 0.46 cm, 300 Å pore-size) from Phenomenex (Aschaffenburg, Germany) were used for RP separations, whereas Biosep-SEC-2000 columns (60 x 0.78 cm, separation range 1300 kDa, Phenomenex) were used for gel filtration. Chromatographic GF separations were normally performed using 50 mM sodium phosphate, pH 7.2, 50 mM NaCl, 2 mM DTE, 10 µM GDP, 1 mM $MgCl_2$ as a running buffer at a flow rate of 0.5 mL/min. Separation was usually complete within 60 min.
For RP separations the following gradient of buffer B (0.1% TFA in acetonitrile) in buffer A (0.1% TFA in water) at a flow rate of 1 mL/min was used: The column was equilibrated with 5% buffer B in buffer A. Upon sample injection this ratio was kept isocratic for 2 min followed by a linear gradient (5-30% buffer B) over another 2 min. Individual components eluted upon a linear gradient (30-70% buffer B) over 10 min and another isocratic phase (70%

buffer B) of 4 min. Afterwards the column was flushed for at least 10 min with 100% buffer B in order to elute hydrophobic compounds (e.g. geranylgeranylated peptides). Data analysis was carried out using the Millenium software package provided by Waters.

Denaturing SDS-PAGE:

Typically 15 % SDS-PAGE gels were used for the analysis of proteins (MW of ca. 20-60 kDa). The corresponding volumes of the individual components as indicated by Table 5-1 were mixed and the resolving gel was cast using a Biorad Multi-casting apparatus (10 gels). After the resolving gel was polymerized, a stacking gel mix was prepared and cast atop the resolving gel. Protein samples were prepared by adding an equal amount of SDS-PAGE sample buffer (2 x) and heated for 5 min at 95 °C. Gels were run at ca. 10 V/cm until the bromphenol blue front had entered the buffer solution. Fluorescently labeled proteins were visualized by exposing the unstained SDS-PAGE gel to UV light. The proteins were subsequently stained using a solution of Coomassie brilliant blue.

Type of gel (%)	Acrylamide/ bisacrylamide (29:1, 30%)	ddH_2O	Resolving gel buffer	Stacking gel buffer	TEMED	10% APS
Resolving gel, 70 mL						
10%	23.5 mL	27.6 mL	17.1 mL	---	29 µL	700 µL
15%	34.2 mL	15.7 mL	17.1 mL	---	29 µL	700 µL
Stacking gel, 30 mL						
5%	4.9 mL	20 mL	---	3.7 mL	300 µL	29 µL

Table 5-1. Pipeting scheme for SDS-PAGE gels. TEMED = *N,N,N′,N′*-tetramethylethylendiamine; APS = ammoniumpersulfate.

Ion exchange chromatography:

Poros HQ (PerSeptive Biosystem) and HiTrap Q Sepharose (Amersham Biosciences) anion-exchange columns were used for ion exchange chromatography. The columns were washed with buffer A (10 mM NaH_2PO_4, pH 7.5, 2 M NaCl, 1 mM $MgCl_2$) and subsequently equilibrated with buffer B (10 mM NaH_2PO_4, pH 7.5, 10 mM NaCl, 1 mM $MgCl_2$, 5 mM MESNA). The proteins were loaded onto the column and eluted with a linear gradient from 10 mM (buffer B) to 500 mM NaCl (buffer C: 10 mM NaH_2PO_4, pH 7.5, 500 mM NaCl, 1 mM $MgCl_2$, 5 mM MESNA).

5.2. Solvents and reagents

Solvent and reagent purification

The reagents were purchased from Acros Chimica, Aldrich, Fluka, Merck, Novabiochem, Riedel de Haen, Roth. The carboxy-PEG_n-amine reagents (n = 8 and 12) were purchased from Thermo scientific (www.thermoscientific.com). Deionized water was obtained using a Millipore Q-plus System. Dichloromethane, acetonitrile, 2,6-lutidine, DIPEA and triethylamine were refluxed and distilled from CaH_2 under argon and stored with KOH. Acetonitrile, xylene and DMF were stored with molecular sieves 4 Å. Absolute ethanol was refluxed with Mg and I_2 under argon and distilled, then stored with molecular sieves 4 Å. Other anhydrous solvents like ethyl acetate, diethylether, DMF, MeOH, toluene and pyridine were directly purchased from Sigma or Fluka. Acetic anhydride was redistilled.

Frequently used buffers and growth media

LB medium

0.5% (w/v)	yeast extract
1% (w/v)	tryptone
1% (w/v)	NaCl

SDS-PAGE running buffer (10 x)

0.25 M Tris-HCl
2 M glycine
1% (w/v) SDS

SDS-PAGE stacking gel buffer

0.5 M	Tris-HCl, pH 6.8
0.4% (w/v)	SDS

SDS-PAGE resolving gel buffer

1.5 M	Tris-HCl, pH 8.8
0.4% (w/v)	SDS

SDS-PAGE loading buffer (2 x)

100 mM	Tris-HCl, pH 6.8
4% (w/v)	SDS
20% (v/v)	glycerol
200 mM	DTT
0.05% (w/v)	bromophenol blue

Coomassie stain solution

10% (v/v)	acetic acid
40% (v/v)	methanol
0.1% (w/v)	Coomassie Blue R250

Coomassie destain solution

10% (v/v)	acetic acid
50% (v/v)	methanol

TAE buffer

40 mM	Tris acetate
2 mM	EDTA

PBS (10 x)

DNA loading buffer (5 x)

80 g	NaCl	10%	Ficoll 400
2 g	KCl	50 mM	Na_2EDTA, pH 8.0
14.4 g	$Na_2HPO_4 \cdot 2H_2O$	0.05% (w/v)	SDS
2.4 g	KH_2PO_4	0.15% (w/v)	bromphenol blue
ddH_2O to 1 L		0.15% (w/v)	xylene cyanol (optional)

5.3. Preparations of chemicals

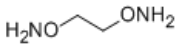

Bis(oxyamine) 1 (Bauer et al., 1963): A mixture of N-hydroxyphthalimide (3.3 g, 0.02 mol) in dimethylformamide (DMF, 20 mL), ethylene bromide (1.9 g, 0.01 mol), triethylamine (Et_3N, 4 g, 0.04 mol) and a catalytic amount of tetramethyl ammonium iodide was allowed to react at 60 °C for 3 h. The precipitate that had formed was filtered off and washed with small amount of DMF and water for several times. The white product was mixed with glacial acetic acid (10 mL) and concentrated HCl (20 mL). The resulting suspension was refluxed for 1 h. On cooling, the filtrate was concentrated to totally remove the solvent. The residue was washed with chloroform, filtered, and crystallized from methanol-chloroform to give 320 mg white crystals **1**, yield 20% over two steps. ^{1}H NMR (400 MHz, D_2O) δ 3.31-3.29 (m, 4H). ^{13}C NMR (100 MHz, D_2O) δ 72.42. ESI-MS for $[M+H]^+$: 93.00 (calculated for $C_2H_9N_2O_2$, 93.07).

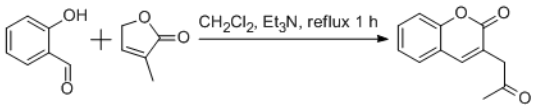

Keto-coumarin 2 (Sethna et al., 1945): A mixture of salicylaldehyde (0.13 g, 1.1 mmol), α-angelica lactone (0.098 g, 1 mmol) and 1 mL Et_3N in CH_2Cl_2 (30 mL) was refluxed for 1 h. The reaction mixture was diluted in CH_2Cl_2 and washed with 1 M HCl, water and brine. The organic layer was dried over anhydrous Na_2SO_4 and concentrated under reduced pressure to give a crude mixture. The product was purified by flash chromatography on silica gel with pentane-EtOAc (2:1) as eluent to yield the desired product as a light yellow solid (155 mg; yield 77%). ^{1}H NMR (400 MHz, $CDCl_3$) δ 7.58 (s, 1H), 7.51-7.39 (m, 2H), 7.33-7.18 (m, 2H), 3.66 (s, 2H), 2.29 (s, 3H). ESI-MS for $[M+H]^+$: 203.27 (calculated for $C_{12}H_{11}O_3$, 203.07).

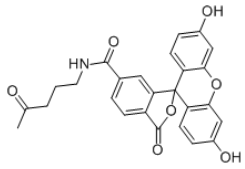

Keto-fluorescein 3. To a solution of fluorescein (0.26 g, 0.69 mmol) and 5-amino-2-pentanone ethylene ketal (0.1 g, 0.68 mmol) in dry DMF was added 1-ethyl-3-(3-dimethyllaminopropyl)carbodiimide (EDC, 0.143 g, 0.75 mmol) and Et_3N 186 µL. The solution was stirred at room temperature overnight. Upon removal of DMF *in vacuo*, the residue was dissolved in ethyl acetate and washed with 1 M HCl, water and brine. The organic layer was dried over anhydrous Na_2SO_4 and concentrated under reduced pressure. The crude product obtained was deprotected by treatment with 10 mL TFA/CH_2Cl_2/H_2O (2:7.5:0.5) at room temperature for 3 h. After removal of the solvent *in vacuo*, the mixture was further purified by flash chromatography using 10% MeOH in CH_2Cl_2, yield 85% (0.26 g). R_f = 0.4 in 10% MeOH in CH_2Cl_2. ^{1}H-NMR (400 MHz, $CDCl_3$) δ 8.41 (s, 1H), 8.19 (d, J = 8.04 Hz, 1H), 7.29 (d, J = 8.04 Hz, 1H) 6.69-6.67 (m, 2H). 6.61-6.51 (m, 4H), 3.42 (t, J = 6.8 Hz, 2H), 2.61 (t, J = 7.2 Hz, 2H), 2.16 (s, 3H), 1.90-1.86 (m, 2H). ^{13}C NMR (100 MHz, $CDCl_3$) δ 210.0, 167.2, 167.0, 152.9, 152.9, 136.7, 134.2, 129.2, 129.1, 124.5, 112.7, 112.6, 109.7, 40.2, 39.3, 28.7, 23.3. ESI-MS for $[M+H]^+$: 460.22 (calculated for $C_{26}H_{22}NO_7$, 460.13). HRMS for $[M+H]^+$: 460.1396 (calculated for $C_{26}H_{22}NO_7$, 460.1383).

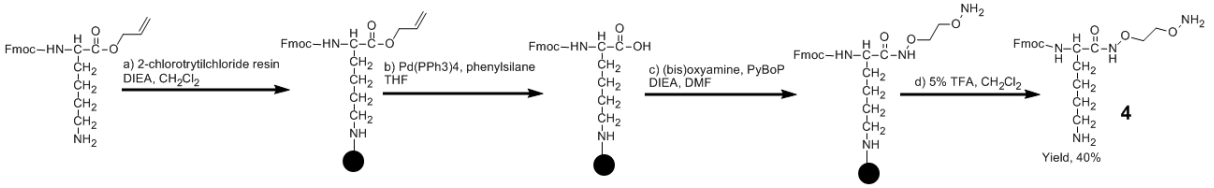

Model molecule 4. Attachment of the building block to the solid support was carried out by shaking the 2-chlorotritylchloride (2-Cl-trt) resin under dry conditions with a CH_2Cl_2 solution containing 3 eq of the Fmoc-LysOAll and N,N'-diisopropylethylamine (DIPEA, 6 eq). Loading efficiency was determined by means of the fluorenylmethoxycarbonyl (Fmoc)-removal method. After deprotection of allyl group, benzotriazol-1-yl-oxytripyrrolidinophosphonium hexafluorophosphate (PyBOP, 5 eq), 1-hydroxy-7-azabenzotriazole (HOAt, 5 eq), DIPEA (10 eq) and **1** (5 eq) in DMF was used for coupling directly (4 h). The result compound was released from the resin with a solution of 2.5% trifluoroacetic acid and 5% triethylsilane in CH_2Cl_2 (twice). Combined filtrates were evaporated to dryness, and the final model molecule **4** was purified by Prep-HPLC. The typical yield is 40%. ^{1}H NMR (400 MHz, MeOD) δ 7.80 (d, J = 7.6 Hz, 2H), 7.65 (d, J = 7.6Hz, 2H), 7.40 (t, J = 7.6 Hz, 2H), 7.31 (t, J = 7.6 Hz, 2H), 4.46-4.36 (m, 2H), 4.22 (b, 5H),

4.05-4.01 (m, 1H), 2.91 (t, J = 7.2 Hz, 2H), 1.85-1.67 (m, 4H), 1.46-1.35 (m, 2H). ^{13}C NMR (100 MHz, $CDCl_3$) δ 173.2, 161.9, 158.5, 145.3, 142.7, 132.4, 129.9, 128.9, 128.2, 126.1, 121.0, 78.3, 73.0, 67.9, 53.9, 40.5, 31.6, 28.1, 23.8. ESI-MS for $[M+H]^+$: 443.10 (calculated for $C_{23}H_{31}N_4O_5$, 443.22). HRMS for $[M+H]^+$: 443.22817 (calculated for $C_{23}H_{31}N_4O_5$, 443.22890).

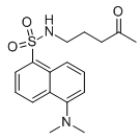

Keto-dansyl 8. To a solution of dansyl chloride (0.185 g, 0.68 mmol) in CH_2Cl_2 was added 5-amino-2-pentanone ethylene ketal (0.1 g, 0.68 mmol) and 2 eq Et_3N. The mixture was allowed to stand overnight at room temperature. The reaction mixture was diluted with CH_2Cl_2 and washed with water and brine. The organic layer was dried over anhydrous Na_2SO_4 and concentrated under reduced pressure to give a crude mixture, which was further purified by flash chromatography using CH_2Cl_2 as the eluent. The product obtained was deprotected with 10 mL TFA/CH_2Cl_2/H_2O (2:7.5:0.5) at room temperature for 3 h. Upon removal of solvent *in vacuo*, the mixture was further purified by flash chromatography using 5% MeOH in CH_2Cl_2, yield 91% (0.207 g). R_f = 0.3 in 5% MeOH in CH_2Cl_2. ^{1}H-NMR (400 MHz, $CDCl_3$) δ 8.80 (d, J = 8.4 Hz, 2H), 8.51 (d, J = 6.8 Hz, 2H), 8.29 (d, J = 7.2 Hz, 2H), 7.78-7.66 (m, 3H), 5.68 (b, 1H), 2.90 (t, J = 6.4 Hz, 2H), 2.45 (t, J = 6.4 Hz, 2H), 2.06 (s, 3H), 1.69-1.64 (m, 2H). ^{13}C-NMR (100 MHz, $CDCl_3$) δ 210.2, 139.2, 136.9, 130.5, 127.6, 127.5, 127.3, 126.2, 125.7, 118.5, 47.3, 47.1, 42.8, 40.4, 30.0, 23.4. ESI-MS for $[M+H]^+$: 335.47 (calculated for $C_{17}H_{23}N_2O_3S$, 335.14). HRMS for $[M+H]^+$: 335.1423 (calculated for $C_{17}H_{23}N_2O_3S$, 335.1424).

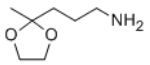

5-Amino-2-pentanone ethylene ketal 9. To a solution of 5-chloro-2-pentanone ethylene ketal (1.5 g, 9.1 mmol) in DMF (20 ml) was added potassium phthalimide (1.7 g, 9.1 mmol). The solution was refluxed for 14 hours. The reaction mixture was added into 1000 ml water, and the resulting white precipitate was filtrated. The white solid was washed with water and ether. Then the solid was dissolved in 95% ethanol and $NH_2NH_2{\cdot}H_2O$ (0.4 g, 8 mmol) was added. After refluxing for 1 hour, the reaction mixture was treated with a 2 N KOH solution. Then ten-times volume ether was added. The ether layer was further washed with water and brine, dried over anhydrous Na_2SO_4 and concentrated to yield compound **1** (0.46 g, 3.2 mmol, yield 35%). ^{1}H NMR (400 MHz, $CDCl_3$) δ 3.90 (m, 4H), 2.69 (t, J = 7.0 Hz, 2H), 2.08 (bs,

2H), 1.64 (m, 2H), 1.53 (m, 2H), 1.29 (s, 3H). ^{13}C NMR (100 MHz, $CDCl_3$) δ 110.0, 64.7, 42.2, 36.5, 27.9, 23.9. ESI-MS for $[M+H]^+$: 146.07 (calculated for $C_{17}H_{23}N_2O_3S$, 146.22). HRMS for $[M+H]^+$: 146.11713 (calculated for $C_{17}H_{23}N_2O_3S$, 146.11756).

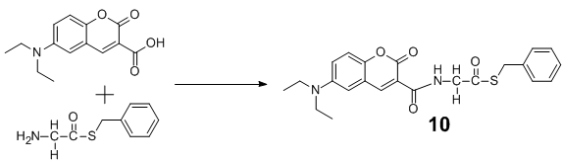

Coumarin-thioester 10: To a solution of coumarin (0.261 g, 1 mmol) in dry THF HATU (0.314 g, 0.83 mmol) and Et_3N (0.22 mL) was added. The mixture was stirred for 10 minutes on ice, followed by addition of amino thioacetic acid S-benzyl ester (0.15 g, 0.83 mmol) dissolved in a minimal amount of DMF. The resulting solution was stirred overnight at room temperature. After removal of the solvent *in vacuo*, the resulting mixture was taken up in ethyl acetate and washed with 1 N HCl, water and brine. The organic layer was dried over anhydrous Na_2SO_4 and concentrated *in vacuo* to afford a yellow solid, which was further purified by flash chromatography (silica gel, n-pentane/EtOAc = 1:2) to afford coumarin-thioester **10** (300 mg, 84%). R_f = 0.7 in 8% MeOH in CH_2Cl_2. ^{1}H NMR (400 MHz, $CDCl_3$) δ 9.26 (t, J = 5.7 Hz, 1H), 8.62 (s, 1H), 7.34 (d, J = 9.0 Hz, 1H), 7.26-6.93 (m, 5H), 6.57 (dd, J = 9.0, 2.4 Hz, 1H), 6.41 (d, J = 1.8 Hz, 1H), 4.31 (d, J = 6.1 Hz, 2H), 4.07 (s, 2H), 3.38 (q, J = 7.1 Hz, 4H), 1.16 (t, J = 7.1 Hz, 6H). ^{13}C NMR (100 MHz, $CDCl_3$) δ 197.0, 163.9, 162.7, 157.9, 152.9, 148.7, 137.1, 131.4, 129.0, 128.7, 127.4, 110.2, 109.4, 108.4, 96.7, 49.3, 45.2, 33.1, 12.5. ESI-MS $[M+H]^+$: found m/z 425.13. HRMS $[M+H]^+$: calculated for $C_{23}H_{24}N_2O_4S$ 425.15295; found 425.15256.

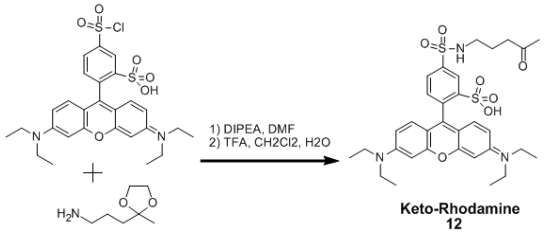

Keto-rhodamine 12. To a solution of sulforhodamine B sulfonyl chloride (0.294 g, 0.51 mmol) in DMF, **9** (0.075 g, 0.51 mmol) and 1 eq triethylamine was added. The mixture was allowed to stand overnight at room temperature. The solvent was evaporated to give a crude product, which was further purified by flash chromatography by using 5% MeOH in CH_2Cl_2 as the eluent. The obtained product was treated with 10 mL TFA/CH_2Cl_2/H_2O (2:7.5:0.5) at room temperature for 3 h. After removal of the solvent *in vacuo*, the keto-rhodamine **12** was obtained without further purify, yield 91%. R_f = 0.4 in 8% MeOH in CH_2Cl_2. ^{1}H NMR (400

MHz, ^{d6}DMSO) δ 8.42 (s, 1H), 7.92 (d, J = 6.1 Hz, 2H), 7.46 (d, J = 6.1 Hz, 2H), 7.02-6.91 (m, 6H), 5.98 (bs, 1H), 3.62 (q, J = 7.2 Hz, 8H), 2.84 (t, J = 6.4 Hz, 2H), 2.48 (t, J = 6.4 Hz, 2H), 2.05 (s, 3H), 1.58 (m, 2H), 1.19 (t, J = 7.2 Hz, 12H). ^{13}C NMR (100 MHz, ^{d6}DMSO) δ 208.5, 156.2, 157.8, 155.8, 148.7, 142.3, 133.7, 133.4, 132.3, 131.3, 127.2, 126.4, 114.9, 114.2, 96.4, 96.1, 46.0, 30.5, 23.9, 13.1. ESI-MS $[M+H]^+$; found m/z 642.67. HRMS $[M+H]^+$ calculated for $C_{32}H_{39}N_3O_7S_2$ 642.23022; found 642.22966.

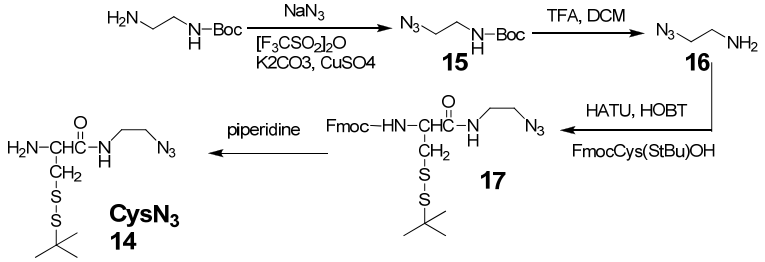

Synthesis of CysN$_3$ 14. 15 was prepared according to literature report methods (Abedin et al., 2009). ^{1}H-NMR (400 MHz, $CDCl_3$) δ 4.81 (br s, 1H), 3.36-3.32 (m, 2H), 3.28 (t, J = 6.0 Hz, 2H), 1.39 (s, 9H); ESI-MS: m/z $[M+H]^+$ = 187.1. **15** (1 g) was treated by 10 mL TFA/DCM (1:1) at room temperature for 2 h to give **16** (95% yield). ^{1}H-NMR (400 MHz, $CDCl_3$) δ 3.67 (t, J = 5.6 Hz, 2H), 3.08 (t, J = 5.6 Hz, 2H). Synthesis of **17**: The coupling reaction of **16** with 1.1 equivalent of Fmoc-Cys(StBu)-OH in the presence of 1.1 equivalent HATU, 1.1 equivalent HOBT and 2.2 equivalent DIPEA in 25 mL CH_2Cl_2 was stirred at room temperature for 24 h. Then the solution was washed with 10% $NaHCO_3$ and brine, dried over Na_2SO_4, and concentrated in vacuo. The residue was purified by chromatography (silica gel, 2% methanol in CH_2Cl_2) to yield 2.5 g (5 mmol, 87%) light yellow solid **17**, R_f = 0.3 (1% MeOH in CH_2Cl_2). ^{1}H NMR (400 MHz, $CDCl_3$) δ 7.76 (d, J = 7.5 Hz, 2H), 7.59 (d, J = 7.4 Hz, 2H), 7.40 (t, J = 7.5 Hz, 2H), 7.31 (td, J = 7.5, 1.1 Hz, 2H), 6.66 (s, 1H), 5.72 (d, J = 6.9 Hz, 1H), 4.45 (dd, J = 10.3, 7.2 Hz, 3H), 4.22 (t, J = 6.9 Hz, 1H), 3.43 (s, 4H), 3.20-2.91 (m, 2H), 1.35 (s, 9H). ^{13}C NMR (100 MHz, $CDCl_3$) δ 170.5, 156.3, 143.8, 141.5, 128.0, 127.3, 125.3, 120.2, 67.6, 54.9, 50.8, 48.7, 47.3, 42.2, 39.3, 30.1. ESI: m/z found, 499.95; calcd for $[M+H]^+$, 500.18. Synthesis of **14**: compound **17** (0.5 g, 1 mmol) in 1:4 piperidine-CH_2Cl_2 was stirred at room temperature for 24 h. After removing the solvent, the product was isolated from the remaining residues by flash chromatography (silica gel, 5% methanol in CH_2Cl_2) to yield **CysN$_3$** as colorless oil in 89% yield (0.247 g). R_f = 0.4 (5% MeOH in CH_2Cl_2). ^{1}H NMR (400 MHz, $CDCl_3$) δ 7.75 (s, 1H), 7.19 (d, J = 0.4 Hz, 2H), 4.29 (s, 1H), 3.50-3.24 (m, 4H), 3.09 (qd, J = 14.4, 6.7 Hz, 2H), 1.27 (s, 8H); ^{13}C NMR (100 MHz, $CDCl_3$) δ 168.1, 53.4, 50.4, 49.2, 40.9, 39.4, 29.8; ESI-MS: m/z found, 277.89; calculated for $[M+H]^+$, 278.11; HRMS (ESI): found, 278.11043; calculated for $C_9H_{20}N_5OS_2$, 278.11038.

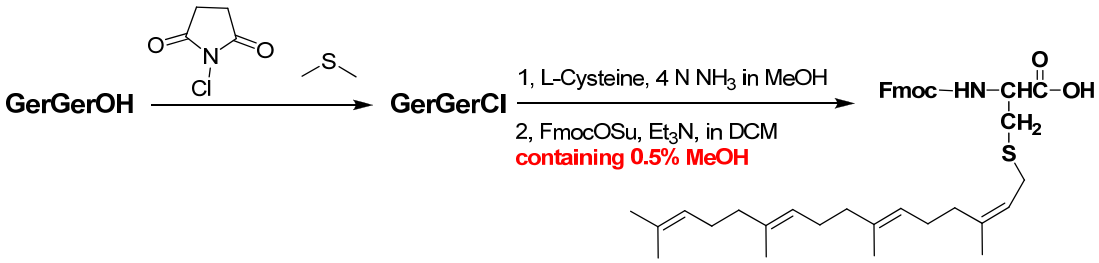

FmocCys(GerGer)OH 18 (Brown et al., 1991): N-chlorosuccinamide (690 mg, 5.1 mmol) in 10 mL dry CH_2Cl_2 was cooled to -40 ºC by using dry-ice-acetone; and then 380 µL $(CH_3)_2S$ was added dropwise. The mixture was stirred at -40 ºC for 5 min, 0 ºC for 5 min, and again kept at -40 ºC. In this stage, GerGerOH (1.0 g, 85%, 2.93 mmol) in 7 mL CH_2Cl_2 was added slowly. The resulting mixture was stirred at -40 ºC for 30 min, 0 ºC for 30 min, and room temperature for 2 h. The reaction solution was poured into ice-cold brine, and extraction with CH_2Cl_2. The CH_2Cl_2 solution was dried by $MgSO_4$, concentrated to obtain 1.04 g geranylgeranyl chloride (GerGerCl), which is directly used in the next-step reaction. L-cysteine (569 mg) was dissolved in 26 mL 4 M solution of ammonia in methanol on ice bath, and the obtained GerGerCl was added into the solution slowly. The reaction solution was allowed to react at 0 ºC for 3 h and room temperature for 1 h. After removing the solvent, 40 mL CH_2Cl_2 containing 0.2 mL MeOH was added at 0 ºC, followed by the supplementation of 1.2 g FmocOSu in 10 mL CH_2Cl_2, and 492 µl triethylamine. The reaction was stirred overnight, and the solvent was removed at reduced pressure. The residue was dissolved in CH_2Cl_2 and washed with water and brine. The organic layer was dried by $MgSO_4$ and concentrated. The product was purified by flash chromatography (silica gel, 2% methanol in CH_2Cl_2) to give light-yellow oil in 83% yield (1.5 g). ^{1}H NMR (400 MHz, $CDCl_3$) δ 10.36 (s, 1H), 7.67 (d, J = 7.5 Hz, 2H), 7.52 (d, J = 5.3 Hz, 2H), 7.31 (t, J = 7.4 Hz, 2H), 7.22 (t, J = 7.4 Hz, 2H), 5.58 (d, J = 7.8 Hz, 1H), 5.14 (t, J = 7.3 Hz, 1H), 5.07-4.92 (m, 3H), 4.53 (d, J = 6.8 Hz, 1H), 4.32 (d, J = 5.3 Hz, 2H), 4.15 (t, J = 7.0 Hz, 1H), 3.12 (p, J = 12.9 Hz, 2H), 2.96-2.82 (m, 2H), 2.06-1.75 (m, 12H), 1.59 (s, 3H), 1.57 (s, 3H), 1.51 (s, 9H). ^{13}C NMR (100 MHz, $CDCl_3$) δ 174.1, 155.1, 142.9, 142.8, 140.4, 139.3, 134.5, 134.0, 130.3, 126.8, 126.2, 124.2, 123.5, 123.3, 122.8, 119.1, 118.6, 66.5, 52.7, 46.2, 38.8, 38.8, 38.7, 32.4, 29.2, 25.9, 25.7, 25.6, 24.79, 15.2, 15.1, 15.1. ESI-MS, found, 615.80; calculated for $[M+H]^+$: 616.34.

Synthesis of alkyne-functionalized lipidated peptides 19-21. Attachment of the building block to the solid support was carried out by shaking the 2-Cl-trt resin under dry conditions with a solution containing 2 eq of the Fmoc-Cys(R)OH (R = StBu or GerGer) and 4 eq of DIPEA. Successful attachment was determined by means of the fluorenylmethoxycarbonyl (Fmoc)-removal method (Brunsveld et al., 2005). For N-terminal elongation, the Fmoc

protecting group was removed with 20% piperidine in dimethylformamide (DMF) (twice, 10 min each). Fmoc-protected amino acids (4 eq) were preactivated by the treatment with O-(6-chlorobenzotriazol-1-yl)-N,N,N′,N′-tetramethyluronium hexafluorophosphate (HCTU) (4 eq) and DIPEA (8 eq) for 5 min in DMF to yield a 0.1 M solution, which was used for coupling directly (2-4 h). The N-terminal alkyne group was incorporated into peptides by the reaction of the activated CH_2Cl_2 solution of 3 eq propiolic acid and 3 eq N,N'-diisopropylcarbodiimide (DIC) with the resin at 0 °C. After completion of the synthesis, the peptides were released from the resin with a solution of 1% trifluoroacetic acid and 3% triethylsilane in CH_2Cl_2 twice. The released solution was evaporated to dryness, and the prenylated peptides were purified by flash chromatography (5% chloroform/methanol as eluent).

Yields for **19**, 53%, 55 mg. R_f = 0.1 (10% MeOH in CH_2Cl_2). ESI-MS ($[M+H]^+$) for **19**: 1085.67 (calculated for $C_{54}H_{81}O_9N_6S_4$, 1085.48); MALDI-TOF MS ($[M+Na]^+$): 1107.83; HRMS ($[M+H]^+$): 1085.49376 (calculated for $C_{54}H_{81}O_9N_6S_4$, 1085.49424).

Yields for **20**, 50%, 48 mg. R_f = 0.2 (10% MeOH in CH_2Cl_2). ESI-MS ($[M+H]^+$) for **20**: 998.73 (calculated for $C_{51}H_{75}O_7N_5S_4$, 998.45); MALDI-TOF MS ($[M+Na]^+$): 1020.65; HRMS ($[M+H]^+$): 998.46270 (calculated for $C_{51}H_{75}O_7N_5S_4$, 998.4622).

Yields for **21**, 70%, 70 mg. R_f = 0.3 (4% MeOH in CH_2Cl_2). ESI-MS ($[M+H]^+$) for **21**: 998.73 (calculated for $C_{51}H_{75}O_7N_5S_4$, 998.45); MALDI-TOF MS ($[M+Na]^+$): 1020.77; HRMS ($[M+H]^+$): 998.46232 (calculated for $C_{51}H_{75}O_7N_5S_4$, 998.4622).

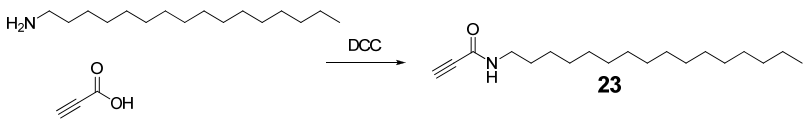

Synthesis of 23. A solution of propiolic acid (280 mg, 4 mmol) in CH_2Cl_2 was cooled to -20 °C. Dicyclohexylcarbodiimide (DCC, 910 mg, 9.1 mmol) and 1-hexadecylamine (536 mg, 2.22 mmol) were added and the reaction was allowed to warm up to room temperature. After overnight, the solution was filtered. After removing the solution, the resulting oil was purified by flash chromatography (2% MeOH in CH_2Cl_2) to give white power **23**, yield, 81% (0.52 g). ^{1}H NMR (400 MHz, $CDCl_3$) δ 6.15 (s, 1H), 3.27 (t, J = 7.1 Hz, 2H), 2.75 (s, 1H), 1.51 (m, 2H), 1.29-1.14 (m, 26H), 0.86 (t, J = 6.9 Hz, 3H). ^{13}C NMR (100 MHz, $CDCl_3$) δ 152.3, 77.6, 72.9, 40.0, 32.0, 29.7, 29.7, 29.7, 29.6, 29.6, 29.4, 29.3, 29.3, 26.9, 22.7, 14.2. ESI-MS for

$[M+H]^+$: 294.18 (calculated for $C_{19}H_{36}ON$, 294.27). HRMS for $[M+H]^+$: 294.27896 (calculated for $C_{19}H_{36}ON$, 294.27914).

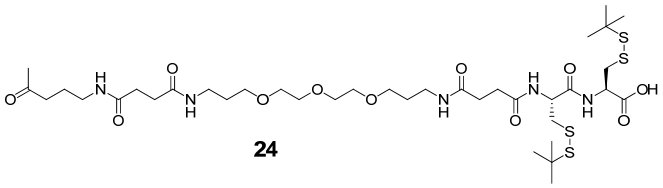

24

PEG-1 24. Attachment of the building block to the solid support was carried out by shaking the tritylchloride resin under dry conditions with a CH_2Cl_2 solution containing 3 eq of the Fmoc-Cys(StBu)OH and 6 eq of DIEA. Loading efficiency was determined by means of the fluorenylmethoxycarbonyl (Fmoc)-removal method. For N-terminal elongation the Fmoc protecting group was removed with 20% piperidine in DMF (twice, 10 min each). Fmoc-protected amino acids (4 eq) were preactivated by treatment with HCTU (4 eq) and DIPEA (8 eq) or PyBOP (5 eq), 1-hydroxy-7-azabenzotriazole (HOAt, 5 eq) and DIPEA (10 eq) for 5 min in DMF to yield a 0.1 M solution, which was used for coupling directly (4 h). After completion of the synthesis, the peptides were released from the resin with a solution of 5% trifluoroacetic acid, 5% triethylsilane and 2% H_2O in CH_2Cl_2 (twice times). Combined filtrates were evaporated to dryness, and the final PEG-1 **24** was purified by Prep-HPLC. The typical yield is around 8%. ^{1}H NMR (400 MHz, MeOD) δ 3.65-3.62 (m, 4H), 3.59-3.57 (m, 4H), 3.51 (t, J = 6, 4H), 3.31-3.29 (m, 10H), 3.27-3.21 (m, 6H), 3.15 (t, J = 7.2, 2H), 2.57-2.49 (m, 4H), 2.13 (s, 3H), 1.79-1.66 (m, 6H), 1.33 (s, 18H). ^{13}C NMR (100 MHz, MeOD) δ 209.3, 173.8, 173.2, 171.2, 169.2, 161.1, 158.1, 76.6, 69.7, 69.2, 69.1, 68.8, 62.2, 50.1, 48.4, 48.2, 46.1, 40.5, 39.2, 33.0, 31.4, 31.4, 31.3, 30.8, 30.5, 29.7, 28.5, 25.5, 25.2, 24.6, 22.9. ESI-MS ($[M+H]^+$): 886.16 (calculated for $C_{37}H_{68}O_{11}N_5S_4$, 886.39); HRMS ($[M+H]^+$): 886.3792 (calculated for $C_{37}H_{68}O_{11}N_5S_4$, 886.3792).

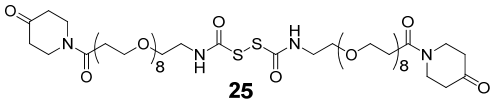

25

PEG-2 25. A mixture of dithiodiglycolic acid (0.5 mmol), N-hydroxysuccinimide (NHS, 1.05 mmol) and DCC (1.05 mmol) in 20 mL CH_2Cl_2 was stirred at room temperature for 1 h and the precipitated dicyclohexylurea (DCU) was removed by filtration. Then, PEG_8 (1 mmol) and Et_3N (1 mmol) were added into the filtrate. The reaction was stirred for another 1 h, and the solvent was removed at reduced pressure. The residue was dissolved in CH_2Cl_2 and washed with water and brine. The organic layer was dried over Na_2SO_4 and the solvent was evaporated under reduced pressure. The resulting intermediate was actived by DCC (1 mmol) and NHS (1 mmol) in 20 mL CH_2Cl_2. After filtration, 1,4-dioxa-8-azaspiro[4.5]decane (1

mmol) and Et_3N (1 mol) were added into the filtrate for reaction. After finishing the reaction, the solution was washed with water and brine, and treated by 20% TFA in CH_2Cl_2 at room temperature overnight. After removing the solution, the resulting oil was purified by flash chromatography (10% MeOH in CH_2Cl_2) to give **25** with 31% yield (0.369 g). TLC: R_f = 0.6 (5% MeOH in CH_2Cl_2). ^{1}H NMR (400 MHz, $CDCl_3$) δ 7.49 (bs, 2H), 3.82 (t, J = 6.0, 4H), 3.78-3.70 (m, 8H), 3.58-3.54 (m, 64H), 3.45 (s, 4H), 3.42 (t, J = 4.4, 4H), 2.67 (t, J = 6.0, 4H), 2.47 (t, J = 6.4, 4H), 2.40 (t, J = 6.0, 4H). ^{13}C NMR (100 MHz, $CDCl_3$) δ 206.9, 172.0, 170.7, 169.3, 70.2, 69.9, 69.2, 67.3, 64.2, 44.3, 42.1, 40.9, 40.7, 39.7, 33.3, 25.2. ESI-MS ($[M+H]^+$): 1191.67 (calculated for $C_{52}H_{95}O_{22}N_4S_2$, 1191.58); HRMS ($[M+H]^+$): 1191.58687 (calculated for $C_{52}H_{95}O_{22}N_4S_2$, 1191.58739).

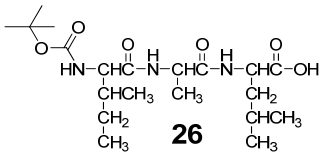

26

Boc-Ile-Ala-Leu 26. The tripeptide was synthesized based on SPPS technique on 2-Cl-trt resin. Attachment of Fmoc-LeuOH to the solid support was carried out by shaking the resin under dry conditions with a CH_2Cl_2 solution containing 3 eq of the Fmoc-LeuOH and 6 eq of DIEA (Loading efficiency, 0.56 mmol/g). For N-terminal elongation the Fmoc protecting group was removed with 20% piperidine in DMF (twice, 10 min each). Fmoc-AlaOH and Boc-IleOH (4 eq) were preactivated by treatment with HCTU (4 eq) and DIPEA (8 eq) for 5 min in DMF to yield a 0.1 M solution, which was used for coupling directly (4 h). After completion of the synthesis, the peptides were released from the resin with a solution of 1% trifluoroacetic acid and 3% triethylsilane in CH_2Cl_2 twice. No obvious deprotection of Boc was observed under such condition. After removing the solution, the resulting oil is pure enough for following synthesis. ^{1}H NMR (400 MHz, $CDCl_3$) δ 7.65-7.20 (m, 2H), 5.36 (bs, 1H), 4.7-4.4 (m, 2H), 4.1-4.0 (m, 1H), 1.82-1.60 (m, 3H), 1.42 (s, 9H), 1.36 (d, J = 5.2, 3H), 0.93-0.87 (m, 12H). ESI-MS ($[M+Na]^+$): 438.53 (calculated for $C_{20}H_{38}O_6N_3$, 438.25); HRMS ($[M+Na]^+$): 438.2571 (calculated for $C_{20}H_{38}O_6N_3$, 438.2574).

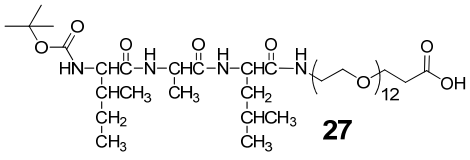

27

Boc-Ile-Ala-Leu-PEG$_{12}$ 27. A mixture of **26** (1.2 mmol, 0.50 g), NHS (1.22 mmol, 0.14 g) and DCC (1.25 mmol, 0.25 g) in 20 mL CH_2Cl_2 was stirred at room temperature for 1 h and the precipitated dicyclohexylurea (DCU) was removed by filtration. Then, PEG_{12} (1.2 mmol,

741 mg) and Et_3N (1.2 mmol, 167 µL) were added into the filtrate. The reaction was stirred for another 1 h, and the solvent was removed at reduced pressure. The residue was dissolved in CH_2Cl_2 and washed with water and brine. The organic layer was dried over Na_2SO_4 and the solvent was evaporated under reduced pressure. The resulting oil was purified by flash chromatography (30% MeOH in CH_2Cl_2) to give **27**. Yield, 89% (1.1 g). TLC: R_f = 0.4 (10% MeOH in CH_2Cl_2). ^{1}H NMR (400 MHz, $CDCl_3$) δ 7.46-7.20 (m, 3H), 5.46-5.40 (m, 1H), 4.58-4.45 (m, 2H), 4.05-3.96 (m, 1H), 3.72 (t, J = 6.8, 2H), 3.66-3.53 (m, 46H), 3.50 (t, J = 5.2, 2H), 2.56 (t, J = 6.4, 2H), 1.84-1.45 (m, 3H), 1.38 (s, 9H), 1.29 (d, J = 6.8, 3H), 0.89-0.81 (m, 12H). ^{13}C NMR (100 MHz, $CDCl_3$) δ 173.9, 172.3, 172.1, 171.7, 155.9, 79.7, 70.4, 70.3, 70.2, 70.0, 69.4, 66.5, 59.2, 51.6, 48.8, 41.3, 39.1, 37.3, 34.8, 28.2, 24.6, 22.7, 21.9, 18.3, 15.4, 11.3. ESI-MS ($[M+Na]^+$): 1037.93 (calculated for $C_{47}H_{90}O_{19}N_4Na$, 1037.61); HRMS ($[M+Na]^+$): 1037.60645 (calculated for $C_{47}H_{90}O_{19}N_4Na$, 1037.60915).

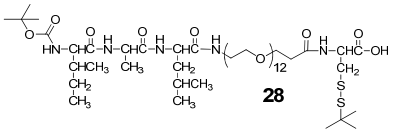

Boc-Ile-Ala-Leu-PEG$_{12}$-Cys 28. A mixture of **27** (0.3 mmol, 0.3 g), NHS (0.35 mmol, 40 mg) and DCC (0.35 mmol, 35 mg) in 20 mL CH_2Cl_2 was stirred at room temperature for 1 h and the precipitated dicyclohexylurea (DCU) was removed by filtration. Then, Cys(StBu)OH (0.3 mmol, 63 mg) and Et_3N (0.35 mmol, 49 µL) were added into the filtrate. The reaction was stirred for another 1 h, and the solvent was removed at reduced pressure. The residue was dissolved in CH_2Cl_2 and washed with water and brine. The organic layer was dried over Na_2SO_4 and the solvent was evaporated under reduced pressure. The resulting oil was purified by flash chromatography (30% MeOH in CH_2Cl_2) to give **28**. Yield, 67% (242 mg). TLC: R_f = 0.5 (10% MeOH in CH_2Cl_2). ^{1}H NMR (400 MHz, $CDCl_3$) δ 7.48-7.12 (m, 3H), 5.53-5.52 (d, J = 7.2, 1H), 4.57-4.41 (m, 2H), 3.97-3.94 (m, 1H), 3.75-3.70 (m, 3H), 3.66-3.56 (m, 46H), 3.49 (t, J = 5.2, 2H), 3.45-3.16 (m, 2H), 2.49 (bs, 1H), 1.81-1.46 (m, 3H), 1.38 (s, 9H), 1.32 (d, J = 6.8, 3H), 1.25 (s, 9H), 0.95-0.83 (m, 12H). ^{13}C NMR (100 MHz, $CDCl_3$) δ 172.3, 171.9, 156.0, 79.7, 70.3, 70.2, 69.9, 69.5, 67.1, 59.6, 53.7, 51.8, 49.3, 47.6, 43.6, 43.5, 41.1, 39.0, 37.2, 36.6, 30.8, 29.7, 28.2, 24.7, 24.6, 22.8, 21.8, 18.1, 15.5, 11.3. ESI-MS ($[M+H]^+$): 1206.47 (calculated for $C_{54}H_{104}O_{20}N_5S_2$, 1206.67); HRMS: 1206.67269 (calculated for $C_{54}H_{104}O_{20}N_5S_2$, 1206.67106).

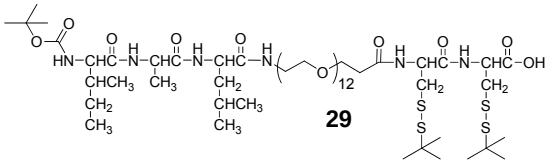

Boc-Ile-Ala-Leu-PEG$_{12}$-CysCys 29. A mixture of **27** (0.2 mmol, 0.2 g), NHS (0.21 mmol, 24 mg) and DCC (0.21 mmol, 21 mg) in 20 mL CH_2Cl_2 was stirred at room temperature for 1 h and the precipitated dicyclohexylurea (DCU) was removed by filtration. Then, Cys(StBu)Cys(StBu)OH (0.2 mmol, 80 mg) and Et_3N (0.4 mmol, 56 µL) were added into the filtrate. The reaction was stirred for another 1 h, and the solvent was removed at reduced pressure. The residue was dissolved in CH_2Cl_2 and washed with water and brine. The organic layer was dried over Na_2SO_4 and the solvent was evaporated under reduced pressure. The resulting oil was purified by flash chromatography (30% MeOH in CH_2Cl_2) to give **29**. Yield, 45% (125 mg). TLC: R_f = 0.7 (10% EtOAc in MeOH). ^{1}H NMR (400 MHz, $CDCl_3$) δ 7.67-7.44 (m, 2H), 7.19-6.88 (m, 2H), 5.31-5.30 (d, J = 7.2, 1H), 4.77-4.65 (m, 1H), 4.50-4.42 (m, 2H), 4.05-3.90 (m, 1H), 3.84-3.71 (m, 3H), 3.68-3.59 (m, 46H), 3.53 (t, J = 5.2, 2H), 3.47-3.10 (m, 4H), 2.54 (bs, 1H), 1.81-1.50 (m, 3H), 1.41 (s, 9H), 1.32-1.25 (m, 21H), 0.91-0.82 (m, 12H). ^{13}C NMR (100 MHz, $CDCl_3$) δ 172.2, 172.0, 171.7, 170.0, 156.0, 80.0, 70.5, 70.1, 69.5, 67.0, 59.4, 51.8, 49.2, 48.1, 47.9, 41.3, 39.2, 37.3, 36.7, 30.5, 29.8, 28.2, 24.7, 22.9, 21.9, 18.3, 15.5, 11.4. ESI-MS ([M+H]$^+$): 1397.36 (calculated for $C_{61}H_{117}O_{21}N_6S_4$, 1397.71); HRMS ([M+2H]$^{2+}$): 699.36226 (calculated for $C_{61}H_{118}O_{21}N_6S_4$, 699.36110).

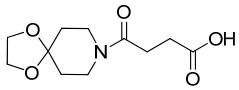

32

A solution of 1,4-dioxa-8-azaspiro[4.5]decane (1 mmol), succinic anhydride (1.2 mmol) and Et_3N (1.2 mmol) in CH_2Cl_2 was stirred at room temperature for 2 h. The solvent was removed at reduced pressure. The residue was dissolved in CH_2Cl_2 and washed with water and brine. The organic layer was dried over Na_2SO_4 and the solvent was evaporated under reduced pressure. The resulted crude product was dissolved in methanol (500 µL), and then ether (25 mL) was added. After keeping the mixture at -20 °C overnight, colorless crystals of **32** were isolated with 40% yield (97 mg). ^{1}H NMR (400 MHz, $CDCl_3$) δ 9.35 (S, 1H), 3.94 (S, 4H), 3.65 (t, J = 6, 2H), 3.52 (t, J = 5.6, 2H), 2.65-2.64 (m, 4H), 1.68 (t, J = 5.6, 2H), 1.64 (t, J = 6.0, 2H). ^{13}C NMR (100 MHz, $CDCl_3$) δ 176.5, 169.9, 106.6, 64.2, 43.3, 40.0, 35.2, 34.5, 29.3, 27.8. ESI-MS ([M+H]$^+$): 244.13 (calculated for $C_{11}H_{18}O_5N$, 244.11); HRMS ([M+H]$^+$): 244.11841 (calculated for $C_{11}H_{18}O_5N$, 244.11795).

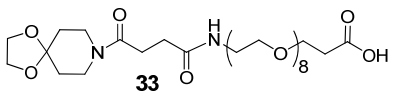

33

Keto-PEG$_8$ 33. A mixture of **32** (0.3 mmol, 73 mg), NHS (0.33 mmol, 36 mg) and DCC (0.33 mmol, 68 mg) in 20 mL CH_2Cl_2 was stirred at room temperature for 1 h and the precipitated dicyclohexylurea (DCU) was removed by filtration. Then, **PEG$_8$** (0.3 mmol, 132 mg) and Et_3N (0.4 mmol, 56 μL) were added into the filtrate. The reaction was stirred for another 1 h, and the solvent was removed at reduced pressure. The residue was dissolved in CH_2Cl_2 and washed with water and brine. The organic layer was dried over Na_2SO_4 and the solvent was evaporated under reduced pressure. The resulting oil was purified by flash chromatography (30% MeOH in CH_2Cl_2) to give **33**. Yield, 90% (180 mg). TLC: R_f = 0.5 (10% MeOH in CH_2Cl_2). ^{1}H NMR (400 MHz, $CDCl_3$) δ 3.85 (s, 4H), 3.61 (t, J = 6.4, 2H), 3.54-3.40 (m, 32H), 3.27 (t, J = 4.2, 2H), 2.57-2.52 (m, 4H), 2.45 (t, J = 6.4, 2H), 2.37 (t, J = 7.2, 2H), 1.77-1.73 (m, 4H). ^{13}C NMR (100 MHz, $CDCl_3$) δ 172.5, 170.2, 157.5, 105.9, 70.1, 69.8, 66.4, 65.4, 64.1, 64.0, 43.2, 39.7, 38.9, 35.0, 34.3, 33.4, 30.7, 28.1, 25.3, 25.1, 24.6. ESI-MS ($[M+H]^+$): 667.47 (calculated for $C_{30}H_{55}O_{14}N_2$, 667.36); HRMS ($[M+H]^+$): 667.36599 (calculated for $C_{30}H_{55}O_{14}N_2$, 667.36478).

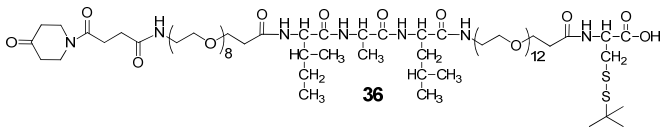

36

Keto-PEG$_8$-IAL-PEG$_{12}$-Cys 36. 28 (0.08 mmol, 97 mg) was dealt with 1:1 TFA-CH_2Cl_2 solution firstly and then the solvents were removed to produce **30**. A mixture of **33** (0.135 mmol, 90 mg), NHS (0.135 mmol, 16 mg) and DCC (0.28 mmol, 28 mg) in 20 mL CH_2Cl_2 was stirred at room temperature for 1 h and the precipitated dicyclohexylurea (DCU) was removed by filtration. A mixture of Et_3N (0.2 mmol, 28 μL) and **30** (0.08 mmol) in CH_2Cl_2 was added into the filtrate. The reaction was stirred for another 1 h, and the solvent was removed at reduced pressure. The residue was dissolved in CH_2Cl_2 and washed with water and brine. The organic layer was dried over Na_2SO_4 and the solvent was evaporated under reduced pressure. The resulting oil was purified by flash chromatography (50% EtOAc in MeOH) to give **34**. Yield, 19% (26 mg). TLC: R_f = 0.2 (10% MeOH in CH_2Cl_2). ^{1}H NMR (400 MHz, $CDCl_3$) δ 4.38-4.27 (m, 2H), 4.17-4.08 (m, 1H), 3.82-3.68 (m, 7H), 3.66-3.55 (m, 80H), 3.49 (t, J = 5.2, 2H), 3.40-3.33 (m, 4H), 2.69 (t, J = 6.4, 2H), 2.54-2.44 (m, 5H), 2.39 (t, J = 7.2, 2H), 2.10 (s, 4H), 1.83-1.48 (m, 7H), 1.37-1.18 (m, 21H), 0.88-0.79 (m, 12H). ^{13}C NMR (100 MHz, $CDCl_3$) δ 206.8, 172.7, 172.4, 172.2, 171.8, 171.6, 171.5, 170.8, 70.4, 70.3, 70.1, 69.7, 69.4, 67.5, 66.9, 58.9, 57.8, 53.3, 52.2, 51.9, 49.6, 48.0, 43.9, 42.3, 41.0, 40.9, 40.7, 39.3, 39.2, 36.8, 36.6, 36.4, 31.0, 30.8, 29.7, 29.6, 28.1, 25.0, 24.8, 22.9, 18.3, 15.4, 11.2, 8.2.

ESI-MS ($[M+H]^+$): 1710.73 (calculated for $C_{77}H_{144}O_{30}N_7S_2$, 1710.94); HRMS ($[M+2H]^{2+}$): 855.97122 (calculated for $C_{77}H_{145}O_{30}N_7S_2$, 855.97331).

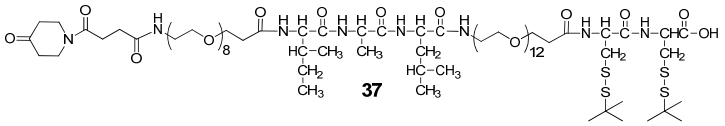

Keto-PEG$_8$-IAL-PEG$_{12}$-Cys-Cys 37. A mixture of **33** (0.135 mmol, 90 mg), NHS (0.135 mmol, 16 mg) and DCC (0.28 mmol, 28 mg) in 20 mL CH_2Cl_2 was stirred at room temperature for 1 h and the precipitated dicyclohexylurea (DCU) was removed by filtration. Then, **31** (0.08 mmol, from deprotection Boc group of **29**) and Et_3N (0.2 mmol, 28 μL) were added into the filtrate. The reaction was stirred for another 1 h, and the solvent was removed at reduced pressure. The residue was dissolved in CH_2Cl_2 and washed with water and brine. The organic layer was dried over Na_2SO_4 and the solvent was evaporated under reduced pressure. The resulting oil was purified by flash chromatography (50% EtOAc in MeOH) to give **37**. Yield, 13% (20 mg). TLC: R_f = 0.2 (10% MeOH in CH_2Cl_2). ^{1}H NMR (400 MHz, $CDCl_3$) δ 4.48-4.31 (m, 2H), 4.13-4.08 (m, 1H), 3.88-3.72 (m, 7H), 3.70-3.57 (m, 80H), 3.54 (t, J = 5.2, 2H), 3.47-3.38 (m, 4H), 3.19-3.13 (m, 2H), 2.75 (t, J = 6.8, 2H), 2.60-2.43 (m, 5H), 2.45 (t, J = 6.0, 2H), 2.15 (s, 4H), 1.86-1.54 (m, 7H), 1.41-1.22 (m, 30H), 0.91-0.86 (m, 12H). ESI-MS ($[M+H]^+$): 1901.60 (calculated for $C_{84}H_{157}N_8O_{31}S_4$, 1901.98); HRMS ($[M+C_2H_5OH+3Na]^{3+}$): 671.99519 (calculated for $C_{86}H_{162}N_8O_{32}S_4Na_3$, 671.99570).

5.4. Biochemical methods

5.4.1. Expression and purification of RabGGTase, REP-1, RabGDI-1, RhoGDI, and Rab7wt

All these proteins were kindly prepared and provided from Goody's group. Mammalian RabGGTase was purified from *E. coli* BL21(DE3) codon plus cells expressing a hexahistidine-GST tagged αsubunit and an untagged β-subunit. Briefly, following cell growth, induction and lysis of the cells, GGTase-II was purified from crude homogenate using Ni-NTA Sepharose columns (Pharmacia). The affinity tag was removed by digestion with TEV protease. A second Ni-NTA chromatography was performed in order to remove the cleaved-off hexahistidine tag, uncleaved GGTase-II and TEV protease. REP-1 was purified from insect cells infected with recombinant baculovirus or from recombinant yeast *S. cerevisiae*. The protein was purified by a combination of Ni-NTA affinity and gel filtration

chromatography. RabGDI and Rab7 wild-type proteins were expressed and purified in a similar manner. RhoGDI was cloned in frame with Maltose Binding Protein (MBP) using the pOPINM vector (Berrow et al., 2007), expressed in *E. coli,* and purified by Ni-NTA chromatography. The MBP tag was removed by proteolysis with Precision protease, and the protein was further purified by gel filtration on a Superdex 200 26/60 column (GE Helthcare).

5.4.2. Expression and purification of thioester proteins

The plasmid coding for the desired protein-Intein-CBD construct was transformed into *E.coli* BL21(DE3) cells using electroporation and transformants were selected on ampicillin (50 mg/L) agar plates. A single colony was inoculated into 5 mL of LB medium containing 125 mg/L Ampicillin and the culture was grown overnight at 37 °C. This pre-culture was used to seed 2 L of fresh LB medium (containing 125 mg/L ampicillin) and the culture was incubated at 37 °C until the absorbance at 600 nm (OD_{600}) reached 0.5-0.7. The cells were cooled down on ice, IPTG was added to a final concentration of 0.5 mM and overnight induction was performed at 20 °C. The cells were cooled down to 4 °C and all subsequent steps were performed at this temperature. Cells were harvested by centrifugation (5000 rpm, 20 min, 4 °C) and washed once in PBS. Cells could be stored frozen at -80 °C at this point. Levels of protein expression before and after induction were determined by SDS-PAGE. The bacterial pellet was resuspended in lysis buffer (25 mM sodium phosphate, pH 7.5, 0.5 M NaCl, 1 mM PMSF, 2 mM $MgCl_2$, 10 μM GDP) and the cells were lysed by passing them twice through a Microfluidizer. A fresh portion of 0.5 mM PMSF and Triton X-100 (1 % final concentration) were added. The lysate was cleared by ultracentrifugation (30000 rpm, 40 min, 4 °C) and the supernatant was transferred to Falcon tubes. An appropriate amount of chitin beads, equilibrated with lysis buffer containing 1 % Triton X-100 was added and the mixture was incubated for 2 h on a rotating wheel at 4 °C (1 mL of beads can bind about 2 mg of fusion-protein. The total amount of expressed fusion protein can be estimated by SDS-PAGE and Coomassie Blue staining. The suspension was centrifuged (2500 rpm, 5 min, 4 °C) and the supernatant removed. To remove unspecifically bound material beads were washed 4 times with lysis buffer containing 1 % Triton X-100 followed by 4 times washing with buffer without detergent. Cleavage of the fusion protein was induced by adding powdered MESNA to the beads suspension to a concentration of 0.5 M and overnight incubation at room temperature. The supernatant was collected by centrifugation and was passed over a gel filtration column equilibrated with ligation buffer (20 mM sodium phosphate, pH 7.5, 1 mM $MgCl_2$, 10 μM GDP). The pooled fractions were concentrated to at least 10 mg/mL and shock

frozen using liquid nitrogen. The proteins could be stored at 80 °C for at least 2 years without observious change in LCMS spectra. Yields typically ranged from 5-10 mg of protein thioester per liter of bacterial culture.

For the plasmid coding for the desired protein-Intein-His construct, the protein expression is similar with that of protein-Intein-CBD. The details of protein purification are optimized in the following part 5.4.3.

5.4.3. Universal C-terminal protein labeling with oxyamine ligation

1. Clone target gene into modified pTWIN vector using NdeI and SapI sites.
2. Express fusion protein (target-Intein-His) in BL21(DE3) cells.
3. Collect cells in 25 mL ice-cold Breaking buffer freshly supplemented with 1 mM PMSF. CRITICAL: PMSF should be added freshly. Don't add any reducing substances.
4. Lyse cells using a microfluidizer or ultrasonication.
5. Add 1% Triton X-100 into cell lysate and centrifuge at 35,000 rpm, 4 °C for 30 min.
6. Filter supernatant through a 0.2 μm filter.
7. Load cell lysate onto a Ni-NTA column equilibrated with buffer A (50 mM NaH_2PO_4, pH 8.0, 0.3 M NaCl).
8. Wash column with Buffer A and continue with 2% Buffer B (Buffer A + 0.5 M imidazole) until absorbance reaches baseline.
9. Elute column with a gradient of 2-100% Buffer B. Collect eluted fractions.
10. Identify and collect fractions of interest by SDS-PAGE.
11. Add MESNA powder to protein solution to a concentration of 0.5 M and incubate overnight at 20 °C.
12. Dilute solution with 5-fold volume of Buffer A
13. Load them onto a Ni-NTA column equilibrated with Buffer A containing 10 mM MESNA. Collect flow-through.
14. Wash column with 2-5% Buffer B containing 10 mM MESNA. Collect and pool flow-through and concentrate protein.
15. Run a gel filtration on a Superdex column using Elution Buffer (30 mM NaH_2PO_4, pH 7.5, 50 mM NaCl, 10 mM MESNA). CRITICAL: Prepare fresh solution, filter buffer through a 0.2 μm filter and degas for 0.5 h at room temperature.
16. Identify and collect fractions of interest by SDS-PAGE. Concentrate protein and snap-freeze in liquid nitrogen. Store protein at -80 °C.

17. Incubate 200 µl protein-thioester (5-25 mg/mL) with 100 µl bis(oxyamine) (1 M stock solution in reaction buffer, final 333 mM) in Reaction Buffer (30 mM NaH_2PO_4, pH 7.5, 50 mM NaCl) on ice overnight. The reaction is monitored by ESI-MS.
18. Dialyze protein twice against 1 L Dialysis Buffer (30 mM NaH_2PO_4 pH 7.5, 50 mM NaCl, 2 mM DTE) at 4 °C.
19. Incubate 50 µM protein-ONH_2 with 0.5 mM Keto-Coumarin **2** for 20 h or 1 mM **2** overnight on ice in the presence of 100 mM Aniline in Incubation Buffer (30 mM NaH_2PO_4, pH 7.0, 50 mM NaCl, 2 mM DTE). CRITICAL: If your protein can tolerate an acidic environment, the reaction can also be performed by incubating 50 µM protein-ONH_2 with 1 mM **2** for 4 h in sodium acetate buffer (50 mM, pH 5.5, 50 mM NaCl, 2 mM DTE).
20. Remove excess dye using a desalting column preequilibrated in Dialysis Buffer.
Note: For GTPases, 1 mM $MgCl_2$ and 10 µM GDP were added in all buffers.

5.4.4. Universal N-terminal protein labeling with NCL

1. Clone target gene containing N-terminal tobacco etch virus (TEV) protease recognition site (ENLYFQC) into modified pET-His vector using NdeI and XhoI sites.
2. Express protein (His-TEV-Cys-protein) in BL21(DE3) cells.
3. Collect cells in 25 mL ice-cold Breaking Buffer freshly supplemented with 1 mM PMSF and 2 mM β-mercaptoethanol. CRITICAL: PMSF and β-mercaptoethanol should be added freshly. Don't add any reducing substances.
4. Lyse cells using a microfluidizer or ultrasonication.
5. Centrifuge cell lysate at 35,000 rpm, 4 °C for 30 min.
6. Filter supernatant through a 0.2 µm filter.
7. Load cell lysate onto a Ni-NTA column equilibrated with Buffer A (50 mM NaH_2PO_4 pH 8.0, 0.3 M NaCl, 2 mM β-mercaptoethanol).
8. Wash column with Buffer A and continue with 2% Buffer B (Buffer A + 0.5 M imidazole) until absorbance reaches baseline.
9. Elute column with a gradient of 2-100% Buffer B. Collect eluted fractions.
10. Identify and collect fractions of interest by SDS-PAGE.
11. Add tobacco etch virus (TEV) protease at 1:20 molar ratio to the protein in the dialysis membrane tubing.
12. Dialyze sample against Dialysis Buffer (30 mM NaH_2PO_4 pH 7.5, 50 mM NaCl, 2 mM DTE) overnight.
13. Centrifuge dialyzed solution at 8000 rpm for 10 min. Collect supernatant.

14. Add $MgCl_2$ and imidazole to the supernatant to a final concentration of 5 mM and 10 mM, respectively.
15. Load onto a Ni-NTA column equilibrated with Buffer A. Collect flow-through.
16. Wash column with 2% Buffer B and collect flowthrough.
17. Pool and concentrate protein from flow-through.
18. Run a gel filtration on a Superdex column using Dialysis Buffer. CRITICAL: Prepare fresh solution, filter buffer through a 0.2 µm filter and degas on a vacuum-membrane pump by stirring for 0.5 h at room temperature.
19. Identify and collect fractions of interest by SDSPAGE. Concentrate protein and snap freeze in liquid nitrogen. Store proteins at -80 °C.
20. Incubate 50 µM N-Cys-protein with 500 µM coumarin-thioester **10** in the presence of 200 mM MPAA in Reaction Buffer (30 mM NaH_2PO_4 pH 7.5, 50 mM NaCl) on ice overnight. The reaction is monitored by ESI-MS.
21. Remove excess dye using a desalting column preequilibrated in Dialysis Buffer.
Note: For GTPases, 1 mM $MgCl_2$ and 10 µM GDP were added in all buffers.

5.4.5. Universal C/N-terminal protein dual-labeling

1. Clone target gene containing N-terminal tobacco etch virus (TEV) protease recognition site (ENLYFQC) into modified pTWIN vector using NdeI and SapI sites.
2. Express fusion protein (TEV-Cys-target-Intein-His) in BL21(DE3) cells.
3. Collect cells in 25 mL ice-cold Breaking Buffer freshly supplemented with 1 mM PMSF. CRITICAL: PMSF should be added freshly. Don't add any reducing substances.
4. Lyse cells using a microfluidizer or ultrasonication.
5. Add 1% Triton X-100 to cell lysate and centrifuge at 35,000 rpm, 4 °C for 30 min.
6. Filter supernatant through a 0.2 µm filter.
7. Load cell lysate onto a Ni-NTA column equilibrated with Buffer A (50 mM NaH_2PO_4, pH 8.0, 0.3 M NaCl).
8. Wash column with Buffer A and continue with 2% Buffer B (50 mM NaH_2PO_4, pH 8.0, 0.3 M NaCl, 0.5 M imidazole) until absorbance reaches baseline.
9. Elute column with a gradient of 2-100% Buffer B. Collect eluted fractions.
10. Identify and collect fractions of interest by SDS-PAGE.
11. Add MESNA powder to protein solution to a concentration of 0.5 M and incubate overnight at 20 °C (intein cleavage).
12. Dilute solution with 5-fold volume of Buffer A

13. Load onto a Ni-NTA column equilibrated with Buffer A containing 10 mM MESNA. Collect flow-through.
14. Wash column with 2-5% Buffer B containing 10 mM MESNA. Collect and pool flow-through and concentrate protein.
15. Run a gel filtration on a Superdex column using Elution Buffer (25 mM NaH_2PO_4, pH 7.2, 30 mM NaCl, 10 mM MESNA). CRITICAL: Prepare fresh solution, filter buffer through a 0.2 μm filter and degas on a vacuum-membrane pump by stirring for 0.5 h at room temperature.
16. Identify and collect fractions of interest by SDS-PAGE. Concentrate protein.
17. Incubate 200 μl TEV-Cys-protein-thioester (5-25 mg/mL) with 100 μl bisoxyamine (1 M stock solution in reaction buffer, final 333 mM) in Reaction Buffer (30 mM NaH_2PO_4, pH 7.5, 50 mM NaCl) on ice overnight. The reaction is monitored by ESI-MS.
18. Dialyze protein twice against 1 L Dialysis Buffer (30 mM NaH_2PO_4, pH 7.5, 50 mM NaCl, 2 mM DTE) at 4 °C.
19. Incubate 50 μM resulting TEV-Cys-protein-ONH_2 with 5 μM TEV protease for 1 h at room temperature.
20. Load solution onto a Ni-NTA column equilibrated with Buffer A containing 2 mM β-mercaptoethanol. Collect flow-through.
21. Wash column with 2-5% Buffer B containing 2 mM β-mercaptoethanol. Collect and pool flowthrough and concentrate protein.
22. Remove peptide and exchange buffer using a desalting column pre-equilibrated with Elution Buffer (30 mM NaH_2PO_4, pH 7.0, 50 mM NaCl).
23. Incubate 50 μM N-Cys-protein-ONH_2 with 0.5 mM **10** and 0.5 mM **3** in the presence of 200 mM MPAA and 100 mM Aniline in Reaction Buffer on ice for 24 h. The reaction is monitored by ESI-MS.
24. Remove excess dyes using a desalting column preequilibrated with Dialysis Buffer.
Note: For GTPases, 1 mM $MgCl_2$ and 10 μM GDP were added in all buffers.

5.4.6. Protein refolding based on the dual-labeling Rab probe

For unfolding: 10-20 μl dual-labeling protein probe (0.1 mg/mL) in buffer A (50 mM HEPES, pH 7.2, 50 mM NaCl, 2 mM $MgCl_2$, 5 mM DTE) was added into 980 μl buffer A containing 0-8 M G.HCl. Then the emission spectrum (420-700 nm) with excitation at 400 nm was recorded. **For refolding**: 20 μL protein (0.1 mg/mL) was added into 200 μL cold methanol. After centrifugation, the supernatant was removed. Then 10 μL denaturing buffer

(50 mM HEPES, pH 7.2, 6 M G.HCl) was added to dissolve the protein, and the solution was added into 990 μL buffer A containing 50 μM GDP or GppNHp. The emission spectra were recorded at different time points with excitation at 400 nm at 25 ºC. The solution was not stirred.

5.4.7. Ligation of PEG-1 24 with Rab-ONH_2

Proteins (about 1 mg/mL) in sodium phosphate buffer (30 mM, pH 7.0) were incubated with ketone molecules **24** (0.5 mM) in the presence of 100 mM aniline on ice overnight. The ESI-MS indicated that the oxyamine-containing proteins were singly and quantitatively modified by ketone molecules. Unreacted small molecules were removed by passing the reaction mixture over a NAP-5 desalting column pre-equilibrated with 30 mM sodium phosphate (pH 7.5, 50 mM NaCl, 1 mM $MgCl_2$, 10 μM GDP, and 5 mM DTE). 500 mM MESNA was added as solid into the protein solution, which was further incubated on ice for 2 h. The ESI-MS indicated that both the StBu groups were totally removed. Then analysis gel filtration was used to purify the ligated protein in prenylation buffer (50 mM HEPES, pH 7.2, 50 mM NaCl, 5 mM DTE, 2 mM $MgCl_2$, 10 μM GDP). The protein fractions were collected by centrifugation and concentrated to about 1-5 mg/mL for further prenylation and microinjection studies.

5.4.8. Preparation of GEF:GTPase complexes

The complex between GEE and nucleotide-free GTPase was generated by mixing 1:1 ratio of the proteins (GEF and its GTPase:GDP) with a 10-fold excess of EDTA (50 mM) over $MgCl_2$ (5 mM) overnight on ice. The resulting complex was further purified by gel filtration with nucleotide-free buffer (50 mM HEPES, pH 7.2, 50 mM NaCl, 5 mM dithioerythritol, 2 mM $MgCl_2$).

5.5. Lipid-Protein ligation by click reaction

Preparation of the 10 × catalysis for click reaction. 10 mM $CuSO_4$ (from 100 mM stock solution), 10 mM ligand tris[(1-benzyl-1H-1,2,3-triazol-4-yl)methyl]amine (TBTA, from 20 mM methanol stock solution), 20 mM sodium ascorbate (from 200 mM freshly stock solution) were prepared, pre-mixed and incubated at room temperature for 5 minutes. For every reaction the catalysis was prepared freshly and used immediately.

Lipid-protein Ligation. Rab proteins (final concentration, 1 mg/mL) in 30 mM sodium phosphate buffer (pH 7.4) containing 10 mM CTAB were mixed with 1 mM (final concentration) alkyne-containing lipopeptide. Then the catalysis solution (final concentration of 1 mM) was added to start the reaction at room temperature. After 30-40 minutes, the reaction solution was centrifuged and 1 mM EDTA was added to quench the reaction. SDS-PAGE indicated the band shift after the click lgation and LC-MS indicated that the click ligation was completed.

Prenylated protein purification. After the click reaction, the solution was diluted with 10 to 15 times in ice-cold acetone or methanol. After centrifuge, the pellet was washed by 4 times with 2 mL of methanol, 4 times with 2 mL of CH_2Cl_2, and 3 times with 1 mL of Milli-Q water. The precipitate was dissolved in denaturing buffer (100 mM Tris-HCl, pH 8.0, 8 M G.HCl, 500 mM MESNA, 1% CHAPS, 1 mM EDTA) to a final protein concentration of 0.5-1.0 mg/mL and incubated overnight at 4 °C with slight agitation. Protein was refolded by diluting it at least 25-fold dropwise into refolding buffer (50 mM HEPES, pH 7.5, 2.5 mM DTE, 2 mM $MgCl_2$, 10 μM GDP, 1% CHAPS, 400 mM arginine-HCl, 400 mM trehalose, 0.5 mM PMSF, 1 mM EDTA) with an equimolar amount of REP-1 or GDI-1 or excess dilipidated BSA. The mixture was further incubated at room temperature for 30 min and on ice for 1 h. The mixture was dialyzed twice against 2 L dialysis buffer (25 mM HEPES, pH 7.5, 2 mM $MgCl_2$, 10 μM GDP, 5 mM DTE, 100 mM $(NH_4)_2SO_4$, 10% glycerol, 0.5 mM PMSF, 1 mM EDTA). The dialyzed material was concentrated to a protein concentration of 2-5 mg/mL using size exclusion concentrators (MWCO, 10 kDa) and loaded on a Superdex-200 gel filtration column (Pharmacia) equilibrated with gel filtration buffer (25 mM HEPES, pH 7.5, 2 mM $MgCl_2$, 10 μM GDP, 5 mM DTE, 50 mM NaCl). The fractions containing Rab-REP complex were collected.

5.6. Protein immobilization by oxyamine ligation

Generation of protein expression lysates. Proteins were expressed as described above. After harvesting the bacteria, the cells were lysed in lysis buffer (25 mM sodium phosphate pH 7.5, 500 mM NaCl, 1 mM $MgCl_2$, 10 μM GDP (for GTPases only), 1 g cells/1 mL lysis buffer) by passing them multiple times through a fluidizer (110 S, Microfluidics) and subsequently centrifuged. Then the soluble fraction was isolated and treated with a 500 mM MESNA solution (final concentration) at room temperature overnight and with a 300 mM bis(oxyamine) solution (final concentration) on ice for at least 4 h. The resulting solution was

dialyzed twice against 1 L of the dialysis buffer at pH 7.5, and against 1 L of dialysis buffer at pH 7.0 to remove the excess of bis(oxyamine). The resulting cell lysates containing oxyamine-modified proteins are ready for spotting. For control experiments, the cellular lysates were treated with 500 mM MESNA only and then dialyzed again dialysis buffers as described.

General procedure for protein spotting and immobilization. Protein spotting was carried out by a non-contact microarray robot to generate five identical subarrays per slide that can be separated by GeneFrames (ABgene, Thermoscientific) (spot volume: 250 pL; spot size: 400 µm diameter). The spotting buffer contains 20 % glycerol to prevent the drying of protein spots on the slides. After incubating in a humidity chamber at room temperature for several hours, the slides were washed with washing buffer (25 mM HEPES pH 7.4, 50 mM NaCl, 2 mM $MgCl_2$, 2 mM DTE, 0.05% Tween 20) three times (3 × 5 min) to remove unreacted proteins. Then, the slides were blocked with blocking buffer (1% BSA in washing buffer) for 30 min at room temperature. The resulted slides were further washed with washing buffer and rinsed with doubly distilled H_2O and dried under an argon stream for subsequent fluorescence scanning or interaction with other proteins. The data were analyzed and quantified with the software ImageQuant TL (GE Healthcare).

Time-dependent immobilization of EGFP-Rab7-ONH_2. A 50 µM solution of EGFP-Rab7-ONH_2 in phosphate buffer (30 mM, pH 7.0, 50 mM NaCl, 2 mM $MgCl_2$, 2 mM DTE, 20 µM GDP, 20% glycerol, 2% Tween 20) was spotted on a ketone-coated slide to generate five identical EGFP-Rab7 subarrays that were separated by applying GeneFrames and incubated in a humid chamber. One subarray was washed with washing buffer at each time point to stop the oxime ligation (2, 4, 5, 6, and 7 hours). Finally, after rinsing with water and drying under argon, the microarray was scanned and analyzed as described above.

pH-dependent immobilization of EGFP-Rab7-ONH_2. Different 45 µM solutions of EGFP-Rab7-ONH_2 in phosphate buffers with different pH values were spotted on the ketone-coated slide to generate five subarrays per slide separated by GeneFrames, followed by incubation in a humid chamber for 6 hours. The microarray was washed, scanned and analyzed as described above.

Aniline-catalysis of EGFP-Rab7-ONH_2. Considering the fact that aniline is insoluble in water, we prepared a 2 M aniline stock solution in methanol. A 50 µM solution of EGFP-Rab7-ONH_2 containing or not 100 mM of aniline was spotted on ketone-coated slides followed by incubation in a humidity chamber for 6 hours. The slide was washed, scanned and analyzed as described above.

Preparation of Cy3-REP-1 and Cy3-RabGDI. To a solution of REP-1 (7.0 mg/mL, 50 µL) in labeling buffer (50 mM HEPES, pH 7.2, 50 mM NaCl, 2 mM $MgCl_2$, 2 mM DTE), Cy3-NHS-ester (GE healthcare PA23001) dissolved in 50 µL labeling buffer (0.1 mM) was added and then the reaction mixture was shaken at room temperature for 30 min and one hour on ice. After this, the labeled protein was separated using Hi-Trap desalting columns (Pharmacia Biotech) to obtain the desired Cy3-REP-1 with a final molar dye/protein (D/P) ratio 1.28. Cy3-RabGDI was prepared analogously with a final molar dye/protein (D/P) ratio 1.10.

Interaction analysis of EGFP-Rab7 microarrays with Cy3-REP-1 and Cy3-RabGDI. The EGFP-Rab7 microarrays were generated as mentioned above. Blocking was done by covering the slide surface with washing buffer containing 1% of BSA for 30 min. Two subarrays separated by GeneFrames were respectively incubated with 100 µL solution of 200 nM Cy3-REP-1 or 1 µM Cy3-RabGDI for 30 min, followed by washing three times with washing buffer (3 x 5 min). After rinsing with doubly distilled H_2O and drying under argon, the slide was scanned and quantified as described above.

Interaction analysis of PKA microarrays with FITC-labeled PKA antibody. The PKA-antibody (sc-365615) was purchased from Santa Cruz Biotechnology. The FITC-labeled antibody was prepared using a FITC protein labeling kit (Invitrogen). Different concentrations of PKA-ONH_2 (5-100 µM) were spotted on ketone-coated slides (pH 7.0) and incubated at room temperature for 6 hours. After washing and blocking, the slide was incubated with 500 nM FITC-labeled antibody for 30 min, followed by washing, drying and fluorescence detection as described above.

Immobilization of protein expression lysates. Both cellular lysates containing expressed EGFP-Rab7 or PKA were prepared as described above. Cellular lysates containing EGFP-Rab7-ONH_2 (0.5 g and 1 g cell/mL lysis buffer) were mixed with glycerol (final concentration 20%) and Tween 20 (final concentration 2%) and then spotted on a ketone-coated slide to generate three identical EGFP-Rab7 subarrays that were separated by applying GeneFrames and incubated in a humidity chamber for 6 h at room temperature. EGFP-Rab7-COSR cellular lysate (1 g cell/mL lysis buffer) was used as negative control. After washing with washing buffer and doubly distilled H_2O, the slide was dried under an argon stream. The microarray was scanned and analyzed as described above. The PKA-ONH_2 cellular lysate (1 g cell/mL lysis buffer) was immobilized using a similar protocol. After washing and blocking, the slide was incubated with 500 nM FITC-labeled PKA antibody for 30 min., followed by washing, drying and fluorescence detection as described above.

5.7. *In vitro* protein prenylation

PEGylated Rab or wild type or mutants (4 μM), REP-1 (6 μM), RabGGTase (6 μM) were incubated in prenylation buffer (50 mM HEPES, pH 7.2, 50 mM NaCl, 5 mM dithioerythritol, 2 mM $MgCl_2$, 10 μM GDP) at 25 °C, and 100 μM NBD-FPP was added to initiate the reaction. At defined time intervals, 10 μL samples were withdrawn and quenched by addition of 10 μL of 2 × SDS-PAGE sample buffer. For an end-point assay, 6 μM PEGylated Rab7 or wild type, 10 μM REP, and 6 μM RabGGTase were mixed with 40 μM NBD-FPP in prenylation buffer and incubated for 1.5 h at 37 °C, followed by quenching with 2 × SDSPAGE sample buffer. The samples were boiled at 95 °C for 10 min and were loaded onto 15% SDS-PAGE. The fluorescence bands corresponding to the NBD-farnesylated protein were visualized in the gel using a Fluorescent Image Reader FLA-5000 (Fuji, excitation laser: 473 nm, cut-off filter: 510 nm) followed by staining with Coomassie Blue and scanning. The fluorescence intensities of the bands were quantitatively analyzed using AIDA densitometry software. The traces were fitted to a single exponential equation using Orgin 6.0.

For lipidated Rabs: For prenylation reactions by fluorescent SDS-PAGE assay, typically RabGGTase (4.5 μM) and Rab1-G:REP-1 complex (4-4.5 μM) was premixed in 10 μL buffer (50 mM HEPES, pH 7.2; 50 mM NaCl, 5 mM DTE, 2 mM $MgCl_2$, 100 μM GDP), and then 20 μM NBD-FPP (final concentration) was added to initiate the reaction. The reaction was allowed to proceed for 1 h at room temperature and was quenched by addition of SDS-PAGE sample buffer, after which the samples were resolved on SDS-PAGE and scanned for fluorescence using a laser fluorescent image reader, and photographed in UV light and visible light after Coomassie blue staining. For real-time monitoring of prenylation reactions, typically 50-100 nM of dansyl-labeled semisynthetic Rab1-G:REP-1 complex was mixed with an equal amount of RabGGTase in a cuvette containing 1 mL buffer (50 mM HEPES, pH 7.2; 50 mM NaCl, 5 mM DTE, 2 mM $MgCl_2$, 10 μM GDP). Following five minutes incubation at 25 °C, the reaction was initiated by adding GGPP to a final concentration of 30 μM. Excitation and emission monochromators were adjusted to 280 and 510 nm, respectively. Data were fitted to a double exponential equation using Orgin 7.5.

5.8. Biophysical methods

Fluorescence measurements were performed either with an Aminco SLM 8100 spectrofluorometer (Aminco, Silver Spring, MD, USA) or a Spex Fluoromax-3 spectrofluorometer (Jobin Yvon, Edison, NJ, USA). Measurements were carried out in 1 mL

quartz cuvettes (Hellma) with continuous stirring and thermostated at 25 °C unless otherwise indicated. Stopped-flow measurements were performed on an Applied Photophysics SX.18MV-R apparatus (Surrey, UK). All buffers used in these experiments were filtered through a 0.2 μm membrane filter (Whatman) and degassed on a vacuum-membrane (ILM/VAC GmbH) pump by stirring for 0.5 h at room temperature. To observe the FRET effect between coumarin and fluorescein, the excitation was at 400 nm in Fluoromax-3 spectrometer or 406 nm in stopped-flow apparatus, and the emission was monitored at 520 nm in the fluorescence spectrometer or observed through a 530 nm cut-off filter.

5.8.1. Fluorescence titrations – determination of K_d

Steady-state fluorescence measurements for monitoring interactions between labeled Rab7 and REP-1 were followed in 50 mM Hepes, pH 7.2, 50 mM NaCl, 5 mM DTE, 1 mM $MgCl_2$ and 10 μM GDP. Typically the fluorophore-labeled Rab7 probe was placed in a cuvette in 1 mL of buffer to give a final concentration of ca. 100-200 nM. Small aliquots of REP-1 or interaction protein were then added to the cuvette, until the fluorescence signal was saturated or showed a continuous linear increase. The change in fluorescence was plotted as a function of the total REP-1 concentration and corrected for unspecific fluorescence. The data was fitted to the following equation using GraFit 5.0 (Erithacus software):

$$Y = Y_{\min} + \left\{ K_d + [L]_0 + [P]_0 - \sqrt{(K_d + [L]_0 + [P]_0)^2 - 4[P]_0[L]_0} \right\} \frac{Y_{\max} - Y_{\min}}{2[P]_0}$$

where Y is the observed fluorescence after each step of titrator addition, $Y_{\min}$ is the initial value at $[L]_0 = 0$, $Y_{\max}$ is the final value at saturation, $[L]_0$ is the total (cumulative) concentration of REP-1, $[P]_0$ is the Rab7:REP-1 complex concentration, and K_d is the equilibrium constant, which is to be determined.

5.8.2. Monitoring the prenylation reaction

The prenylation of the semisynthetic Rab7 proteins was analysed using a Spex Fluoromax-3 spectrofluorometer (Jobin Yvon, Edison, NJ, USA) for long-term measurements, whereas a stopped-flow apparatus (Applied Photophysics, Surrey, UK) was used for examining the fast events occurring upon start of the reaction.

Long-term measurements

Typically, 50-100 nM of dansyl labeled semisynthetic Rab7:REP-1 complex was mixed with an equal amount of GGTase-II in a cuvette, containing 1 mL of buffer (50 mM Hepes, pH 7.2,

50 mM NaCl, 5 mM DTE, 1 mM $MgCl_2$, 10 µM GDP). Following a 5 min incubation at 25° C permitting temperature equilibration, the reaction was started by adding geranylgeranyl-pyrophosphate to a final concentration of approximately 10 µM. Excitation and emission monochromators were adjusted to 280 nm and 510 nm, respectively. The data were fitted to a double exponential equation using GraFit 5.0 (Erithacus software):

$$Y = Y_0 + A_1 e^{-k_1 t} + A_2 e^{-k_2 t}$$

where Y is the observed fluorescence, Y_0 is the fluorescence at $t = \infty$, A_1 and A_2 are the signal amplitudes, t is the time, and k_1 and k_2 are the rate constants.

5.8.3. Transient kinetics

Stopped-flow measurements

Fluorescent reactant A in buffer (50 mM HEPES, pH 7.2, 50 mM NaCl, 5 mM DTE, 1 mM $MgCl_2$) was rapidly mixed in the stopped-flow apparatus with an equal volume of reactant B in the same buffer. Excitation was at 406 nm for coumarin, while fluorescene was recorded through a 530 nm cut-off filter. Mixing and measuring chamber were thermostated at 25 °C using a water bath. Typically, traces of 3 independent experiments were averaged using the software package provided by Applied Photophysics. The data were fitted to a single- or double-exponential equation using GraFit 5.0 (Erithacus software)

Determination of k_{off}

For determination of k_{off}, the coumarin-GEF:GTPase-fluorescein complex (50 nM for DrrA:Rab1 and 500 nM for Ran:Rcc1) was mixed with 10-20 equal amount of GEF at 25 °C in the stopped-flow apparatus (buffer: 50 mM Hepes, pH 7.2, 50 mM NaCl and 5 mM DTE, 1 mM $MgCl_2$). Excitation was at 406 nm for coumarin, while fluorescene was recorded through a 530 nm cut-off filter. The obtained displacement curve could be fitted to a single exponential equation:

$$Y = Y_0 + A e^{-k_{off} t}$$

where Y is the observed fluorescence, Y_0 is the fluorescence at $t = \infty$, A is the signal amplitude, t is the time, and k is the rate constant, which equals k_{off} for dissociation of GEF from the GEF:GTPase complex. Data analysis was carried out using GraFit 5.0 (Erithacus software).

5.9. Molecular biology method

5.9.1 Preparation and transformation of competent cells

1 L of LB medium was inoculated with 1 mL of an overnight-grown culture of the desired *E.coli* strain. Cells possessing antibiotic resistance genes (e.g. BL21(DE3) codon plus RIL) were grown in the presence of the corresponding antibiotic. The culture was incubated at 37 °C on a shaker, until the OD_{600} reached 0.5 (ca. 4 h). The culture was cooled on ice for 20 min, transferred to sterile centrifugation vessels and centrifuged for 10 min at 4 °C and 2000 rpm. The supernatant was decanted.

Variant A.: Transformation by Electroporation

The bacterial cell pellet was gently (!) resuspended in 5 mL of ice-cold sterile GYT (0.125% (w/v) yeast extract, 0.25% (w/v) tryptone, 10% (v/v) glycerol) and recentrifuged as described above. Cells were resuspended in a final volume of 1 mL GYT, dispensed in 50 µL aliquots, shock frozen in liquid nitrogen and stored at 80 °C. For transformation, approximately 1 ng of DNA was added to the thawed cell suspension in a chilled cuvette. Electrotransformation was carried out by applying a high voltage pulse using a *E.coli* Pulser from Biorad (conditions: 25 µF, 200 Ω, 2.5 kV). 1 mL of LB medium was added to the cell suspension and the culture was grown at 37 °C for 1 h. Transformed Cells were selected on agar plates containing the corresponding antibiotics.

Variant B.: Transformation using $CaCl_2$

The pellet was gently resuspended in 20 mL of ice-cold sterile 100 mM $CaCl_2$ solution and incubated on ice for 30 min. The cells were centrifuged at 2000 rpm for 5 min at 4 °C and were resuspended in 1-5 mL of TFBII buffer (10 mM MOPS, pH 7.0, 75 mM $CaCl_2$, 10 mM NaCl, 15 % glycerol). Aliquots of 50-100 µL were shock frozen in liquid nitrogen and stored frozen at 80 °C. For transformation, cells were thawed rapidly and approximately 1 ng of the desired plasmid DNA was added. The mixture was incubated on ice for 30 min without shaking. Cells were heat-shocked at 42 °C for 60 s and immediately cooled on ice for 2 min. 1 mL of LB medium was added to the tube and the culture was incubated at 37 °C for 1 h, before recombinants were selected on agar plates supplemented with the corresponding antibiotics.

5.9.2. Purification of DNA

DNA fragments

DNA fragments produced by PCR amplification or restriction enzyme digestion were purified by preparative agarose gel electrophoresis. The band of interest was excised and extracted from the gel using a gel extraction kit from Quiagen or PQLab according to the instructions of the manufacturer.

Agarose gel electrophoresis

Depending on the size of the DNA fragment, the agarose concentration was between 0.8 and 1.2% (w/v). The required amount of agarose was solubilized by heating in TAE buffer. Ethidium bromide was added to a final concentration of 0.01% (w/v), the gel was poured into the gel casting equipment and allowed to polymerize. Samples were prepared in DNA loading buffer and the gels were run horizontally at 10 V/cm immersed in TAE-buffer until fragment separation was complete. A 1 kb DNA ladder (GibcoBRL) was used as a molecular weight standard.

Preparation of Plasmid DNA

Plasmid DNA was prepared using the plasmid mini-prep kit (Quiagen or PQLab) as follows: A single bacterial colony was used to seed 2 mL of LB medium containing the appropriate antibiotic(s). The culture was grown overnight (10-12 h) at 37 °C. Cells were harvested by centrifugation (2000 rpm, 5 min) and lysed by alkaline/SDS treatment. The precipitate (chromosomal DNA, lipids, proteins) was removed by centrifugation and the supernatant was loaded on a silica spin column. Following washing, the plasmid DNA was eluted using sterile TAE buffer or deionized water.

Ethanol precipitation

The salt concentration of the DNA sample was adjusted to 250-300 mM sodium acetate, pH 5.5 and DNA was precipitated by adding ethanol (96%) to a final concentration of ca. 70% followed by a 30 min incubation at room temperature. After centrifugation (13000 rpm, 10 min, RT) and removal of the supernatant, the precipitate was washed once with 70 % ethanol and dried under vacuum.

5.9.3. PCR

Preparative PCR

Typically, a 50 µL reaction mixture comprised 1-5 ng of template (plasmid) DNA, 0.5-1.0 µM of upstream and downstream primers, 200 µM of each dNTP, 2-3 units of Expand High Fidelity Polymerase mix (Roche Diagnostics, Mannheim, Germany) and the corresponding reaction buffer and salts. A Biorad PE 9700 thermocycler from Applied Biosystems (Weiterstadt, Germany) was used for temperature control and cycling.

Denaturation was for 1 min at 96 °C, annealing for 1 min at 50-62 °C depending on primer length and GC content, and extension was for 2-4 min (depending on the length of the amplicon). In general, 20-25 cycles were sufficient for efficient amplification.

Colony PCR screen

Colonies were picked and resuspended in 20 µL of sterile ddH_2O in a PCR test tube using sterile eppendorf tips. 6 µL of this suspension were mixed with 6 µL of PCR mix (containing 400 µM of each dNTP, 5 pmol of each primer, 1 unit of Taq polymerase (Sigma, Taufkirchen, Germany) in Taq buffer (2 x)). The PCR reactions were carried out under the following conditions: Cells were disrupted by heating the PCR tubes for 3 min at 96 °C followed by 25 cycles of denaturation for 30 s at 96 °C, annealing for 30 s at 50-62 °C, and primer extension for 40 sec at 72 °C. The PCR products were analyzed by agarose gel electrophoresis. An aliquot (1 µL) of the initially obtained cell suspension was plated on agar plates containing the corresponding antibiotics.

DNA Sequencing

For DNA sequencing of the cloned fragments the BigDyeDesoxy terminator cycle sequencing kit and a ABI Prism 373XL machine (Applied Biosystems, Weiterstadt, Germany) was used. The sequencing reactions contained 0.5-1 µg plasmid DNA, 3 pmol of the corresponding primers, and 8 µL BigDye termination mix in a final volume of 20 µL. 25 cycles were performed with the following parameters: denaturation for 30 s at 96 °C (for the first cycle 1 min), annealing for 1 min at 50 °C, and primer extension for 4 min at 60 °C. The DNA was ethanol precipitated (see above), washed twice with 70% ethanol, dried, and analyzed by the in house sequencing facility.

5.9.4. Restriction enzyme digestion

Restriction enzyme digests of DNA fragments were performed as recommended by the manufacturer. The reaction was stopped by addition of DNA loading buffer. Fragments produced by restriction enzyme digestion were separated using agarose gel electrophoresis.

5.9.5. Ligation

For ligation 1-10 *f*mol plasmid DNA was mixed with a 10 fold molar excess of fragment DNA. Ligation was performed in T4 DNA ligase buffer in a volume of 12.5 µL, using 0.2 units of T4 DNA ligase (Roche Diagnostics, Mannheim, Germany) for 16 h at 16 °C.

6. References

Abedin,M.J., Liepold,L., Suci,P., Young,M., and Douglas,T. (2009). Synthesis of a cross-linked branched polymer network in the interior of a protein cage. J. Am. Chem. Soc. *131*, 4346-4354.

Alexandrov,K., Horiuchi,H., Steelemortimer,O., Seabra,M.C., and Zerial,M. (1994). Rab escort protein-1 is a multifunctional protein that accompanies newly prenylated Rab proteins to their target membranes. EMBO J. *13,* 5262-5273.

Alexandrov,K., Simon,I., Iakovenko,A., Holz,B., Goody,R.S., and Scheidig,A. (1998). Moderate discrimination of REP-1 between Rab7·GDP and Rab7·GTP arises from a difference of an order of magnitude in dissociation rates. FEBS Lett. *425*, 460-464.

Alexandrov,K., Simon,I., Yurchenko,V., Iakovenko,A., Rostkova,E., Scheidig,A.J., and Goody,R.S. (1999). Characterization of the ternary complex between Rab7, REP-1 and Rab geranylgeranyl transferase. Eur. J. Biochem. *265*, 160-170.

Alexandrov,K., Heinemann,I., Durek,T., Sidorovitch,V., Goody,R.S., and Waldmann,H. (2002). Intein-mediated synthesis of geranylgeranylated Rab7 protein in vitro. J. Am. Chem. Soc. *124*, 5648-5649.

Alexander,M., Gerauer,M., Pechlivanis,M., Popkirova,B., Dvorsky,R., Brunsveld,L., Waldmann,H., and Kuhlmann,J. (2009). Mapping the isoprenoid binding pocket of PDEδ by a semisynthetic, photoactivatable N-Ras lipoprotein. ChemBioChem. *10*, 98-108.

Ali,B.R., Wasmeier,C., Lamoreux,L., Strom,M., and Seabra,M.C. (2004). Multiple regions contribute to membrane targeting of Rab GTPases. J. Cell Sci. *117*, 6401-6412.

Ali,B.R., and Seabra,M.C. (2005). Targeting of Rab GTPases to cellular membranes. Biochem. Soc. Trans. *33,* 651-656.

Allan,B.B., Moyer,B.D., and Balch,W.E. (2000). Rab1 recruitment of p115 into a cis-SNARE complex: Programming budding COPII vesicles for fusion. Science. *289*, 444-448.

Anant,J.S., Desnoyers,L., Machius,M., Demeler,B., Hansen,J.C., Westover,K.D., Deisenhofer,J., and Seabra,M.C. (1998). Mechanism of Rab geranylgeranylation: formation of the catalytic ternary complex. Biochemistry. *37*, 12559-12568.

Andres,D.A., Seabra,M.C., Brown,M.S., Armstrong,S.A., Smeland,T.E., Cremers,F.P., and Goldstein,J.L. (1993). cDNA cloning of component A of rab geranylgeranyl transferase and demonstration of its role as a rab escort protein. Cell. *73*, 1091-1099.

Antos,J.M., Miller,G.M., Grotenbreg,G.M., and Ploegh,H.L. (2008). Lipid modification of proteins through sortase-catalyzed transpeptidation. J. Am. Chem. Soc. *130*, 16338-16343.

Antos,J.M., Chew,G.L., Guimaraes,C.P., Yoder,N.C., Grotenbreg,G.M., Popp,M.W., and Ploegh,H.L. (2009). Site-specific N- and C-terminal labeling of a single polypeptide using sortases of different specificity. J. Am. Chem. Soc. *131*, 10800-10801.

Araki,S., Kikuchi,A., Hata,Y., Isomura,M., and Takai,Y. (1990). Regulation of reversible binding of Smg P25a, a Ras P21-Like GTP-Binding protein, to synaptic plasma-membranes and vesicles by its specific regulatory protein, GDP dissociation inhibitor. J. Biol. Chem. *265*, 13007-13015.

Araki,S., Kaibuchi,K., Sasaki,T., Hata,Y., and Takai,Y. (1991). Role of the C-terminal region of Smg P25a in its interaction with membranes and the GDP/GTP exchange protein. Mol. Cell. Biol. *11*, 1438-1447.

Ayad,N., Hull,M., and Mellman,I. (1997). Mitotic phosphorylation of rab4 prevents binding to a specific receptor on endosome membranes. EMBO J. *16*, 4497-4507.

Bader,B., Kuhn,K., Owen,D.J., Waldmann,H., Wittinghofer,A., and Kuhlmann,J. (2000). Bioorganic synthesis of lipid-modified proteins for the study of signal transduction. Nature. *403*, 223-226.

Bahadoran,P., Aberdam,E., Mantoux,F., Busca,R., Bille,K., Yalman,N., Saint-Basile,G., Casaroli-Marano,R., Ortonne,J.P., and Ballotti,R. (2001). Rab27a: A key to melanosome transport in human melanocytes. J. Cell Biol. *152*, 843-849.

Barbero,P., Bittova,L., and Pfeffer,S.R. (2002). Visualization of Rab9-mediated vesicle transport from endosomes to the trans-Golgi in living cells. J. Cell Biol. *156*, 511-518.

Barrowman,J., and Novick,P. (2003). Three Yips for Rab recruitment. Nat. Cell Biol. *5*, 955-956.

Bauer,L., and Suresh,K.S. (1963). S-(w-(Aminooexy)alkyl)isothiuronium salts, w,w`-bis(aminooxy)alkanes and related compounds. J. Org. Chem. *28*, 1604-1608.

Becker,C.F., Liu,X., Olschewski,D., Castelli,R., Seidel,R., and Seeberger,P.H. (2008). Semisynthesis of a glycosylphosphatidylinositol-anchored prion protein. Angew. Chem. Int. Ed. *47*, 8215-8219.
Bernards,A. (2003). GAPs galore! A survey of putative Ras superfamily GTPase activating proteins in man and Drosophila. Biochim. Biophys. Acta-Rev. Cancer. *1603*, 47-82.
Berrow,N.S., Alderton,D., Sainsbury,S., Nettleship,J., Assenberg,R., Rahman,N., Stuart,D.I., and Owens,R.J. (2007). A versatile ligation-independent cloning method suitable for highthroughput expression screening applications. Nucleic Acids Res. *35*, e45.
Berry,A.F.H., Heal,W.P., Tarafder,A.K., Tolmachova,T., Baron,R.A., Seabra,M.C., and Tate,E.W. (2010). Rapid multilabel detection of geranylgeranylated proteins by using bioorthogonal ligation chemistry. ChemBioChem. *11*, 771-773.
Bill,A., Blockus,H., Stumpfe,H., Bajorath,J., Schmitz,A., and Famulok,M. (2011). A homogeneous fluorescence resonance energy transfer system for monitoring the activation of a protein switch in real time. J. Am. Chem. Soc. *133*, 8372-8379.
Binda,O., Boyce,M., Rush,J.S., Palaniappan,K.K., Bertozzi,C.R., and Gozani,O. (2011). A chemical method for labeling lysine methyltransferase substrates. ChemBioChem. *12*, 330-334.
Blangy,A., Bouquier,N., Gauthier-Rouviere,C., Schmidt,S., Debant,A., Leonetti,J.P., and Fort,P. (2006). Identification of TRIO-GEFD1 chemical inhibitors using the yeast exchange assay. Biol. Cell. *98*, 511-522.
Blaschke,U.K., Silberstein,J., and Muir,T.W. (2000). Protein engineering by expressed protein ligation. Methods Enzymol. *328*, 478-496.
Bock,J.B., Matern,H.T., Peden,A.A., and Scheller,R.H. (2001). A genomic perspective on membrane compartment organization. Nature. *409*, 839-841.
Bos,J.L., Rehmann,H., and Wittinghofer,A. (2007). GEFs and GAPs: Critical Elements in the Control of Small G Proteins. Cell. *29*, 865-877.
Bourne,H.R., Sanders,D.A., and McCormick,F. (1990). The GTPase superfamily: a conserved switch for diverse cell functions. Nature. *348*, 125-132.
Bourne,H.R., Sanders,D.A., and McCormick,F. (1991). The GTPase superfamily: conserved structure and molecular mechanism. Nature. *349*, 117-127.
Bouquier,N., Vignal,E., Charrasse,S., Weill,M., Schmidt,S., Leonetti,J.P., Blangy,A., and Fort,P. (2009). A cell active chemical GEF inhibitor selectively targets the Trio/RhoG/Rac1 signaling pathway. Chem. Biol. *16*, 657-666.
Brennwald,P., and Novick,P. (1993). Interactions of 3 Domains Distinguishing the Ras-Related GTP-Binding Proteins Ypt1 and Sec4. Nature. *362*, 560-563.
Brown,M.J., Milano,P.D., Lever,D.C., Epstein,W.W., and Poulter,C.D. (1991). Prenylated proteins. A convenient synthesis of farnesyl cysteinyl thioethers. J. Am. Chem. Soc. *113*, 3176-3177.
Brunsveld,L., Kuhlmann,J., Alexandrov,K., Wittinghofer,A., Goody,R.S., and Waldmann,H. (2006). Lipidated Ras and Rab peptides and proteins – synthesis, structure, and function. Angew. Chem. Int. Ed. *45*, 6622-6646.
Brunsveld,L., Watzke,A., Durek,T., Alexandrov,K., Goody,R.S., and Waldmann,H. (2005). Synthesis of functionalized Rab GTPases by a combination of solution- or solid-phase lipopeptide synthesis with expressed protein ligaiton. Chem. Eur. J. *11*, 2756-2772.
Brustad,E.M., Lemke,E.A., Schultz,P.G., and Deniz,A.A. (2008). A general and efficient method for the site-specific dual-labeling of proteins for single molecule fluorescence resonance energy transfer. J. Am. Chem. Soc. *130*, 17664-17665.
Cai,H., Huang,Z.-H., Shi,L., Zhao,Y.-F., Kunz,H., and Li,Y.-M. (2011). Towards a fully synthetic MUC1-based anticancer vaccine: efficient conjugation of glycopeptides with mono-, di-. And tetravalent lipopeptides using click chemistry. Chem. Eur. J. *17*, 6396-6406.
Calero,M., and Collins,R.N. (2002). Saccharomyces cerevisiae Pra1p/Yip3p interacts with yip1p and Rab proteins. Biochem. Biophys. Res. Commun. *290*, 676-681.
Calero,M., Winand,N.J., and Collins,R.N. (2002). Identification of the novel proteins Yip4p and Yip5p as Rab GTPase interacting factors. FEBS Lett. *515*, 89-98.
Calero,M., Chen,C.Z., Zhu,W.Y., Winand,N., Havas,K.A., Gilbert,P.M., Burd,C.G., and Collins,R.N. (2003). Dual prenylation is required for Rab protein localization and function. Mol. Biol. Cell. *14*, 1852-1867.

Camarero,J.A., Kwon,Y., and Coleman,M.A. (2004). Chemoselective attachment of biologically active proteins to surfaces by expressed protein ligation and its application for "protein chip" fabrication. J. Am. Chem. Soc. *126*, 14730-14731.
Canne,L.E., Ferredamare,A.R., Burley,S.K., and Kent,S.B.H. (1995). Total chemical synthesis of a unique transcription factor-related protein: cMyc-Max. J. Am. Chem. Soc. *117*, 2998-3007.
Canne,L.E., Bark,S.J., and Kent,S.B.H. (1996). Extending the applicability of native chemical ligation. J. Am. Chem. Soc. *118*, 5891-5896.
Caplin,B.E., Hettich,L.A., and Marshall,M.S. (1994). Substrate characterization of the saccharomyces-cerevisiae protein farnesyltransferase and Type-I protein geranylgeranyltransferase. Biochim. Biophys. Acta-Protein Struct. Molec. Enzym. *1205*, 39-48.
Carroll,K.S., Hanna,J., Simon,I., Krise,J., Barbero,P., and Pfeffer,S.R. (2001). Role of Rab9 GTPase in facilitating receptor recruitment by TIP47. Science. *292*, 1373-1376.
Cao,X.C., Ballew,N., and Barlowe,C. (1998). Initial docking of ER-derived vesicles requires Uso1p and Ypt1p but is independent of SNARE proteins. EMBO J. *17*, 2156-2165.
Casey,P.J., and Seabra,M.C. (1996). Protein prenyltransferases. J. Biol. Chem. *271*, 5289-5292.
Chan,A.O.Y., Ho,C.M., Chong,H.C., Leung,Y.C., Huang,J.S., Wong,M.K., and Che,C.M. (2012) Modification of N-Terminal α-Amino Groups of Peptides and Proteins Using Ketenes. J. Am. Chem.Soc. *134*, 2589-2598.
Chan,T.R., Hilgraf,R., Sharpless,K.B., and Fokin,V.V. (2004). Polytriazoles as Copper(I)-Stabilizing Ligands in Catalysis. Org. Lett. *6*, 2853-2855.
Chavrier,P., Gorvel,J.P., Stelzer,E., Simons,K., Gruenberg,J., and Zerial,M. (1991). Hypervariable C-Terminal Domain of Rab Proteins Acts as a Targeting Signal. Nature. *353*, 769-772.
Chen,I., Howarth,M., Lin,W.Y., and Ting,A.Y. (2005). Site-specific labeling of cell surface proteins with biophysical probes using biotinligase. Nat. Methods. *2*, 99-104.
Christman,K.L., Broyer,R.M., Tolstyka,Z.P., and Maynard,H.D. (2007). Site-specific protein immobilization through N-terminal oxime linkages. J. Mater. Chem. *17*, 2021-2027.
Christoforidis,S., McBride,H.M., Burgoyne,R.D., and Zerial,M. (1999). The Rab5 effector EEA1 is a core component of endosome docking. Nature. *397*, 621-625.
Chytil,M., Peterson,B.R., Erlanson,D.A., and Verdine,G.L. (1998). The orientation of the AP-1 heterodimer on DNA strongly affects transcriptional potency. Proc. Natl. Acad. Sci. U.S.A. *95*, 14076-14081.
Cornish,V.W., Mendel,D., and Schultz,P.G. (1996). Site-specific protein modification using a ketone handle. J. Am. Chem. Soc. *118*, 8150-8151.
Constantinescu,A.T., Rak,A., Alexandrov,K., Esters,H., Goody,R.S., and Scheldig,A.J. (2002). Rab-subfamily-specific regions of Ypt7p are structurally different from other RabGTPases. Structure. *10*, 569-579.
Cordes,E.H., and Jencks,W.P. (1962). Nucleophilic Catalysis of Semicarbazone Formation by Anilines. J. Am. Chem. Soc. *84*, 826-831.
Cotton,G.J., Ayers,B., Xu,R., and Muir,T.W. (1999). Insertion of a synthetic peptide into a recombinant protein framework: A protein biosensor. J. Am. Chem. Soc. *121*, 1100-1101.
Cotton,G.J., and Muir,T.W. (2000). Generation of a dual-labeled fluorescence biosensor for Crk-II phosphorylation using solid-phase expressed protein ligation. Chem. Biol. *7*, 253-261.
Cremers,F.P.M., Armstrong,S.A., Seabra,M.C., Brown,M.S., and Goldstein,J.L. (1994). Rep-2, a Rab Escort Protein Encoded by the Choroideremia-Like Gene. J. Biol. Chem. *269*, 2111-2117.
Dawson,P.E., Muir,T.W., Clark-Lewis,I., and Kent,S.B.H. (1994). Synthesis of proteins by native chemical ligation. Science. *266*, 776-779.
Dawson,P.E., and Kent,S.B.H. (2000). Synthesis of native proteins by chemical ligation. Annu. Rev. Biochem. *69*, 923-960.
De Araujo,A.D., Palomo,J.M., Cramer,J., Kohn,M., Schroder,H., Wacker,R., Niemeyer,C., Alexandrov,K., and Waldmann,H. (2006). Diels-Alder-ligation and immobilization of proteins. Angew. Chem. Int. Ed. *45*, 296-301.
Delprato,A., and Lambright,D.G. (2007). Structural basis for Rab GTPase activation by VPS9 domain exchange factors. Nat. Struct. Mol. Biol. *14*, 406-412.
Delprato,A., Merithew,E., and Lambright,D.G. (2004). Structure, exchange determinants, and familywide rab specificity of the tandem helical bundle and Vps9 domains of Rabex-5. Cell. *118*, 607-617.

Deneka,M., Neeft,M., and Sluijs,P. (2003). Regulation of membrane transport by rab GTPases. Crit. Rev. Biochem. Mol. Biol. *38*, 121-142.
De Renzis,S., Sonnichsen,B., and Zerial,M. (2002). Divalent Rab effectors regulate the sub-compartmental organization and sorting of early endosomes. Nat. Cell Biol. *4*, 124-133.
Dettin,M., Muncan,N., Bugatti,A., Grezzo,F., Danesin,R., and Rusnati,M. (2011). Chemoselective surface immobilization of proteins through a cleavable peptide. Bioconjugate Chem. *22*, 1753-1757.
Devaraj,N.K., Miller,G.P., Ebina,W., Kakaradov,B., Collman,J.P., Kool,E.T., and Chidsey,C.E.D. (2005). Chemoselective covalent coupling of oligonucleotide probes to self-assembled monolayers. J. Am. Chem. Soc. *127*, 8600-8601.
Dirac-Svejstrup,A.B., Soldati,T., Shapiro,A.D., and Pfeffer,S.R. (1994). Rab-GDI presents functional Rab9 to the intracellular transport machinery and contributes selectivity to Rab9 membrane recruitment. J. Biol. Chem. *269*, 15427-15430.
DiracSvejstrup,A.B., Sumizawa,T., and Pfeffer,S.R. (1997). Identification of a GDI displacement factor that releases endosomal Rab GTPases from Rab-GDI. EMBO J. *16*, 465-472.
Dirksen,A., Dirksen,S., Hackeng,T.M., and Dawson,P.E. (2006). Nucleophilic catalysis of hydrazone formation and transimination: implications for dynamic covalent chemistry. J. Am. Chem. Soc. *128*, 15602-15603.
Dirksen,A., Hackeng,T.M., and Dawson,P.E. (2006). Nucleophilic catalysis of oxime ligation. Angew. Chem. Int. Ed. *45*, 7581-7584.
Dong,G., Medkova,M., Novick,P., and Reinisch,K.M. (2007). A catalytic coiled coil: structural insights into the activation of the Rab GTPase Sec4p by Sec2p. Mol. Cell. *25*, 455-462.
Dumas,J.J., Zhu,Z.Y., Connolly,J.L., and Lambright,D.G. (1999). Structural basis of activation and GTP hydrolysis in Rab proteins. Struct. Fold. Des. *7*, 413-423.
Dunn,B., Stearns,T., and Botstein,D. (1993). Specificity domains distinguish the Ras-Related GTPases Ypt1 and Sec4. Nature. *362*, 563-565.
Durek,T., Alexandrov,K., Goody,R.S., Hildebrand,A., Heinemann,I., and Waldmann,H. (2004). Synthesis of fluorescently labeled mono- and diprenylated Rab7 GTPase. J. Am. Chem. Soc. *126*, 16368-16378.
Dursina,B., Reents,R., Delon,C., Wu,Y., Kulharia,M., Thutewohl,M., Veligodsky,A., Kalinin,A., Evstifeev,V., Ciobanu,D., Szedlacsek,S.E., Waldmann,H., Goody,R.S., and Alexandrov,K. (2006). Identification and specificity profiling of protein prenyltransferase inhibitors using new fluorescent phosphoisoprenoids. J. Am. Chem. Soc. *128*, 2822-2835.
Echard,A., Jollivet,F., Martinez,O., Lacapere,J.J., Rousselet,A., Janoueix-Lerosey,I., and Goud,B. (1998). Interaction of a Golgi-associated kinesin-like protein with Rab6. Science. *279*, 580-585.
Erlanson,D.A., Chytil,M., and Verdine,G.L. (1996). The leucine zipper domain controls the orientation of AP-1 in the NFAT center dot AP-1 center dot DNA complex. Chem. Biol. *3*, 981-991.
Esters,H., Alexandrov,K., Constantinescu,A.T., Goody,R.S., and Scheidig,A.J. (2000). High-resolution crystal structure of S. cerevisiae Ypt51(Delta C15)-GppNHp, a small GTP-binding protein involved in regulation of endocytosis. J. Mol. Biol. *298*, 111-121.
Farnsworth,C.C., Seabra,M.C., Ericsson,L.H., Gelb,M.H., and Glomset,J.A. (1994). Rab geranylgeranyl transferase catalyzes the geranylgeranylation of adjacent cysteines in the small GTPases RablA, Rab3A, and Rab5A. Proc. Natl. Acad. Sci. U.S.A. *91*, 11963-11967.
Figueroa,C., Taylor,J., and Vojtek,A.B. (2001). Prenylated Rab acceptor protein is a receptor for prenylated small GTPases. J. Biol. Chem. *276*, 28219-28225.
Flavell,R.R., Kothari,P., Bar-Dagan,M., Synan,M., Vallabhajosula,S., Friedman,J.M., Muir,T.W., and Ceccarini,G. (2008). Site-specific ^{18}F-labeling of the protein hormone leptin using a general two-step ligation procedure. J. Am. Chem. Soc. *130*, 9106-9112.
Förster,T. (1946). Energiewanderung und fluoreszenz. Naturwissenschaften. *6*, 166-175.
Fujimura,K., Tanaka,K., Nakano,A., and Tohe,A. (1994). The saccharomyces-cerevisiae Msi4 gene encodes the yeast counterpart of component-a of Rab geranylgeranyltransferase. J. Biol. Chem. *269*, 9205-9212.
Fukuda,M., Kuroda,T.S., and Mikoshiba,K. (2002). Slac2-a/melanophilin, the missing link between Rab27 and myosin Va - Implications of a tripartite protein complex for melanosome transport. J. Biol. Chem. *277*, 12432-12436.

Fukui,K., Sasaki,T., Imazumi,K., Matsuura,Y., Nakanishi,H., and Takai,Y. (1997). Isolation and characterization of a GTPase activating protein specific for the Rab3 subfamily of small G proteins. J. Biol. Chem. *272*, 4655-4658.
Galperin,E., and Sorkin,A. (2003). Visualization of Rab5 activity in living cells by FRET microscopy and influence of plasma-membrane-targeted Rab5 on clathrin-dependent endocytosis. J. Cell Sci. *116*, 4799-4810.
Gao,Y., Dickerson,J.B., Guo,F., Zheng,J., and Zheng,Y. (2004). Rational design and characterization of a Rac GTPase-specific small molecule inhibitor. Proc. Natl. Acad. Sci. U.S.A. *101*, 7618-7623.
Garcia-Mata,R., and Burridge,K. (2007). Catching a GEF by its tail. Trends Cell Biol. *17*, 36-43.
Garrett,M.D., Zahner,J.E., Cheney,C.M., and Novick,P.J. (1994). GDI1 encodes a GDP dissociation inhibitor that plays an essential role in the yeast secretory pathway. EMBO J. *13,* 1718-1728.
Gauchet,C., Labadie,G.R., and Poulter,C.D. (2006). Regio- and chemoselective covalent immobilization of proteins through unnatural amino acids. J. Am. Chem. Soc. *128*, 9274-9275.
Geoghegan,K.F., and Stroh,J.G. (1992). Site-directed conjugation of nonpeptide groups to peptides and proteins via periodate oxidation of a 2-amino alcohol. Application to modification at N-terminal serine. Bioconjugate Chem. *3*, 138-146.
Giepmans,B.N., Adams,S.R., Ellisman,M.H., and Tsien,R.Y. (2006). The fluorescent toolbox for assessing protein location and function. Science. *312*, 217-224.
Gilmore,J.M., Scheck,R.A., Esser-Kahn,A.P., Joshi,N.S., and Francis,M.B. (2006). N-terminal protein modification through a biomimetic transamination reaction. Angew. Chem. Int. Ed. *45*, 5307-5311.
Girish,A., Sun,H.Y., Yeo,D.S.Y., Chen,G.Y.J., Chua,T.K., and Yao,S.Q. (2005). Site-specific immobilization of proteins in a microarray using intein-mediated protein splicing. Bioorg. Med. Chem. Lett. *15*, 2447-2451.
Gomes,A.Q., Ali,B.R., Ramalho,J.S., Godfrey,R.F., Barral,D.C., Hume,A.N., and Seabra,M.C. (2003). Membrane targeting of Rab GTPases is influenced by the prenylation motif. Mol. Biol. Cell. *14*, 1882-1899.
Gonzalez-Garcia,A., Pritchard,C.A., Paterson,H.F., Mavria,G., Stamp,G., and Marshall,C.J. (2005). RalGDS is required for tumor formation in a model of skin carcinogenesis. Cancer Cell. *7*, 219-226.
Goody,R.S., and Hofmann-Goody,W. (2002). Exchange factors, effectors, GAPs and motor proteins: common thermodynamic and kinetic principles for different functions. Eur. Biophys. J. *31*, 268-274.
Gottlieb,D., Grunwald,C., Nowak,C., Kuhlmann,J., and Waldmann,H. (2006). Intein-Mediated in vitro Synthesis of Lipidated Ras Proteins. Chem. Commun. 260-262.
Govindaraju,T., Jonkheijm,P., Gogolin,L., Schroeder,H., Becker,C.F.W., Niemeyer,C.M., and Waldmann,H. (2008). Surface immobilization of biomolecules by click sulfonamide reaction. Chem. Commun. 3723-3725.
Grogan,M.J., Kaizuka,Y., Conrad,R.M., Groves,J.T., and Bertozzi,C.R. (2005). Synthesis of lipidated green fluorescent protein and its incorporation in supported lipid bilayers. J. Am. Chem. Soc. *127*, 14383-14387.
Gromadski,K.B., Wieden,H.J., and Rodnina,M.V. (2002). Kinetic mechanism of elongation factor Ts-catalyzed nucleotide exchange in elongation factor tu. Biochemistry. *41*, 162-169.
Guo,W., Roth,D., Walch-Solimena,C., and Novick,P. (1999). The exocyst is an effector for Sec4p, targeting secretory vesicles to sites of exocytosis. EMBO J. *18*, 1071-1080.
Guo,Z.., Ahmadian,M.R., and Goody,R.S. (2005). Guanine nucleotide exchange factors operate by a simple allosteric competitive mechanism. Biochemistry. *44*, 15423-15429.
Guo,Z., Wu,Y.W., Tan,K.T., Bon,R.S., Guiu-Rozas,E., Delon,C., Nguyen,T.U., Wetzel,S., Arndt,S., Goody,R.S., Alexandrov,K., and Waldmann,H. (2008). Development of selective RabGGTase inhibitors and crystal structure of a RabGGTase-inhibitor complex. Angew. Chem. Int. Ed. *47*, 3747-3750.
Hackenberger,C.P.R., and Schwarzer,D. (2008). Chemoselective ligation and modification strategies for peptides and proteins. Angew. Chem. Int. Ed. *47*, 10030-10074, and references cited therein.
Hafner,M., Schmitz,A., Grune,I., Srivatsan,S.G., Paul,B., Kolanus,W., Quast,T., Kremmer,E., Bauer,I., and Famulok,M. (2006). Inhibition of cytohesins by SecinH3 leads to hepatic insulin resistance. Nature. *444*, 941-944.
Hammer,J.A., and Wu,X.F.S. (2002). Rabs grab motors: defining the connections between Rab GTPases and motor proteins. Curr. Opin. Cell Biol. *14*, 69-75.

Heidtman,M., Chen,C.Z., Collins,R.N. and Barlowe,C. (2003). A Role for Yip1p in COPII Vesicle Biogenesis. J. Cell Biol. *163*, 57-69.
Heo,W.D., Inoue,T., Park,W.S., Kim,M.L., Park,B.O., Wandless,T.J., and Meyer,T. (2006). PI(3,4,5)P3 and PI(4,5)P2 Lipids Target Proteins with Polybasic Clusters to the Plasma Membran. Science. *314*, 1458-1461.
Hill,E., Clarke,N., and Barr,F.A. (2000). The Rab6-binding kinesin, Rab6-KIFL, is required for cytokinesis. EMBO J. *19*, 5711-5719.
Hong,S.H., and Maret,W. (2003). A fluorescence resonance energy transfer sensor for the beta-domain of metallothionein. Proc. Natl. Acad. Sci. U.S.A. *100*, 2255-2260.
Horiuchi,H., Lippe,R., McBride,H.M., Rubino,M., Woodman,P., Stenmark,H., Rybin,V., Wilm,M., Ashman,K., Mann,M., and Zerial,M. (1997). A novel Rab5 GDP/GTP exchange factor complexed to Rabaptin-5 links nucleotide exchange to effector recruitment and function. Cell. *90*, 1149-1159.
Huang,Y., Wan,W., Russell,W.K., Pai,P.J., Wang,Z.Y., Russell,D.H., and Liu,W. (2010). Genetic incorporation of an aliphatic keto-containing amino acid into proteins for their site-specific modificaiton. Bioorg. Med. Chem. Lett. *20*, 878-880.
Huisgen,R. (1963). 1,3-Dipolar Cycloadditions. Past and Future. Angew. Chem. Int. Ed. *2*, 565-598.
Hume,A.N., Collinson,L.M., Rapak,A., Gomes,A.Q., Hopkins,C.R., and Seabra,M.C. (2001). Rab27a regulates the peripheral distribution of melanosomes in melanocytes. J. Cell Biol. *152*, 795-808.
Hutchinson,J.P., and Eccleston,J.F. (2000). Mechanism of nucleotide release from Rho by the GDP dissociation stimulator protein. Biochemistry. *39*, 11348-11359.
Ingmundson,A., Delprato,A., Lambright,D.G., and Roy,C.R. (2007). Legionella pneumophila proteins that regulate Rab1 membrane cycling. Nature. *450*, 365-369.
Itzen,A., Pylypenko,O., Goody,R.S., Alexandrov,K., and Rak,A. (2006). Nucleotide exchange via local protein unfolding--structure of Rab8 in complex with MSS4. EMBO J. *25*, 1445-1455.
Itzen,A., Rak,A., and Goody,R.S. (2007). Sec2 is a highly efficient exchange factor for the Rab protein Sec4. J. Mol. Biol. *365*, 1359-1367.
Iwai,H., and Pluckthun,A. (1999). Circular beta-lactamase: stability enhancement by cyclizing the backbone. FEBS Lett. *459*, 166-172.
John,J., Sohmen,R., Feuerstein,J., Linke,R., Wittinghofer,A., and Goody,R.S. (1990). Kinetics of interaction of nucleotides with nucleotide-free H-ras p21. Biochemistry. *29*, 6058-606.
Johnson,E.C.B., and Kent,S.B.H. (2006). Insights into the mechanism and catalysis of the native chemical ligation reaction. J. Am. Chem. Soc.*128*, 6640-6646.
Jones,S., Newman,C., Liu,F.L., and Segev,N. (2000). The TRAPP complex is a nucleotide exchanger for Ypt1 and Ypt31/32. Mol. Biol. Cell. *11*, 4403-4411.
Jonkheijm,P., Weinrich,D., Schroder,H., Niemeyer,C.M., and Waldmann,H. (2008). Chemical strategies for generating protein biochips. Angew. Chem. Int. Ed. *47*, 9618-9647.
Joo,C., Balci,H., Ishitsuka,Y., Buranachai,C., and Ha,T. (2008). Advances in single-molecule fluorescence methods for molecular biology. Annu. Rev. Biochem. *77*, 51-76.
Kadereit,D., Kuhlmann,J., and Waldmann,H. (2000). Linking the fields-the interplay of organic synthesis, biophysical chemistry, and cell biology in the chemical biology of protein lipidation. ChemBioChem. *1*, 144-169.
Kalia,J., and Raines,R.T. (2010). Advances in bioconjugation. Curr. Org. Chem. *14*, 138-147.
Katadae,M., Hagiwara,K., Wada,A., Ito,M., Umeda,M., Casey,P.J., and Fukada,Y. (2008). Interacting targets of the farnesyl of transducin gamma-subunit. Biochemistry. *47*, 8424-8433.
Keppler,A., Gendreizig,S., Gronemeyer,T., Pick,H., Vogel,H., and Johnsson,K. (2002). A general method for the covalent labeling of fusion proteins with small molecules in vivo. Nat. Biotechnol. *21*, 86-89.
Khosravifar,R., Clark,G.J., Abe,K., Cox,A.D., McLain,T., Lutz,R.J., Sinensky,M., and Der,C.J. (1992). Ras (CXXX) and Rab (CC/CXC) prenylation signal sequences are unique and functionally distinct. J. Biol. Chem. *267*, 24363-24368.
Khosravifar,R., Lutz,R.J., Cox,A.D., Conroy,L., Bourne,J.R., Sinensky,M., Balch,W.E., Buss,J.E., and Der,C.J. (1991). Isoprenoid modification of Rab proteins terminating in CC or CXC motifs. Proc. Natl. Acad. Sci. U.S.A. *88,* 6264-6268.
Kinsella,B.T., and Maltese,W.A. (1991). Rab Gtp-Binding proteins implicated in vesicular transport are isoprenylated in vitro at cysteines within a novel carboxyl-terminal motif. J. Biol. Chem. *266*, 8540-8544.

Kinsella,B.T., and Maltese,W.A. (1992). Rab Gtp-Binding proteins with 3 different carboxyl-terminal cysteine motifs are modified in vivo by 20-Carbon isoprenoids. J. Biol. Chem. *267*, 3940-3945.
Kishida,S., Shirataki,H., Sasaki,T., Kato,M., Kaibuchi,K., and Takai,Y. (1993). Rab3a GTPase-Activating Protein-Inhibiting Activity of Rabphilin-3a, a Putative Rab3a Target Protein. J. Biol. Chem. *268*, 22259-22261.
Klebe,C., Prinz,H., Wittinghofer,A., and Goody,R.S. (1995). The kinetic mechanism of rannucleotide exchange catalyzed by RCC1. Biochemistry. *34*, 12543-12552.
Kleinecke,J., Düls,C., and Söling,H.D. (1979). Subcellular compartmentation of guanine nucleotides and functional relationships between the adenine and guanine nucleotide systems in isolated hepatocytes. FEBS Lett. *107*, 198-202.
Knaus,U.G., Bamberg,A., and Bokoch,G.M. (2007). Rac and Rap GTPase activation assays. Methods Mol. Biol. *412*, 59-67.
Knickerbocker,T., and MacBeath,G. (2011). Detecting and quantifying multiple proteins in clinical samples in high-throughput using antibody microarrays. Methods Mol. Biol. *723*, 3-13.
Kolb,H.C., Finn,M.G., and Sharpless,K.B. (2001). Click Chemistry: Diverse Chemical Function from a Few Good Reactions. Angew. Chem. Int. Ed. *40*, 2004-2021.
Kraynov,V.S., Chamberlain,C., Bokoch,G.M., Schwartz,M.A., Slabaugh,S., and Hahn,K.M. (2000). Localized Rac Activation Dynamics Visualized in Living Cells. Science. *290*, 333-337.
Kurpiers,T., and Mootz,H.D. (2009). Bioorthogonal ligation in the spotlight. Angew. Chem. Int. Ed. *48*, 1729-1731.
Lee,A.J., Ensign,A.A., Krauss,T.D., and Bren,K.L. (2010). Zinc porphyrin as a donor for FRET in Zn(II)cytochrome *c*. J. Am. Chem. Soc. *132*, 1752-1753.
Lee,B.W.K.L., Sun,H.G., Zang,T., Kim,J.B., Alfaro,J.F., and Zhou,Z.S. (2010). Enzyme-catalyzed transfer of a ketone group from an *S*-adenosylmethionine analogue: a tool for the functional analysis of methyltransferases. J. Am. Chem. Soc. *132*, 3642-3643.
Lee,H.J., Wark,A.W., and Corn,R.M. (2008). Microarray methods for protein biomarker detection. Analyst. *133*, 975-983.
Lempens,E.H.M., Helms,B.A., Merkx,M., and Meijer,E.W. (2009). Efficient and chemoselective surface immobilization of proteins by using aniline-catalyzed oxime chemistry. ChemBioChem. *10*, 658-662.
Lenzen,C., Cool,R.H., Prinz,H., Kuhlmann,J., and Wittinghofer,A. (1998). Kinetic analysis by fluorescence of the interaction between Ras and the catalytic domain of the guanine nucleotide exchange factor Cdc25Mm. Biochemistry. *37*, 7420-7430.
Lim,B.K.V., and Lin,Q. (2010). Bioorthogonal chemistry: recent progress and future directions. Chem. Commun. 1589-1600.
Lin,P.C., Ueng,S.H., Tseng,M.C., Ko,J.L., Huang,K.T., Yu,S.C., Adak,A.K., Chen,Y.J., and Lin,C.C. (2006). Site-specific protein modification through CuI-catalyzed 1,2,3-triazole formation and its implementation in protein microarray fabrication. Angew. Chem. Int. Ed. *45*, 4286-4290.
Lin,P.C., Weinrich,D., and Waldmann,H. (2010). Protein biochips: oriented surface immobilization of proteins. Macr. Chem. Phys. *211*, 136-144.
Li,X.F., Zhang,L.S., Hall,S.E., and Tam,J.P. (2000). A new ligation method for N-terminal tryptophan-containing peptides using the Pictet-Spengler reaction. Tetrahedron Lett. *41*, 4069-4073.
Luan,P., Balch,M.E., Emr,S.D., and Burd,C.G. (1999). Molecular dissection of guanine nucleotide dissociation inhibitor function in vivo - Rab-independent binding to membranes and role of Rab recycling factors. J. Biol. Chem. *274*, 14806-14817.
Lue,R.Y., Chen,G.Y., Hu,Y., Zhu,Q., and Yao,S.Q. (2004). Versatile protein biotinylation strategies for potential high-throughput proteomics. J. Am. Chem. Soc. *126*, 1055-1062.
Lynch,M., Mosher,C., Huff,J., Nettikadan,S., Johnson,J., and Henderson,E. (2004). Functional protein nanoarrays for biomarker profiling. Proteomics. *4*, 1695-1702.
MacBeath,G., and Schreiber,S.L. (2000). Printing proteins as microarrays for high-throughput function determination. Science. *289*, 1760-1763.
Machner,M.P., and Isberg,R.R. (2006). Targeting of host Rab GTPase function by the intravacuolar pathogen Legionella pneumophila. Dev. Cell. *11*, 47-56.
Machner,M.P., and Isberg,R.R. (2007). A bifunctional bacterial protein links GDI displacement to Rab1 activation. Science. *318*, 974-977.

Mahal,L.K., Yarema,K.J., and Bertozzi,C.R. (1997). Engineering Chemical Reactivity on Cell Surfaces Through Oligosaccharide Biosynthesis. Science. *276*, 1125-1128.
Malliri,A., Kammen,R.A., Clark,K., Valk,M., Michiels,F., and Collard,J.G. (2002). Mice deficient in the Rac activator Tiam1 are resistant to Ras-induced skin tumours. Nature. *417*, 867-871.
Martincic,I., Peralta,M.E., and Ngsee,J.K. (1997). Isolation and characterization of a dual prenylated Rab and VAMP2 receptor. J. Biol. Chem. *272*, 26991-26998.
Matern,H., Yang,X.P., Andrulis,E., Sternglanz,R., Trepte,H.H., and Gallwitz,D. (2000). A novel Golgi membrane protein is part of a GTPase-binding protein complex involved in vesicle targeting. EMBO J. *19*, 4485-4492.
McBride,H.M., Rybin,V., Murphy,C., Giner,A., Teasdale,R., and Zerial,M. (1999). Oligomeric complexes link Rab5 effectors with NSF and drive membrane fusion via interactions between EEA1 and syntaxin 13. Cell. *98*, 377-386.
Mcgeady,P., Kuroda,S., Shimizu,K., Takai,Y., and Gelb,M.H. (1995). The farnesyl group of H-Ras facilitates the activation of a soluble upstream activator of mitogen-activated protein kinase. J. Biol. Chem. *270*, 26347-26351.
McLauchlan,H., Newell,J., Morrice,N., Osborne,A., West,M., and Smythe,E. (1998). A novel role for Rab5-GDI in ligand sequestration into calthrin-coated pits. Curr. Biol. *8*, 34-45.
Merithew,E., Hatherly,S., Dumas,J.J., Lawe,D.C., Heller-Harrison,R., and Lambright,D.G. (2001). Structural plasticity of an invariant hydrophobic triad in the switch regions of Rab GTPases is a determinant of effector recognition. J. Biol. Chem. *276*, 13982-13988.
Menasche,G., Pastural,E., Feldmann,J., Certain,S., Ersoy,F., Dupuis,S., Wulffraat,N., Bianchi,D., Fischer,A., Le Deist,F., and de Saint Basile,G. (2000). Mutations in RAB27A cause Griscelli syndrome associated with haemophagocytic syndrome. Nature Genet. *25*, 173-176.
Merithew,E., Hatherly,S., Dumas,J.J., Lawe,D.C., Heller-Harrison,R., and Lambright,D.G. (2001). Structural plasticity of an invariant hydrophobic triad in the switch regions of Rab GTPases is a determinant of effector recognition. J. Biol. Chem. *276*, 13982-13988.
Michael,A. (1893). Ueber die Einwirkung von Diazobenzolimid auf Acetylendicarbonsauremethylester. J. Prakt. Chem. *48*, 94-95.
Milburn,M.V., Tong,L., Devos,A.M., Brunger,A., Yamaizumi,Z., Nishimura,S., and Kim,S.H. (1990). Molecular switch for signal transduction - structural differences between active and inactive forms of protooncogenic Ras proteins. Science. *247*, 939-945.
Mochizuki,N., Yamashita,S., Kurokawa,K., Ohba,Y., Nagai,T., Miyawaki,A., and Matsuda,M. (2001). Spatio-temporal images of growth-factor-induced activation of Ras and Rap1. Nature. *411*, 1065-1068.
Moores,S.L., Schaber,M.D., Mosser,S.D., Rands,E., Ohara,M.B., Garsky,V.M., Marshall,M.S., Pompliano,D.L., and Gibbs,J.B. (1991). Sequence Dependence of Protein Isoprenylation. J. Biol. Chem. *266*, 14603-14610.
Morishige,M., Hashimoto,S., Ogawa,E., Toda,Y., Kotani,H., Hirose,M., Wei,S., Hashimoto,A., Yamada,A., Yano,H., Mazaki,Y., Kodama,H., Nio,Y., Manabe,T., Wada,H., Kobayashi,H., and Sabe,H. (2008). GEP100 links epidermal growth factor receptor signalling to Arf6 activation to induce breast cancer invasion. Nat. Cell Biol. *10*, 85-92.
Muir,T.W., Sondhi,D., and Cole,P.A. (1998). Expressed protein ligation: A general method for protein engineering. Proc. Natl. Acad. Sci. U.S.A. *95*, 6705-6710.
Müller,M.P., Peters,H., Blümer,J., Blankenfeldt,W., Goody,R.S., and Itzen,A. (2010). The Legionella effector protein DrrA AMPylates the membrane traffic regulator Rab1b. Science. *329*, 946-949.
Muir,T.W. (2003). Semisynthesis of proteins by expressed protein ligation. Annu. Rev. Biochem. *72*, 249-289.
Mukherjee,S., Liu,X.Y., Arasaki,K., McDonough,J., Galán,J.E., and Roy,C.R. (2011). Modulation of Rab GTPase function by a protein phosphocholine transferase. Nature. *477*, 103-106.
Munro,S. (2002). Organelle identity and the targeting of peripheral membrane proteins. Curr. Opin. Cell Biol. *14*, 506-514.
Muralidharan,V., and Muir,T.W. (2006). Protein ligation: an enabling technology for the biophysical analysis of proteins. Nat. Methods. *3*, 429-438.
Murray,J.W., and Wolkoff,A.W. (2003). Roles of the cytoskeleton and motor proteins in endocytic sorting. Adv. Drug Deliv. Rev. *55*, 1385-1403.
Neukamm,M.A., Pinto,A., and Metzler-Nolte,N. (2008). Synthesis and cytotoxicity of a cobaltcarbonyl-alkyne enkephalin bioconjugate. Chem. Commun. 232-234.

Newman,C.M.H., Giannakouros,T., Hancock,J.F., Fawell,E.H., Armstrong,J., and Magee,A.I. (1992). Posttranslational processing of schizosaccharomyces-pombe Ypt proteins. J. Biol. Chem. *267*, 11329-11336.
Niebel,B., Weiche,B., Mueller,A.L., Li,D.Y., Karnowski,N., Famulok,M., Nakamura,T., Aoki,K., and Matsuda,M. (2005). Monitoring spatio-temporal regulation of ras and rho gtpases with gfp-based fret probes. Methods. *37*, 146-153.
Nicolini,C., Baranski,J., Schlummer,S., Palomo,J., Lumbierres-Burgues,M., Kahms,M., Kuhlmann,J., Sanchez,S., Gratton,E., and Waldmann,H. (2006). Visualizing association of N-ras in lipid microdomains: influence of domain structure and interfacial adsorption. J. Am. Chem. Soc. *128*, 192-201.
Nolte,C., Mayer,P., and Straub,B.F. (2007). Isolation of a copper(I) triazolide: a "click" intermediate. Angew. Chem. Int. Ed. *46*, 2101-2103.
Nguyen,U.T., Cramer,J., Gomis,J., Reents,R., Gutierrez-Rodriguez,M., Goody,R.S., Alexandrov,K., and Waldmann,H. (2007). Exploiting the substrate tolerance of farnesyltransferase for site-selective protein derivatization. ChemBioChem. *8*, 408-423.
Nguyen,U.T., Guo,Z., Delon,C., Wu,Y., Deraeve,C., Franzel,B., Bon,R.S., Blankenfeldt,W., Goody,R.S., Waldmann,H., and Alexandrov,K. (2009). Analysis of the eukaryotic prenylome by isoprenoid affinity tagging. Nat. Chem. Biol. *5*, 227-235.
Nguyen,U.T.T., Goody,R.S., and Alexandrov,K. (2010). Understanding and Exploiting Protein Prenyltransferases. ChemBioChem. *11*, 1194-1201.
Oesterlin,L.K., Goody,R.S., and Itzen,A. (2012). Posttranslational modifications of Rab proteins cause effective displacement of GDP dissociation inhibitor. Proc. Nat. Acad. Sci. U.S.A. *109*, 5621-5626.
Ohbayashi,N., and Fukuda,M. (2012). Role of Rab family GTPases and their effectors in melanosomal logistics. J. Biochem. *151*, 343-351.
Ortiz,D., Medkova,M., Walch-Solimena,C., and Novick,P. (2002). Ypt32 recruits the Sec4p guanine nucleotide exchange factor, Sec2p, to secretory vesicles; evidence for a Rab cascade in yeast. J. Cell Biol. *157*, 1005-1015.
Ostermeier,C., and Brunger,A.T. (1999). Structural basis of Rab effector specificity: Crystal structure of the small G protein Rab3A complexed with the effector domain of Rabphilin-3A. Cell. *96*, 363-374.
Owen,D.J., Alexandrov,K., Rostkova,E., Scheidig,A.J., Goody,R.S., and Waldmann,H. (1999). Chemo-enzymatic synthesis of fluorescent Rab 7 proteins: Tools to study vesicular trafficking in cells. Angew. Chem. Int. Ed. *38*, 509-512.
Pasqualato,S., Senic-Matuglia,F., Renault,L., Goud,B., Salamero,J., and Cherfils,J. (2004). The structural GDP/GTP cycle of Rab11 reveals a novel interface involved in the dynamics of recycling endosomes. J. Biol. Chem. *279*, 11480-11488.
Pastural,E., Barrat,F.J., Dufourcq-Lagelouse,R., Certain,S., Sanal,O., Jabado,N., Seger,R., Griscelli,C., Fischer,A., and DesaintBasile,G. (1997). Griscelli disease maps to chromosome 15q21 and is associated with mutations in the myosin-Va gene. Nature Genet. *16*, 289-292.
Paulick,M.G., Forstner,M.B., Groves,J.T., and Bertozzi,C.R. (2007). A chemical approach to unraveling the biological function of the glycosylphosphatidylinositol anchor. Proc. Natl. Acad. Sci. U.S.A. *104*, 20332-20337.
Pauloehrl,T., Delaittre,G., Winkler,V., Welle,A., Bruns,M., Börner,H.G., Greiner,A.M., Bastmeyer,M., and Barner-Kowollik,C. (2012). Adding spatial control to click chemistry: phototriggered Diels–Alder surface (Bio)functionalization at ambient temperature. Angew. Chem. Int Ed. *51*, 1071-1074.
Pedersen,H., Hölder,S., Sutherlin,D.P., Schwitter,U., King,D.S., and Schultz,P.G. (1998). A method for directed evolution and functional cloning of enzymes. Proc. Natl. Acad. Sci. U.S.A. *95*, 10523-10528.
Pedersen,E., and Brakebusch,C. (2012). Rho GTPase function in development: How in vivo models change our view. Exp. Cell Res. *318*, 1779-1787.
Pereira-Leal,J.B., and Seabra,M.C. (2000). The mammalian Rab family of small GTPases: Definition of family and subfamily sequence motifs suggests a mechanism for functional specificity in the Ras superfamily. J. Mol. Biol. *301*, 1077-1087.
Pereira-Leal,J.B., Strom,M., Godfrey,R.F., and Seabra,M.C. (2000). Structural determinants of Rab and Rab Escort Protein interaction: Rab family motifs define a conserved binding surface. Biochem. Biophys. Res. Commun. *301*, 92-97.

Pereira-Leal,J.B., and Seabra,M.C. (2001). Evolution of the Rab family of small GTP-binding proteins. J. Mol. Biol. *313*, 889-901.
Pereira-Leal,J.B., Hume,A.N., and Seabra,M.C. (2001). Prenylation of Rab GTPases: molecular mechanisms and involvement in genetic disease. FEBS Lett. *498*, 197-200.
Peters,C., Wolf,A., Wagner,M., Kuhlmann,J., and Waldmann,H. (2004). The cholesterol membrane anchor of the Hedgehog protein confers stable membrane association to lipid-modified proteins. Proc. Natl. Acad. Sci. U.S.A. *101*, 8531-8536.
Phizicky,E., Bastiaens,P.I.H., Zhu,H., Snyder,M., and Fields,S. (2003). Protein analysis on a proteomic scale. Nature. *422*, 208-215.
Piston,D.W., and Kremers,G.J. (2007). Fluorescent protein FRET: the good, the bad and the ugly. Trends Biochem. Sci. *32*, 407-414.
Prior,I.A., and Hancock,J.F. (2012). Ras trafficking, localization and compartmentalized signalling. Semin Cell Dev. Biol. *23*, 145-153.
Pylypenko,O., Rak,A., Reents,R., Niculae,A., Sidorovitch,V., Cioaca,M.D., Bessolitsyna,E., Thoma,N.H., Waldmann,H. , Schlichting,I., Goody,R.S., and Alexandrov,K. (2003). Structure of Rab escort protein-1 in complex with Rab geranylgeranyltransferase. Mol. Cell. *11*, 483-494.
Pylypenko,O., Rak,A., Durek,T., Kushnir,S., Dursina,B.E., Thomae,N.H., Constantinescu,A.T., Brunsveld,L., Watzke,A., Waldmann,H., Goody,R.S., and Alexandrov,K. (2006). Structure of doubly prenylated Ypt1: GDI complex and the mechanism of GDI-mediated Rab recycling. EMBO J. *25*, 13-23.
Quilliam,L.A., Rebhun,J.F., and Castro,A.F. (2002). A growing family of guanine nucleotide exchange factors is responsible for activation of Ras-family GTPases. Prog. Nucleic Acid Res. Mol. Biol. *71*, 391-444.
Rak,A., Pylypenko,O., Durek,T., Watzke,A., Kushnir,S., Brunsveld,L., Waldmann,H., Goody,R.S., and Alexandrov,K. (2003). Structure of Rab GDP-dissociation inhibitor in complex with prenylated YPT1 GTPase. Science. *302*, 646-650.
Rak,A., Pylypenko,O., Niculae,A., Pyatkov,K., Goody,R.S., and Alexandrov,K. (2004). Structure of the Rab7:REP-1 complex: insights into the mechanism of Rab prenylation and choroideremia disease. Cell. *117*, 749-760.
Resh,M.D. (2006). Trafficking and signaling by fatty-acylated and prenylated proteins. Nat. Chem. Biol. *2*, 584-590.
Richardson,C.J., Jones,S., Litt,R.J., and Segev,N. (1998). GTP hydrolysis is not important for Ypt1 GTPase function in vesicular transport. Mol. Cell. Biol. *18*, 827-838.
Riedrich,M., Harkal,S., and Arndt,H.D. (2007). Peptide-Embedded Heterocycles by Mild Single and Multiple Aza-Wittig Ring Closures. Angew. Chem. Int. Ed. *46*, 2701-2703.
Robinson,W.H., DiGennaro,C., Huber,W., Haab,B.B., Kamachi,M., Dean,E.J., Founel,S., Fong,D., Genovese,M.C., de Vegvar,H.E., Skriner,K., Hirschberg,D.L., Monis,R.J., Muller,S., Pruijn,G.J., van Venrooij,W.J., Smolen,J.S., Brown,P.O., Steinman,L., and Utz,P.J. (2002). Autoantigen microarrays for multiplex characterization of autoantibody responses. Nat. Med. *8*, 295-301.
Rocks,O., Peyker,A., Kahms,M., Verveer,P.J., Koerner,C., Lumbierres,M., Kuhlmann,J., Waldmann,H., Wittinghofer,A., and Bastiaens,P.I. (2005). An acylation cycle regulates localization and activity of palmitoylated Ras isoforms. Science. *307*, 1746-1752.
Rocks,O., Gerauer,M., Vartak,N., Koch,S., Huang,Z.P., Pechlivanis,M., Kuhlmann,J., Brunsveld,L., Chandra,A., Ellinger,B., Waldmann,H., and Bastiaens,P.I.H. (2010). The Palmitoylation Machinery Is a Spatially Organizing System for Peripheral Membrane Proteins. Cell. *141*, 458-471.
Rose,K. (1994). Facile synthesis of homogeneous artificial proteins. J. Am. Chem. Soc. *116*, 30-33.
Rosenberg,S., Silver,S.M., Sayer,J.M., and Jencks,W.P. (1974). Evidence for two concurrent mechanisms and a kinetically significant proton transfer process in acid-catalyzed O-methyloxime formation. J. Am. Chem. Soc. *96*, 7986-7998.
Roskoski,R., and Ritchie,P. (1998). Role of the carboxyterminal residue in peptide binding to protein farnesyltransferase and protein geranylgeranyltransferase. Arch. Biochem. Biophys. *356*, 167-176.
Rostovtsev,V.V., Green,L.G., Fokin,V.V., and Sharpless,K.B. (2002). A stepwise huisgen cycloaddition process: copper(I)-catalyzed regioselective ligation of azides and terminal alkynes. Angew. Chem. Int. Ed. *41*, 2596-2599.
Roy,R., Hohng,S., and Ha,T. (2008). A practical guide to single-molecule FRET. Nat. Methods. *5*, 507-516.

Rybin,V., Ullrich,O., Rubino,M., Alexandrov,K., Simon,I., Seabra,M.C., Goody,R., and Zerial,M. (1996). GTPase activity of Rab5 acts as a timer for endocytic membrane fusion. Nature, *383*, 266-269.
Sacher,M., Jiang,Y., Barrowman,J., Scarpa,A., Burston,J., Zhang,L., Schieltz,D., Yates,J.R., Abeliovich,H., and Ferro-Novick,S. (1998). TRAPP, a highly conserved novel complex on the cis-Golgi that mediates vesicle docking and fusion. EMBO J. *17*, 2494-2503.
Sakisaka,T., Meerlo,T., Matteson,J., Plutner,H., and Balch,W.E. (2002). Rab-alpha GDI activity is regulated by a Hsp90 chaperone complex. EMBO J. *21*, 6125-6135.
Sapsford,K.E., Berti,L., and Medintz,I.L. (2006). Materials for fluorescence resonance energy transfer analysis: beyond traditional donor-acceptor combinations. Angew. Chem. Int. Ed. *45*, 4562-4589.
Sasaki,T., Kikuchi,A., Araki,S., Hata,Y., Isomura,M., Kuroda,S., and Takai,Y. (1990). Purification and characterization from bovine brain cytosol of a protein that inhibits the dissociation of GDP from and the subsequent binding of GTP to Smg-P25a, a Ras P21-like GTP-binding protein. J. Biol. Chem. *265*, 2333-2337.
Sato,T.K., Rehling,P., Peterson,M.R., and Emr,S.D. (2000). Class C Vps protein complex regulates vacuolar SNARE pairing and is required for vesicle docking/fusion. Mol. Cell. *6*, 661-671.
Sayer,J.M., Pinsky,B., Schonbrunn,A., and Washtien,W. (1974). Mechanism of carbinolamine formation. J. Am. Chem. Soc. *96*, 7998-8009.
Scheck,R.A., Dedeo,M.T., Iavarone,A.T., and Francis,M.B. (2008). Optimization of a biomimetic transamination reaction. J. Am. Chem. Soc. *130*, 11762-11770.
Scheffzek,K., Klebe,C., Fritz-Wolf,K., Kabsch,W., and Wittinghofer,A. (1995). Crystal structure of the nuclear Ras-related protein Ran in its GDP-bound form. Nature. *374*, 378-381.
Schleifenbaum,A., Stier,G., Gasch,A., Sattler,M., and Schultz,C. (2004). Genetically encoded FRET probe for PKC activity based on pleckstrin. J. Am. Chem. Soc. *126*, 11786-117687.
Schlichting,I., Almo,S.C., Rapp,G., Wilson,K., Petratos,K., Lentfer,A., Wittinghofer,A., Kabsch,W., Pai,E.F., Petsko,G.A., and Goody,R.S. (2004). Time-Resolved X-Ray Crystallographic Study of the Conformational Change in Ha-Ras P21 Protein on Gtp Hydrolysis. Nature. *345*, 309-315.
Schoebel,S., Oesterlin,L.K., Blankenfeldt,W., Goody,R.S., and Itzen,A. (2009). RabGDI displacement by DrrA from Legionella is a consequence of its guanine nucleotide exchange activity. Mol. Cell. *36*, 1060-1072.
Seabra,M.C., Goldstein,J.L., Sudhof,T.C., and Brown,M.S. (1992). Rab geranylgeranyl transferase - a multisubunit enzyme that prenylates GTP-Binding proteins terminating in Cys-X-Cys or Cys-Cys. J. Biol. Chem. *267*, 14497-14503.
Seabra,M.C., Brown,M.S., and Goldstein,J.L. (1993). Retinal degeneration in choroideremia - deficiency of Rab geranylgeranyl transferase. Science. *259*, 377-381.
Seabra,M.C., Ho,Y.K., and Anant,J.S. (1995). Deficient geranylgeranylation of Ram/Rab27 in choroideremia. J. Biol. Chem. *270*, 24420-24427.
Seabra,M.C. (1996). Nucleotide dependence of Rab geranylgeranylation - Rab escort protein interacts preferentially with GDP-bound Rab. J. Biol. Chem. *271*, 14398-14404.
Seabra,M.C., Mules,E.H., and Hume,A.N. (2002). Rab GTPases, intracellular traffic and disease. Trends Mol. Med. *8*, 23-30.
Seabra,M.C., and Wasmeier,C. (2004). Controlling the location and activation of Rab GTPases. Curr. Opin. Cell Biol. *16*, 451-457.
Seals,D.F., Eitzen,G., Margolis,N., Wickner,W.T., and Price,A. (2000). A Ypt/Rab effector complex containing the Sec1 homolog Vps33p is required for homotypic vacuole fusion. Proc. Natl. Acad. Sci. U.S.A. *97*, 9402-9407.
Segev,N. (2001). Ypt and Rab GTPases: insight into functions through novel interactions. Curr. Opin. Cell Biol. *13*, 500-511.
Seo,M.H., Han,J., Jin,Z., Lee,D.W., Park,H.S., and Kim,H.S. (2011). Controlled and oriented immobilization of protein by site-specific incorporation of unnatural amino acid. Anal. Chem. *83*, 2841-2845.
Sethna,S.M., and Shah,N.M. (1945). The chemistry of coumarins. Chem. Rev. *36*, 1-62.
Shen,F., and Seabra,M.C. (1996). Mechanism of Digeranylgeranylation of Rab Proteins: formation of a complex between monogeranylgeranyl geranyl-Rab and Rab escort protein. J. Biol. Chem. *271*, 3692-3698.

Sidorovitch,V., Niculae,A., Kan,N., Ceacareanu,A.C., and Alexandrov,K. (2002). Expression of mammalian Rab escort protein-1 and -2 in yeast saccharomyces cerevisiae. Protein Expr. Purif. *26*, 50-58.
Sielaff,I., Arnold,A., Godin,G., Tugulu,S., Klok,H.A., and Johnsson,K. (2006). Protein function microarrays based on self-immobilizing and self-labeling fusion proteins. ChemBioChem. *7*, 194-202.
Simon,I., Zerial,M., and Goody,R.S. (1996). Kinetics of interaction of Rab5 and Rab7 with nucleotides and magnesium ions. J. Biol. Chem. *271*, 20470-20478.
Sivars,U., Aivazian,D., and Pfeffer,S.R. (2003). Yip3 catalyses the dissociation of endosomal Rab-GDI complexes. Nature. *425*, 856-859.
Sakisaka,T., Meerlo,T., Matteson,J., Plutner,H., and Balch,W.E. (2002). Rab-αGDI activity is regulated by a Hsp90 chaperone complex. EMBO J. *21*, 6125-6135.
Sletten,E.M., and Bertozzi,C.R. (2009). Bioorthogonal chemistry: fishing for selectivity in a sea of functionality. Angew. Chem. Int. Ed. *48*, 6974-6998.
Smeland,T.E., Seabra,M.C., Goldstein,J.L., and Brown,M.S. (1994). Geranylgeranylated Rab proteins terminating in Cys-Ala-Cys, but not Cys-Cys, are carboxyl-methylated by bovine brain membranes in-Vitro. Proc. Natl. Acad. Sci. U.S.A. *91*, 10712-10716.
Smythe,E. (2002). Direct interactions between rab GTPases and cargo. Mol. Cell, *9*, 205-206.
Soellner,M.B., Dickson,K.A., Nilsson,B.L., and Raines,R.T. (2003). Site-specific protein immobilization by Staudinger ligation. J. Am. Chem. Soc. *125*, 11790-11781.
Sohma,Y., and Kent,S.B.H. (2009). Biomimetic synthesis of lispro insulin via a chemically synthesized “mini-proinsulin” prepared by oxime-forming ligation. J. Am. Chem. Soc. *131*, 16313-16318.
Soldati,T., Shapiro,A.D., Svejstrup,A.B.D., and Pfeffer,S.R. (1994). Membrane Targeting of the Small GTPase Rab9 Is Accompanied by Nucleotide Exchange. Nature. *369*, 76-78.
Sonnichsen,B., de Renzis,S., Nielsen,E., Rietdorf,J. and Zerial,M. (2000). Distinct membrane domains on endosomes in the recycling pathway visualized by multicolor imaging of Rab4, Rab5, and Rab11. J. Cell Biol. *149*, 901-914.
Sprang,S.R. (1997). G protein mechanisms: Insights from structural analysis. Annu. Rev. Biochem. *66*, 639-678.
Stein,M.P., Dong,J.B., and Wandinger-Ness,A. (2003). Rab proteins and endocytic trafficking: potential targets for therapeutic intervention. Adv. Drug Deliv. Rev. *55*, 1421-1437.
Stenmark,H., Parton,R.G., Steelemortimer,O., Lutcke,A., Gruenberg,J., and Zerial,M. (1994). Inhibition of Rab5 GTPase Activity Stimulates Membrane-Fusion in Endocytosis. EMBO J. *13*, 1287-1296.
Stenmark,H., Valencia,A., Martinez,O., Ullrich,O., Goud,B., and Zerial,M. (1994). Distinct structural elements of Rab5 define its functional specificity. EMBO J. *13*, 575-583.
Stenmark,H. (2009). Rab GTPases as coordinators of vesicle traffic. Nat. Rev. Mol. Cell Biol. *10*, 513-525.
Stroupe,C., and Brunger,A.T. (2000). Crystal structures of a Rab protein in its inactive and active conformations. J. Mol. Biol. *304*, 585-598.
Suh,H.Y., Lee,D.W., Lee,K.H., Ku,B., Choi,S.J., Woo,J.S., Kim,Y.G., and Oh,B.H. (2010). Structural insights into the dual nucleotide exchange and GDI displacement activity of SidM/DrrA. EMBO J. *29*, 496-504.
Szilvay,G.R., Blenner,M.A., Shur,O., Cropek,D.M., and Banta,S.A. (2009). FRET-Based method for probing the conformational behavior of an intrinsically disordered repeat domain from bordetella pertussis adenylate cyclase. Biochemistry. *48*, 11273-11282.
Tang,B.L., Ong,Y.S., Huang,B., Wei,S., Wong,E.T., Qi,R., Horstmann,H., and Hong,W. (2001). A membrane protein enriched in endoplasmic reticulum exit sites interacts with COPII. J. Biol. Chem. *276*, 40008-40017.
Terstappen,G.C., Schlupen,C., Raggiaschi,R., and Gaviraghi,G. (2007). Target deconvolution strategies in drug discovery. Nature Rev. Drug Discov. *6*, 891-903.
Thomä,N.H., Iakovenko,A., Kalinin,A., Waldmann,H., Goody,R.S., and Alexandrov,K. (2001). Allosteric regulation of substrate binding and product release in geranylgeranyltransferase type II. Biochemistry. *40*, 268-274.

Thomä,N.H., Niculae,A., Goody,R.S., and Alexandrov,K. (2001). Double prenylation by RabGGTase can proceed without dissociation of the mono-prenylated intermediate. J. Biol. Chem. *276*, 48631-48636.
Tolbert,T.J., and Wong,C.H. (2002). New methods for proteomic research: Preparation of proteins with N-terminal cysteines for labeling and conjugation. Angew. Chem. Int. Ed. *41*, 2171-2174.
Tron,G.C., Pirali,T., Billington,R.A., Canonico,P.L., Sorba,G., and Genazzani,A.A. (2008). Click chemistry reactions in medicinal chemistry: applications of the 1,3-dipolar cycloaddition between azides and alkynes. Med. Res. Rev. *28*, 278-308.
Tsukiji,S., and Nagamune,T. (2009). Sortase-mediated ligation: A gift from Gram-positive bacteria to protein engineering. ChemBioChem. *10*, 787-798.
Ullrich,O., Horiuchi,H., Bucci,C., and Zerial,M. (1994). Membrane asociation of Rab5 mediated by GDP-dissociation inhibitor and accompanied by GDP/GTP exchange. Nature. *368*, 157-160.
Ungermann,C., Sato,K., and Wickner,W. (1998). Defining the functions of trans-SNARE pairs. Nature. *396*, 543-548.
Valencia,A., Chardin,P., Wittinghofer,A., and Sander,C. (1991). The Ras protein family - evolutionary tree and role of conserved amino-acids. Biochemistry. *30*, 4637-4648.
Vandersluijs,P., Hull,M., Huber,L.A., Male,P., Goud,B., and Mellman,I. (1992). Reversible phosphorylation dephosphorylation determines the localization of Rab4 during the cell-cycle. EMBO J. *11*, 4379-4389.
Vega,F.M., and Ridley,A.J. (2008). Rho GTPases in cancer cell biology. FEBS Lett. *582*, 2093-2101.
Vetter,I.R., and Wittinghofer,A. (2001). The guanine nucleotide-binding switch in three dimensions. Science. *294*, 1299-1304.
Volkert,M., Uwai,K., Tebbe,A., Popkirova,B., Wagner,M., Kuhlmann,J., and Waldmann,H. (2003). Synthesis and biological activity of photoactivatable N-ras peptides and proteins. J. Am. Chem. Soc. *125*, 12749-12758.
Wada,M., Nakanishi,H., Satoh,A., Hirano,H., Obaishi,H., Matsuura,Y., and Takai,Y. (1997). Isolation and characterization of a GDP/GTP exchange protein specific for the Rab3 subfamily Small G proteins. J. Biol. Chem. *272*, 3875-3878.
Watzke,A., Köhn,M., Gutierrez-Rodriguez,M., Wacker,R., Schröder,H., Breinbauer,R., Kuhlmann,J., Alexandrov,K., Niemeyer,C.M., Goody,R.S., and Waldmann,H. (2006). Site-selective protein immobilization by staudinger ligation. Angew. Chem. Int. Ed. *45*, 1408-1412.
Wang,R., Zheng,W., Yu,H., Deng,H., and Luo,M. (2011). Labeling Substrates of Protein Arginine Methyltransferase with Engineered Enzymes and Matched *S*-Adenosyl-l-methionine Analogues. J. Am. Chem. Soc. *133*, 7648-7651.
Weikart,N.D., and Mootz,H.D. (2010). Generation of site-specific and enzymatically stable conjugates of recombinant proteins with ubiquitin-like modifiers by the CuI-catalyzed azide–alkyne cycloaddition. ChemBioChem. *11*, 774-777.
Weinrich,D., Jonkheijm,P., Niemeyer,C.M., and Waldmann,H. (2009). Applications of protein biochips in biomedical and biotechnological research. Angew. Chem. Int. Ed., *48*, 7744-7751.
Weinrich,D., Lin,P.C., Jonkheijm,P., Nguyen,U.T.T., Schroder,H., Niemeyer,C.M., Alexandrov,K., Goody,R.S., and Waldmann,H. (2010). Oriented immobilization of farnesylated proteins by the thiol-ene reaction. Angew. Chem. Int. Ed. *49*, 1252-1257.
Weise,K., Triola,G., Brunsveld,L., Waldmann,H., and Winter,R. (2009). Influence of the lipidation motif on the partitioning and association of N-Ras in model membrane subdomains. J. Am. Chem. Soc. *131*, 1557-1564.
Weiss,S. (1999). Fluorescence Spectroscopy of Single Biomolecules. Science. *283*, 1676-1683.
Whyte,J.R.C., and Munro,S. (2002). Vesicle tethering complexes in membrane traffic. J. Cell Sci. *115*, 2627-2637.
Wong,L.S., Khan,F., and Micklefield,J. (2009). Selective covalent protein immobilization: strategies and applications. Chem. Rev. *109*, 4025-4053.
Wu,B., Wang,Z., Huang,Y., and Liu,W.R. (2012). Catalyst-free and site-specific one-pot dual-labeling of a protein directed by two fenetically incorporated noncanonical amino acids. ChemBioChem. *13*, 1405-1408.
Wu,M., Wang,T., Loh,E., Hong,W., and Song,H. (2005). Structural basis for recruitment of RILP by small GTPase Rab7. EMBO J. *24*, 1491-1501.

Wurmser,A.E., Sato,T.K., and Emr,S.D. (2000). New component of the vacuolar class C-Vps complex couples nucleotide exchange on the Ypt7 GTPase to SNARE-dependent docking and fusion. J. Cell Biol. *151*, 551-562.
Wu,S.K., Zeng,K., Wilson,I.A., and Balch,W.E. (1996). Structural insights into the function of the Rab GDI superfamily. Trends Biochem. Sci. *21*, 472-476.
Wu,Y.W., Waldmann,H., Reents,R., Ebetino,F.H., Goody,R.S., and Alexandrov,K. (2006). A protein fluorescence amplifier: continuous fluorometric assay for rab geranylgeranyltransferase. ChemBioChem. *7*, 1859-1861.
Wu,Y.W., Alexandrov,K., and Brunsveld,L. (2006). Nature Protoc. *2*, 2704-2711.
Wu,Y.W., Tan,K.T., Waldmann,H., Goody,R.S., and Alexandrov,K. (2007). Quantitative analysis of the interaction of prenylated Rab proteins with REP and GDI explains the requirement for both regulators in Rab function. Proc. Nat. Acad. Sci. U.S.A. *104*, 12294-12299.
Wu,Y.W., Goody,R.S., Abagyan,R., and Alexandrov,K. (2009). Structure of the disordered C terminus of Rab7 GTPase induced by binding to the Rab geranylgeranyl transferase catalytic complex reveals the mechanism of Rab prenylation. J. Biol. Chem. *284*, 13185-13192.
Wu,Y.W., and Goody,R.S. (2010). Probing protein function by chemical modification. J. Pept. Sci. *16*, 514-523.
Wu,Y.W, Oesterlin1,L.K., Tan,K.T., Waldmann,H., Alexandrov,K., and Goody,R.S. (2010). Membrane targeting mechanism of Rab GTP aseselucidated by semisynthetic protein probes. Nature Chem. Biol. *6*, 534-540.
Xiao,J., and Tolbert,T.J. (2009). Synthesis of N-terminally linked protein dimers and trimers by a combined native chemical ligation-CuAAC click chemistry strategy. Org. Lett. *11*, 4144-4147.
Xu,M.Q., Paulus,H., and Chong,S.R. (2000). Fusions to self-splicing inteins for protein purification. Methods Enzymol. *326*, 376-418.
Yang,J.Y., and Yang,W.Y. (2009). Site-specific two-color protein labeling for FRET studies using split inteins. J. Am. Chem. Soc. *131*, 11644-11645.
Yang,X.P., Matern,H.T., and Gallwitz,D. (1998). Specific binding to a novel and essential Golgi membrane protein (Yip1p) functionally links the transport GTPases Ypt1p and Ypt31p. EMBO J. *17*, 4954-4963.
Yi,L., Shi,J., Gao,S., Li,S., Niu,C., and Xi,Z. (2009). Sulfonium alkylation followed by 'click' chemistry for facile surface modification of proteins and tobacco mosaic virus. Tetrahedron Lett. *50*, 759-762.
Yi,L., Sun,H.Y., Wu,Y.W., Triola,G., Waldmann,H., and Goody,R.S. (2010). A highly efficient strategy for modification of proteins at the C terminus. Angew. Chem. Int. Ed. *49*, 9417-9421.
Yi,L., Sun,H.Y., Itzen,A., Triola,G., Waldmann,H., Goody,R.S., and Wu,Y.W. (2011). One-pot dual-labeling of a protein by two chemoselective reactions. Angew. Chem. Int. Ed. *50*, 8287-8290.
Yoshimura,S., Gerondopoulos,A., Linford,A., Rigden,D.J., and Barr,F.A. (2010). Family-wide characterization of the DENN domain Rab GDP-GTP exchange factors. J. Cell Biol. *191*, 367-381.
Yu,M., Wang,Q., Patterson,J.E., and Woolley,A.T. (2011). Multilayer polymer microchip capillary array electrophoresis devices with integrated on/-chip labeling for high-throughput protein Analysis. Anal. Chem. *83*, 3541-3547.
Zeng,Y., Ramya,T.N.C., Diksen,A., Dawson,P.E., and Paulson,J.C. (2009). High-efficiency labeling of sialylated glycoproteins on living cells. Nat. Methods. *6*, 207-209.
Zerial,M., and McBride,H. (2001). Rab proteins as membrane organizers. Nat. Rev. Mol. Cell Biol. *2*, 107-117.
Zhang,Z., Smith,B.A.C., Wang,L., Brock,A., Cho,C., and Schultz,P. (2003). A new strategy for the site-specific modification of proteins in vivo. Biochemistry. *42*, 6735-6746.

7. Appendices

7.1. Selected LCMS spectra of proteins

ESI-MS spectra of proteins in the project for FRET-based GEF sensors

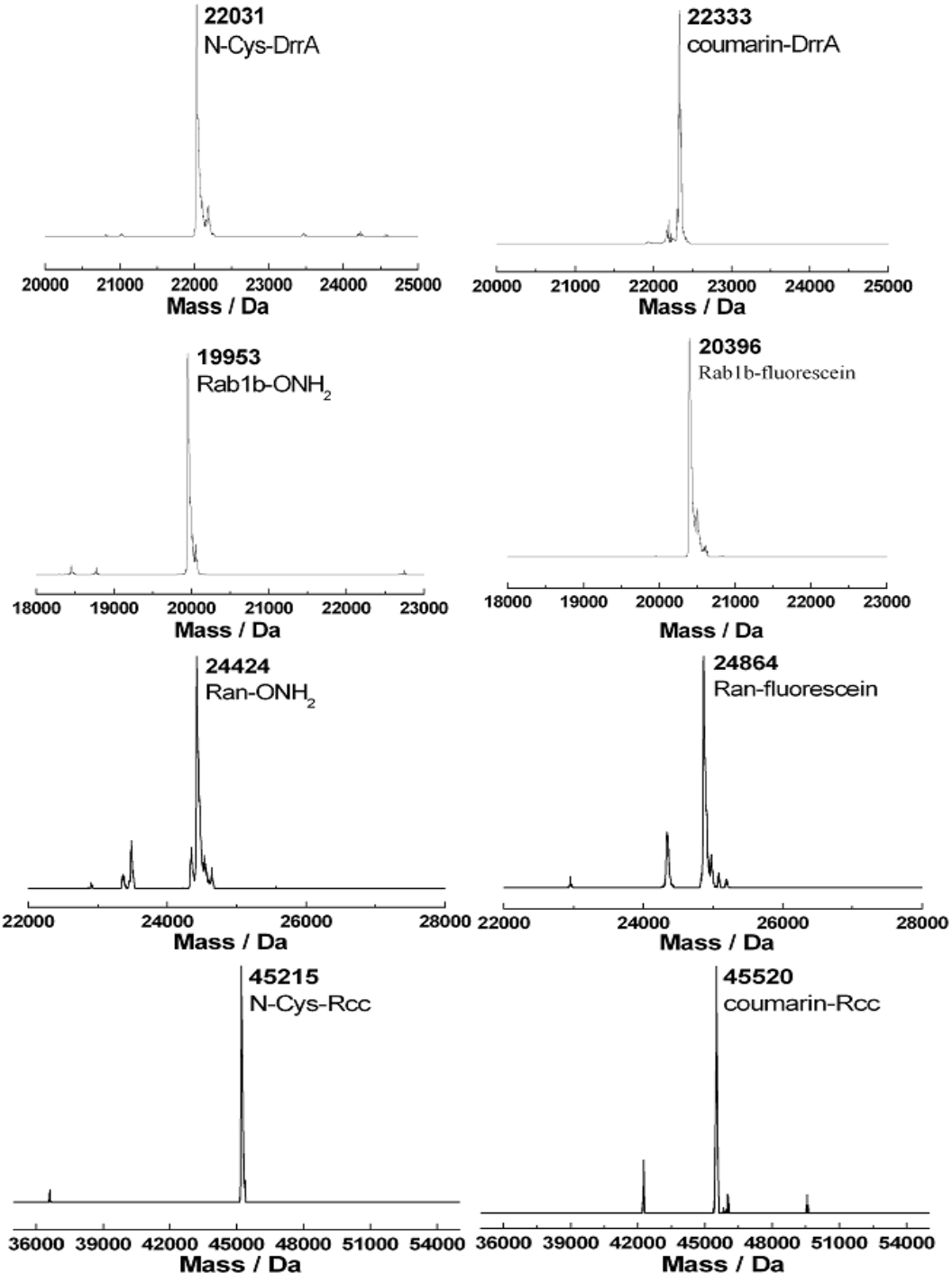

ESI-MS spectra of proteins in the project for dual-labeling Rab7

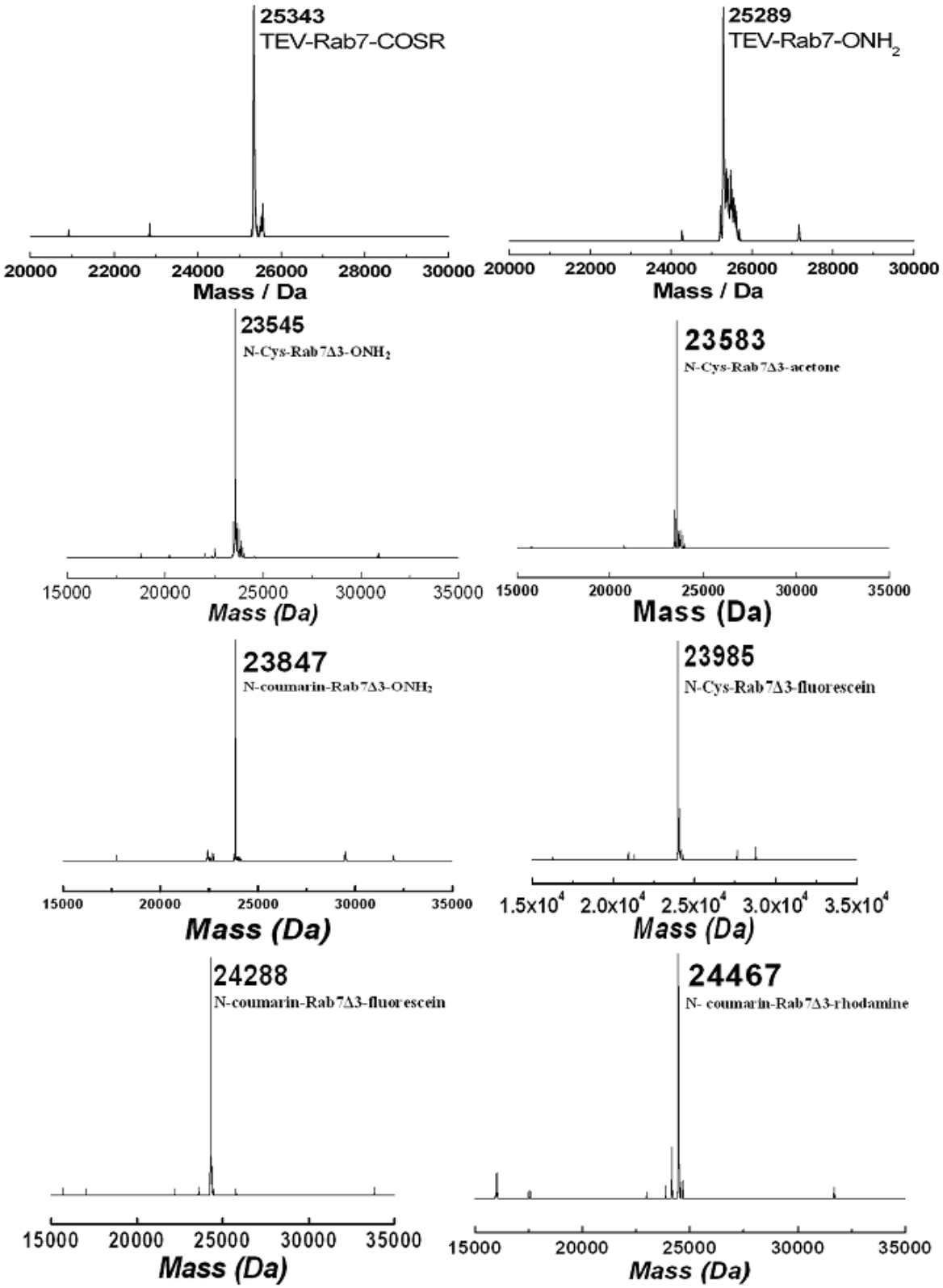

ESI-MS spectra of proteins in the project of PEGylated Rab probe

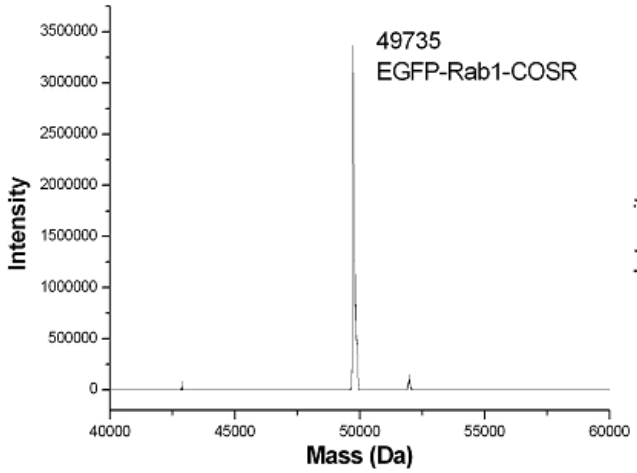

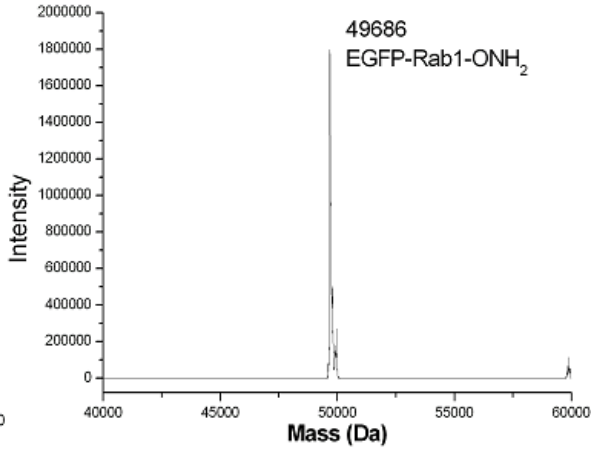

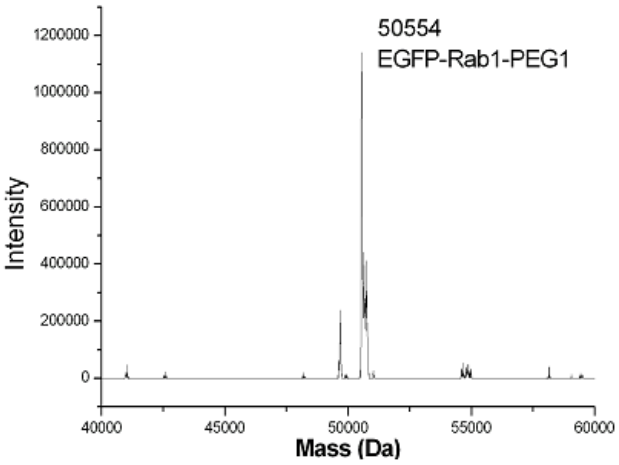

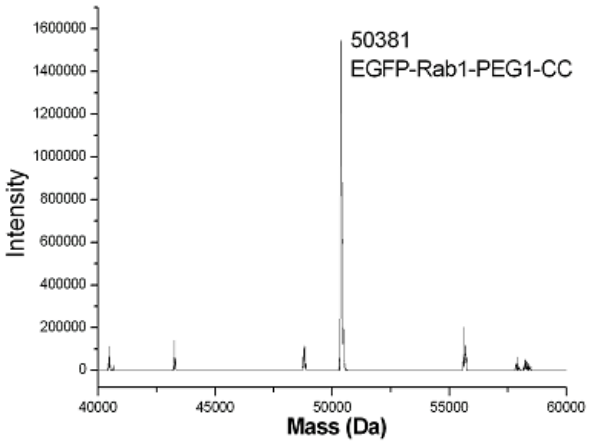

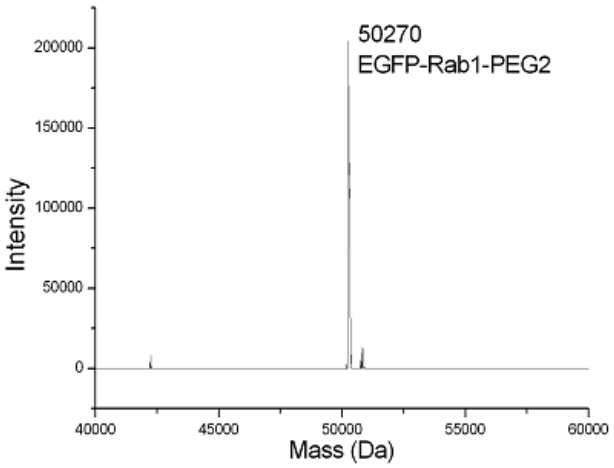

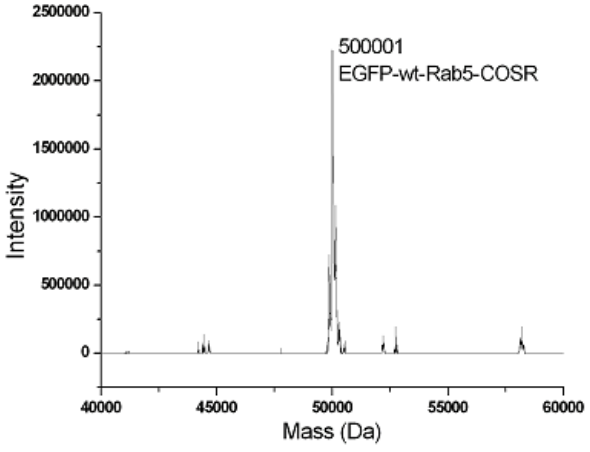

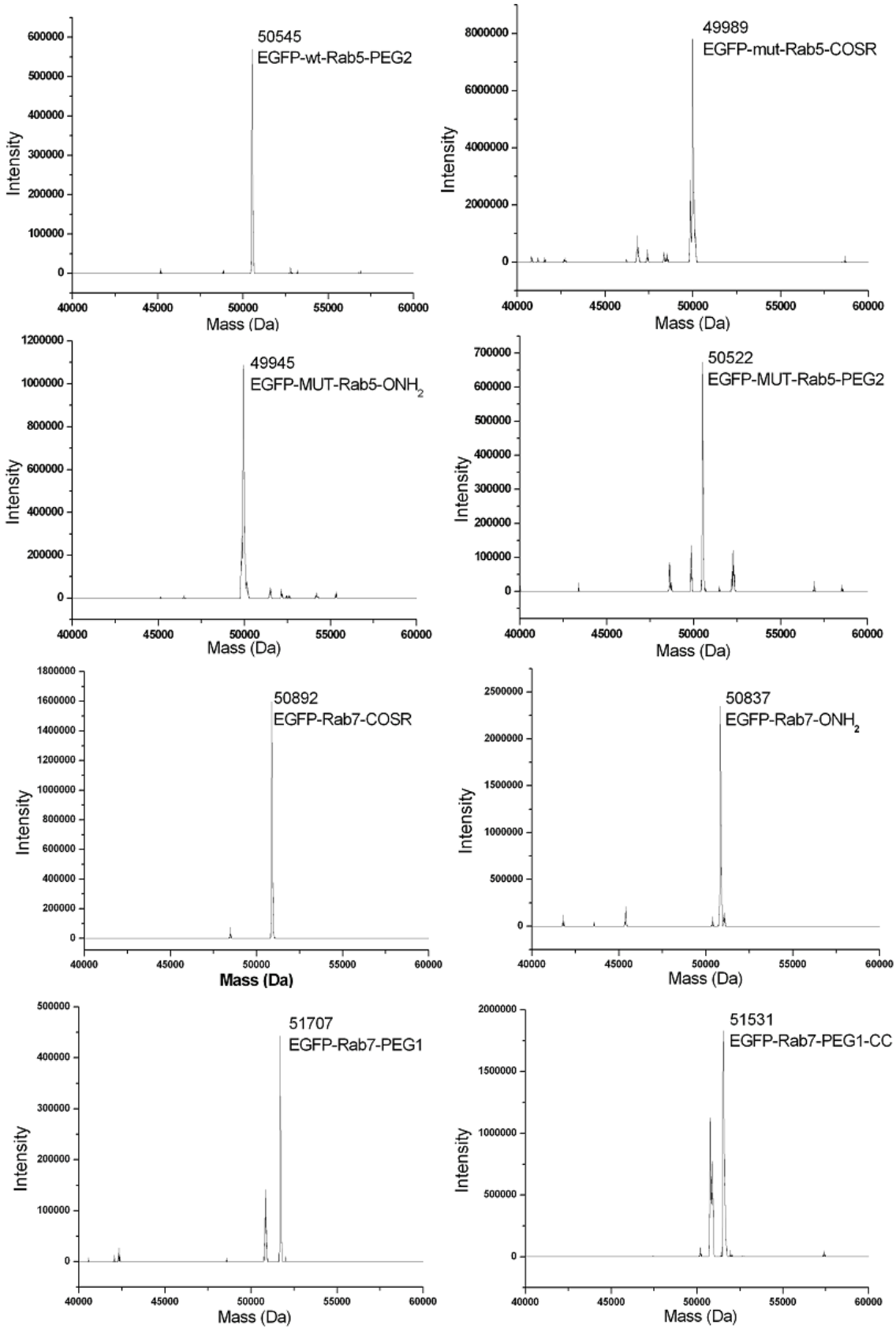
50545
EGFP-wt-Rab5-PEG2
49989
EGFP-mut-Rab5-COSR
49945
EGFP-MUT-Rab5-ONH2
50522
EGFP-MUT-Rab5-PEG2
50892
EGFP-Rab7-COSR
50837
EGFP-Rab7-ONH2
51707
EGFP-Rab7-PEG1
51531
EGFP-Rab7-PEG1-CC
Intensity
Mass (Da)

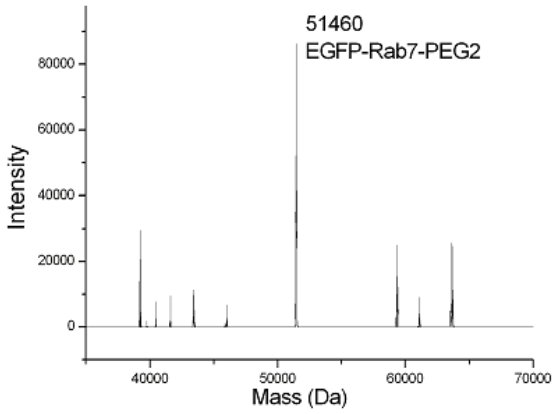
51460
EGFP-Rab7-PEG2
Intensity
Mass (Da)

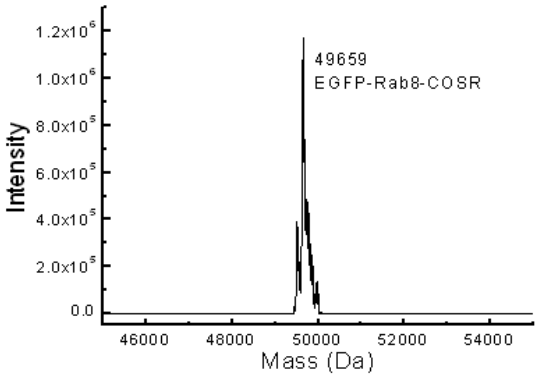
49659
EGFP-Rab8-COSR
Intensity
Mass (Da)

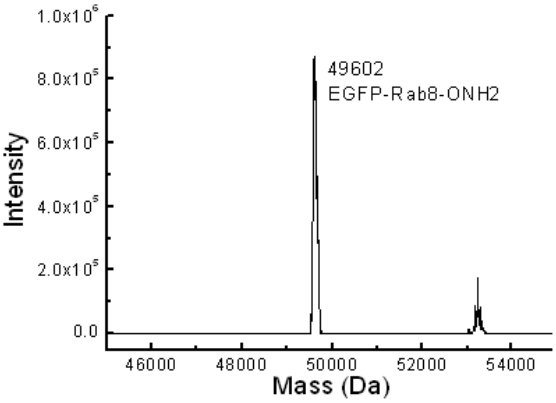
49602
EGFP-Rab8-ONH2
Intensity
Mass (Da)

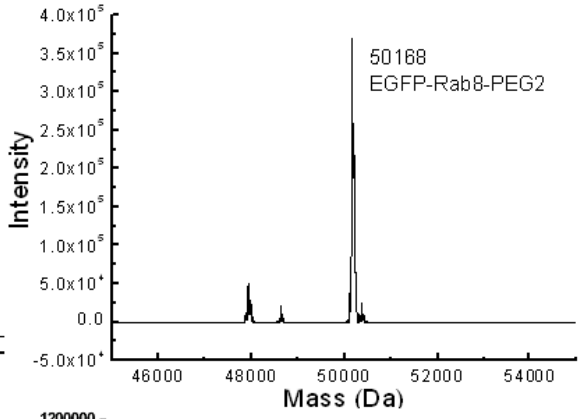
50168
EGFP-Rab8-PEG2
Intensity
Mass (Da)

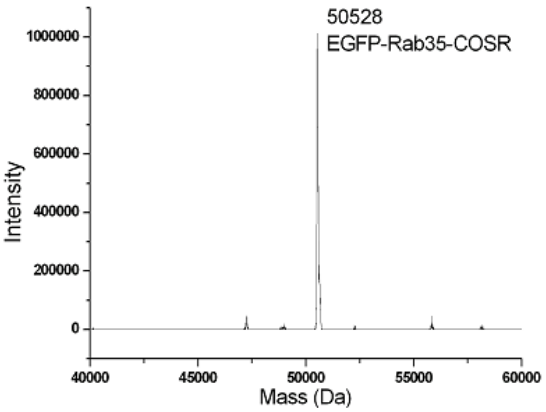
50528
EGFP-Rab35-COSR
Intensity
Mass (Da)

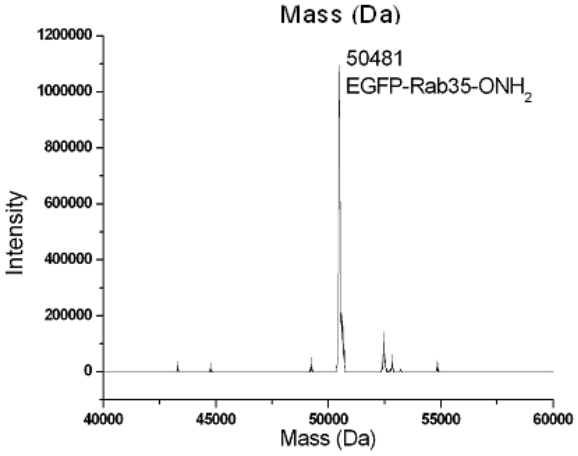
50481
EGFP-Rab35-ONH2
Intensity
Mass (Da)

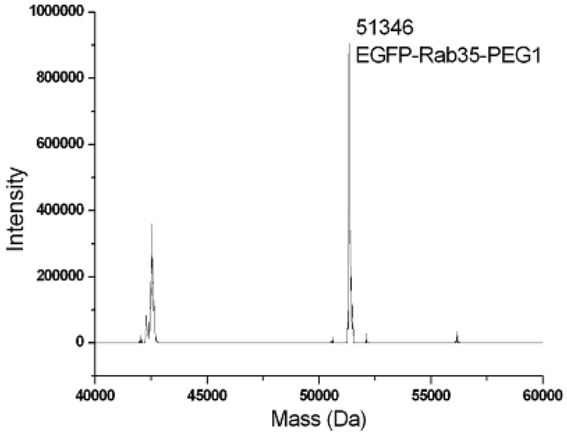
51346
EGFP-Rab35-PEG1
Intensity
Mass (Da)

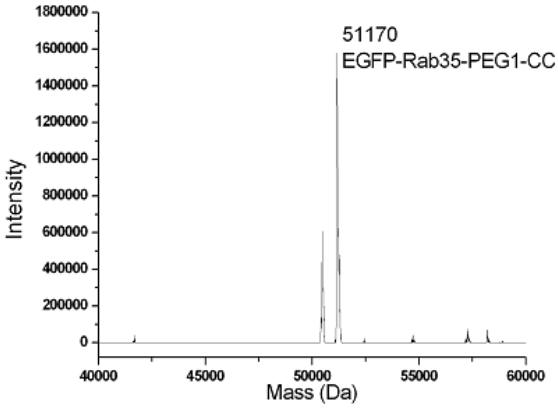
51170
EGFP-Rab35-PEG1-CC
Intensity
Mass (Da)

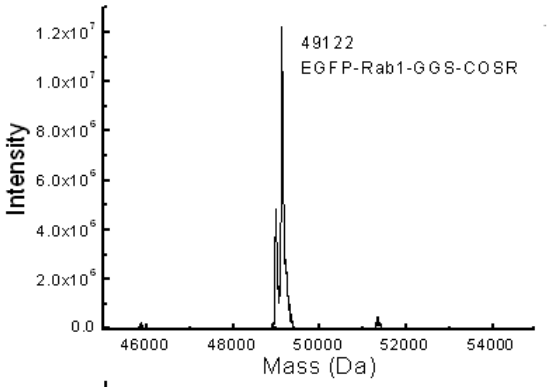
49122
EGFP-Rab1-GGS-COSR
Intensity
Mass (Da)

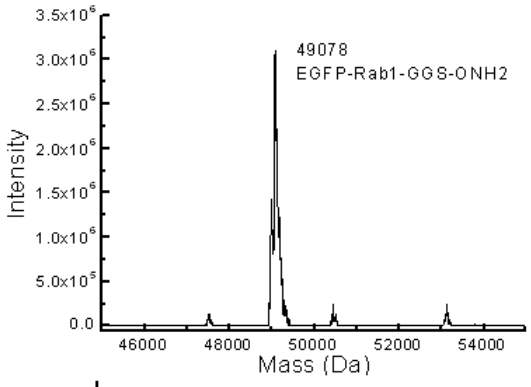
49078
EGFP-Rab1-GGS-ONH2
Intensity
Mass (Da)

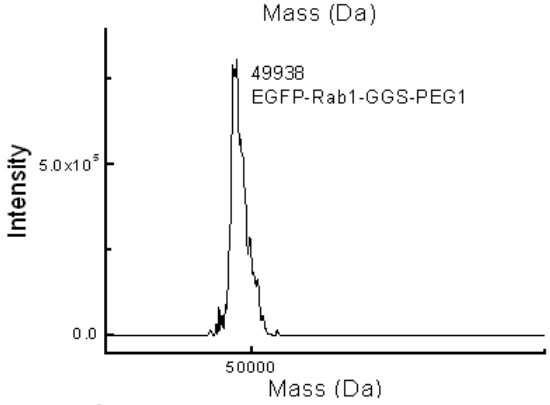
49938
EGFP-Rab1-GGS-PEG1
Intensity
Mass (Da)

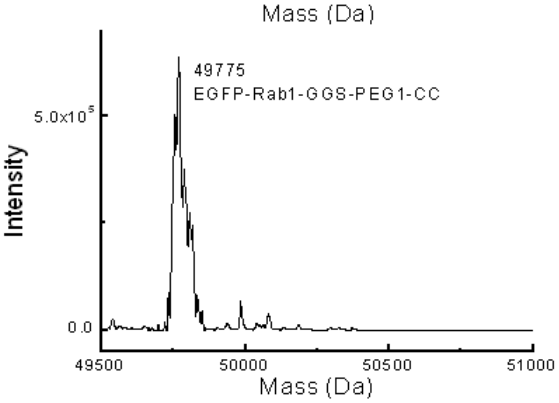
49775
EGFP-Rab1-GGS-PEG1-CC
Intensity
Mass (Da)

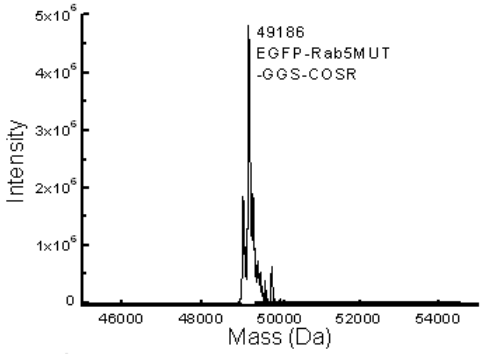
49186
EGFP-Rab5MUT
-GGS-COSR
Intensity
Mass (Da)

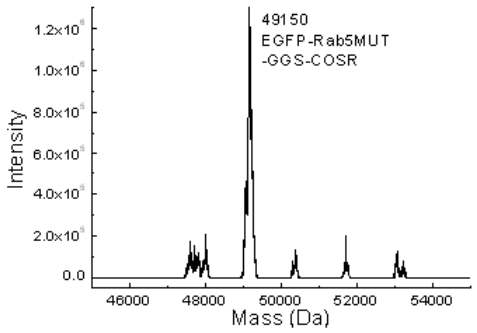
49150
EGFP-Rab5MUT
-GGS-COSR
Intensity
Mass (Da)

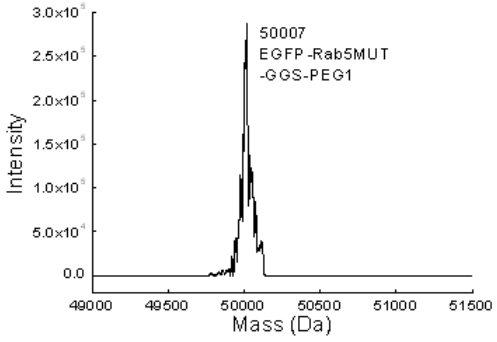
50007
EGFP-Rab5MUT
-GGS-PEG1
Intensity
Mass (Da)

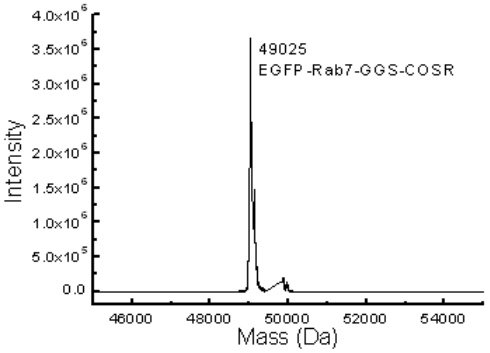
49025
EGFP-Rab7-GGS-COSR
Intensity
Mass (Da)

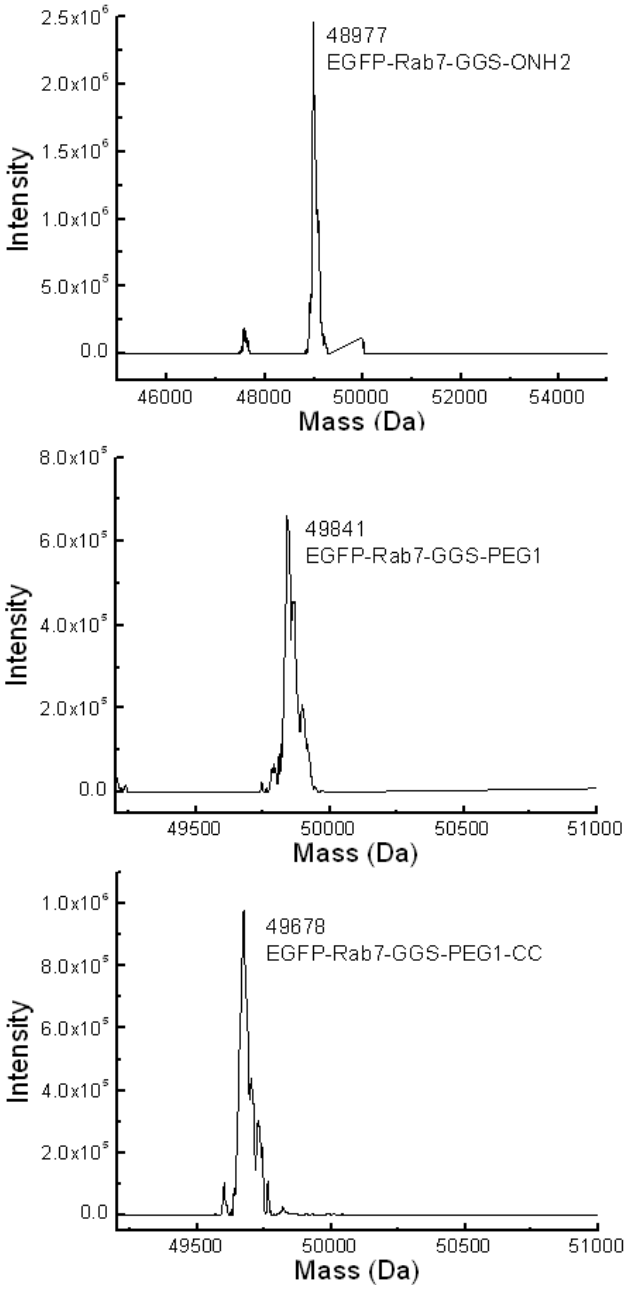
48977
EGFP-Rab7-GGS-ONH2
Intensity
Mass (Da)
49841
EGFP-Rab7-GGS-PEG1
Intensity
Mass (Da)
49678
EGFP-Rab7-GGS-PEG1-CC
Intensity
Mass (Da)

7.2. Selected NMR spectra

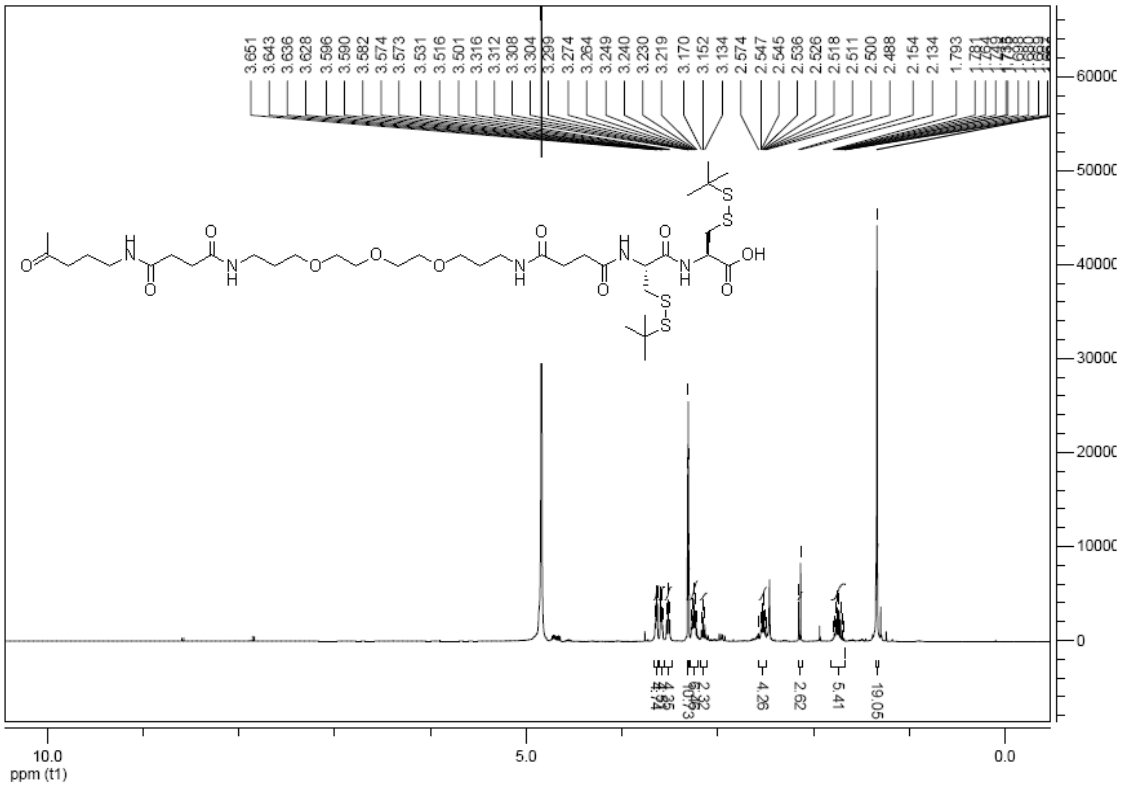

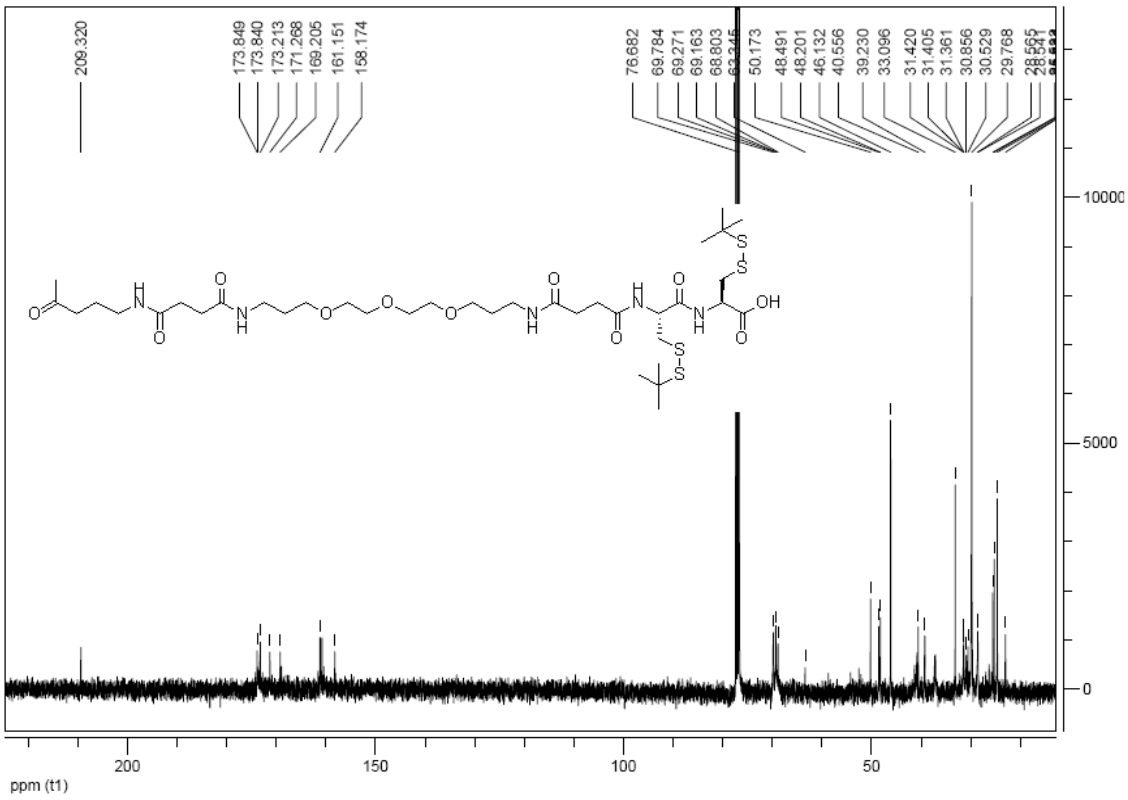

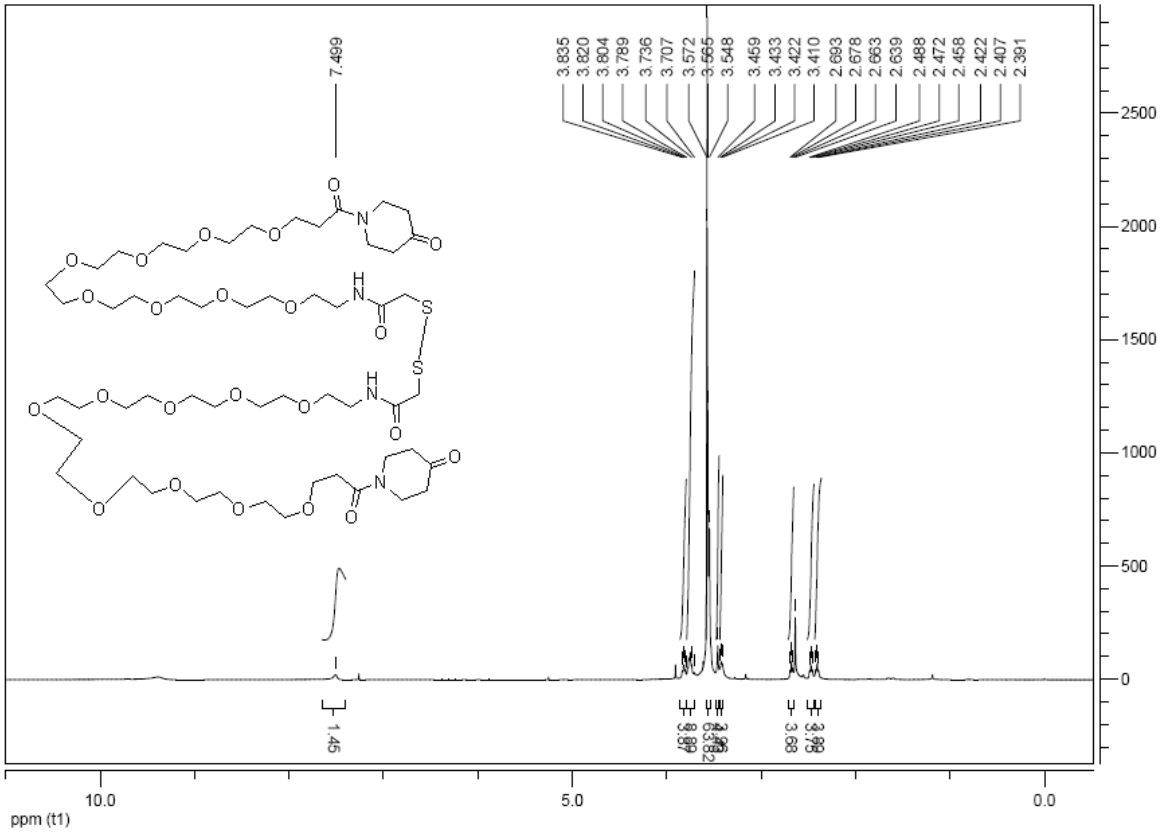
7.499
3.835
3.820
3.804
3.789
3.736
3.707
3.572
3.565
3.548
3.459
3.433
3.422
3.410
2.693
2.678
2.663
2.639
2.488
2.472
2.458
2.422
2.407
2.391
1.46
3.68
2500
2000
1500
1000
500
0
10.0
5.0
0.0
ppm (t1)

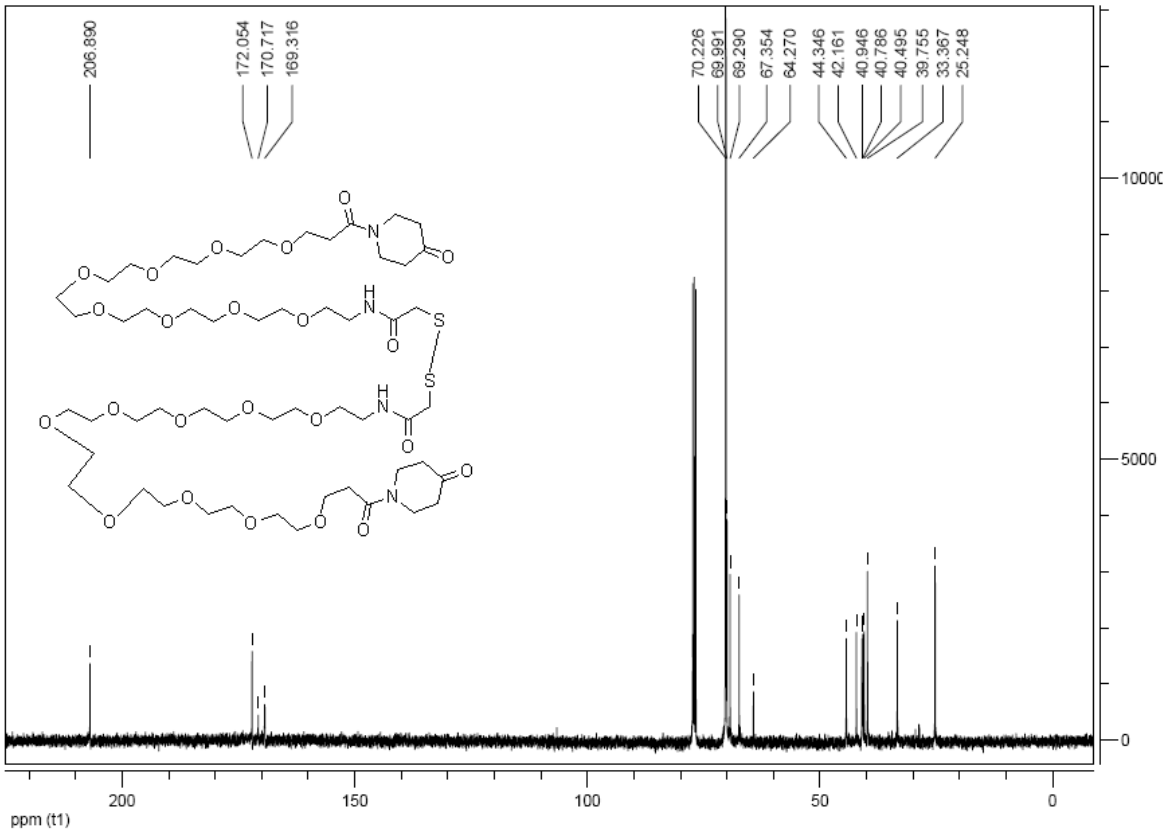
206.890
172.054
170.717
169.316
70.226
69.991
69.290
67.354
64.270
44.346
42.161
40.946
40.786
40.495
39.755
33.367
25.248
10000
5000
0
200
150
100
50
0
ppm (t1)

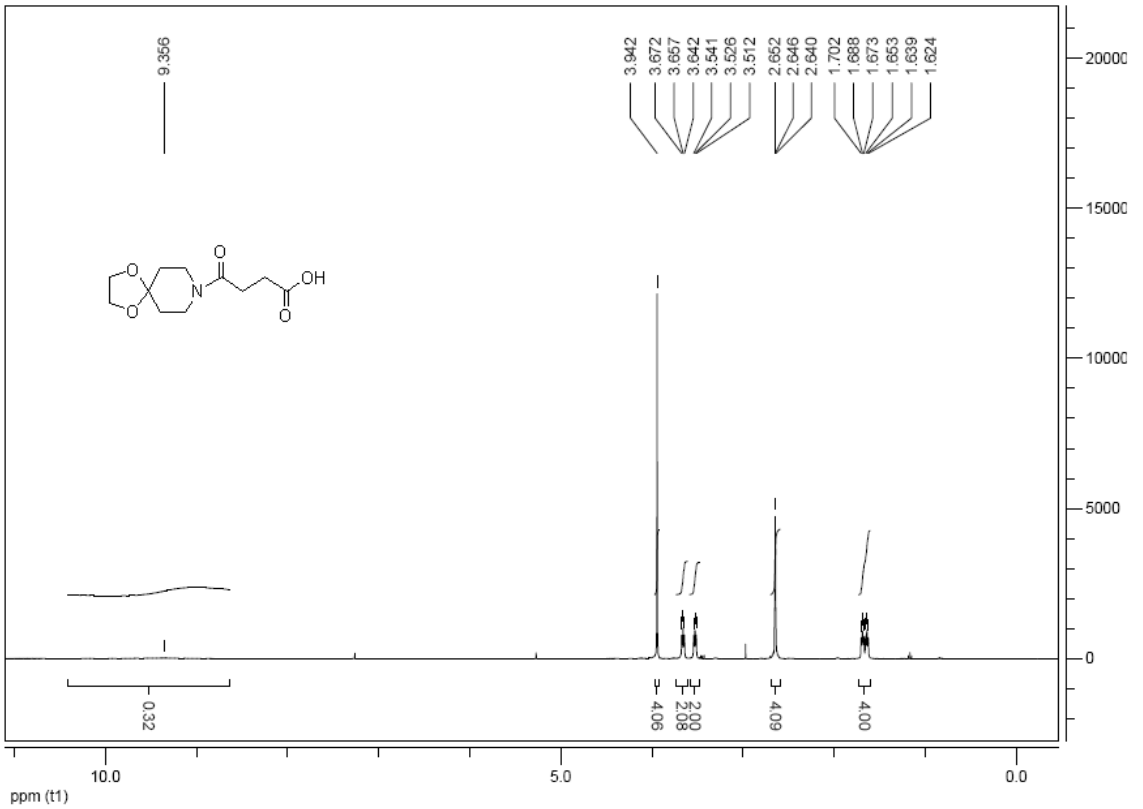
9.356
3.942
3.672
3.657
3.642
3.541
3.526
3.512
2.652
2.646
2.640
1.702
1.688
1.673
1.653
1.639
1.624
O
OH
O
N
O
O
0.32
4.06
2.08
2.00
4.09
4.00
20000
15000
10000
5000
0
10.0
5.0
0.0
ppm (t1)

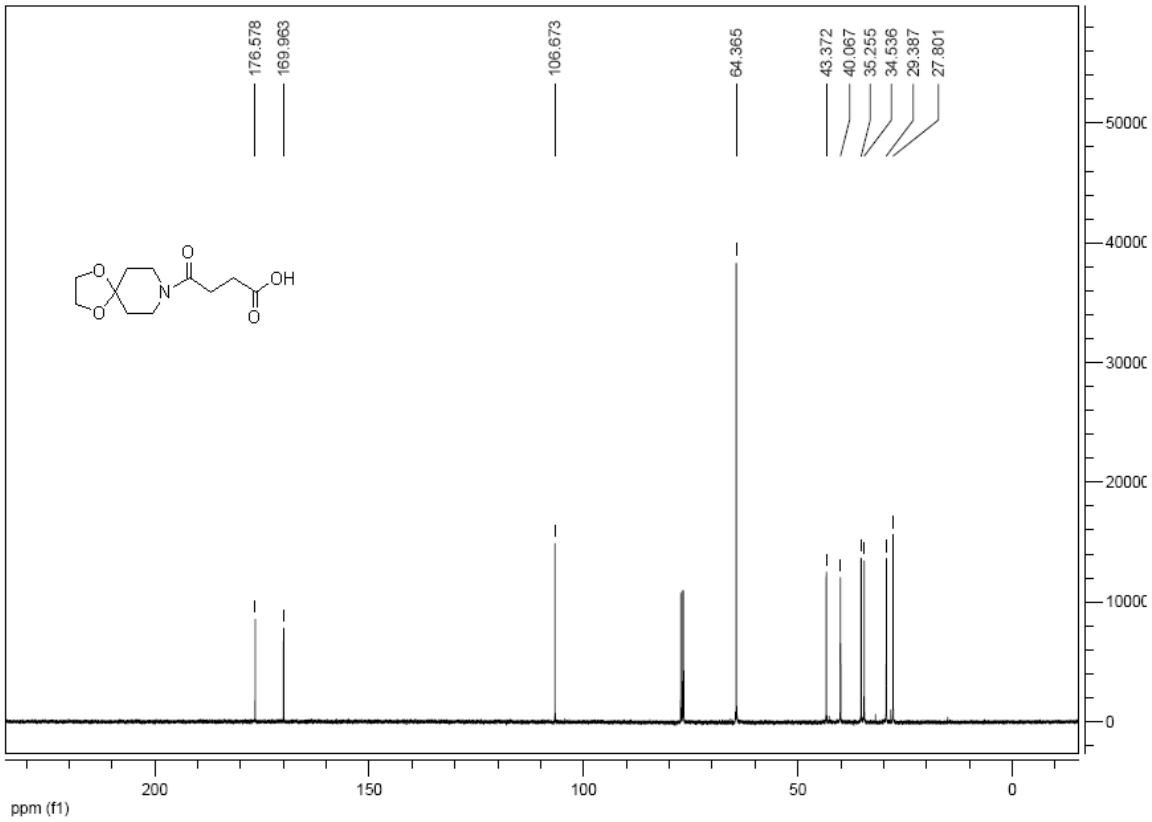
176.578
169.963
106.673
64.365
43.372
40.067
35.255
34.536
29.387
27.801
O
OH
O
N
O
O
50000
40000
30000
20000
10000
0
200
150
100
50
0
ppm (f1)

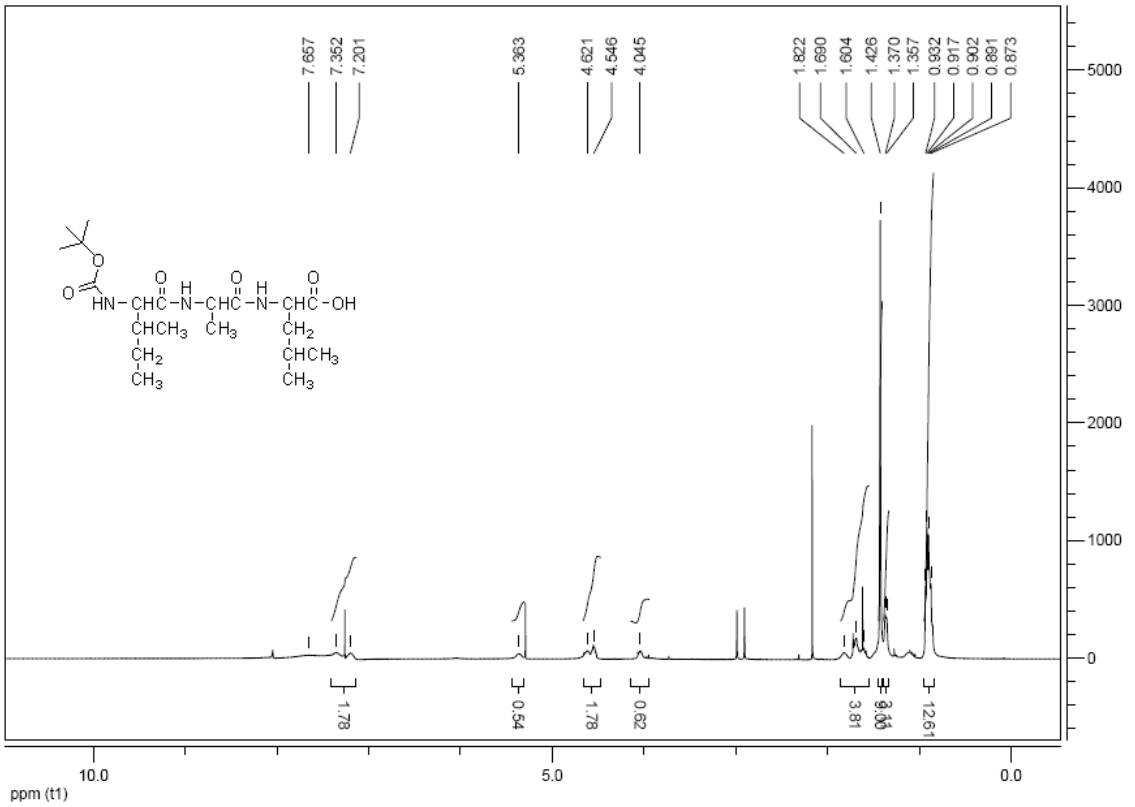
7.657
7.352
7.201
5.363
4.621
4.546
4.045
1.822
1.690
1.604
1.426
1.370
1.357
0.932
0.917
0.902
0.891
0.873
1.78
0.54
1.78
0.62
3.81
9.00
12.61
10.0
5.0
0.0
ppm (t1)

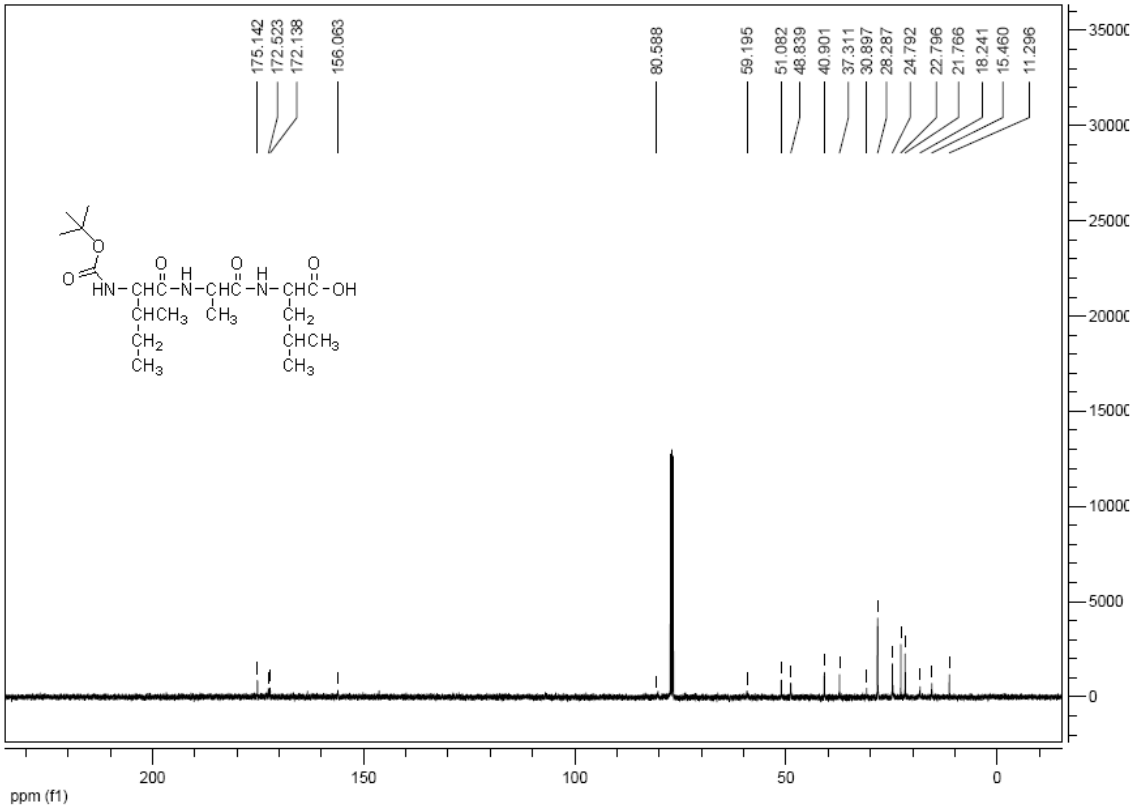
175.142
172.523
172.138
156.063
80.588
59.195
51.082
48.839
40.901
37.311
30.897
28.287
24.792
22.796
21.766
18.241
15.460
11.296
200
150
100
50
0
ppm (f1)

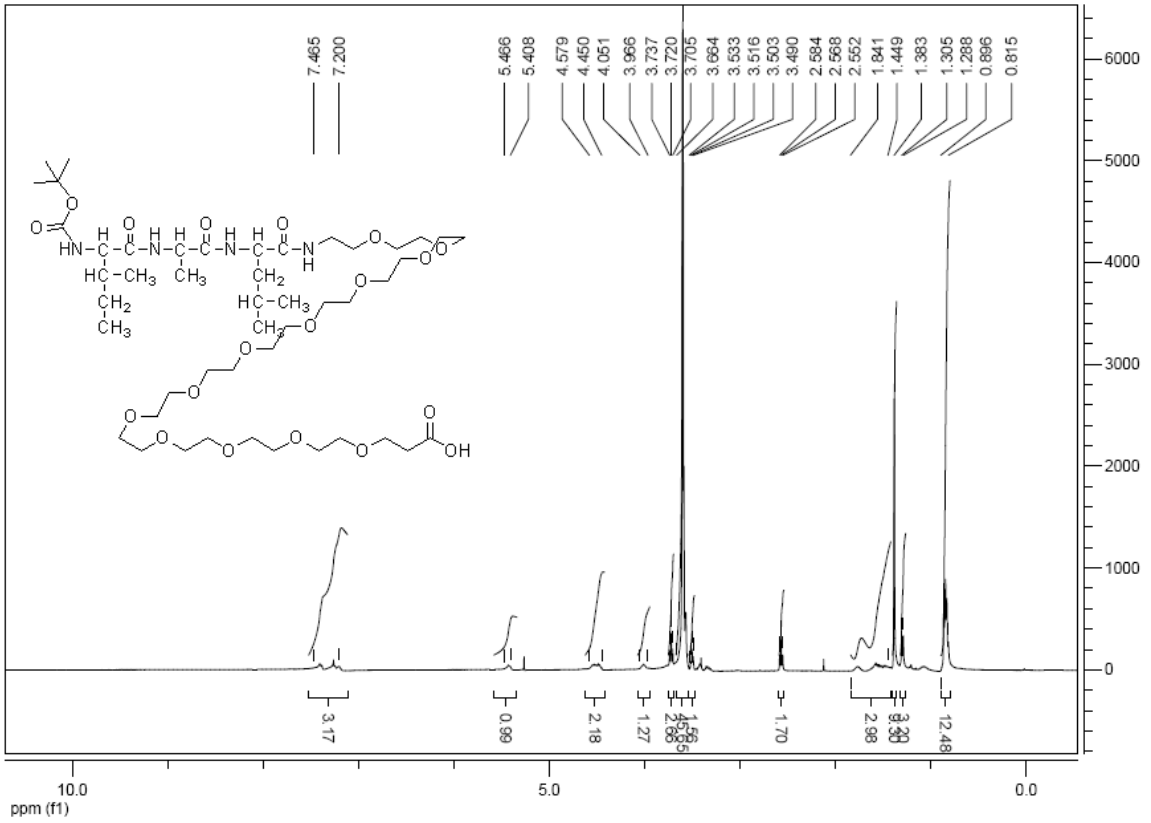
7.465
7.200
5.466
5.408
4.579
4.450
4.051
3.966
3.737
3.720
3.705
3.664
3.533
3.516
3.503
3.490
2.584
2.568
2.552
1.841
1.449
1.383
1.305
1.288
0.896
0.815
3.17
0.99
2.18
1.27
1.70
2.98
12.48
ppm (f1)

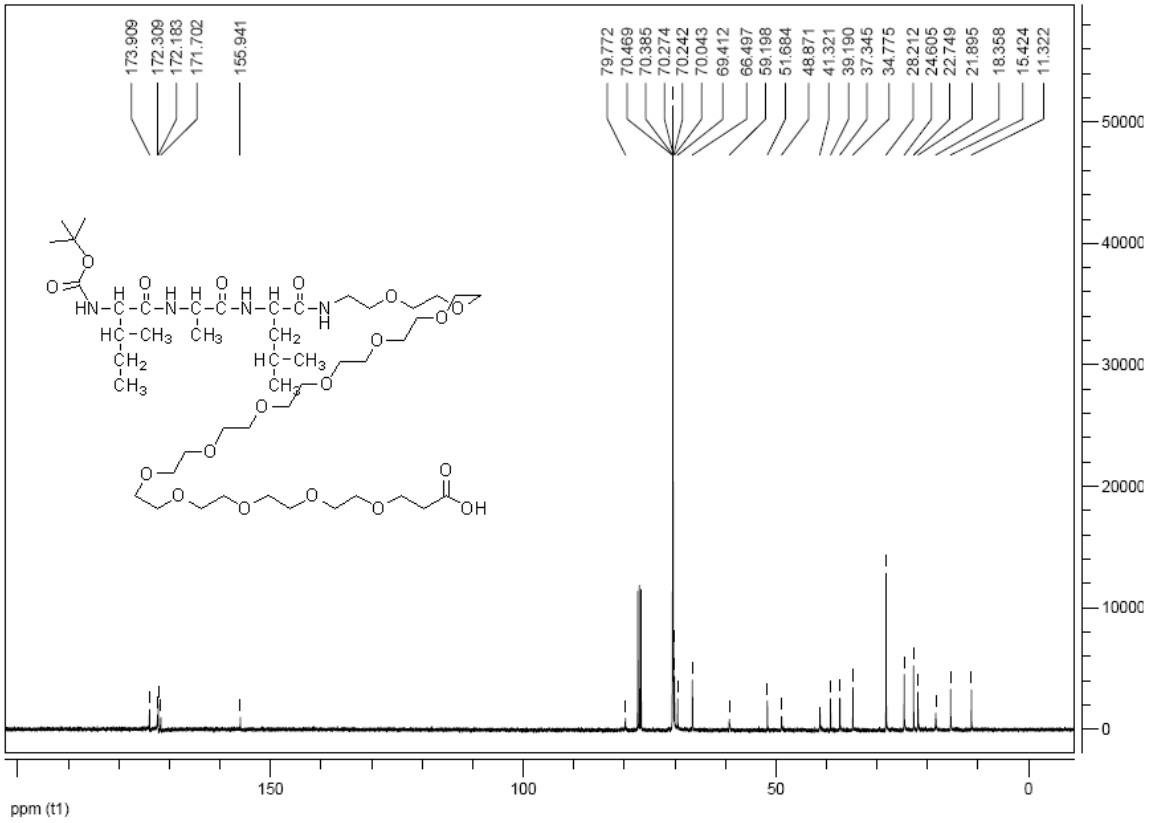
173.909
172.309
172.183
171.702
155.941
79.772
70.469
70.385
70.274
70.242
70.043
69.412
66.497
59.198
51.684
48.871
41.321
39.190
37.345
34.775
28.212
24.605
22.749
21.895
18.358
15.424
11.322
ppm (t1)

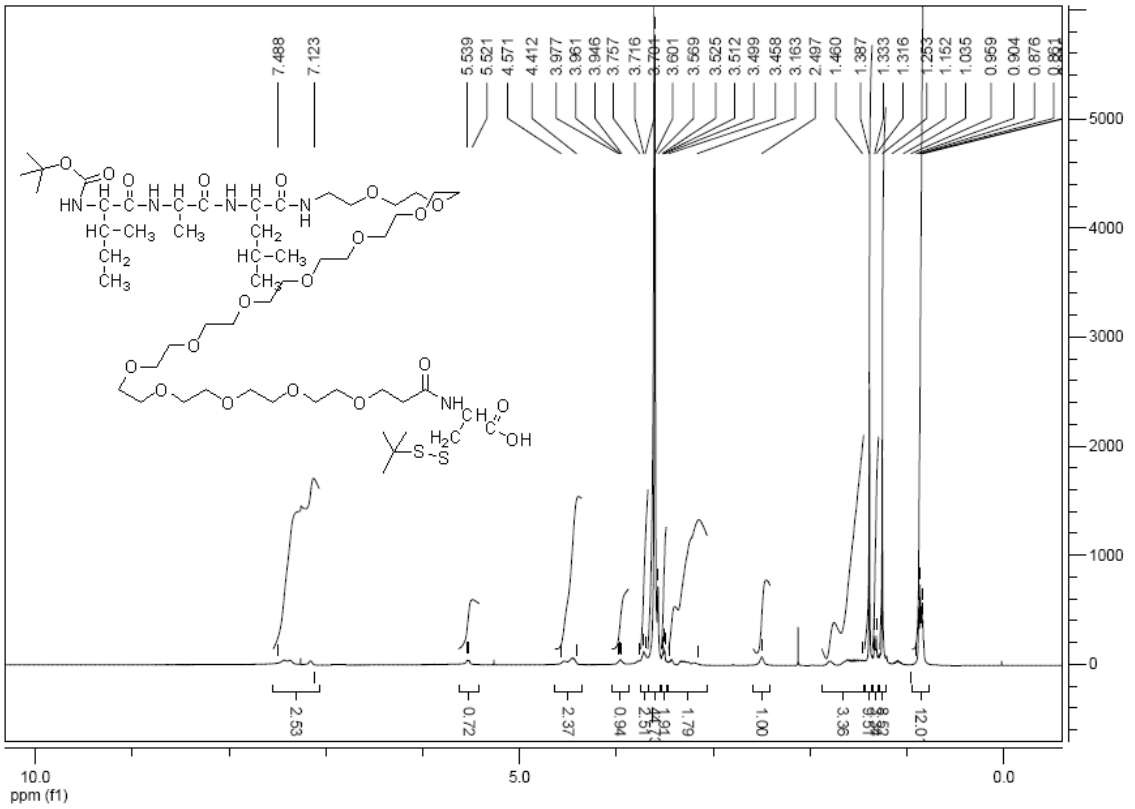
7.488
7.123
5.539
5.521
4.571
4.412
3.977
3.961
3.946
3.757
3.716
3.704
3.601
3.569
3.525
3.512
3.499
3.458
3.163
2.497
1.460
1.387
1.333
1.316
1.253
1.152
1.035
0.959
0.904
0.876
2.53
0.72
2.37
0.94
1.79
1.00
3.36
12.01
10.0
5.0
0.0
ppm (f1)

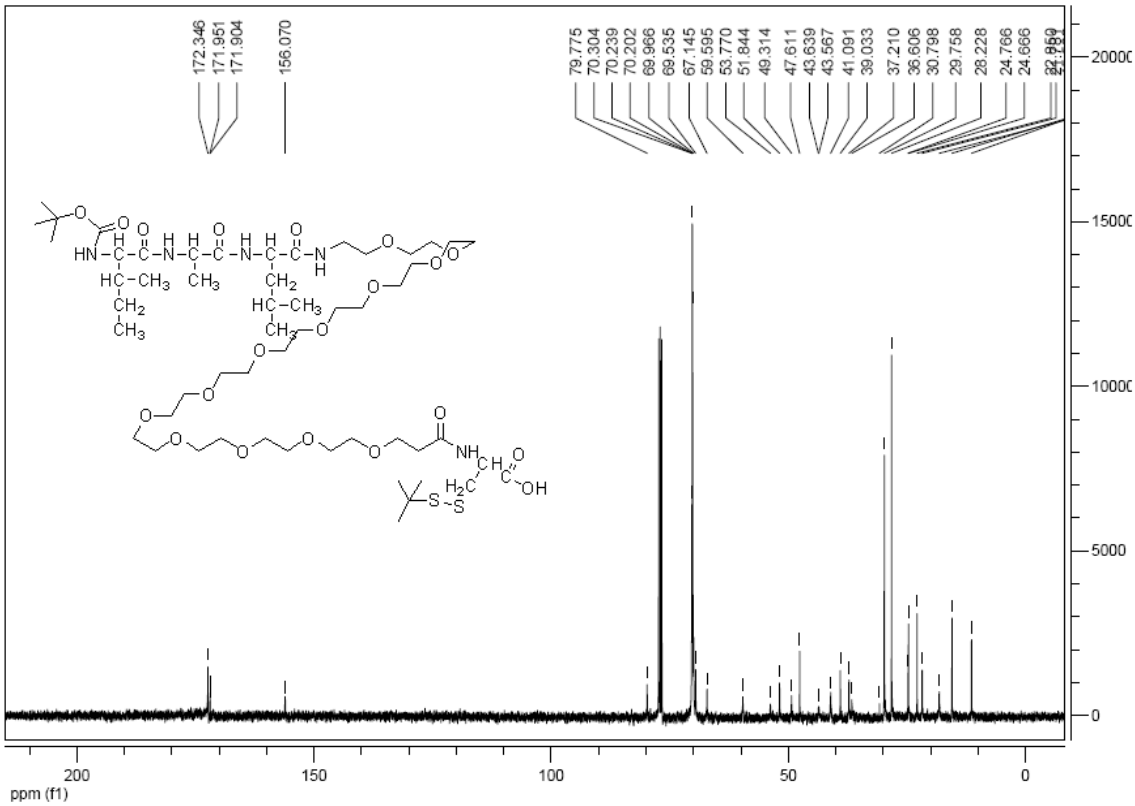
172.346
171.951
171.904
156.070
79.775
70.304
70.239
70.202
69.966
69.535
67.145
59.595
53.770
51.844
49.314
47.611
43.639
43.567
41.091
39.033
37.210
36.606
30.798
29.758
28.228
24.766
24.666
200
150
100
50
0
ppm (f1)

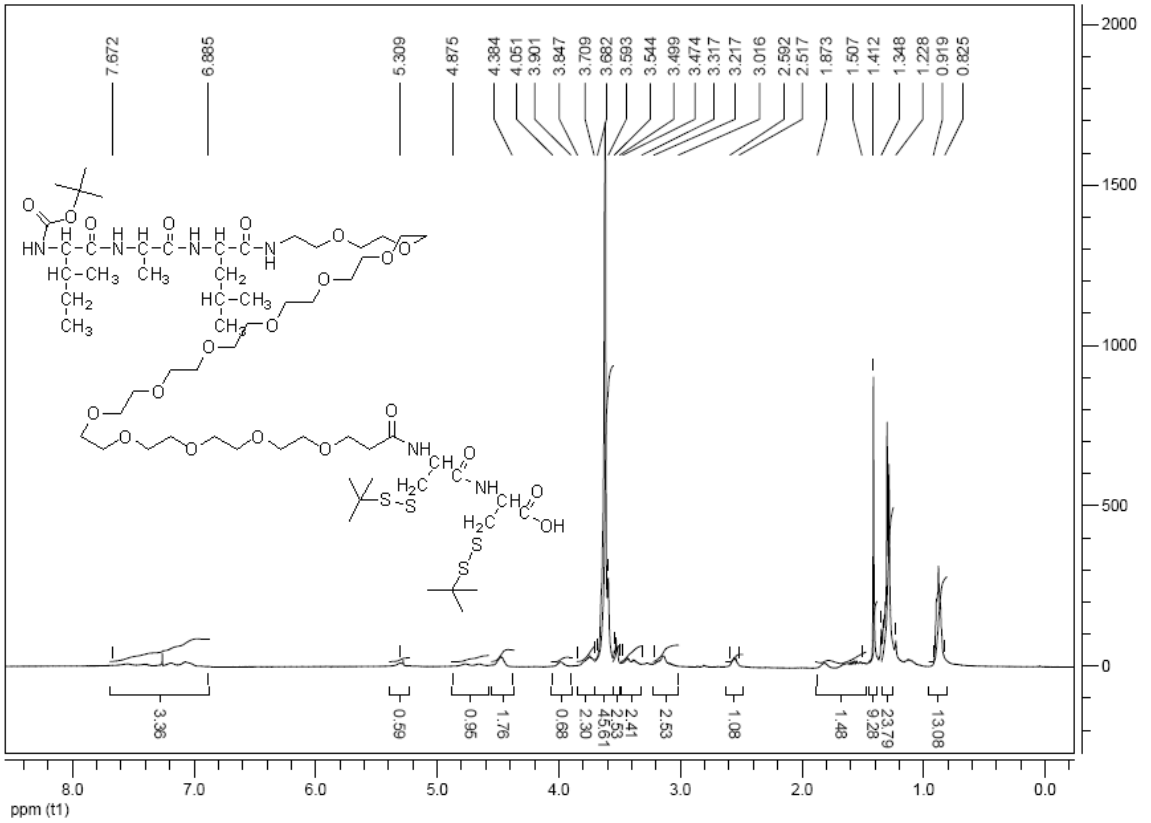
7.672
6.885
5.309
4.875
4.384
4.051
3.901
3.847
3.709
3.682
3.593
3.544
3.499
3.474
3.317
3.217
3.016
2.592
2.517
1.873
1.507
1.412
1.348
1.228
0.919
0.825
3.36
0.59
0.95
1.76
0.89
2.30
4.56
2.53
2.41
2.53
1.08
1.48
6.28
23.79
13.08
ppm (t1)

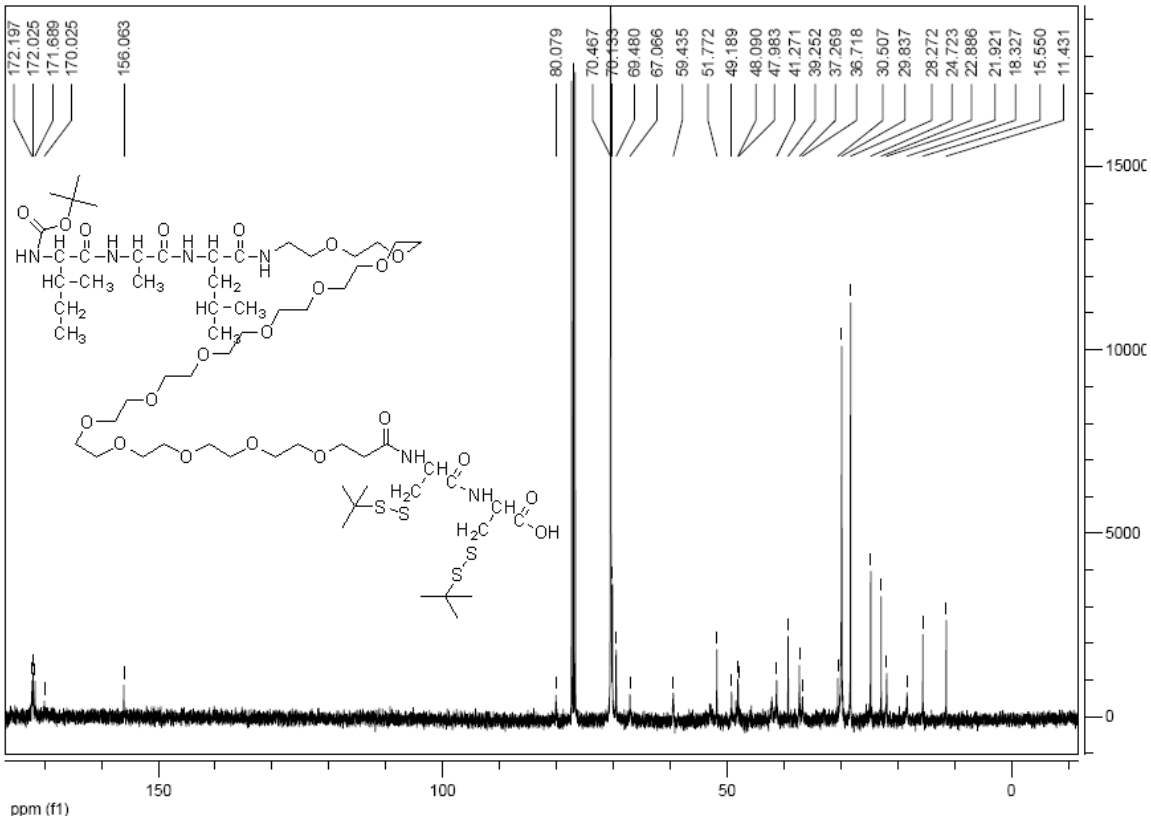
172.197
172.025
171.689
170.025
156.063
80.079
70.467
70.133
69.480
67.066
59.435
51.772
49.189
48.090
47.983
41.271
39.252
37.269
36.718
30.507
29.837
28.272
24.723
22.886
21.921
18.327
15.550
11.431
ppm (f1)

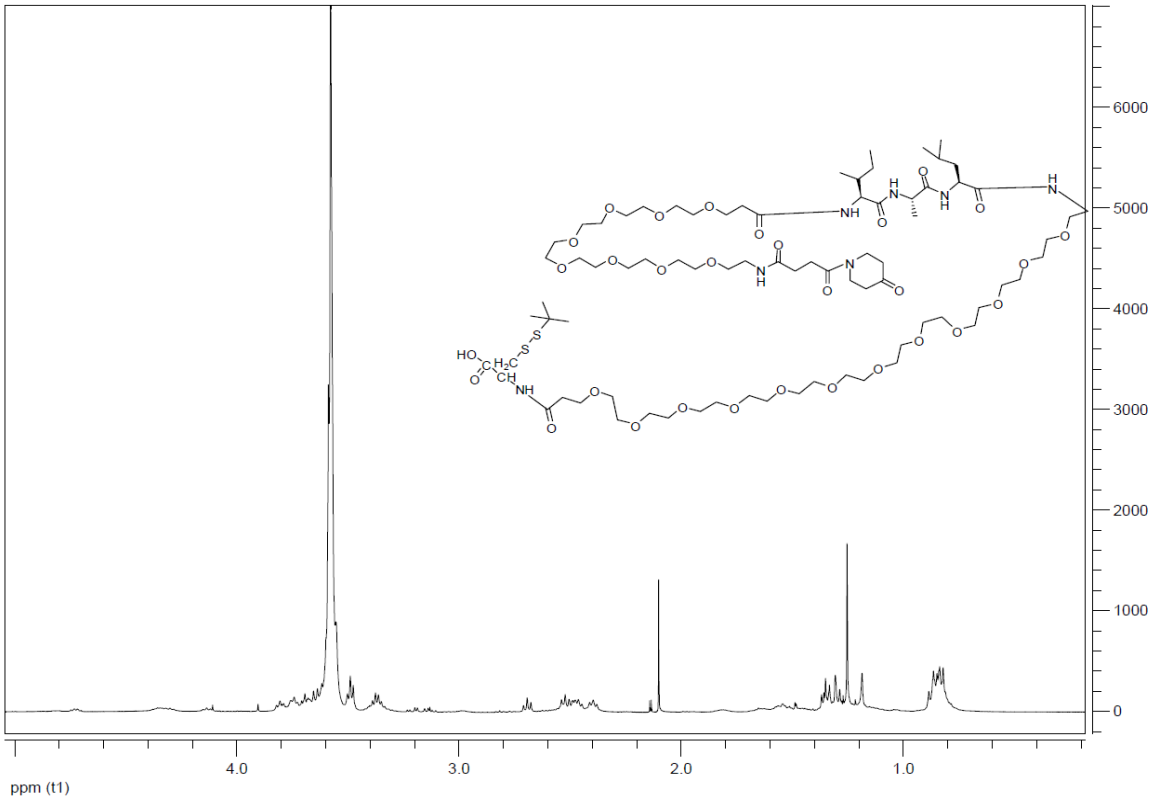
6000
5000
4000
3000
2000
1000
0
4.0
3.0
2.0
1.0
ppm (t1)

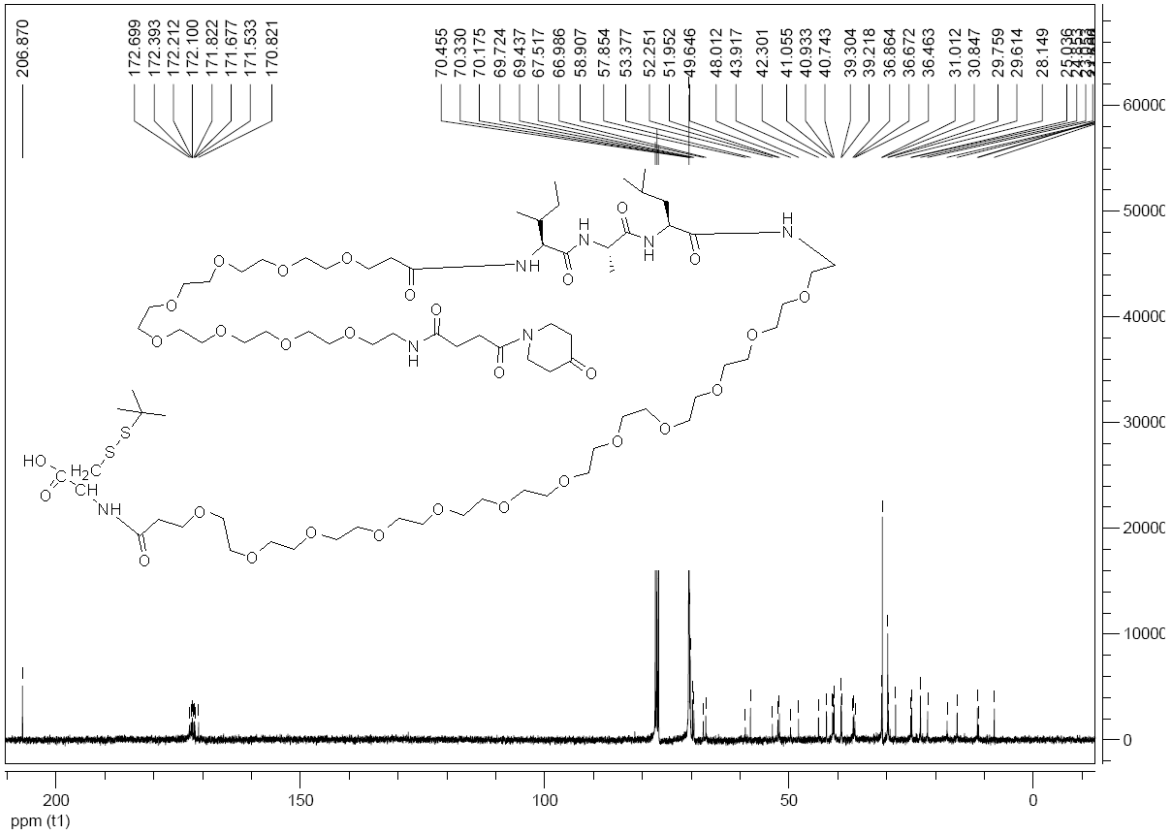
206.870
172.699
172.393
172.212
172.100
171.822
171.677
171.533
170.821
70.455
70.330
70.175
69.724
69.437
67.517
66.986
58.907
57.854
53.377
52.251
51.952
49.646
48.012
43.917
42.301
41.055
40.933
40.743
39.304
39.218
36.864
36.672
36.463
31.012
30.847
29.759
29.614
28.149
25.036
6000
5000
4000
3000
2000
1000
0
200
150
100
50
0
ppm (t1)

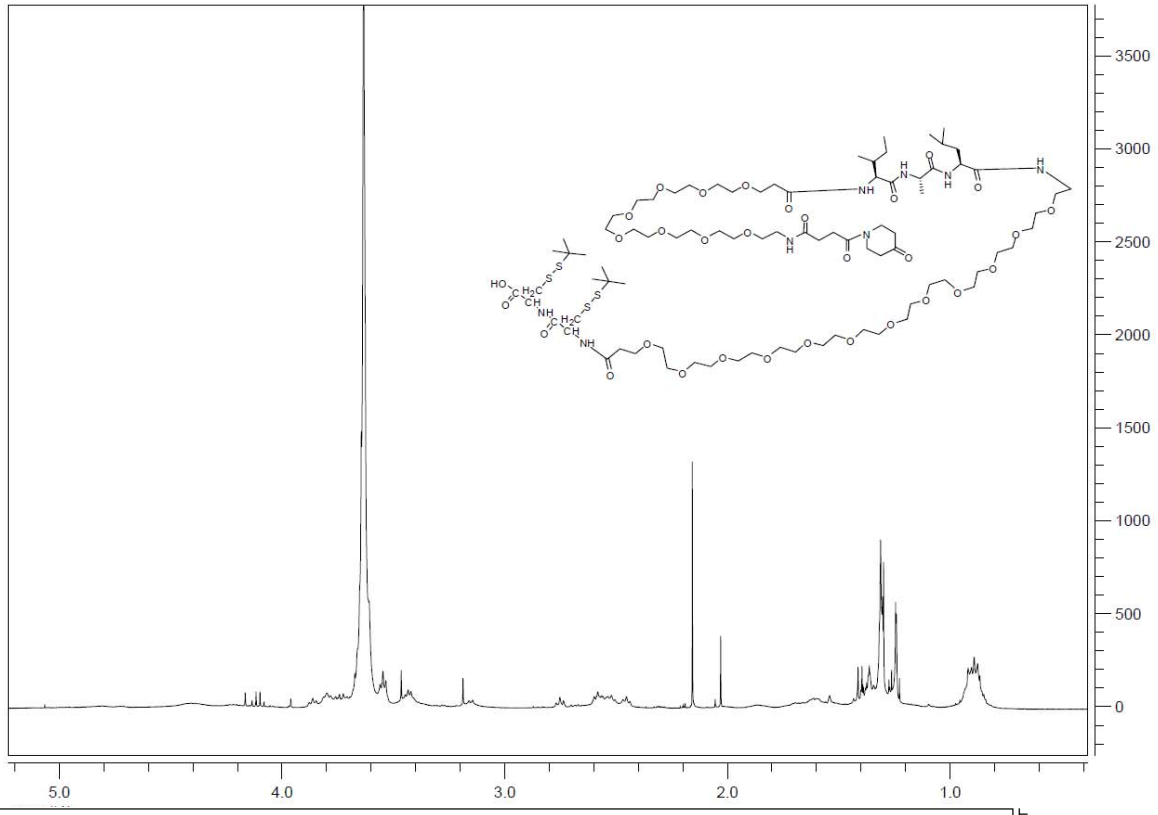
3500
3000
2500
2000
1500
1000
500
0
5.0
4.0
3.0
2.0
1.0

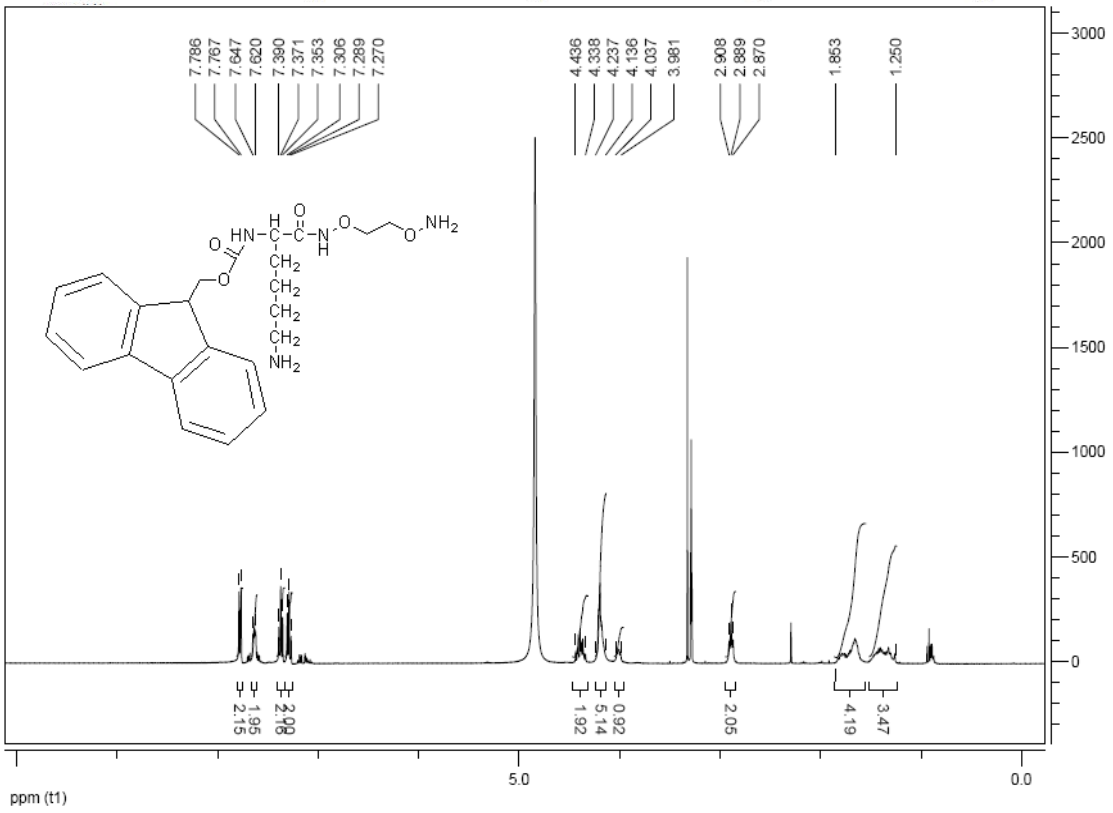
7.786
7.767
7.647
7.620
7.390
7.371
7.353
7.306
7.289
7.270
4.436
4.338
4.237
4.136
4.037
3.981
2.908
2.889
2.870
1.853
1.250
2.15
1.95
2.09
1.92
5.14
0.92
2.05
4.19
3.47
3000
2500
2000
1500
1000
500
0
5.0
0.0
ppm (t1)

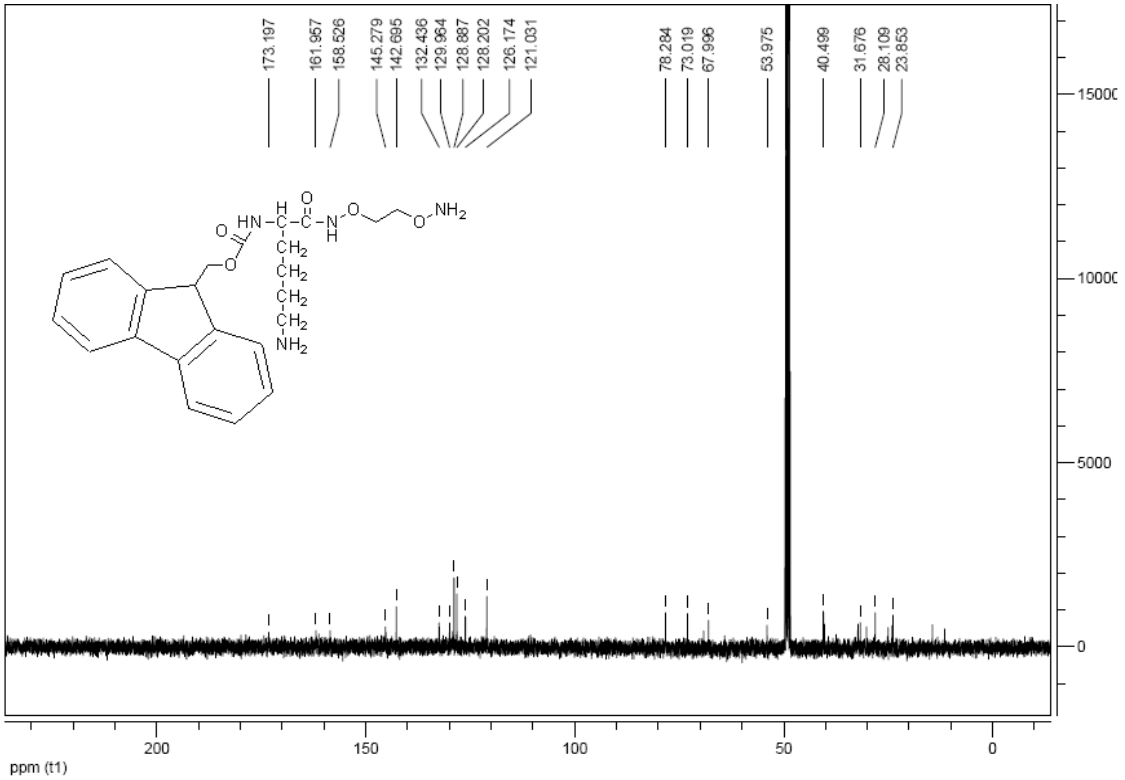
173.197
161.957
158.526
145.279
142.695
132.436
129.964
128.887
128.202
126.174
121.031
78.284
73.019
67.996
53.975
40.499
31.676
28.109
23.853
15000
10000
5000
0
200
150
100
50
0
ppm (t1)

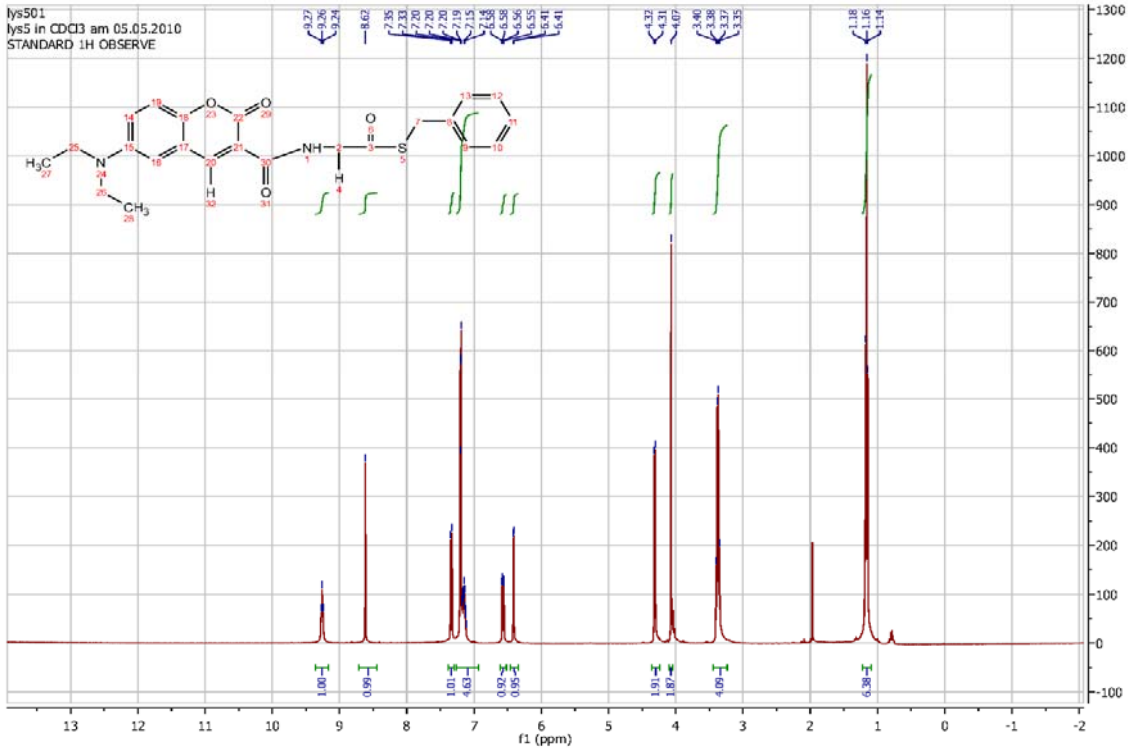
lys501
lys5 in CDCl3 am 05.05.2010
STANDARD 1H OBSERVE
1300
1200
1100
1000
900
800
700
600
500
400
300
200
100
0
-100
13
12
11
10
9
8
7
6
5
4
3
2
1
0
-1
-2
f1 (ppm)

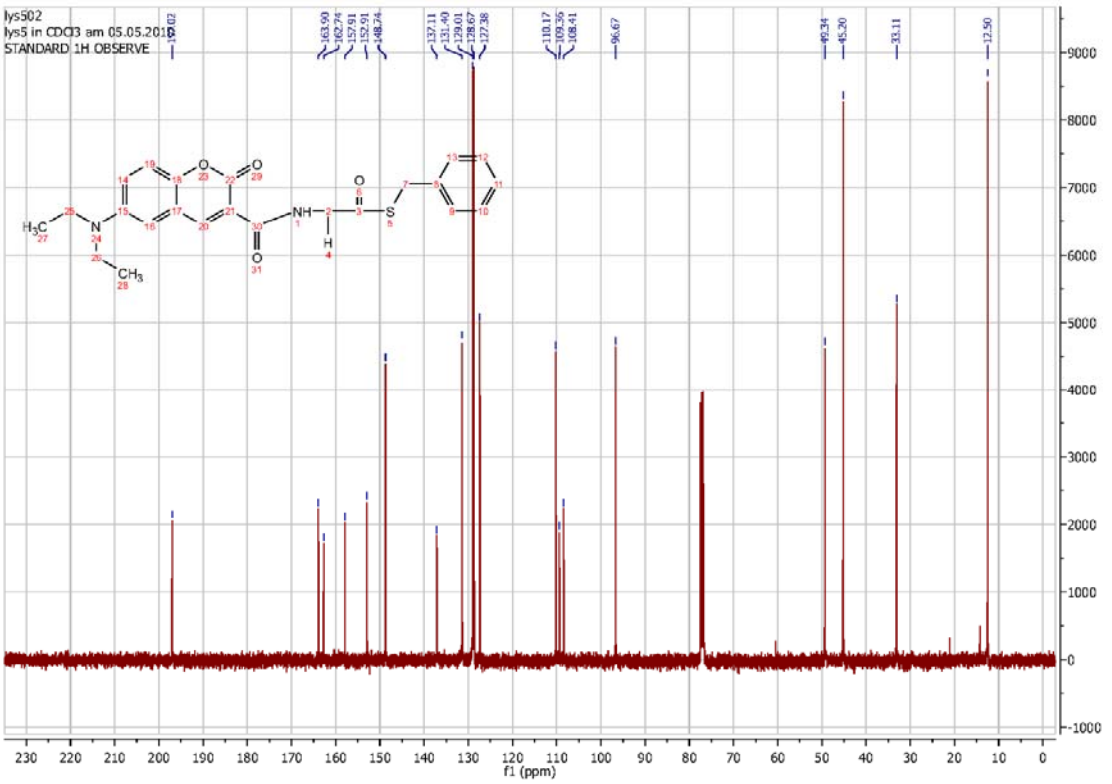
lys502
lys5 in CDCl3 am 05.05.2011
STANDARD 1H OBSERVE
163.90
162.74
157.91
152.91
148.74
137.11
131.40
129.01
128.67
127.38
118.17
109.55
108.41
96.67
49.34
45.30
33.11
12.50
f1 (ppm)

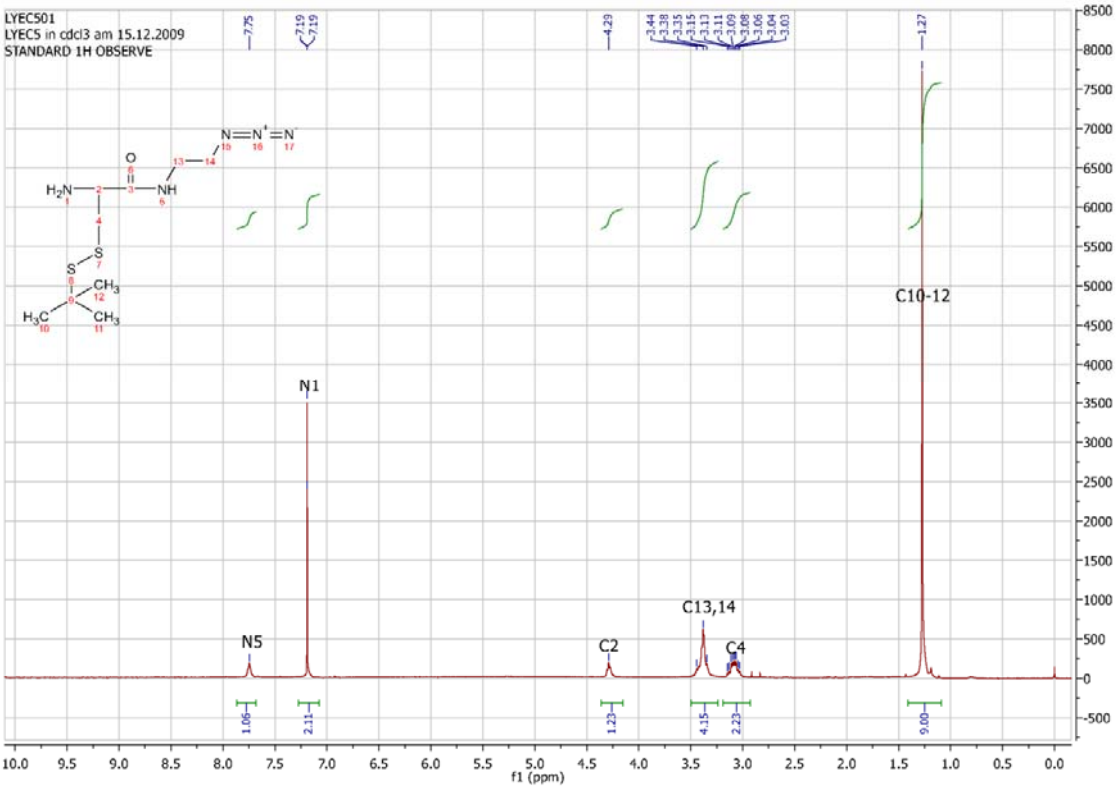
LYEC501
LYEC5 in cdcl3 am 15.12.2009
STANDARD 1H OBSERVE
7.75
7.19
7.19
4.29
3.44
3.38
3.35
3.15
3.13
3.11
3.09
3.08
3.06
3.04
3.03
1.27
C10-12
N1
C13,14
N5
C2
C4
1.06
2.11
1.23
4.15
2.23
9.00
f1 (ppm)

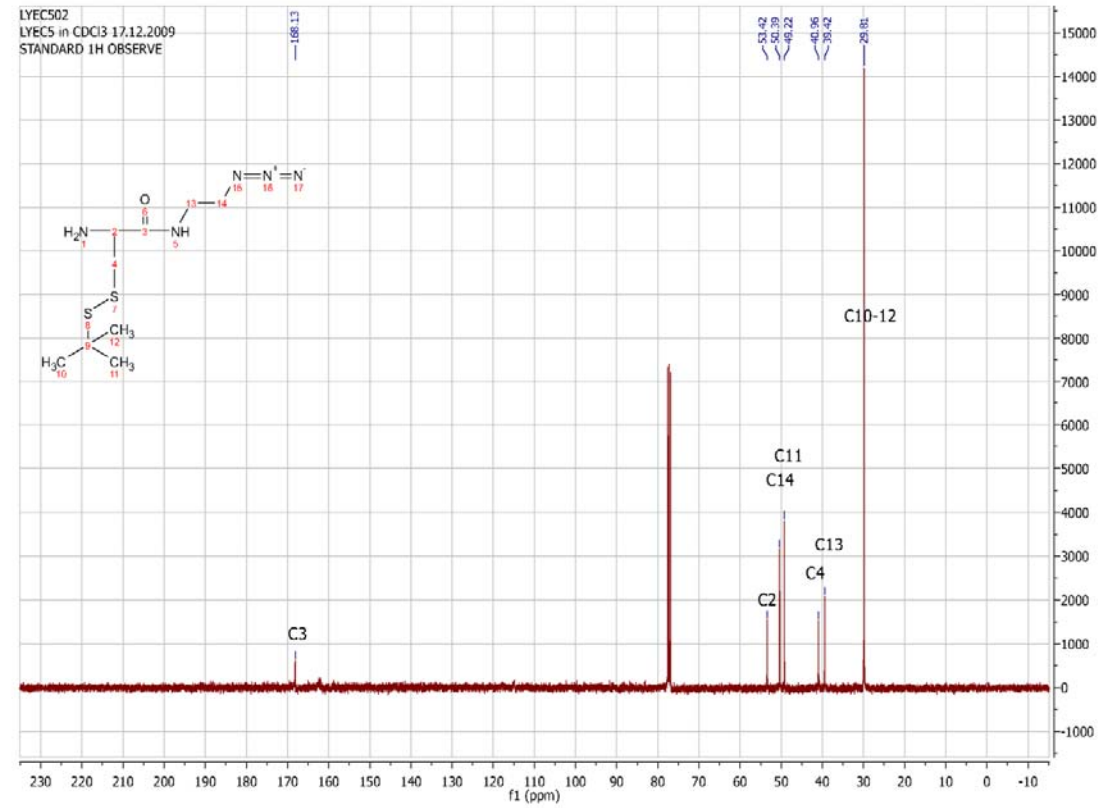
LYEC502
LYEC5 in CDCl3 17.12.2009
STANDARD 1H OBSERVE
C10-12
C11
C14
C13
C4
C2
C3
f1 (ppm)

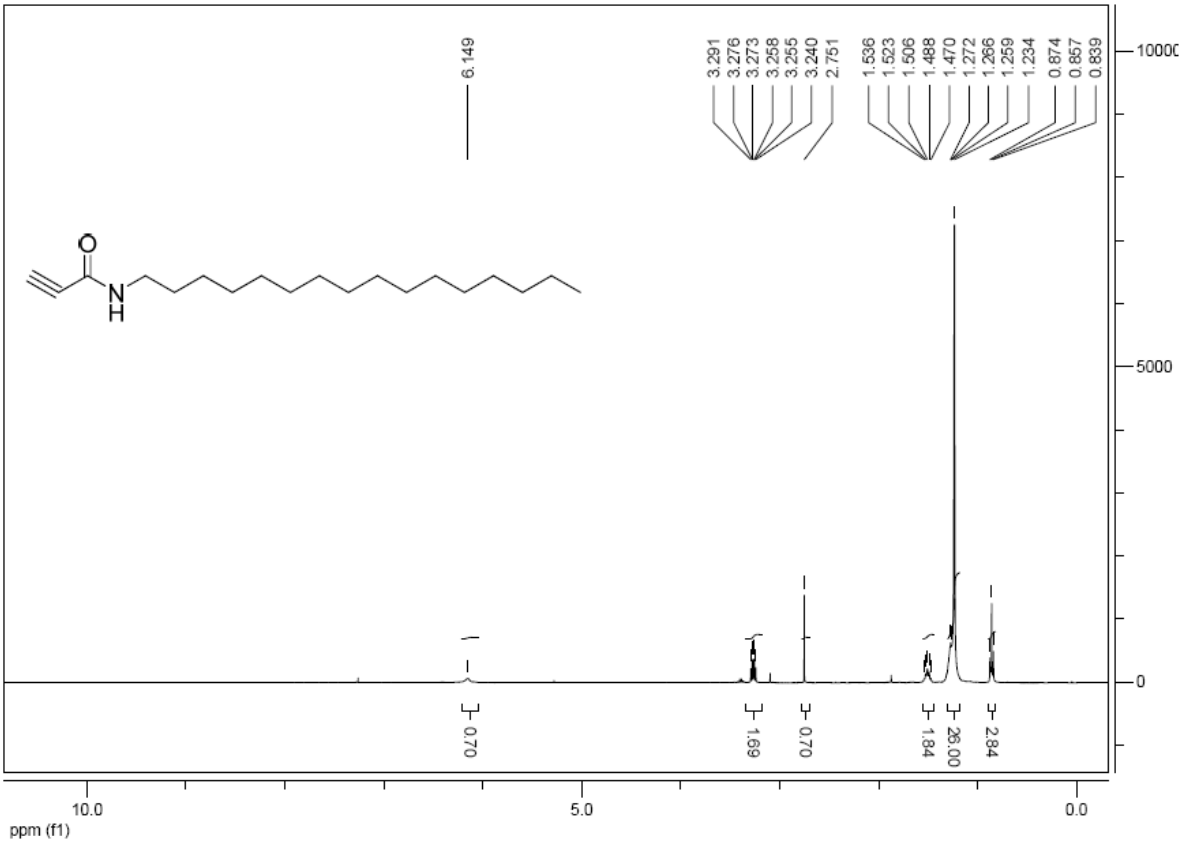
6.149
3.291
3.276
3.273
3.258
3.255
3.240
2.751
1.536
1.523
1.506
1.488
1.470
1.272
1.266
1.259
1.234
0.874
0.857
0.839
0.70
1.69
0.70
1.84
26.00
2.84
ppm (f1)

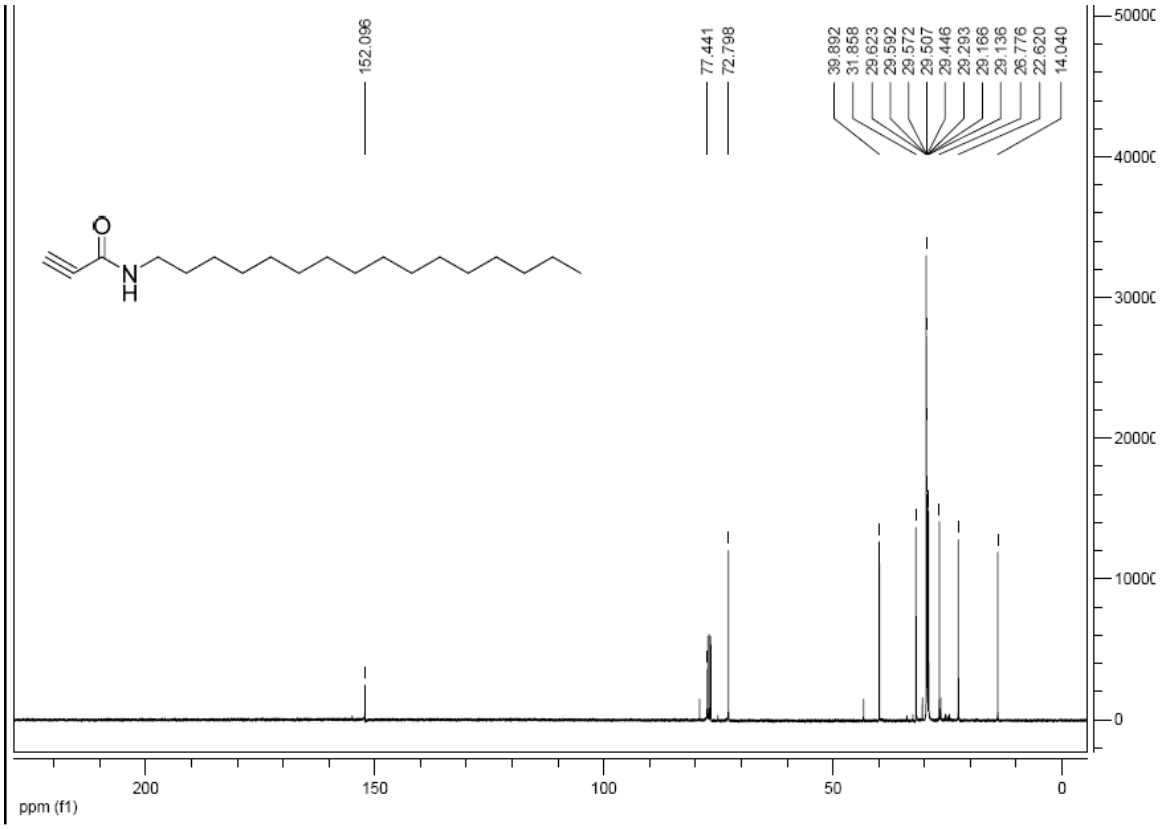
152.096
77.441
72.798
39.892
31.858
29.623
29.592
29.572
29.507
29.446
29.293
29.166
29.136
26.776
22.620
14.040
O
N
H
50000
40000
30000
20000
10000
0
200
150
100
50
0
ppm (f1)

Acknowledgements

I am taking this opportunity to thank all those who have assisted me in one way or the other with my Ph.D. project.

Firstly, I would like to express my gratitude to my supervisors Prof. Dr. Roger Goody and Dr. Yao-Wen Wu. They have always been extremely generous with their time, knowledge and ideas and allowed me great freedom in my research. I am grateful for their persistent motivation and their concerns for my well being. I would also like to thank many people from the Goody Department who have collaborated with me and contributed to various parts of this research, in particular Dr. Aymelt Itzen and Dr. Xiao-Min Hou (for FRET-based GEF sensor project), Fu Li and Dr. Wei Liu (for PEGylated Rab probe project), and particularly grateful to Nathalie Bleimling for preparing many plasmids I consumed throughout my studies. I am also grateful to all who have been a part of the Goody group. I have enjoyed working with skilful colleagues and friends, in a very inspiring and helpful atmosphere.

I would like to thank my second supervisors, Prof. Dr. Herbert Waldmann and Dr. Gemma Triola, for their suggestions and comments on my thesis and for part supervision of my Ph.D. work, especially in the lipidated protein semisynthesis and protein immobilization project. I would also like to thank the many people from the Waldmann Department who have collaborated with me and contributed to various parts of this research, in particular Dr. Debapratim Das (for synthesis of lipopeptides and introduction at the beginning in labs), Dr. Yong-Xiang Chen and Dr. Po-Chiao Lin (for protein immobilization project), Dr. HongYan Sun (for protein modification project), and Dr. Andrey P. Antonchick (for organic synthesis) and all members in Universary labs of the Waldmann Department. Without their skilfull help and cooperation this work would not have been possible.

Special thanks go to Dr. Ralf Seidel for LCMS help in protein test. I would also like to thank Dr. Hendrik Schröder and Prof. Dr. Christof M. Niemeyer for their kind help in protein immobilization project. I would like to thank the International Max-Planck Research School in Chemical Biology (IMPRS-CB) for setting the opportunity of becoming a member. My sincere gratitude gave to Christa Hornemann, Brigitte Rose, Waltraud Hofmann-Goody and Prof. Dr. Martin Engelhard for their kind support and help in official matters.

Last but not least, I would like to thank my wife Yali Yao. She gives me full support here. I am also greatly indebted to my family and friends for their understanding, patience and support during the entire period of my study.

Publications during PhD

'**Oriented Immobilization of Oxyamine-Modified Proteins**'
Long Yi,[1] Yong-Xiang Chen,[1] Po-Chiao Lin, Hendrik Schröder, Christof M. Niemeyer, Yao-Wen Wu, Roger S. Goody, Gemma Triola,* Herbert Waldmann* ([1]equal contribution)
Chem Commun **2012**, *48*, 10829 **COVER STORY**

'**One-Pot Dual-Labeling of a Protein by Two Chemoselective Reactions**'
Long Yi, Hongyan Sun, Aymelt Itzen, Gemma Triola, Herbert Waldmann, Roger S Goody,* Yao-Wen Wu*
Angew Chem Int Ed **2011**, *50*, 8287

'**Semi-synthesis of Prenylated Rab GTPase by Click Ligation**'
Long Yi, Mostafa Abootorabi, Yao-Wen Wu*
ChemBioChem, **2011**, *12*, 2413

'**A highly efficient strategy for modification of proteins at the C terminus**'
Long Yi, Hongyan Sun, Yao-Wen Wu, Gemma Triola, Herbert Waldmann,* Roger S. Goody*
Angew Chem Int Ed **2010**, *49*, 9417

'**A FRET Strategy for Monitoring GEF-Mediated Activation of a GTPase**'
Long Yi, Roger S. Goody, Yao-Wen Wu*
ChemBioChem, acceptance